12-2003

Mechanistic Studies of the Oxidation of Lignin and Cellulose Models

Oh-Kyu Lee

MECHANISTIC STUDIES OF THE OXIDATION OF LIGNIN AND CELLULOSE MODELS

By

Oh-Kyu Lee

B.S. Konkuk University, Korea, 1988

M.S. Konkuk University, Korea, 1990

M.S. University of Maine, 1999

A THESIS

Submitted in Partial Fulfillment of the

Requirements for the Degree of

Doctor of Philosophy

(in Chemistry)

The Graduate School

The University of Maine

December, 2002

Advisory Committee:

Barbara J. W. Cole, Professor of Chemistry, Co-Advisor

Raymond C. Fort, Jr., Professor of Chemistry, Co-Advisor

Bruce L. Jensen, Associate Professor of Chemistry

Joseph M. Genco, Professor of Chemical Engineering

Adriaan R. P. van Heiningen, Professor of Chemical Engineering

MECHANISTIC STUDIES OF THE OXIDATION OF LIGNIN AND CELLULOSE MODELS

By Oh-Kyu Lee

Thesis Co-Advisors: Dr. Barbara J. W. Cole and Dr. Raymond C. Fort, Jr.

An Abstract of the Thesis Presented
in Partial Fulfillment of the Requirements for the
Degree of Doctor of Philosophy
(in Chemistry)
December, 2002

Oxygen delignification is an environmentally friendly pulp bleaching system. To develop a selective delignification process that results in high DP retention of carbohydrate with lignin being removed, obtaining better knowledge of reactions occurring during oxygen delignification is essential.

In this work, mixtures of guaiacol (model lignin) and methyl-β-D-glucoside (model cellulose) were reacted in a pressurized oxygen reaction system (pH 12, 65 psi O_2, and 95 °C in a glass reaction vessel). In the results, methyl-β-D-glucoside degraded only in the presence of lignin. This indicates that hydroxyl radicals, that subsequently react with methyl-β-D-glucoside, are generated in the system. Unfortunately, we could not develop the degradation mechanisms of methyl-β-D-glucoside in this study because the identification of products derived from methyl-β-D-glucoside could not be accomplished. Therefore, we undertook an alternative

study of the oxidation reactions of cellulose using a UV/H_2O_2 system, which is a hydroxyl radical generation system.

For the UV/H_2O_2 system, the cellulose models used were methyl-β-D-glucoside, methyl-β-D-cellobioside, and cellulose fiber. The reactions using hydroxyl radical scavengers in the UV/H_2O_2 system strongly support the hydroxyl radical reactions proposed in our lab previously. The results, from the qualitative analysis of the organic acids produced during the reaction, suggest that hydroxyl radicals have an important role in the formation of aldonic acids from aldoses.

In the reactions with methyl-β-D-cellobioside, the reaction chemistry was the same as in the reactions with methyl-β-D-glucoside. However, the reactivity of methyl-β-D-cellobioside toward hydroxyl radicals is considered to be larger than that of methyl-β-D-glucoside.

The cellulose fiber (filter paper) was degraded in the UV/H_2O_2 system.

In the presence of hydroxyl radical scavengers, *tert*-BuOH and 2-propanol, the degradation was inhibited in all three cellulose models used in this study. This supports that cellulose can be protected from the degradation by the hydroxyl radical using scavengers, *tert*-BuOH and 2-propanol.

ACKNOWLEDGEMENTS

I acknowledge the USDA for the financial support.

I gratefully thank Dr. Cole and Dr. Fort, co-advisors, for their support, guidance, encouragement, and patience through my whole academic program. I also would like to thank other members of advisory committee, Dr. Genco, Dr. van Heiningen, and Dr. Jensen, for their advice and support.

I would like to thank Johnna Brazier for her endless technical support and kindness. I thank Don Guay and Meg Hausman for helping me to start the lab work in my first academic year in this program. I also thank Jon Spender and other graduate students in the wood chem group for sharing information.

I thank all faculty and staff, especially, Dave Labrecque, Margaret Forbes, Linda Maynard, and Cindy Commeau.

I gratefully thank Dr. Kwon and his family for their enormous help during entire years in Maine.

I thank my parents and other family members and will never forget constant support and encouragement from them.

My greatest thank goes to my wife Sora, son Jongsun, and daughter Soyoung for their love, patience, support, and sacrifice.

TABLE OF CONTENTS

LIST OF TABLES

LIST OF FIGURES

CHAPTER 1

INTRODUCTION

This thesis describes our progress on the understanding of chemistry occurring during oxygen-alkali delignification (denoted as oxygen delignification).

During chemical wood pulping and bleaching, lignin is removed to produce high quality paper, since lignin reduces fiber-fiber bond strength of paper and contributes to color reversion in paper when it is oxidized. Recent environmental regulations have forced the elimination of the use of chlorine for delignification, and the oxygen-alkali system is becoming the leading method of delignification that is environmentally benign. However, oxygen-alkali delignification results in low yield and strength of paper since carbohydrates are degraded during these processes. To develop a carbohydrate-preserving delignification method, it is necessary to obtain a better knowledge of the chemical reaction mechanisms occurring during oxygen-alkali delignification.

1.1. Wood components

Wood is a heterogeneous organic polymer that consists of carbohydrates and lignin as the major components.

Carbohydrates in wood are classified into cellulose and hemicelluloses. Cellulose and hemicelluloses comprise about 40-45 % and 20-30 % of dry wood weight, respectively (Sjöström, 1993). A cellulose molecule (Figure 1.1) of wood is a linear homopolysaccharide composed of about 10,000 β-D-glucopyranose units linked by

(1 → 4)-glucosidic bonds (Sjöström, 1993). Cellulose molecules are bound by intra- and intermolecular hydrogen bonds to build "microfibrils" that contain 50-70% crystalline regions that alternate with amorphous regions (Biermann, 1996). The microfibrils grow to become "fibrils", and the fibrils build up to become cellulose fibers that comprise the "back-bone" structure of a wood fiber (Biermann, 1996). Because of the hydrogen bonding between cellulose molecules, wood fibers have high strength which provides important physical properties of paper.

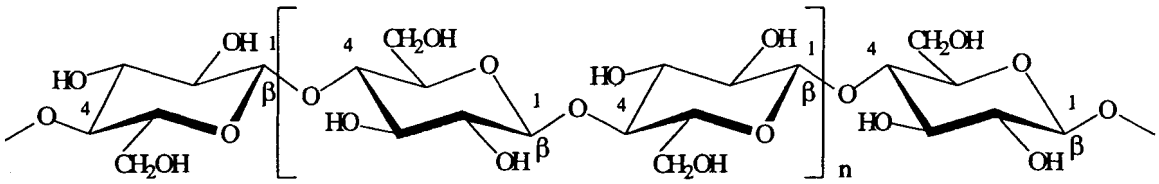

Figure 1.1. Structure of a cellulose molecule (Biermann, 1996; Sjöström, 1993).

Hemicelluloses are primarily branched heteropolysaccharides composed of various sugars including D-glucose, D-mannose, D-galactose, D-xylose, L-arabinose, L-rhamnose, and their derivatives (Figure 1.2). Most hemicelluloses have a degree of polymerization of around 200. In hardwoods, glucuronoxylans (or xylans) are the principal hemicelluloses. Glucuronoxylans have a β-(1 → 4)-xylose backbone containing side branches of 4-O-methylglucuronic acids with α-(1 → 2) linkages. Xylans vary from 15–30 % of the dry wood weight in different hardwood species (Sjöström, 1993). In softwoods, galactoglucomanans are the major hemicellulose. They which contain (1→ 4)-linked β-D-glucopyranose and β-D-mannopyranose

units with side chains of α-D-galactopyranoses in (1→ 6) linkages. These galactoglucomanans make up about 20 % of the dry wood weight (Sjöström, 1993).

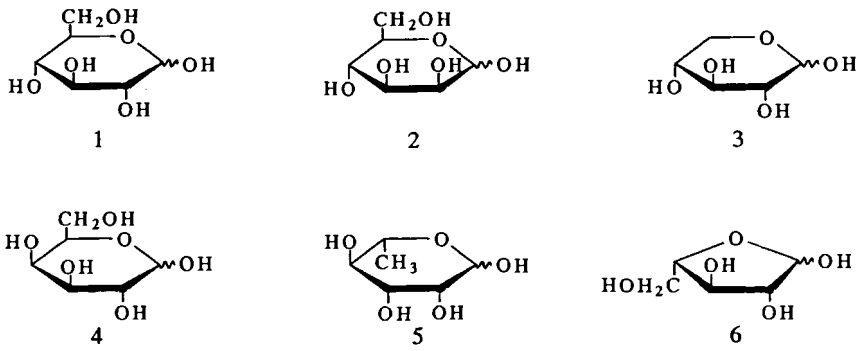

Figure 1.2. Sugar units that compose hemicellulose in wood cell: 1- D-glucose, 2- D-mannose, 3- D-xylose, 4- D-galactose, 5- L-rhamnose , 6- L-arabinose.

Lignin is a macromolecular compound built up of phenylpropane units (Figure 1.3) with a weight-average mole weight of approximately 20,000 (Sjöström, 1993). Derivatives of phenylpropane are linked together to develop its structure, which is three-dimensional and amorphous. Because of the uncertain linkage patterns of phenylpropane units, the structure of lignin is not completely understood.

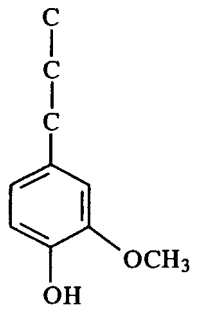

Figure 1.3. A phenylpropane unit.

There are several types of linkages between phenylpropane units as shown in Figure 1.4 (Sjöström, 1993) and Figure 1.5 (Karhunen *et al.*, 1995). β-O-4 linkages are the major likages comprising about 50 and 60 % of the total linkages in softwoods and hardwoods, respectively.

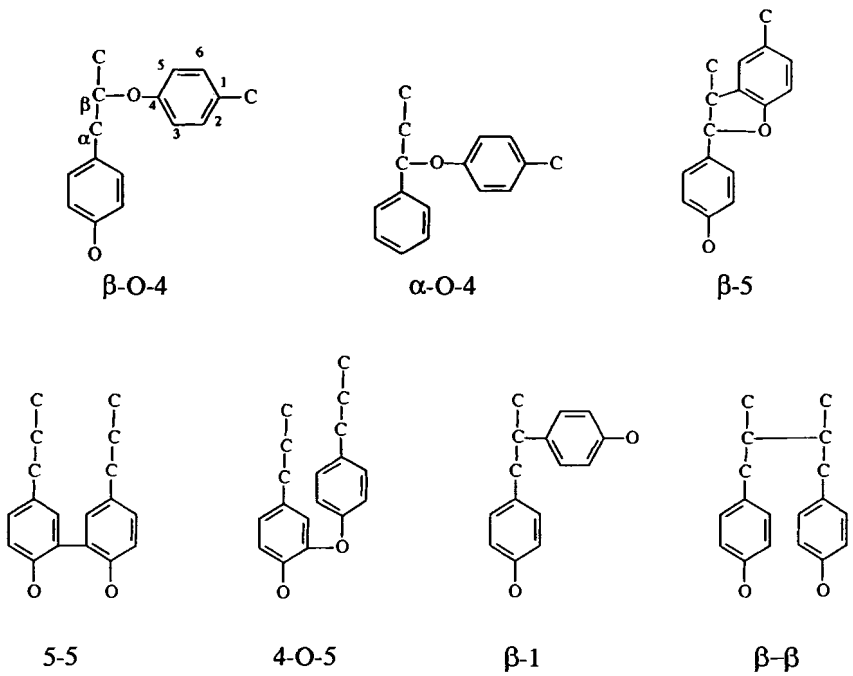

Figure 1.4. Common linkage types between phenylpropane units in lignin (Sjöström, 1993).

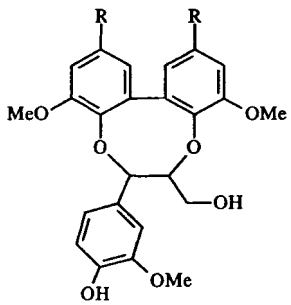

Figure 1.5. The cross coupling structure between a phenylpropane and an o, o'-dihydroxybiphenyl unit (Karhunen *et al.*, 1995).

Functional groups on lignin phenylpropane units also vary with wood species (Table 1.1) (Sjöström, 1993). Based on the information of linkage patterns and

Table 1.1. Functional groups of lignin (per 100 phenylpropane units) (Sjöström, 1993).

Group	Softwood lignin	Hardwood lignin
Methoxyl	92-97	139-158
Phenolic hydroxyl	15-30	10-15
Benzyl alcohol	30-40	40-50
Carbonyl	10-15	

functional groups, Brunow (1998) proposed a revised structure of softwood lignin (Figure 1.6).

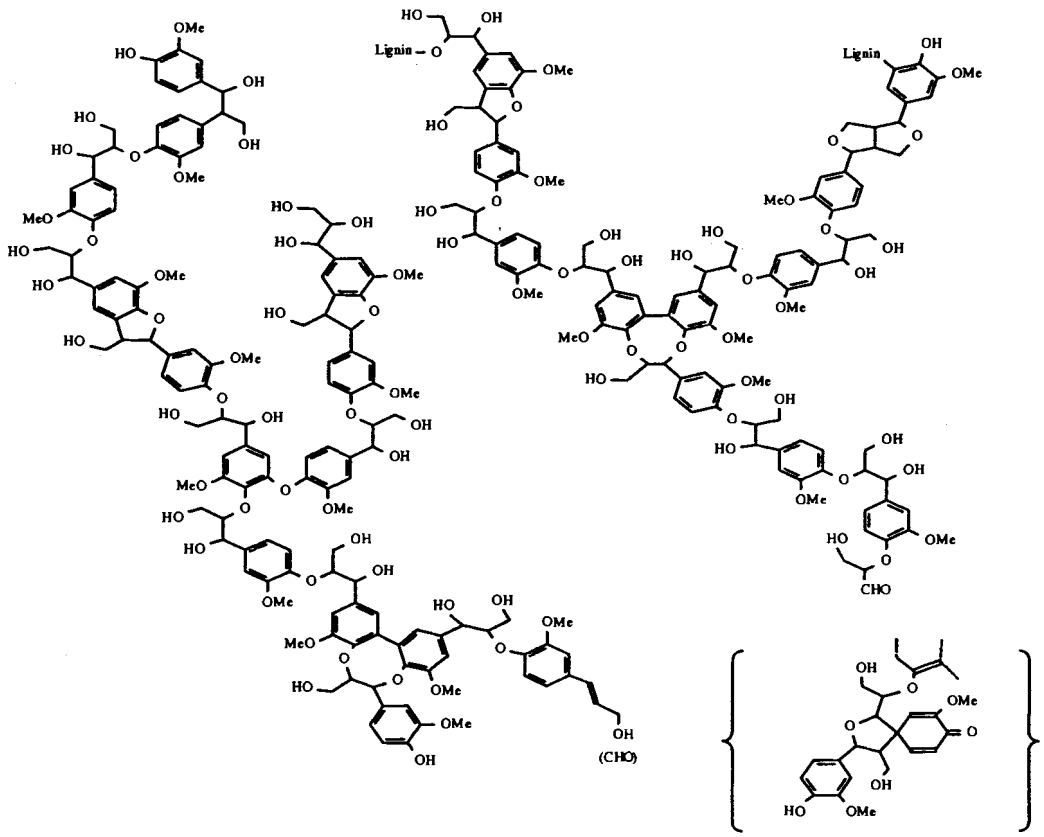

Figure 1.6. A proposed softwood lignin (Brunow, 1998).

1.2. Chemical pulping and bleaching

Chemical pulping is a process used to break down wood chips chemically into fibers by removing lignin (Biermann, 1996; Sjöström, 1993). Delignification (the removal of lignin) is necessary to obtain high quality paper because lignin negatively affects paper properties. Various types of commercial chemical pulping processes have been employed. Kraft pulping is predominant these days, in that it occupies more than 80 % of the chemical pulp produced in the world (Sjöström, 1993). Sodium hydroxide and sodium sulfide (Na_2S) are used as the pulping chemicals in this process. Advantages of kraft pulping over other pulping processes are simpler process, more economic recovery of chemicals, and better quality of pulp.

Although most lignin is removed during the chemical pulping processes, there are still residual lignin, contaminants, and chromophores existing in the system. The bleaching process is used to eliminate those remaining substances and to make the pulp cleaner and brighter. Common bleaching chemicals are chlorine (Cl_2), chlorine dioxide (ClO_2), oxygen (O_2), hydrogen peroxide (H_2O_2), and ozone (O_3). Chlorine was the most popular pulp bleaching chemical from the early 1930s to the early 1990s. However, chlorine treatment of pulp results in production of toxic chlorinated compounds like dioxins. Today, chlorine is not used in pulp bleaching because of environmental regulations. Chlorine dioxide was introduced into pulp bleaching in the mid 1940s. In chlorine dioxide bleaching, the formation of absorbable chlorinated organic compounds occurs although dioxin is not produced in detectable quantities. Due to environmental issues in recent years, environmentally benign methods of pulping and bleaching are desired. Thus, ozone, hydrogen peroxide, and oxygen have

received significant attention as the bleaching chemicals although they are less selective toward lignin degradation than are chlorine and chlorine dioxide.

Ozone has been used in pulp bleaching since the mid 1990s. Ozone is a powerful oxidizing agent that reacts with most organic materials. However, its application is not easy since ozone is generated in low concentrations diluted with a carrier gas, like oxygen, and its solubility in water is limited (van Lierop *et al.*, 1996).

Hydrogen peroxide has been used in commercial pulp bleaching since the late 1970s. Hydrogen peroxide is used in an alkaline medium to form hydroperoxide anion (HO_2^-), which is believed to eliminate chromophores that contain carbonyl groups in lignin structures (Pan *et al.*, 1993). In the presence of transition metals, however, alkaline hydrogen peroxide decomposes to hydroxyl radicals, and the radicals degrade not only lignin but also cellulose in the pulp (Lachenal, 1996). To reduce decomposition of hydrogen peroxide, chelating agents, such as DTPA (diethylenetetraminepentaacetic acid), are used before alkaline hydrogen peroxide treatment.

Oxygen in alkaline conditions was introduced in commercial bleaching in the 1970s. Alkaline oxygen often is used in combination with other bleaching chemicals, such as chlorine-containing chemicals, because of its low selectivity toward lignin. To minimize carbohydrate degradation, oxygen bleaching (or oxygen delignification) is conducted only up to about 50 % lignin degradation. The oxygen step allows for lower amounts of bleaching chemicals in subsequent bleaching stages. This results in the formation of fewer chlorinated compounds, in a decrease in biochemical

oxygen demand (BOD) and chemical oxygen demand (COD), and in a decrease in color of the effluents (McDonough, 1996).

CHAPTER 2

LITERATURE REVIEW

To investigate the complex chemistry of oxygen delignification, it is necessary to consider the relationships between lignin, carbohydrates, and oxygen species.

2.1. Oxygen species

In oxygen delignification, molecular oxygen (O_2), superoxide radical ($O_2^{\cdot-}$), hydrogen peroxide (H_2O_2), hydroxyl radical ($HO^{\cdot}$), and their conjugates are the main species involved during the process. These oxy-compounds are called oxygen species. Molecular oxygen is a precursor of the other oxygen species, which are formed by one-electron and proton transfers (Gratzl, 1992) as shown in Figure 2.1.

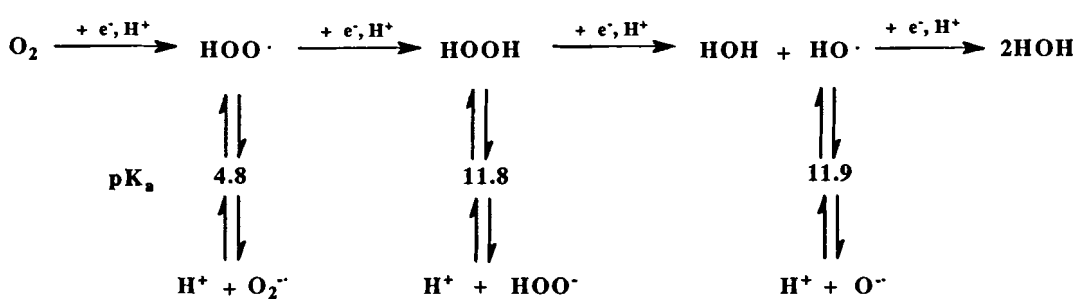

Figure 2.1. Oxygen species derived from molecular oxygen in aqueous solution (Gratzl, 1992).

2. 1. 1. Molecular oxygen (O_2 or $^{\cdot}O_2^{\cdot}$)

Molecular oxygen (or dioxygen) is a diradical in its ground state (a triplet state). This diradical has two unpaired electrons in two different $2p$ anti-bonding orbitals (π^*) with parallel spin orientation (Hund's rule). The orbital energy in this arrangement is lower than when the two electrons are in the same orbital. When dioxygen attempts to oxidize another atom or molecule (electron donors), as an electrophile, it can accept only one electron at a time. The reason is that only one electron can each half-filled molecular orbital and pair with the electron already present (Pauli exclusion principle). Moreover, only one of the spin-paired electrons of the donor has the appropriate spin to pair spin in the acceptor (molecular oxygen). This spin restriction on electron transfer prevents molecular oxygen from having fast reactions with most singlet state organic compounds. Nevertheless, molecular oxygen is the primary oxidant in most combustion processes of hydrocarbons, such as the following reactions (Sawyer and Nanni, Jr., 1981):

$$^{\cdot}O_2^{\cdot} + RH \longrightarrow R^{\cdot} + HO_2^{\cdot} \longrightarrow \textbf{Further reactions by radical processes}$$

The spin restriction of molecular oxygen, however, doesn't affect the reactions with radicals, carbanions (March, 1977), and single electrons (Fee and Valentine, 1977; Sawyer, 1991). Dioxygen reacts with a hydrogen atom (March, 1977; Sawyer, 1991) to form a perhydroxyl radical both in the gas-phase and in solution (Samuel and Steckel, 1974). Also, it is well known that dioxygen forms complexes with transition metals which are in low oxidation states (Collman, 1977; Sawyer, 1991).

It is widely accepted that the one-electron reduction potential of molecular oxygen into superoxide radical in water is –0.33 V vs. NHE (Normal Hydrogen Electrode) while other reduced oxygen species have higher one-electron reduction potentials as shown in Table 2.1. As a result, the first one-electron reduction of molecular oxygen is the limiting factor of its reactivity, since after the first one-electron reduction, molecular oxygen is reduced to a much more reactive species as shown in Figure 2.1.

Table 2.1. Standard reduction potential (E^0) of oxygen species in water at pH 7.25 (Sawyer, 1988).

	E^0(V) vs. NHE
$O_2 + e^- \longrightarrow O_2^-$	- 0.33
$O_2^- + e^- + 2H^+ \longrightarrow H_2O_2$	+ 0.89
$H_2O_2 + e^- + H^+ \longrightarrow H_2O + HO\cdot$	+ 0.38
$HO\cdot + e^- + H^+ \longrightarrow H_2O$	+ 2.31

Because of the low reducing potential of dioxygen, in oxygen delignification there must be easily oxidized substrates in the system for the first one-electron reduction to occur. Another important factor for the use of dioxygen is its solubility in aqueous solution. The non-polar character of dioxygen makes it less soluble in water than in organic solvents (Sawyer, 1991). As a result, at least 4 atm (about 60 psi) is needed during oxygen delignification (McDonough, 1996).

2.1.2. Superoxide anion radical ($O_2^{\cdot-}$)

Two features, an anion and a radical, exist in superoxide anion ($O_2^{\cdot-}$), although the anion character dominates the radical character (Sawyer, 1991). Also, with regard to superoxide anion reactions, it is important to take into account the reactions of its conjugate acid (hydroperoxy radical, $HOO^{\cdot}$). The reactivity of superoxide anion and hydroperoxy radical is highly dependent on the pH and solvent system. For example, the $O_2^{\cdot-}/HOO^{\cdot}$ couple will be in equilibrium in aqueous media as shown in Figure 2.1. As a result, superoxide anion will be predominant at high pH, whereas hydroperoxy radical will be the primary species at low pH. Because of dual character, the chemistry superoxide anion depends on its basicity and nucleophilicity in the reacting system.

The weak basicity of superoxide anion is defined by the low pK_a value (4.8) of its conjugate acid (hydroperoxy radical). However, in reality, in both protic and aprotic media superoxide anion is a strong base, which can be explained by the step-wise reactions shown in Figure 2.2 (Sawyer and Gibian, 1979; Roberts and Sawyer, 1983; Afanas'ev, 1989). After the first proton abstraction, hydroperoxy anions form, and

$$O_2^{\cdot-} + HA \rightleftharpoons HOO^{\cdot} + A^{-} \quad \textbf{(HA = Proton donor)}$$

$$HOO^{\cdot} + O_2^{\cdot-} \longrightarrow HOO^{-} + O_2$$

Figure 2.2. Protonation reaction of superoxide anion (Afanas'ev, 1989).

therefore the basicity will increase (Frimer, 1982). When the proton donor is water (weak acid), superoxide anion acts as a base with a pK_a value equivalent to 23. This

is calculated using the equilibrium constant in the combination of the two equations in Figure 2.2 (Gibian *et al.*, 1979; Sawyer and Valentine, 1981). It can be argued that the basicity of superoxide anion would be greater in aprotic medium than in protic medium since superoxide anion is more basic without a solvation shell than when it is solvated. However, in the cases of the deprotonation of ascorbic acid and α-tocopherol by superoxide anion, the reactivity is unexpectedly higher in aqueous solution than in dimethylformamide (DMF) (aprotic) (Afanas'ev, *et al.*, 1986; 1987). This is because in the aprotic medium, the basicity of the proton donors is increased even more than that of superoxide anion. Thus, deprotonation by superoxide anion in aqueous solution is faster (Afanas'ev, 1989). The basicity of superoxide anion, therefore, should be judged not only by its pK_a value in aqueous solution, but also by the solvent system and acidity (or basicity) of the proton donor.

There not much evidences that superoxide anions have nucleophilic activity in protic media (Frimer, 1982; Sawyer, 1991). This is due to the strong solvation of superoxide anions by the protic solvents that provide hydrogen bonds and rapid disportionation (Sawyer, 1991). On the other hand, superoxide anion is a powerful nucleophile in aprotic media. It reacts with alkyl halides (Dietz *et al.*, 1970; Merritt and Sawyer, 1970; Merritt and Johnson, 1977), acyl halides (Johnson, 1976), esters (San Filippo *et al.*, 1976; Kornblum and Singaram, 1976; McDonald and Chowdhury, 1985), and acyl anhydrides (Forrester and Purushotham, 1984) to form peroxy radical intermediates ($ROO^{\cdot}$) through nucleophilic substitution reactions (Figure 2.3). For acyl halides, the most probable nucleophilic reaction mechanism of superoxide anion is an addition reaction to the carbonyl carbons to form radical anion intermediates

(Afanas'ev, 1989). Esters can also react with superoxide anion *via* a nucleophilic addition mechanism as well as the nucleophilic substitution mechanism mentioned above (McDonald and Chowdhury, 1985). It should be pointed out that, in the nucleophilic substitution of superoxide anion to a carbonyl carbon, a leaving group must be attached to the carbonyl carbon so that the tetrahedral intermediate can collapsed to product (Sawyer *et al.*, 1983).

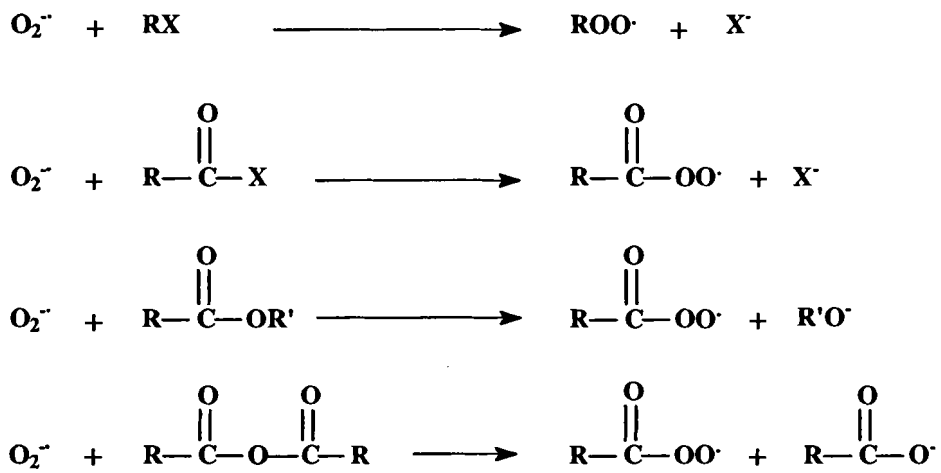

Figure 2.3. Formation of peroxy radical intermediates by nucleophilic substitution reactions between an superoxide anion and an alkyl halide, an acyl halide, an ester, or an anhydride in aprotic media (Afanas'ev, 1989).

Superoxide anions can also add to positively charged carbon-carbon double bonds (Kobayashi, *et al.*, 1979) and carbon-nitrogen double bonds (Frimer, 1982; Shibata *et al.*, 1986) (Figure 2.4).

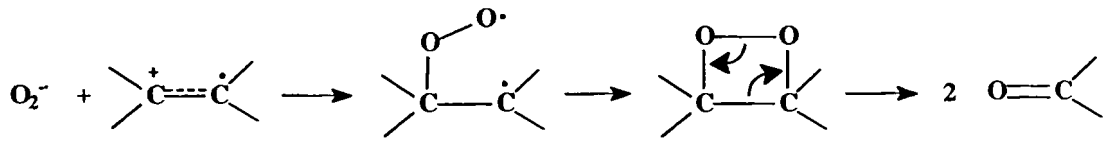

Figure 2.4. Addition reaction of a superoxide anion to a radical cation form of double which is followed by bond cleavage (Frimer, 1982).

Another addition reaction of superoxide anion is to metal complexes ($M^{m+}L_n$) (Figure 2.5) (Afanas'ev, 1989).

$$O_2^- + M^{m+}L_n \longrightarrow M^{m+}L_n(O_2^-) \rightleftharpoons M^{(m-1)+}L_nO_2$$

Figure 2.5. Addition of a superoxide anion to a metal complex (Afanas'ev, 1989).

As a radical reaction of superoxide anion, it has been proposed that it could abstract allylic hydrogen atom ($H^{\cdot}$) (Frimer, 1982). However, there is no convincing evidence of such a reaction. Afanas'ev (1989) explained that superoxide anion has a low possibility of the hydrogen abstraction due to the weakness of the bond ($H\text{-}O_2^-$), which will form by the abstraction, and the competition between proton and hydrogen atom abstraction by superoxide anion. Nevertheless, numerous hydrogen atom abstractions by superoxide anion have been published for catechols (Miller, 1970; Lee-Ruff *et al.*, 1976; Moro-oka and Foote, 1976; Nanni *et al.*, 1980), other hydroquinones (Rao and Hayon, 1973; Afanas'ev and Polozova, 1976), and ascorbic acid (Nishikimi, 1975; Nanni, Jr. *et al.*, 1980). The pathways of the hydrogen abstraction reaction in these compounds by superoxide anion have been debated.

Afanas'ev and Polozova (1976) assumed that *ortho-* and *para*-hydroquinone reacts with superoxide anion through one-step reaction (concerted reaction) to form semi-quinones in DMF. Conversely, Lee-Ruff and co-workers (1976) insisted that the concerted abstraction of a proton and a hydrogen atom is not likely since there is a large inter-hydrogen distance between the two hydrogen atoms in *para*-hydroquinone. They suggested that a hydrogen atom and proton are abstracted in a two-step reaction mechanism, but offered no specific sequences. Later, Sawyer (1991) proposed that the proton abstraction occurs first to form a hydroperoxy radical (HOO·) and a substrate anion, and then the hydrogen atom abstraction is performed as shown in Figure 2.6 because the hydrogen abstraction reactivity of hydroperoxy radical is much greater than that of superoxide anion. If hydroperoxyl radicals form first, they are the more reactive hydrogen abstractors.

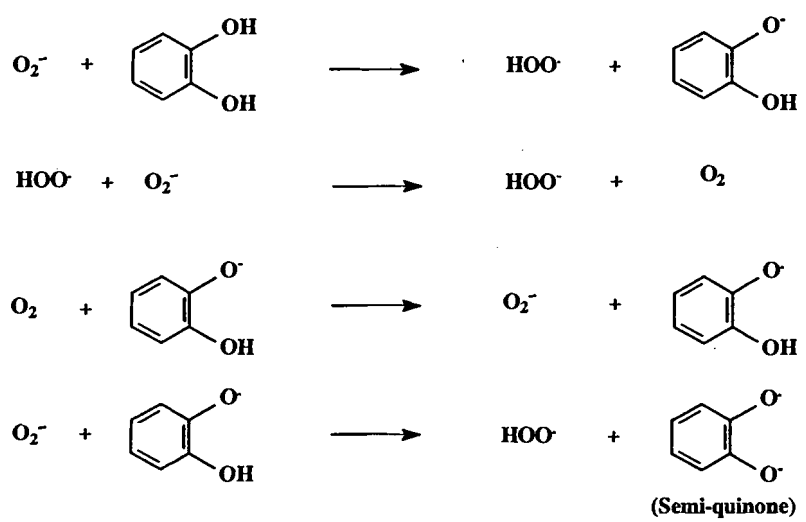

Figure 2.6. Proposed mechanism of the formation semi-quinone by the reaction between superoxide anion and catechol (Modified from Frimer, 1982).

Superoxide anion also acts as a moderate one-electron reductant. Quinones have been used in studies of one-electron transfer by superoxide anion in aqueous solution (Willson, 1971) and aprotic media (Afanas'ev *et al.,* 1973; Poupko and Rosenthal, 1973). In both protic and aprotic media, one-electron transfer occurred from superoxide anion to quinone (Q) to produce semi-quinone ($Q^{\cdot-}$) (Afanas'ev, 1989) although the reactivity may be lower in aqueous solutions due to solvation (Frimer, 1982). Many other aromatic organic compounds can undergo one-electron transfer reaction from superoxide anion, such as nitro compounds including dinitrobenzenes (Poupko and Rosenthal, 1973; Frimer and Rosenthal, 1976) and diphenylcyclopropenone (Rosenthal and Frimer, 1975; Necker and Hauck, 1983).

It is widely accepted, also, that superoxide anion can transfer one electron to many inorganic substances like metals (Fe^{3+}, Cu^{2+}, Mn^{3+}, Cr^{3+}, etc.) and metal complexes ($M^{n+}L_m$). The products are dioxygen and reduced forms of the metal or metal complexes. In addition, superoxide anion can transfer one electron to halogens in benzene and dimethylsulfoxide (DMSO) (Kim *et al.,* 1979), as well as to bromine and iodine (Sutton and Downes, 1972; Schwarz and Bielski, 1980) and hypochlorous acid (HOCl) (Long and Bielski, 1980) in aqueous solution.

Although radical coupling reactions of superoxide anion with radical cations (Nanni, Jr. and Sawyer, 1980) and metal complexes (Tsang and Sawyer, 1990) have seen proposed at certain conditions, these are not common reactions. They may result from suppression of the other favored reactions (Sawyer and Valentine, 1981).

2.1.3. Hydrogen peroxide (H_2O_2)

Hydrogen peroxide has both electrophilic and nucleophilic properties as well as being a weak oxidant. The electrophilic character results from the fact that the bond between the two oxygen atoms can be easily polarized as shown below (Jones, 1999):

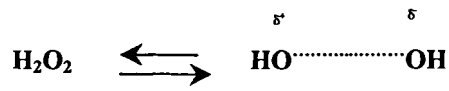

Although the nucleophilic character of hydrogen peroxide is 10^4 times higher than that of water, hydrogen peroxide still has limited ability to react with organic compounds such as olefins and aromatic hydrocarbons (Jones, 1999).

The chemistry involving hydrogen peroxide is mostly related to its activated derivatives. It can be directly activated and turned into much more reactive species such as hydroperoxy anion (HOO^-) in base, hydroxy cation ($O_2H_3^+$) in acid, and hydroxyl radical ($HO^\cdot$) by treatment with ultraviolet light or transition metals (M^+) (Figure 2.7) (Jones, 1999).

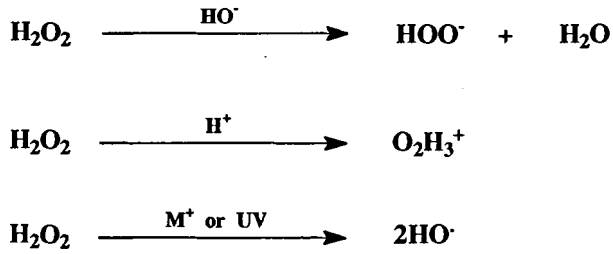

Figure 2.7. Direct activation modes of hydrogen peroxide.

In acidic conditions, hydrogen peroxide can produce peroxy acids from carboxylic acids or their derivatives (March, 1977) as shown in Figure 2.8.

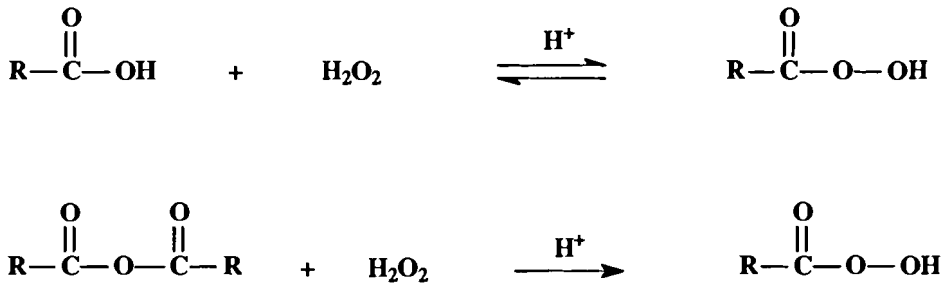

Figure 2.8. Peroxy acid formation in the presence of hydrogen peroxide under acidic conditions (March, 1977).

Hydrogen peroxide reacts with transition metals (M^{n+}) under acidic conditions to produce hydroxyl radicals through Fenton-type reactions (Cohen, 1985; Sawyer, 1991) according to the following reaction:

$$H_2O_2 + M^{n+} \longrightarrow HO^{\cdot} + HO^{\cdot} + M^{(n+1)+}$$

Hydrogen peroxide is equilibrium with hydroperoxy anion (HOO^-) in alkaline conditions. Hydroperoxy anion is a strong nucleophile, and can react with α–β unsaturated ketones, including quinones and aldehydes, to form epoxides (Jones, 1999; Schumb *et al.*, 1955) (Figure 2.9). Also, in basic conditions, hydrogen peroxide oxidizes aromatic aldehydes to carboxylic acids at pH 10.5 or higher (Jones, 1999) or leads to rearrangement reactions (Dakin reaction) with aromatic aldehydes that have electron-donating group(s) attached at the *ortho* and/or *para* positions of the ring (Figure 2.10) (March, 1977).

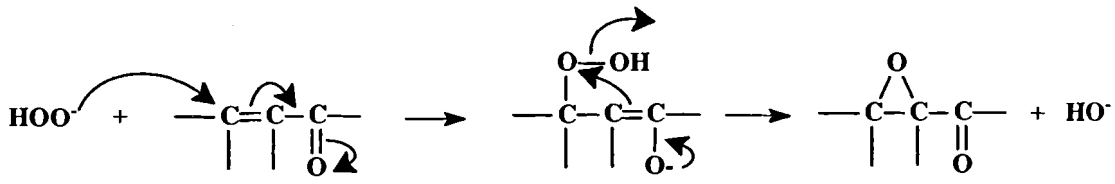

Figure 2.9. Epoxidation of α–β unsaturated ketones or aldehydes by hydrogen peroxide in alkaline solution (March, 1977).

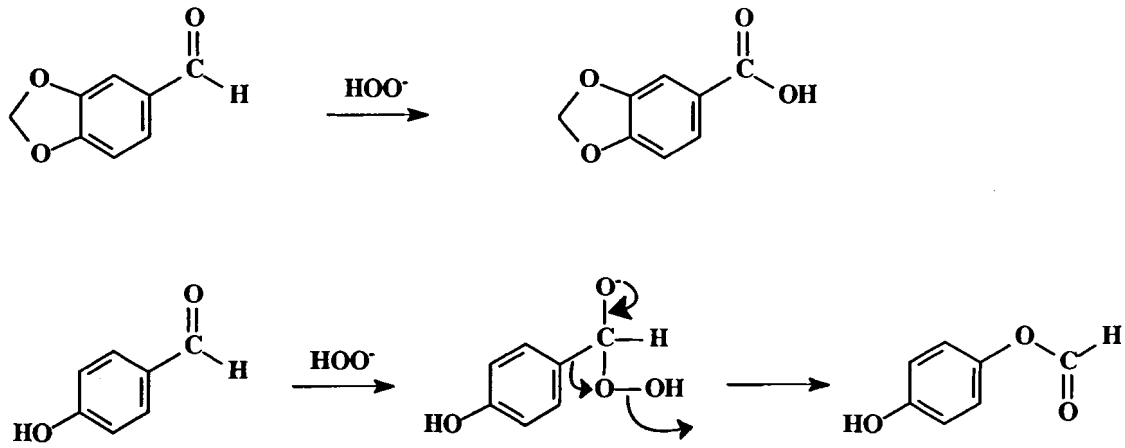

Figure 2.10. Oxidation of aromatic aldehyde (top) (Jones, 1999) and Dakin reaction of aromatic aldehyde (bottom) (March, 1977) by hydrogen peroxide in alkaline conditions.

2.1.4. Hydroxyl radical (HO·)

Hydroxyl radical is known as the most reactive member of the oxygen radical family (Sawyer, 1991). It can react with most organic compounds *via* hydrogen atom abstraction, electrophilic addition, electron abstraction, and radical coupling reactions

(Atkinson, 1985; Legrini *et al.,* 1993; Barnes and Sugden, 1986). The reactions involving hydroxyl radicals are similar in both gas and liquid phase, although solvation may cause some differences in solution (Mayo, 1967; March, 1977). Oxy radical anions ($O^{\cdot-}$) are the conjugate bases of hydroxyl radicals ($pK_a = 11.9$). In strongly basic aqueous solutions, oxy radical anions are easily produced by the hydrogen atom abstraction by hydroxyl radicals from hydroxide anions (Buxton *et al.,* 1988; Lee *et al.,* 1992). These oxy radical anions have high redox potential (1.73 V) although it is lower than that of hydroxyl radicals (2.73 V). Thus, the reactions of oxy radical anions should be kept in mind, especially in strongly alkaline conditions.

Hydrogen atom abstraction by hydroxyl radical can occur in alkanes, halo-alkanes, aldehydes, ketones, esters, ethers, alcohols, carboxylic acids, amines, thiols, and hydroperoxides (Atkinson, 1985; Barnes and Sugden, 1986). The hydrogen abstraction reactivity of hydroxyl radicals depends on the strength of R-H bond in the substrates which can be defined by the difference between the bond formation energy of the product (HO-H) and the bond dissociation energy of the substrate (R-H) (Atkinson, 1985; Sawyer, 1991). Of course, the bond dissociation energy of R-H depends on the degree of substitution and identity of R, class(es) of the substituent(s), and the ring strain , if it is a cyclic compound. For example, C-H bond dissociation energies are 438, 401, and 390 kJ/mol in methane (1°), C-2 (2°) of propane, and C-2 (3°) of 2-methylpropane, respectively (McMurry, 1996). As a result, hydrogen attached to tertiary carbon will have higher reactivity than those of others. In fact, Atkinson (1985) reported that tertiary hexyl radical is the most abundant product in

the reaction between hydroxyl radical and 2-methylpentane in gas phase at 25 °C (Figure 2.11).

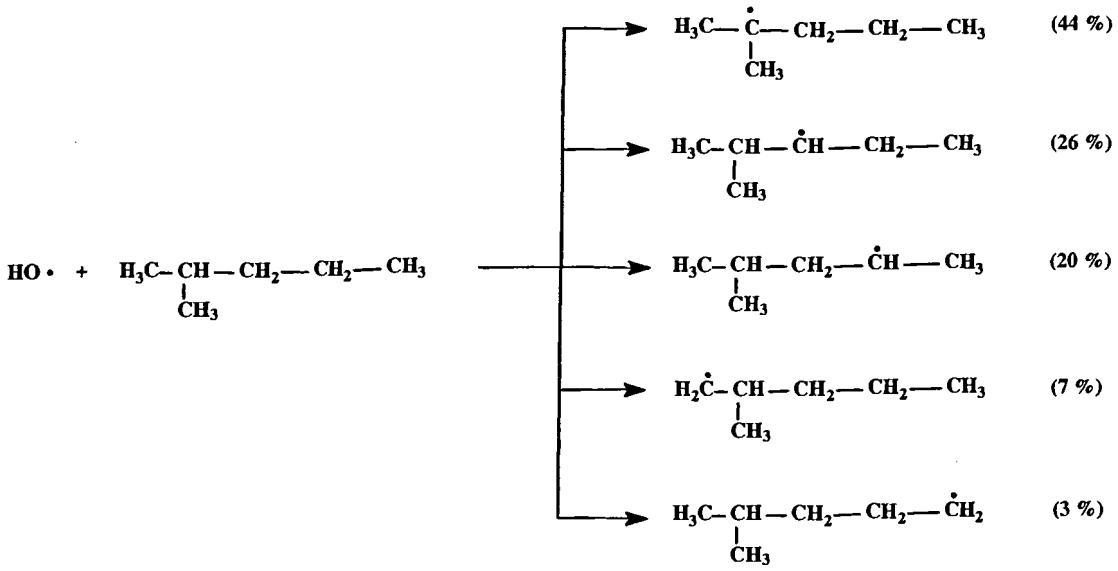

Figure 2.11. Proportions of hexyl radicals produced in the reaction between hydroxyl radical and 2-methylpentane (Atkinson, 1985).

In aliphatic aldehydes, hydrogen atom abstraction by hydroxyl radical occurs at the hydrogen attached to the carbonyl group (Singleton *et al.*, 1977; Kerr and Sheppard, 1981; McMillen and Golden, 1982). In the case of formaldehyde, the two reaction pathways in Figure 2.12 can occur with approximately equal probability in the gas phase (Atkinson, 1985). Addition of hydroxyl radicals to aldehydes is

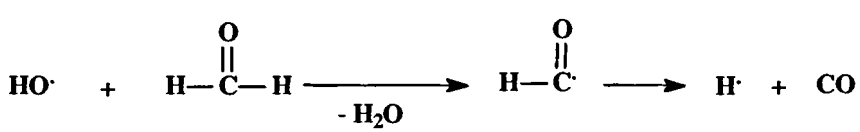

Figure 2.12. Pathway in the reaction of hydroxyl radical and formaldehyde (Atkinson, 1985).

negligible (Temps and Wagner, 1984). For α–β unsaturated aldehydes reacting with hydroxyl radicals, two different pathways have been reported; hydrogen abstraction from a –CHO group is significant in the gas phase (Atkinson, 1985), whereas hydroxyl addition to β-position is the usual reaction in aqueous solution (Barnes and Sugden, 1986).

Ketones also react with hydroxyl radicals by a hydrogen abstraction pathway. Carbonyl groups in ketones decrease the reactivity of the α-H but increase β-H reactivity (Atkinson, 1985) because of their electronegativity. α-Dicarbonyls react with hydroxyl radicals in analogous mode to those for the simple aldehydes and ketones (Atkinson, 1985).

In alcohols, hydrogen abstraction can occur at both C-H and O-H. However, it will be dominant at C-H since the bond dissociation energy of C-H is lower than that of O-H (Meier *et al.,* 1984; 1985). Reaction examples of primary, secondary, and tertiary alcohol are shown in Figure 2.13. Hydroxyl radicals abstract hydrogen from

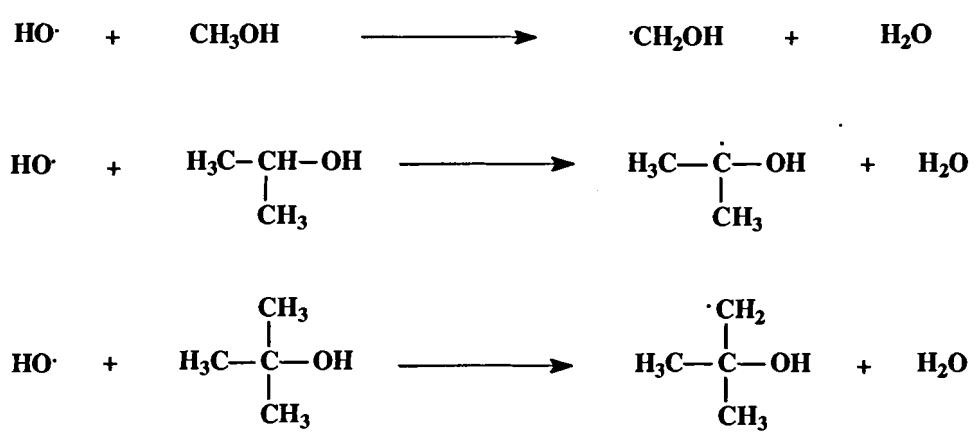

Figure 2.13. Hydrogen abstraction from methanol, 2-propanol (isopropanol), 2-methyl-2-propanol (*tert*-butanol) by hydroxyl radicals.

the C-H bond in methanol to form its radical, which leads to formaldehyde by further oxidation (Meier *et al.,* 1984;1985). In 2-propanol, the hydrogen at the α-position is the most probable target in the abstraction pathway (Luo *et al.,* 1997; Hislop and Bolton, 1999), and the final product is acetone by elimination of the hydrogen atom. In the same molecule, the hydrogens attached to the β-position will be reactive when there is no hydrogen bonding by water molecules (Luo *et al.,* 1997). 2-Methyl-2-propanol (*tert*-butanol) has only one type of hydrogen atoms on the three methyl groups which will give only one reaction pathway (Chitose *et al.,* 1999; Tauber *et al.,* 1999). The final product will be acetone by elimination of a methyl radical ($^{\cdot}CH_3$) and enolization.

Under Fenton reaction conditions using H_2O_2-Fe^{2+}-Cu^{2+} to produce hydroxyl radicals, 2-methyl-1,2-propandiol was the major oxidation product in the reaction with 2-methyl-2-propanol (Walling and Kato, 1971). Also, 1,2-diols react with hydroxyl radicals by a dehydration reaction in acidic conditions (Figure 2.14) (Barnes and Sugden, 1986).

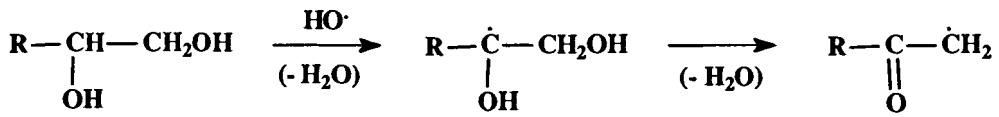

Figure 2.14. Dehydration reaction of 1,2-diols by hydroxyl radical (Barnes and Sugden, 1986).

In amines, hydrogens at both C-H and N-H can be abstraction targets (Atkinson *et al.,* 1977; 1978). In primary amines such as CH_3NH_2 and $C_2H_5NH_2$, hydrogen

abstractions by hydroxyl radicals mostly occur at C-H, whereas in secondary amines the hydrogen abstraction from N-H will be competitive with that from C-H. (Atkinson *et al.,* 1978).

Ethers react with hydroxyl radicals by hydrogen abstraction reactions at the C-H adjacent to the ether group (Barnes and Sugden, 1986) because the oxygen atom makes the bond dissociation energy of C-H significantly lower than that of C-H in alkanes (Lenhardt *et al.,* 1980). This phenomenon can be explained by the formation of the stabilized radical product (Figure 2.15). In the case of esters, hydrogen abstraction occurs in the –OR entity for similar reasons.

Figure 2.15. Resonance stabilization of an ether radical (McMillen and Golden, 1982).

Carboxylic acids also undergo hydrogen abstraction by hydroxyl radicals (Hoare and Peacock, 1966; Barnes and Sugden, 1986). Usually, hydrogen abstraction occurs at the furthest position from the –COOH group but α-hydroxy acids tend to react with hydroxyl radicals by α-hydrogen abstraction (Dixon *et al,* 1964; Barnes and Sugden, 1986). Similarily to the reactions of hydroxyl radicals but more slowly, oxy radical anions can abstract hydrogen atoms from alkanes, alkenes, alcohols, ethers, esters, and epoxides (Lee *et al.,* 1992).

Where the bond energy of C-H is too high to permit abstraction of hydrogen atoms, hydroxyl radical proceeds through electrophilic addition reactions. Alkenes,

alkynes, thiols, and aromatic compounds fall into the groups that can undergo hydroxyl radical addition. However, some alkenes undergo limited hydrogen abstraction (Hoyermann and Sievert, 1979; 1983). Oxy radical anions and hydroxyl radicals have similar chemistry but the formers prefer to act like nucleophiles, and do not add to double bonds (Buxton *et al.*, 1988). The reactions of unsaturated 1,4-dicarbonyls proceed by hydroxyl radical addition to the carbon-carbon double bonds (Atkinson, 1985). Hydroxyl radical prefers to attack the less substituted carbon atom (Figure 2.16) (Barnes and Sugden, 1986).

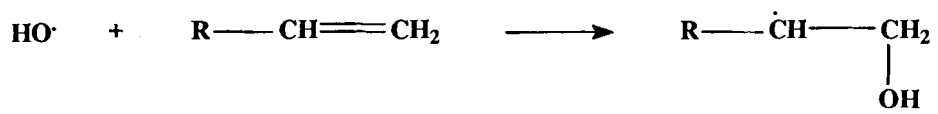

Figure 2.16. Addition of a hydroxyl radical to a carbon-carbon double bond.

Haloalkenes generally act similarly to aliphatic alkenes in the reaction with hydroxyl radicals. However, they also undergo elimination of halogen atoms either by direct addition of hydroxyl radical to the α-position in the double bond or less commonly by 1,2-migration of the hydroxyl group after the addition to the β-position (Perry *et al.*, 1977; Whytock *et al.*, 1976).

For thiols, hydroxyl radical addition to the sulfur atom is the primary reaction pathway (Hatakeyama and Akimoto, 1983; Barnes and Sugden, 1986).

In the reactions of phenol under Ti^{3+}-H_2O_2 treatment, which is a hydroxyl radical producing method, hydroxyl addition occurrs in both acidic and basic conditions (Jefcoate *et al.*, 1968).

Aromatic compounds can react with hydroxyl radical by addition to the aromatic ring (Sawyer, 1991; Legrini *et al.,* 1993; Schuchmann *et al.,* 1998) (Figure 2.17).

Figure 2.17. Electrophilic hydroxyl radical addition to benzene (Sawyer, 1991).

This is because the conjugated π-system provides a relatively stable OH-adduct radical by delocalization (Sawyer, 1991). Another role of hydroxyl radicals is electron abstraction from aromatic compounds (Tripathi, 1998; Peller *et al.,* 2001), metal ions, and other electron rich components (Cohen, 1985; Barnes and Sudgen, 1986). For aromatic compounds, electron transfer reaction competes with a hydroxyl radical addition reaction in experiments with pulse radiolysis of N_2O-saturated water at pH 7 (Tripathi, 1998). In this reaction, it was found using time-resolved Raman spectroscopy that there are two possible electron transfer pathways (Tripathi, 1998) (Figure 2.18). One is the direct electron transfer (ET) and the other is the adduct-

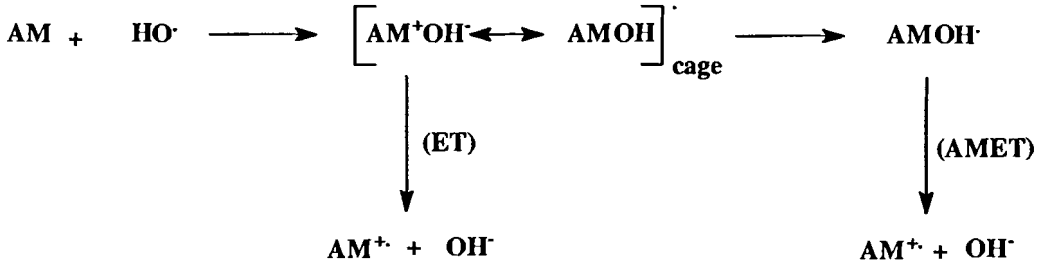

Figure 2.18. The two pathways of the electron transfer reaction between hydroxyl radical and aromatic molecules (AM) (Modified from Tripathi (1998)).

mediated electron transfer (AMET) pathway. The mechanism described in Figure 2.18 depends on ionization potential (IP) of the molecules, so that the neutral molecules having IP < 7eV proceed *via* electron transfer, whereas the molecules having IP > 8eV will undergo hydroxyl radical addition reaction (Tripathi, 1998).

These investigations found that electron transfer ranged from 6 % in *p*-dimethoxybenzene to 30 % in *p*-ainisidine and 85 % in *p*-phenylenediamine. The proposed pathways are shown in Figure 2.19. For metals having coordinated water molecules ($[M(H_2O)_x]^{n+}$) and electron rich compounds such as halides (X^-), the electron transfer reactions occur through an AMET process (Buxton *et al.*, 1988).

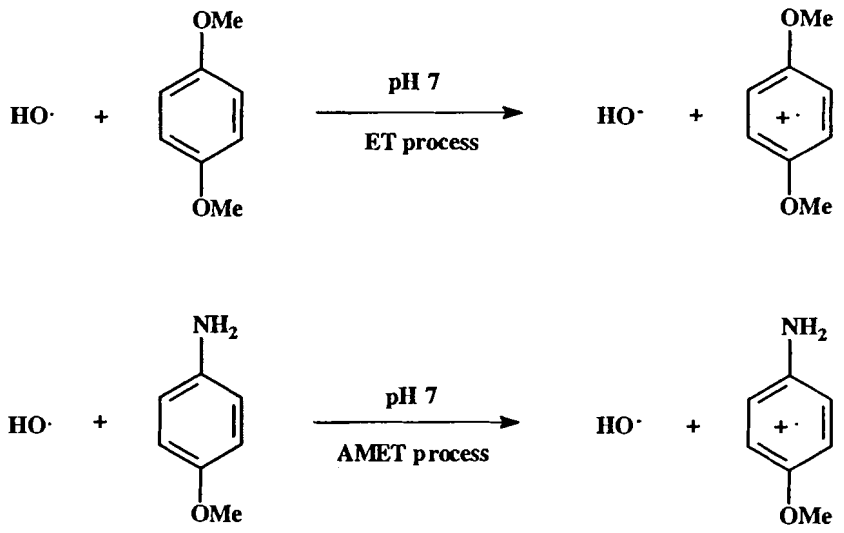

Figure 2.19. Electron transfer pathways in *p*-dimethoxybenzene and *p*-anisidine during pulse radiolysis of N_2O-saturated water (Tripathi, 1998).

2.2. Chemistry of oxygen delignification

2.2.1. Lignin reactions

Lignin reactions are very complex since lignin is heterogeneous and is composed of various chemical structures as mentioned previously. Moreover, the co-existence of the numerous oxygen species increases the complexity of the lignin reactions. Thus, mechanistic studies on lignin reactions are often performed with relatively simple model lignins.

From previous studies, it was proposed that phenolic groups have an extremely important role in initiating the radical reactions during delignification (Gierer, 1987, Gierer *et al.*, 2001, Reitberger *et al.*, 2001). Phenolic groups exist in equilibrium with phenoxy anions in oxygen delignification. It was suggested that hydroxyl radical is

produced by thermal homolytic cleavage of the hydroperoxide group originating from phenoxy anion in the presence of molecular oxygen (Gierer *et al.,* 2001). Also the phenoxy anion can react with molecular oxygen to produce phenoxy radical and superoxide anion radical (Reitberger *et al.,* 2001). The superoxide anion can be converted to hydroperoxy radical, or to hydrogen peroxide and its conjugate base (hydroperoxy anion) as shown in Figure 2.1. This hydrogen peroxide in turn can generate hydroxyl radical and water. These oxygen species and the phenoxy radical can react with any other molecules in the delignification system.

Typical lignin reactions with oxygen species are hydroxylation, hydroxyl substitution (dealkoxylation), side chain oxidation, side chain cleavage, cleavage of the ether linkage, aromatic ring cleavage, and oxidative coupling (Gierer, 1993; 1997). Hydroxylation and hydroxyl substitution occur in the reactions between hydroxyl radicals and electron-rich moieties in the lignin, which are the aromatic rings (Figure 2.20) and olefinic groups (Figure 2.21) (Gierer, 1997). First, hydroxyl

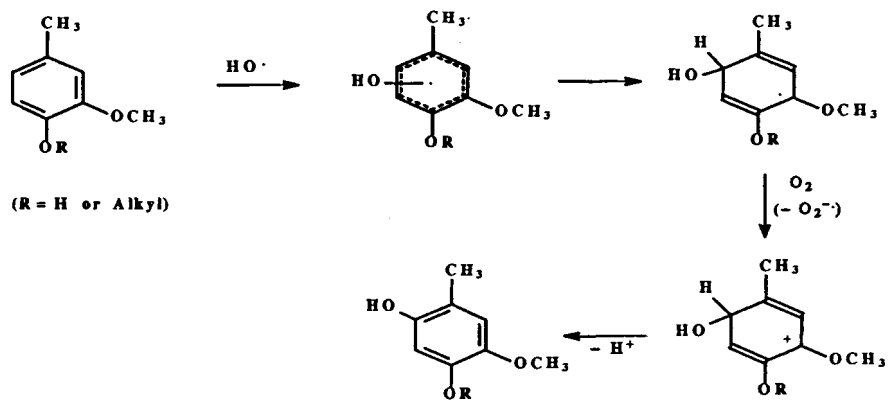

Figure 2.20. Hydroxylation reaction of aromatic compound with hydroxyl radical (Gierer, 1997).

radical is added to the conjugated aromatic ring to form a radical adducts. The radical adducts reacts with molecular oxygen, and then the hydroxylated product is formed after elimination of a superoxide anion radical and a proton.

In lignin some of the side chains have a double bond conjugated with the aromatic ring. Hydroxyl can be added to the side chain in this case. The compound hydroxylated in the side chain in Figure 2.21 can react further to give C_α-C_β side chain cleavage.

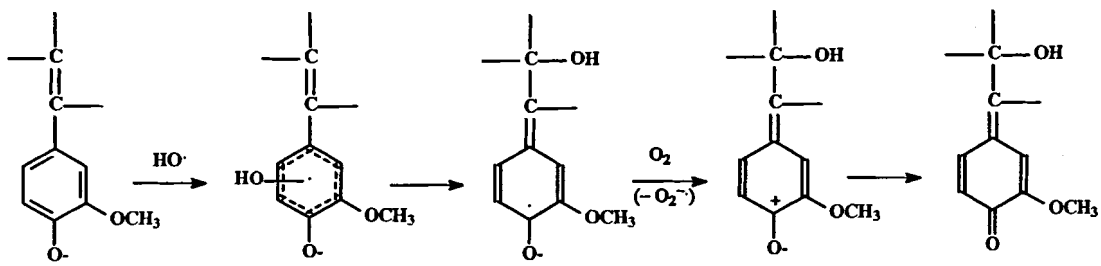

Figure 2.21. Hydroxylation of conjugated double bond with hydroxyl radical (Gierer, 1997).

Hydroxyl radicals also can react with the aromatic rings to replace substitutents such as methoxyl (Figure 2.22). Tatsumi and Terashima (1984; 1985b) proposed, in

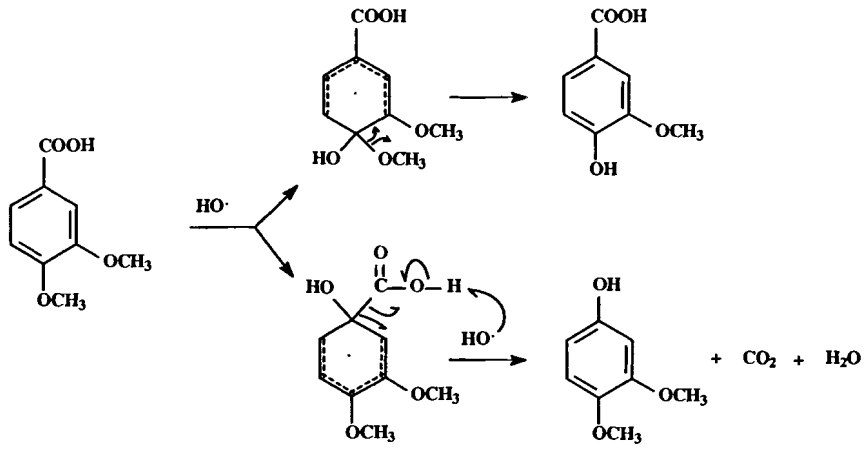

Figure 2.22. Hydroxyl substitution (dealkoxylation) reactions of aromatic compound (Tatsumi and Terashima, 1984 (Top); 1985b (Bottom)).

the studies on the oxidative degradation of lignin reacted with hydroxyl radicals produced from UV (254 nm) irradiation on $H_2{}^{18}O_2$, that hydroxyl radicals can attack the aromatic ring. Subsequent loss of methoxyl, or decarboxylation, gives net substitution.

Side chain cleavage reactions (C_α-C_β cleavage) can occur in different ways, induced by hydroxyl radical, superoxide anion, and hydroperoxy anion. It was suggested that abstraction of one electron from the ring followed by addition of superoxide anion to the side chain (Figure 2.23).

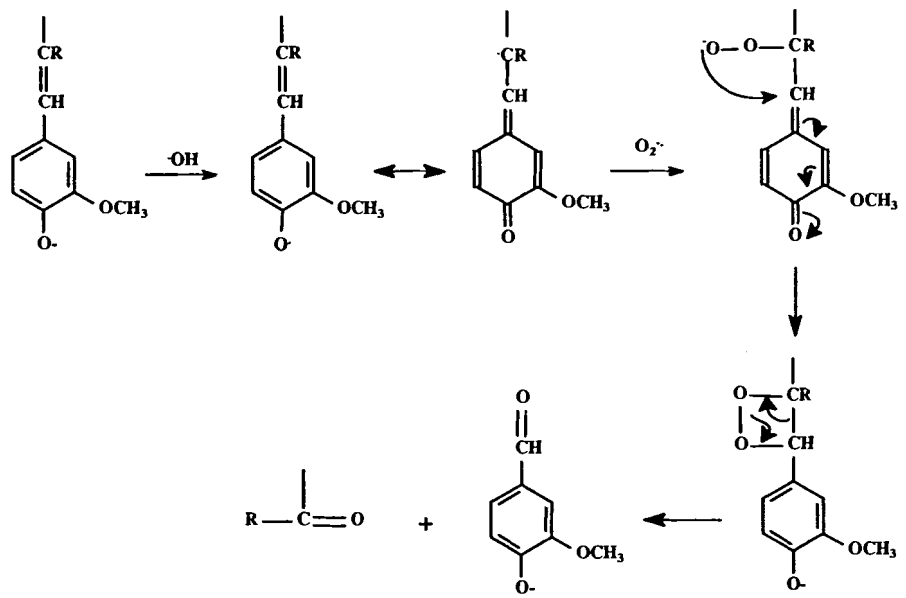

Figure 2.23. Side chain cleavage by superoxide anion (Modified from Gierer, 1997).

It has been suggested that side chain cleavage also can occur by nucleophilic addition of hydroperoxy anion to the carbonyl groups in the side chain followed by Dakin reaction (Figure 2.24).

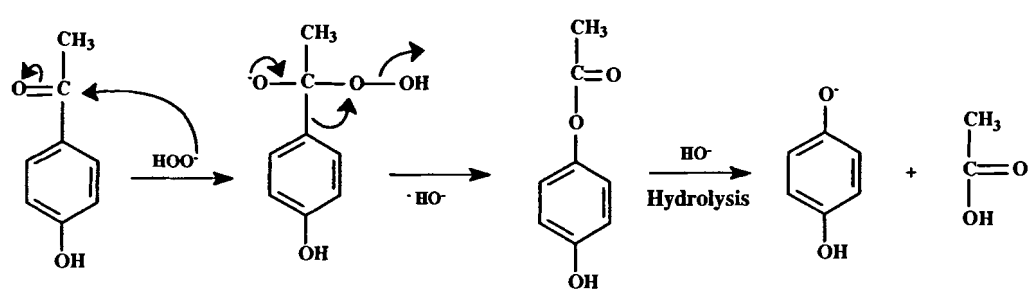

Figure 2.24. Side chain cleavage by hydroperoxy anion (March, 1992).

The cleavage of an ether linkage is another way of the separation of the aromatic moieties in lignin by hydroxyl radical reactions (Figure 2.25).

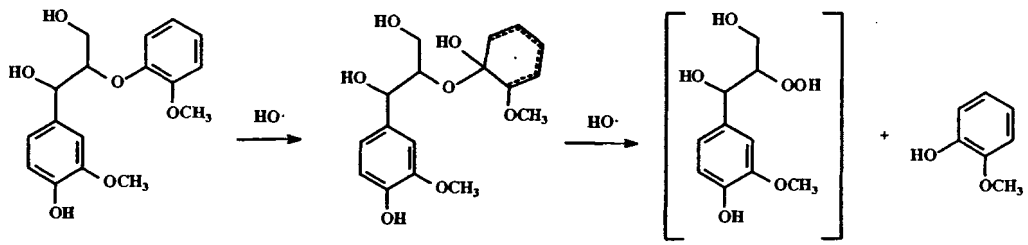

Figure 2.25. Ether linkage cleavage by hydroxyl radicals (Tatsumi and Terashima, 1985a).

Aromatic ring cleavage occurs through the formation of phenoxy radical (Gierer, 1993; 1997; Hausman, 1999). It was suggested, for the formation of phenoxy radical in oxygen delignification, that hydroxide anion leaves from the radical adduct (Gierer, 1997) (Figure 2.26).

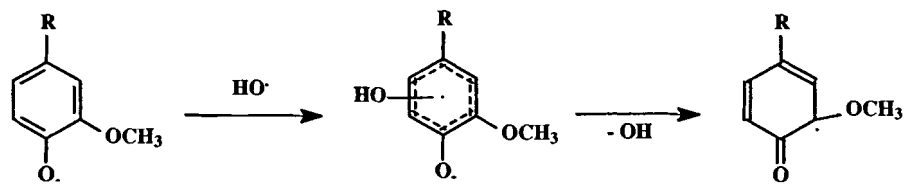

Figure 2.26. Previously suggested mechanisms of the formation of phenoxy radical (Gierer,1997).

Hausman (1999) reported that phenoxy radical forms *via* hydrogen atom abstraction or demethylation from the aromatic compounds by hydroxyl radical (Figure 2.27) and those reactions are energetically favorable.

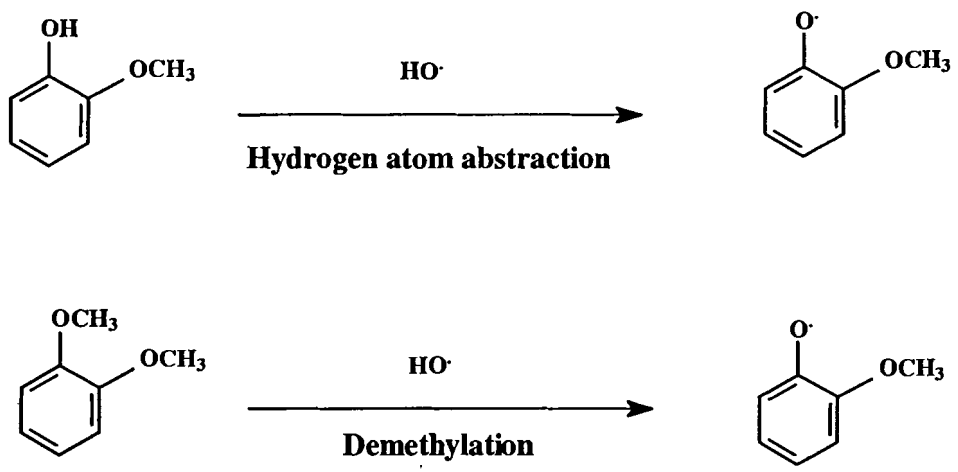

Figure 2.27. Energetically favorable mechanisms of the formation of phenoxy radical (Hausman, 1999).

The phenoxy radicals can react with superoxide anion to form dioxetane as a precursor to the opened ring (Gierer, 1997; Hausman, 1999) (Figure 2.28). The

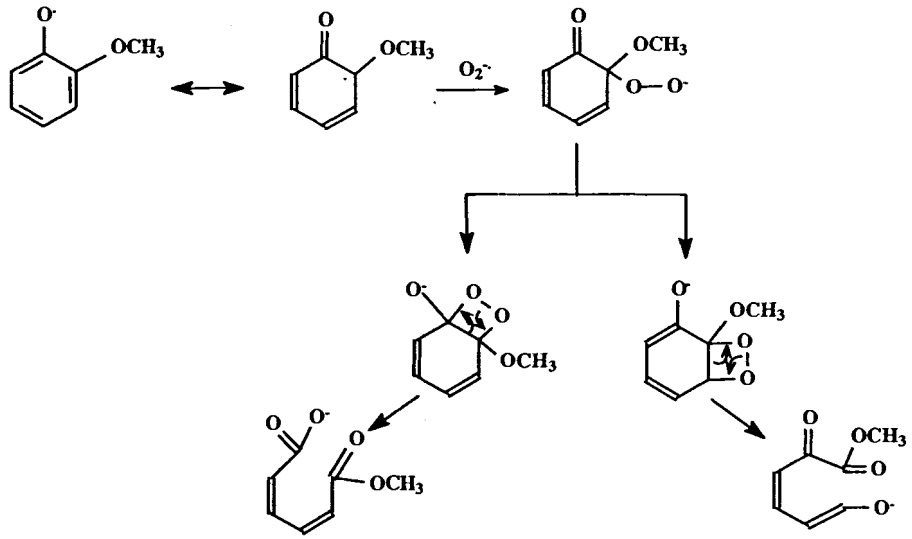

Figure 2.28. Ring cleavage by addition of superoxide anion to the phenoxy radical (modified from Gierer, 1997; Hausman, 1999).

opened ring is oxidized further to smaller organic acids by oxygen species. It was reported that organic acids were detected at significantly greater amounts at higher pH (12) than at lower pH (9.5) (Hausman, 1999). This supports the suggestion that superoxide anion is the major oxygen species that can open the aromatic ring at pH 12. As further evidence of the existence of abundant superoxide anion at higher pH, the pH of the reaction solution after the reaction increased due to the reactions shown in Figure 2.29 (Hausman, 1999). Because of the dominant superoxide anion, the

$$O_2^{\cdot-} + H_2O \longrightarrow HO^{\cdot} + HOO^-$$

$$O_2^{\cdot-} + HO^{\cdot} \longrightarrow O_2 + HO^-$$

$$2\,O_2^{\cdot-} + H_2O \longrightarrow O_2 + HO^- + HOO^-$$

Figure 2.29. Generation of anions by superoxide anion radicals (Hausman, 1999).

concentrations of hydroxide and hydroperoxide anion increased, and these anions raise the pH of the reaction solution.

Oxidative coupling of lignin was reported in oxygen delignification. Two phenoxy radicals can couple to form a condensed structure (Figure 2.30) (Gierer, 1994).

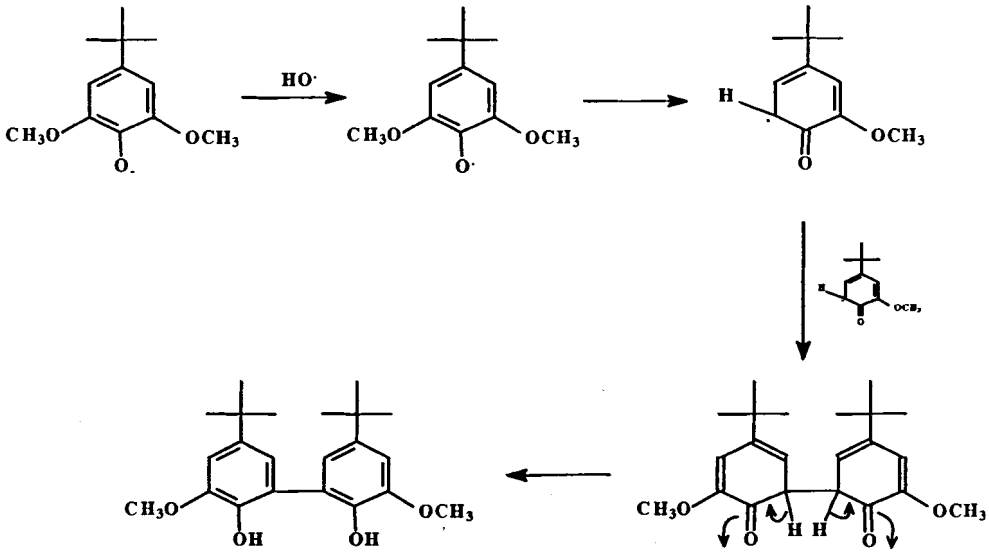

Figure 2.30. Oxidative coupling reaction pathway of lignin (Gierer, 1994).

2.2.2. Carbohydrate reactions

It is known that there are two degradation pathways of carbohydrates in oxygen delignification. One is the "peeling" reaction. In the "peeling" reaction, the "reducing" carbonyl end group of the cellulose chain is cleaved as a result of the alkaline hydrolysis of glycosidic bonds one unit by one unit (Sjöström, 1993). The

"peeling" reaction stops when the reducing end group is converted to a carboxylic group as a competing reaction.

The other degradation pathway is random chain cleavage caused by the reaction with oxygen species (McDonough, 1996). Both pathways can occur in oxygen delignification. However, the random chain cleavage will be significant during oxygen delignification since not many "reducing" end groups remain after the Kraft pulping process (McDonough, 1996). The most probable oxygen species for the random chain cleavage is hydroxyl radical because it has the highest redox potential among them. To initiate the random chain cleavage, it has long been suggested that a hydroxyl radical abstracts a hydrogen atom at the C-2 position in the glucose unit in the cellulose chain, followed by reaction with molecular oxygen (Figure 2.31) (Gierer, 1997).

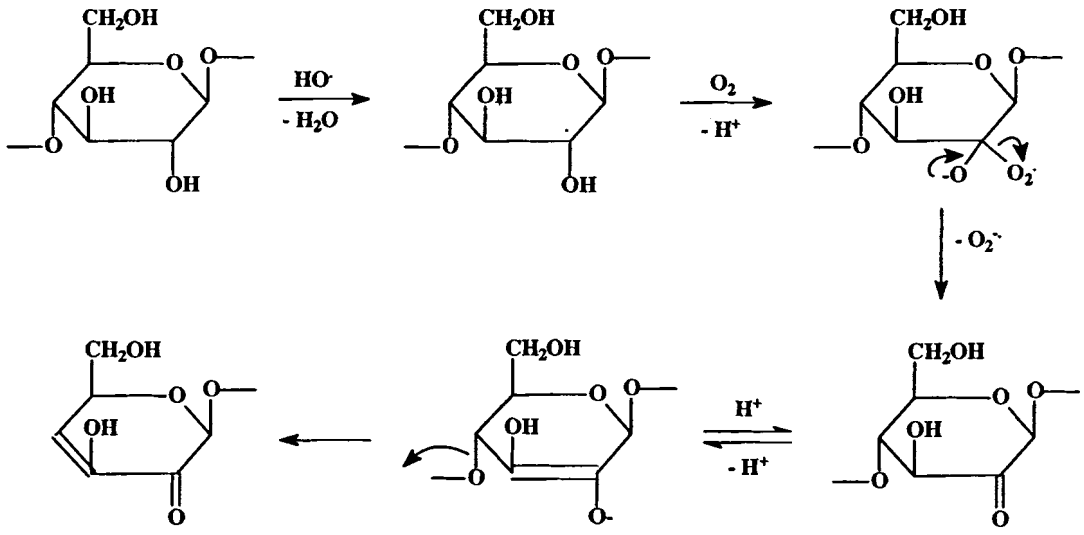

Figure 2.31. A previously suggested oxidative mechanism of carbohydrate during oxygen delignification (Gierer, 1997).

When superoxide anion leaves from the C-2 position, a carbonyl forms as an enolate after loss of a proton at the C-3 position. This enolate develops to a conjugated carbonyl as a result of the elimination of the ether linkage from the C-4 position. The eliminated part of the cellulose chain remains as a "reducing" end group. Some carbonyl compounds were observed in the studies of carbohydrates treated with γ-irradiation in aqueous solution in the presence of oxygen (Schumann and Sonntag, 1977). However, it is reported that cellulose degrades directly by γ-irradiation (Lind *et al.*, 1997). Recently, the heat of reaction (ΔH) for the first step in the mechanism in Figure 2.31 was calculated using the Spartan V5.0 *ab initio* program and 3-21G(*) basis set, and the result was 6.82 kcal/mol (Guay, 1999). This indicates that the reaction is endothermic and is unfavorable. Also, in a previous study in our laboratory, Guay and co-workers (2000; 2001) proposed a new mechanism of random cleavage in the study of carbohydrate reactions with photochemically generated hydroxyl radical. In this mechanism, hydroxyl radical attacks the C-1 position in the glucosidic unit rather than the C-2 to eliminate the –OR group. The heat of reaction (ΔH) of these steps are negative numbers which indicate that these reactions are favorable, as shown in Figure 2.32 (Guay, 1999).

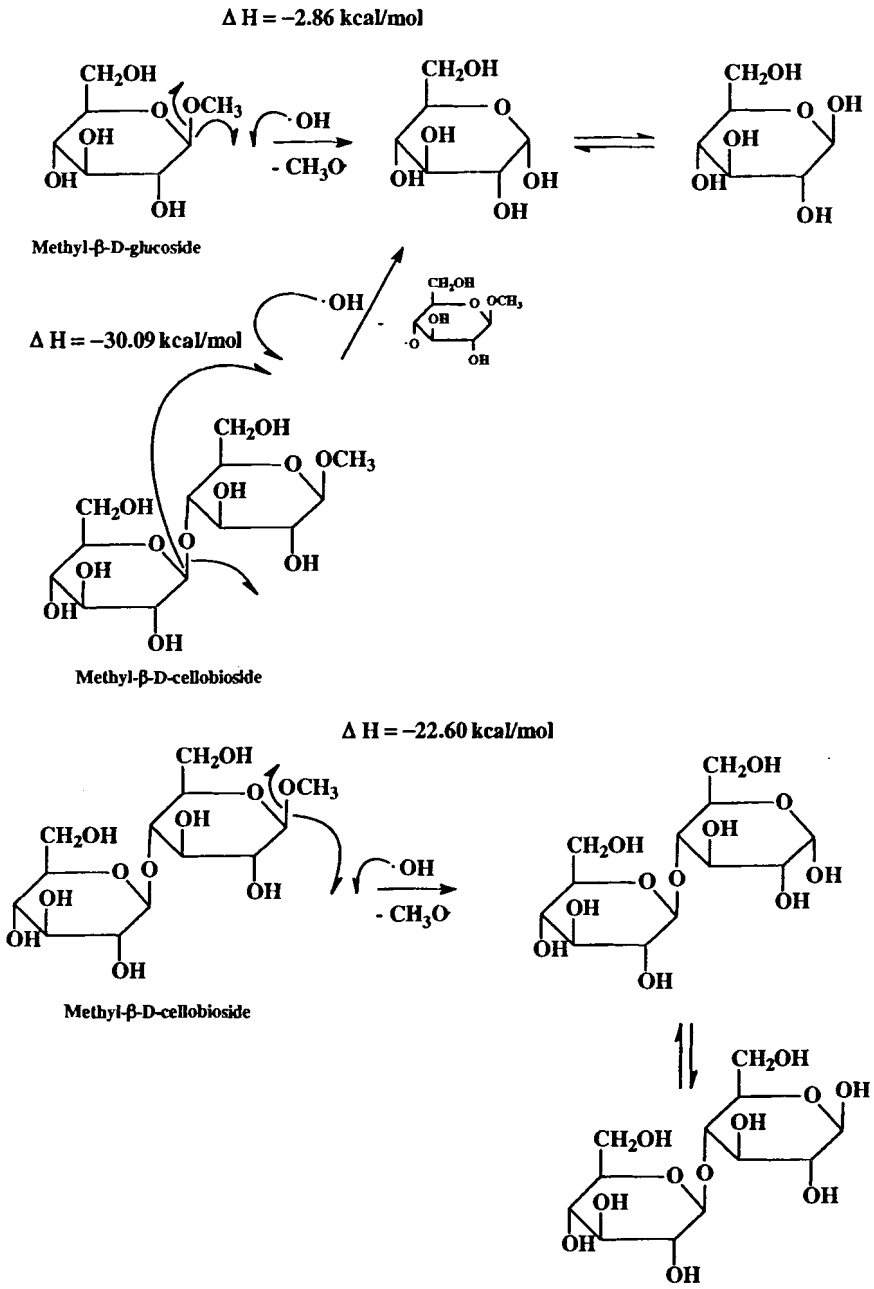

Figure 2.32. Mechanisms proposed by Guay *et al.* for the random cleavage of carbohydrates during oxygen delignification (Modified from Guay, 1999; Guay *et al.*, 2000; 2001).

Also, in the same research by Guay (1999), it is also found that the degradation rates of the carbohydrates are significantly higher at pH 9.5 than at pH 12. This observation supports the idea that hydroxyl radicals are the major oxygen species at lower pH. In addition, the reaction products were analyzed by HPLC and GC/MS in both reactions of methyl-β-D-glucoside and methyl-β-D-cellobioside with hydroxyl radicals. The major products were D-glucose, D-gluconic acid, D-arabinose, D-arabinoic acid, D-erythrose, D-erythronic acid, D-glyceric acid, glycolic acid, and tartaric acid from the reaction of methyl-β-D-glucoside with hydroxyl radicals (Figure 2.33).

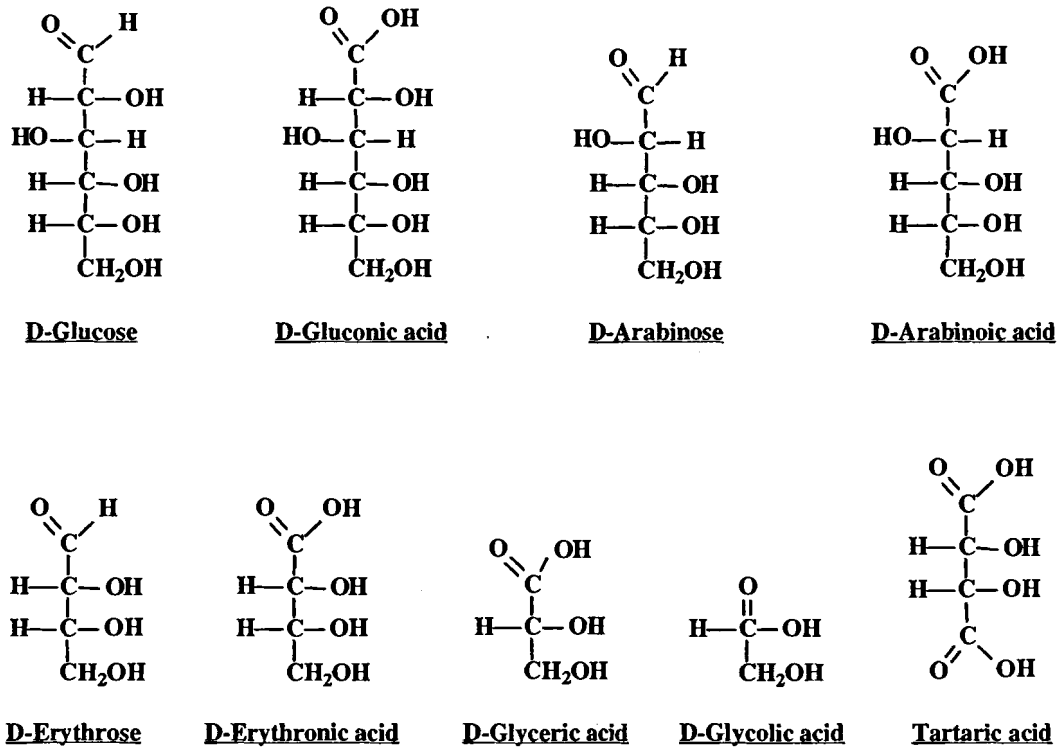

Figure 2.33. Major products determined by HPLC and GC/MS from the carbohydrates reacted with photochemically generated hydroxyl radicals (Modified from Guay, 1999; Guay *et al.*, 2000; 2001).

The reaction of methyl-β-D-cellobioside with hydroxyl radicals produced the same products in addition to D-cellobiose and D-cellobionic acid. Our group also proposed the pathways in Figure 2.34 for the formation of aldonic acids (shown in Figure 2.33) from the aldoses (D-glucose and D-cellobiose) (shown in Figure 2.32).

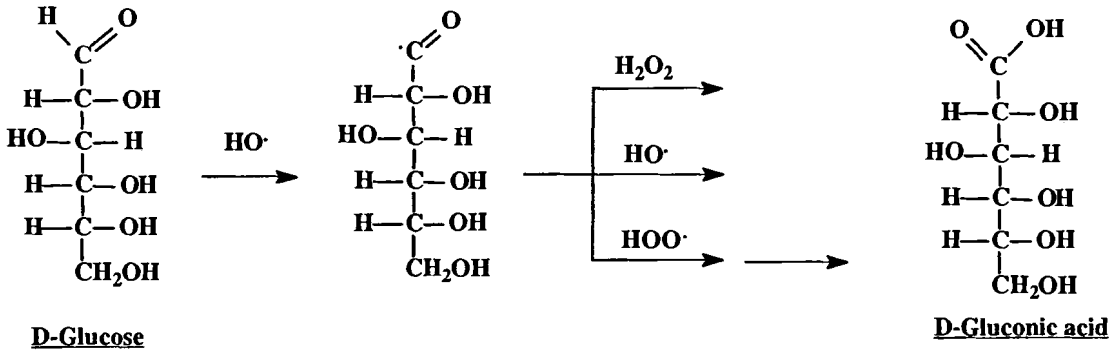

Figure 2.34. D-Gluconic acid (aldonic acid) formation pathways from D-glucose (aldose) (Guay, 1999).

In the proposed mechanisms, hydroxyl radical abstracts hydrogen atom from the acyl group in D-glucose to form an acyl radical. Subsequent reaction can occur with hydrogen peroxide, hydroxyl radical, or hydroperoxy radical. However, hydrogen peroxide was considered as the most likely species since radical coupling is unfavorable because of low concentrations and limited lifetime of radicals.

The next reaction step is suggested to be decarboxylation of D- gluconic acid (Figure 2.35), by Ruff degradation, which is not completely understood. Through this cycle of oxidation and Ruff decarboxylation reactions, higher aldoses become lower aldoses and aldonic acids. That is, the sugars are degraded one carbon at a time.

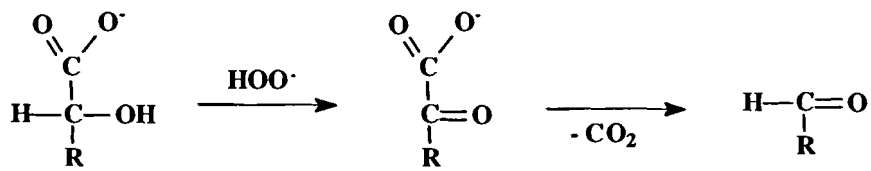

Figure 2.35. Ruff degradation (Based on Pigman and Horton, 1972).

2.3. Summary of review

Oxygen radical species evolve from molecular oxygen during oxygen delignification. In the most probable initiation reaction for the formation of radicals, molecular oxygen reacts with labile oxygen-reducing substrates, such as phenolic moieties, in lignin under alkaline conditions. It is suggested that superoxide anion or hydroxyl radical can be produced from the initiation reaction. Once these radicals are produced, there will be other oxygen species generated by the series of electron transfer reactions. The oxygen species react with the substrates in the delignification system in different ways due to their different oxidation potentials and electrostatic properties.

It is likely that lignin degradation proceeds mainly by hydroxyl radicals, superoxide anions, and hydroperoxy anions after the initiation reaction. Hydroxyl radicals hydroxylate the aromatic rings or the conjugated side chains. The hydroxylation of the aromatic ring causes dealkoxylation or initiation of α-β cleavage or cleavage of ether linkages between two aromatic moieties. Also, hydroxyl radicals can abstract electrons from the conjugated systems in lignin structures to make lignin more reactive. From the electron abstraction, phenoxy radicals can form. Although superoxide anions can abstract electrons from lignin, the most distinct role of them is

ring cleavage. Once a phenoxy radical forms, it can react with a superoxide anion to form a dioxetane, which undergoes the ring cleavage. The ring cleavage occurs substantially more at pH 12 than at pH 10. This supports the notion that superoxide anions are the most abundant species at higher pH. Hydroperoxy anion can add to the conjugated side chain. After the addition of hydroperoxy anion, α-β cleavage occurs.

It appears that hydroxyl radicals are the major species remarkable for degradation of carbohydrates during oxygen delignification. Also, it is reported that the C-1 position is the most probable spot to react with photochemically generated hydroxyl radicals. Here, a hydroxyl radical is attached to the C-1 position when the -OR group is leaving from the same position. This results in the formation of an aldose. The aldose is thought to be oxidized by another hydroxyl radical to become an aldonic acid after the reaction with hydrogen peroxide, hydroxyl radical, or hydroperoxy radical. The aldonic acid can lose the carboxylic group by the reaction with hydroperoxy radicals (Ruff degradation) or with hydroxyl radicals. As a result, a lower aldose forms. Through the series of oxidation and decarboxylation, carbohydrates are degraded to lower aldoses and aldonic acids. The final products will be carbon dioxide and water.

CHAPTER 3

RESULTS AND DISCUSSION

The long-term goal of this project is to understand the reactions occurring during oxygen delignification. The understanding of the reaction mechanisms during oxygen delignification is essential to develop a selective delignification process, which results in a high yield of carbohydrates with lignin being removed. The chemical reactions in delignification processes are complex to analyze because of the numerous variables. Therefore, to better understand the oxidation chemistry of lignin and carbohydrates during oxygen delignification, the simplest lignin and carbohydrate models were separately reacted with photochemically generated oxygen species, which are controllable, and analyzed by Hausman (1999) and Guay (1999) in our laboratory.

Hausman (1999) suggested that phenolic lignin reacts more effectively with oxygen species than non-phenolic lignin and the formation of phenoxy radical intermediates is the key step for the cleavage of aromatic rings of lignin. In the research with model carbohydrates, Guay (1999) suggested that hydroxyl radicals are the major oxygen species to attack carbohydrate at anomeric positions. On the other hand, Ericsson *et al.* (1971) reported that methyl-β-D-glucoside (model carbohydrate) was not degraded by oxygen but degraded in the presence of guaiacol and catechol (model lignins). They did not develop a reaction mechanism, however.

In this work, as a continuation of the works mentioned above, mixtures of a model lignin and a model carbohydrate were reacted in a pressurized oxygen delignification system which will be described in the following section. From this work, as will be

described in the next section, the identification of products derived from methyl-β-D-glucoside could not be accomplished, although lignin derived products were detected. Therefore, further work with the combined models was discontinued. We then undertook an alternative study of the oxidation reactions of cellulose.

In the alternative study, a UV/H_2O_2 system was used, so that the model cellulose reactions were conducted with photochemically generated hydroxyl radicals. Using the work of Guay (1999), we are able to analyze the products from carbohydrate oxidation reactions in UV/H_2O_2 system. In all UV/H_2O_2 reactions performed in this thesis, the wavelength of UV was 254 nm. This work also examined the effects of hydroxyl radical scavengers to investigate the inhibition of oxidation reactions of the cellulose models. The scavengers used were *tert*-BuOH and 2-propanol, which are well known hydroxyl radical inhibitors (Hislop and Bolton, 1999; Tauber, *et al.*, 1999).

3.1. Results of the pressurized oxygen reactions

The objective of this work was to investigate the reactions in the mixture of a model lignin and a model cellulose, which could provide reaction mechanisms relevant to oxygen delignification.

To minimize the complexity of the reactions, simple models for lignin and cellulose were used. Guaiacol was used as the model lignin because it contains one hydroxyl and one methoxyl group on a benzene ring, so that the structure represents the simplest phenolic lignin in wood. Methyl-β-D-glucoside was chosen as the model cellulose since it represents the smallest unit of a cellulose chain that does not

have a reducing group, so that it is not oxidized in ambient conditions. Thus, the mixture of guaiacol and methyl-β-D-glucoside was treated as the simplest representative of wood. Figure 3.1 shows the structures of guaiacol and methyl-β-D-glucoside. The initial reaction pH of the aqueous solution was 12, the oxygen

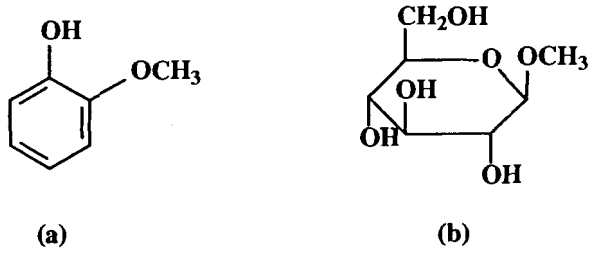

Figure 3.1. Structures of guaiacol (a) and methyl-β-D-glucoside (b).

pressure was 65 psi (steady), and the temperature was 95 °C, which are similar to the industrial conditions. The reactor was a 60 mL borosilicate glass pressure vessel to avoid the potential reactions between oxygen species and metals. A stir bar was used to provide better solubility of oxygen. The reaction time was four hours. Details may be found in the experimental section.

3.1.1. Control reactions

Control I was conducted with 1.5 mmol of guaiacol only in the pressurized oxygen reaction system to investigate if guaiacol is degraded by molecular oxygen. Control II was conducted with 1.5 mmol of methyl-β-D-glucoside only to determine

if methyl-β-D-glucoside is degraded by molecular oxygen. Table 3.1 shows the results of the control reactions.

Table 3.1. Results of the control reactions in the pressurized oxygen reactions.

	mmol* of Methyl-β-D-glucoside Degraded	mmol* of Guaiacol Degraded	pH Initial	pH Final
Control I	N/A	0.84 ± 0.027	12.0	7.9
Control II	0.00	N/A	12.0	11.8

* Calculated based on the recoveries. - All of the data are the average of triplicates.

In Control I, the amount of guaiacol degraded was calculated as 0.84 mmol and the pH of the solution changed to 7.9 from the initial pH of 12.0. These results indicate that guaiacol is decomposed to organic acids by oxygen species, and consequently the pH of the solution decreased as proposed by Hausman (1999). The major reaction products found in Control I are listed in Table 3.2. The HPLC chromatogram of Control I is shown in Appendix B.

Table 3.2. Major reaction products from Control I in the pressurized oxygen reaction.

Product	Retention Time (min)
Glycolic Acid (Hydroxy acetic Acid)*	7.51
Oxalic Acid (Ethanedioic Acid)*	9.13
Malonic Acid (Propanedioic Acid)*	10.52
Maleic Acid (2-Butenedioic Acid (Z))*	12.20
Succinic Acid (Butanedioic Acid)*	12.33
Fumaric Acid (2-Butenedioic Acid (E))*	12.82
Tartronic Acid (Hydroxy propanedioic Acid)**	13.60
Malic Acid (Hydroxy butanedioic Acid)*	14.88

*Match with the authentic compounds. ** Match with the reference MS.

Figure 3.2 is the GC/MS chromatogram of silylated guaiacol and organic acids in the reaction solution of Control I.

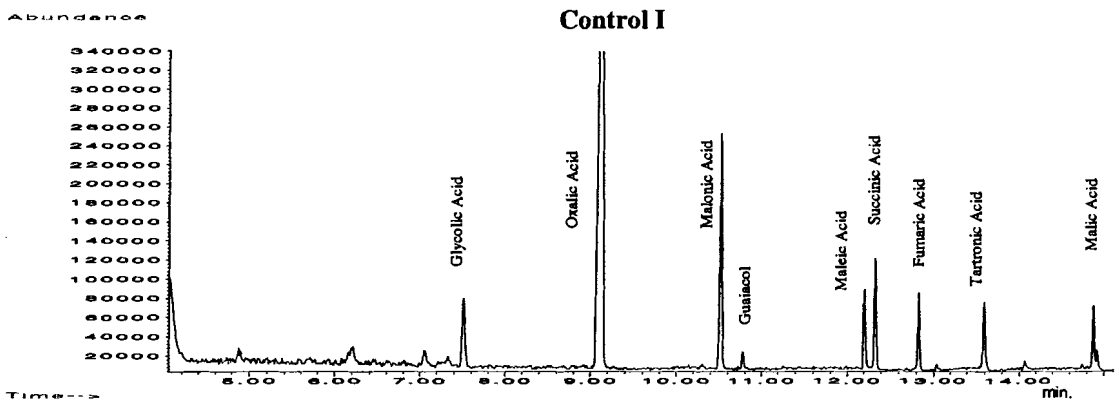

Figure 3.2. GC/MS chromatogram of reaction Control I.

The GC/MS chromatograms and spectra of the authentic compounds are in Appendix A.

The major reaction products in the pressurized oxygen reaction of guaiacol were very similar to what Hausman (1999) determined in the UV/H_2O_2 reaction of guaiacol.

To form the organic acids shown in Table 3.2 from guaiacol, the aromatic ring of guaiacol has to be cleaved. In the previously suggested reaction mechanisms of guaiacol with oxygen species, as described in the review section, the formation of phenoxy radicals is the first step in the ring cleavage. It was suggested that phenoxy radical would form through electron transfer by molecular oxygen from phenoxy anion. However, it was shown that electron transfer by molecular oxygen from phenoxy anion is an unfavorable reaction according to the results of computations

(Hausman, 1999). Hausman (1999) also suggested that phenoxy radicals can form *via* hydrogen atom abstraction or demethylation of guaiacol by oxygen species (Hausman, 1999). Figure 3.3 shows the computed heat of formation for hydrogen atom abstraction and demethylation from guaiacol by molecular oxygen and for one electron abstraction from guaiacol anion by molecular oxygen.

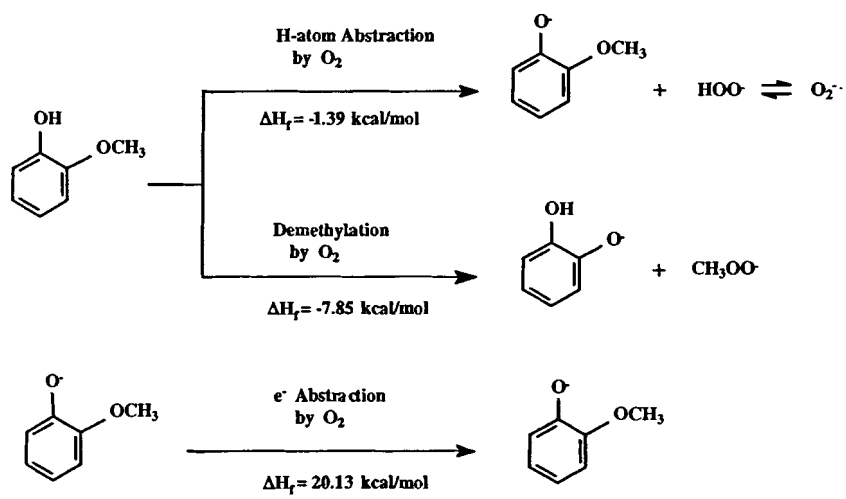

Figure 3.3. Computed heat of formation for hydrogen atom abstraction and demethylation from guaiacol by molecular oxygen and for one electron abstraction from guaiacol anion by molecular oxygen (Modified from Hausman, 1999).

Hydroperoxy radicals form through hydrogen abstraction by molecular oxygen as shown in Figure 3.3. The hydroperoxy radicals are in equilibrium with superoxide anions. These superoxide anions react with phenoxy radicals to form dioxetanes and the ring is opened when the bond between the two oxygen atoms in dioxetane is cleaved. The opened ring is oxidized further to smaller organic acids by reactions with various oxygen species, as described by Hausman (1999).

In Control II, no methyl-β-D-glucoside was degraded and the pH of the solution was not changed significantly. Also, no product was detected in the HPLC and GC/MS analyses. These results demonstrate that molecular oxygen can not degrade methyl-β-D-glucoside in alkaline conditions. The HPLC chromatograms of Control II are in Appendix B and GC/MS spectra are included in Appendix C.

3.1.2. Reactions with the mixtures of methyl-β-D- glucoside and guaiacol

In this work, the mixtures of guaiacol and methyl-β-D-glucoside were reacted in different ratios to investigate the effects of concentrations. The results of these reactions are shown in Table 3.3.

Table 3.3. The results of pressurized oxygen reactions with the mixtures of methyl-β-D-glucoside and guaiacol in alkaline conditions.

Molar Ratio (mmol*) (Guaiacol To Methyl-β-D-glucoside)	mmol** of Methyl-β-D-glucoside Degraded (a)	mmol** of Guaiacol Degraded (b)	Average mmol*** of Methyl-β-D-glucoside Remained (c)	Rate constant = (a /b)/c	pH Initial Final
1 : 1 (1.5 : 1.5)	0.05 ± 0.005	0.86 ± 0.028	1.48	0.04	12.0
1 : 2 (1.5 : 3.1)	0.26 ± 0.050	0.82 ± 0.035	2.93	0.11	12.0
1 : 4 (1.5 : 6.2)	0.68 ± 0.098	0.91 ± 0.039	5.86	0.13	12.0
2 : 1 (3.0 : 1.5)	0.24 ± 0.015	1.66 ± 0.039	1.38	0.10	12.0
2 : 2 (3.0 : 3.1)	0.81 ± 0.164	1.58 ± 0.095	2.70	0.18	12.0

* Actual amounts used. ** Calculated based on the % recoveries determined in HPLC analyses.
*** Average of the initial and final amounts of methyl-β-D-glucoside.

- All of the data are the average of triplicates.

The results in Table 3.3 show that methyl-β-D-glucoside is degraded in the presence of guaiacol under pressurized oxygen in alkaline conditions, compared to Control II. The pH change, from pH 12 to pH 8~9.4, suggests the formation of organic acids during the reaction.

The extent of degradation of methyl-β-D-glucoside and guaiacol depends on the molar ratios of the two substances, and the total amounts of them. As shown in the first three rows (1:1, 1:2, and 1:4 ratio) in Table 3.3, greater amounts of methyl-β-D-glucoside used result in greater degradation of methyl-β-D-glucoside, whereas the amounts of guaiacol degraded were similar in the three cases to that of Control I. The trends were the same in the last two cases (2:1 and 2:2) in Table 3.3. These results suggest that the concentrations of both methyl-β-D-glucoside and guaiacol affect the degradation of methyl-β-D-glucoside.

Guaiacol is degraded through the formation of phenoxy radical by molecular oxygen, followed by the ring opening by superoxide radical as discussed earlier. It was suggested by Hausman (1999) and Guay (1999) that methyl-β-D-glucoside can be degraded by hydroxyl radical but is not attacked by superoxide radical anion. Therefore, methyl-β-D-glucoside may be degraded by hydroxyl radical possibly generated in the reaction system.

Hydroxyl radical generation can be initiated by radical species and molecular oxygen as shown in Figure 3.4. In the very beginning of the reaction in the mixtures of methyl-β-D-glucoside and guaiacol, the radical species ($R^{\cdot}$) is phenoxy radical formed from guaiacol by molecular oxygen. This phenoxy radical can react with a molecular oxygen to form a peroxy radical, which can abstract a hydrogen atom from

another guaiacol molecule to form a peroxide. A hydroxyl radical can form through a homolytic cleavage of the bond between the two oxygen atoms in the peroxide.

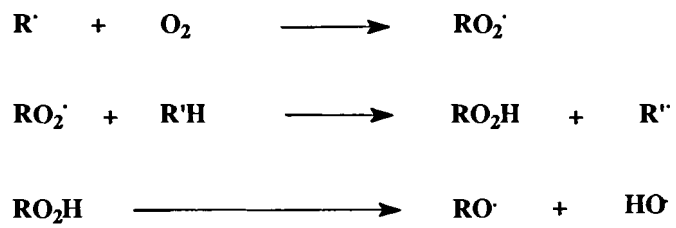

Figure 3.4. A suggested scheme of the formation of hydroxyl radical.

Once hydroxyl radical is formed, D-glucose can be generated by the substitution of hydroxyl radical at the C-1 position in methyl-β-D-glucoside, according to Guay (1999), and hydroxyl radicals can abstract the hydrogen atom at C-1 position in D-glucose to form a D-glucose radical. In addition, hydroxyl radicals can abstract hydrogen atoms from the hydroxyl groups in guaiacol even faster than molecular oxygen (Hausman, 1999). As a result, species R· can be both phenoxy radical and D-glucose radical (or smaller aldose radical, if glucose is decomposed) after the decomposition of methyl-β-D-glucoside by hydroxyl radicals.

Hydroxyl radical is the most reactive oxygen species, so it reacts with any organic compounds non-selectively. Because of the non-selective reaction of hydroxyl radical, hydroxyl radicals react with methyl-β-D-glucoside, with guaiacol, and with others derived from methyl-β-D-glucoside and guaiacol. We can expect that higher amounts of guaiacol provide more phenoxy radicals, thus more hydroxyl radicals can form as depicted in Figure 3.4. Therefore, more hydroxyl radicals degrade more

methyl-β-D-glucoside. On the other hand, if we assume the concentrations of hydroxyl radicals are the same, greater amounts of methyl-β-D-glucoside result in more frequent collisions between hydroxyl radicals and methyl-β-D-glucoside molecules. Additionally, greater degradation of methyl-β-D-glucoside produces more aldose radicals, such as D-glucose radical. These aldose radicals can contribute to produce more hydroxyl radicals as alkyl radicals (R·) shown in Figure 3.4. Therefore, greater concentrations in both methyl-β-D-glucoside and guaiacol can increase the degradation rate of methyl-β-D-glucoside of the mixtures in the pressurized oxygen reactions under alkaline conditions.

These results support the work of Ericsson *et al.* (1971). They ran a pressurized oxygen reaction with a mixture of methyl-β-D-glucoside (0.050 M) and guaiacol (0.025 M) in 0.5 M NaOH solution under 88.2 psi (6 atm) for 20 hours. The recovery of methyl-β-D-glucoside was 89 and 85 % in two runs.

The reaction rate constant shown in Table 3.3 was calculated under the assumption that hydroxyl radicals are generated through the reaction between phenoxy radical from guaiacol and molecular oxygen shown as in Figure 3.4. Thus the degradation of methyl-β-D-glucoside is proportional to the degradation of guaiacol as well as to concentration of methyl-β-D-glucoside available which is represented by the average amount of methyl-β-D-glucoside in Table 3.3. Thus, we attempted to compare the reaction constants shown in Table 3.3 to investigate if we can see correlation between the three factors, the degraded amounts of guaiacol and methyl-β-D-glucoside and amounts of methyl-β-D-glucoside available. The results suggested that there was a correlation between the three factors mentioned above

although the reactions with 1:1 and 2:2 ratios did not show the similar reaction constants as other three points. The discrepancy may be due to experimental error, and further tests should be performed to verify the constant value of the rate constant.

We found that the guaiacol derived reaction products from the mixture of methyl-β-D-glucoside and guaiacol were similar to those of Control I, except the products showing after 16 minutes in the chromatogram, which originate from acid hydrolysis of methyl-β-D-glucoside during sample preparation (Figure 3.5).

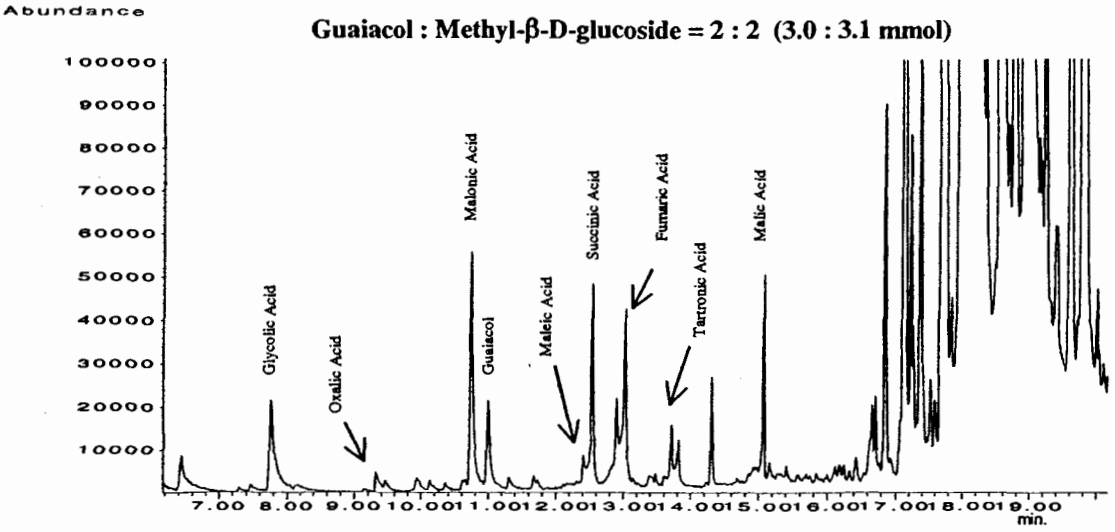

Figure 3.5. GC/MS chromatogram of the guaiacol-derived products in the mixture of guaiacol and methyl-β-D-glucoside.

Although methyl-β-D-glucoside appeared to degrade during the reactions, we were not able to determine the reaction products derived from methyl-β-D-glucoside. For the GC/MS analyses, the reaction mixtures were silylated and acetylated

separately as described in the experimental section. However, only methyl-β-D-glucoside was detected in the two analyses.

The HPLC chromatograms of the reactions of the mixtures of guaiacol and methyl-β-D-glucoside are placed in Appendix B and GC/MS chromatograms are in Appendix C.

As previously suggested, our inability to detect products from methyl-β-D-glucoside led us to alter our original plan. We chose to pursue further studies with the UV/H_2O_2 system, for which analytical protocols were well worked out by Hausman (1999) and Guay (1999).

3.2. Results of UV/H_2O_2 reactions

These experiments were conducted to reinforce our knowledge of the role of hydroxyl radicals in carbohydrate degradation during oxygen delignification. The model celluloses were methyl-β-D-glucoside, methyl-β-D-cellobioside, and cellulose fiber (Filter paper). As mentioned earlier, methyl-β-D-glucoside is the simplest representative of wood cellulose. Methyl-β-D-cellobioside consists of the two glycosidic rings connected with β-linkage (Figure 3.6) which more closely models wood cellulose.

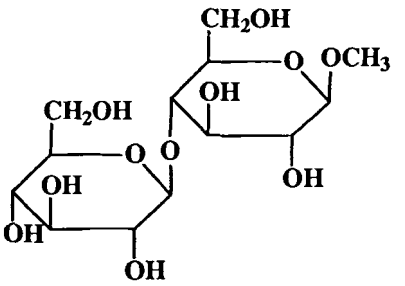

Figure 3.6. Structure of methyl-β-D-cellobioside.

It is known that carbohydrates are degraded more at pH 10 than at pH 12 because hydroxyl radicals are predominant at lower pH (Guay, 1999). In this work, the starting pH was 9.5, to ensure significant degradation of the model celluloses. The end pH of the reaction solutions was above pH 7, which avoids acid hydrolysis of the model celluloses.

This work also considered the effects of hydroxyl radical scavengers to investigate the inhibition of the oxidation reactions of the cellulose models. The scavengers used were *tert*-BuOH and 2-propanol, which are well known hydroxyl radical inhibitors.

3.2.1. Methyl-β-D-glucoside

3.2.1.1. Control reactions

Two control reactions were conducted to investigate if the irradiation with ultraviolet (UV) light affects the degradation of methyl-β-D-glucoside. Control III contained 1.5 mmol of methyl-β-D-glucoside only in the buffer solution. Control IV

contained 1.5 mmol methyl-β-D-glucoside and 11.3 mmol of hydrogen peroxide in the buffer solution. Both were irradiated with UV light at 254 nm.

Table 3.4 shows the results of the control reactions with methyl-β-D- glucoside.

Table 3.4. The results of control reactions with methyl-β-D- glucoside: UV treated.

	mmol* of Methyl-β-D-glucoside Degraded	mmol** of D-glucose Isolated	mmol** of D-Arabinose Isolated	pH Initial	pH Final
Control III	0***	0	0	9.4	9.5
Control IV	1.11 ± 0.012	0.04 ± 0.0007	0.01 ± 0.0002	9.4	7.3

* Calculated based on the percent recoveries.
** Calculated based on the percentages compared to the starting material.
*** The percent recovery was 98.5% which reflects an experimental error.
- All of the data are the average of triplicates.

In Control III, the recovery of methyl-β-D-glucoside was 98.5 %. However, no D-glucose or D-arabinose was detected. Also, there was no significant pH change in the reaction solution. These results suggest that the recovery (98.5 %) in Control III reflects experimental error in the analysis, and methyl-β-D-glucoside is not degraded by UV light in the system. In Control IV, methyl-β-D-glucoside was significantly decomposed, so that about 1.1 mmol out of 1.5 mmol were degraded. These data agree with the results of Guay *et al.* (2000). The pH of the solution dropped to 7.3, because of the formation of organic acids, as proposed by Guay *et al.* (2000). The major reaction products are shown in Table 3.5.

Table 3.5. The major reaction products from UV/H_2O_2 reaction of methyl-β-D-glucoside.

Product	Retention time (min)
Glycolic Acid	**8.65**
D-Glyceric Acid	**16.63**
D-Erythronic Acid	**22.23**
D-Arabinose	**23.87**
Tartaric Acid	**24.52**
D-Arabinoic Acid	**27.61**
D-Glucose	**32.80**
D-Gluconic Acid	**33.14**

- All of the GC/MS data match with those of the authentic compounds.

Figure 3.7 is the GC/MS chromatogram of the reaction Control IV. The HPLC chromatograms are included in Appendix B. The GC/MS chromatograms and spectra of the authentic compounds are included in Appendix A.

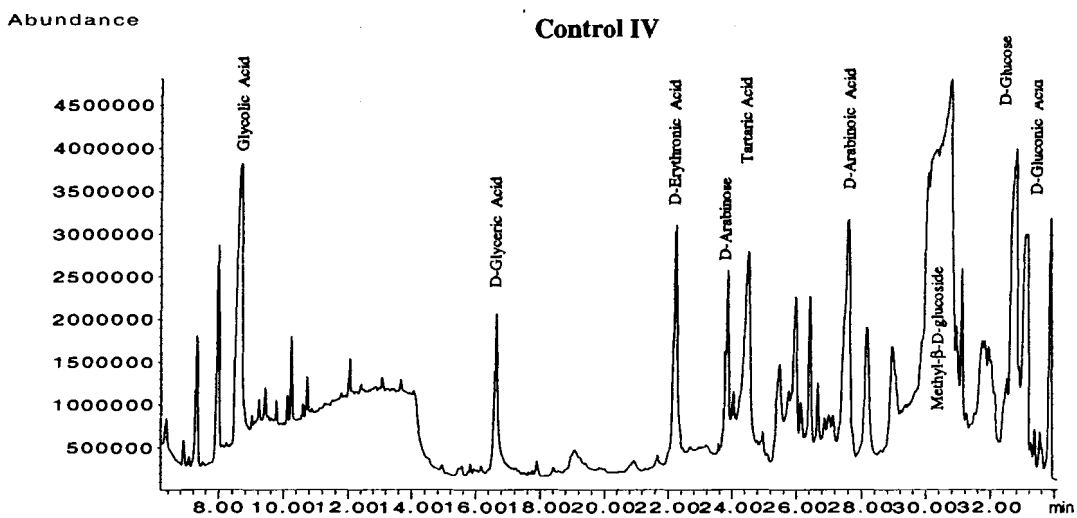

Figure 3.7. A GC/MS spectrum of the reaction mixture of Control IV.

3.2.1.2. Reactions with methyl-β-D-glucoside in the presence of hydroxyl radical scavengers

To investigate the effects of hydroxyl radical scavengers on the degradation of methyl-β-D-glucoside by hydroxyl radical, *tert*-BuOH and 2-propanol were used as hydroxyl radical scavengers in the UV/H_2O_2 reactions of methyl-β-D-glucoside. The scavengers were employed in different molar ratios with methyl-β-D-glucoside.

Table 3.6 shows the recoveries of methyl-β-D-glucoside and the percentages of D-glucose and D-arabinose isolated as results of the UV/H_2O_2 reactions of methyl-β-D-glucoside conducted in the presence of *tert*-BuOH.

Table 3.6. The results of UV/H_2O_2 reactions with methyl-β-D-glucoside in the presence of *tert*-BuOH in different ratios of the mixtures.

Molar Ratio (mmol*) (Methyl-β-D-glucoside To *tert*-BuOH)	mmol** of Methyl-β-D-glucoside Degraded	mmol*** of D-glucose Isolated	mmol*** of D-Arabinose Isolated	pH Initial	pH Final
1 : 1 (1.5 : 1.6)	0.95 ± 0.009	0.04 ± 0.0015	0.01 ± 0.0002	9.6	8.5
1 : 2 (1.5 : 3.1)	0.87 ± 0.018	0.04 ± 0.0017	0.01 ± 0.0001	9.6	8.9
1 : 4 (1.5 : 6.3)	0.75 ± 0.019	0.03 ± 0.0009	0.01 ± 0.0002	9.6	9.0

* Actual amounts used.
** Calculated based on the percent recoveries
*** Calculated based on the percentages compared to the starting material.
- All of the data are the average of triplicates.

In the presence of *tert*-BuOH, as shown in Table 3.6, the amounts of methyl-β-D-glucoside degraded in the three reactions were significantly lower than that of reaction Control IV which did not contain *tert*-BuOH. This observation is consistent with the scavenging of hydroxyl radicals by *tert*-BuOH. The reaction mechanism of

tert-BuOH with hydroxyl radical is depicted in Figure 3.8. One hydrogen atom is abstracted by a hydroxyl radical, followed by elimination of a methyl radical to form the enol of acetone.

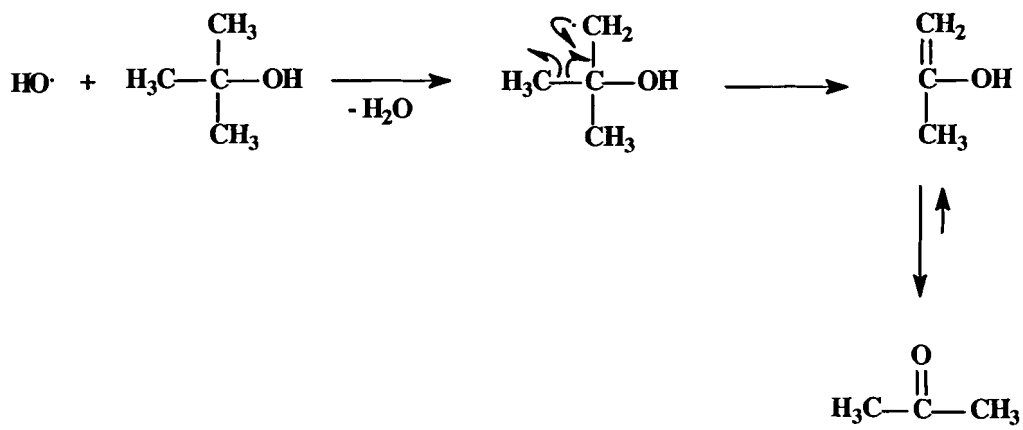

Figure 3.8. The reaction mechanism of *tert*-BuOH with hydroxyl radical (Modified from Tauber *et al.*,1999).

Acetone was collected by the Solid Phase Microextraction (SPME) method and detected with GC/MS. The SPME-GC/MS data are shown in Appendix D. In the SPME-GC/MS data in Appendix D, the retention times of acetone and *tert*-BuOH varied less than 0.3 minute in different reactions. This variation is caused by GC/MS column conditions. To make the differences clear, the mass spectra of acetone and *tert*-BuOH were included in each GC/MS chromatogram in Appendix D. Also, the GC/MS chromatograms and spectra of the authentic acetone, *tert*-BuOH, and 2-propanol are included in Appendix D.

The final pHs of the three mixtures having different ratios of methyl-β-D-glucoside to *tert*-BuOH were higher than that of Control II. Also the final pH in the reaction having a 1:1 ratio of methyl-β-D-glucoside to *tert*-BuOH was lower than those at 1:2 and 1:4. Greater degradation of methyl-β-D-glucoside results in greater formation of organic acids, which decrease the final pH of the solution. According to the results of Guay *et al.* (2000), methyl-β-D-glucoside is degraded to D-glucose, which in turn is the precursor of D-gluconic acid. The D-gluconic acid is decomposed to D-arabinose, which is degraded to the smaller aldoses and organic acids.

Although the recoveries of methyl-β-D-glucoside differ in the three reactions, the amounts of D-glucose and D-arabinose formed were not substantially different. In other words, only limited quantities of D-glucose and D-arabinose remained, even though significantly different amounts of methyl-β-D-glucoside were degraded in the three reactions. This suggests that the formation of D-glucose from methyl-β-D-glucoside is the rate-determining step. After the rate-determining step, the D-glucose formed undergoes fast decomposition by oxygen species. As a result, the concentrations of D-glucose and D-arabinose are found to be low in all three reactions. The overall chemistry in the reactions is not changed from the reaction Control II although the amounts of the products are decreased by increasing concentration of *tert*-BuOH. That is, the relative proportions of products remain the same, even as the total amount decreases.

Table 3.7 shows the recovery of methyl-β-D-glucoside and the amounts of D-glucose and D-arabinose isolated when reactions were run in the presence of 2-propanol.

Table 3.7. The results of UV/H_2O_2 reactions with methyl-β-D-glucoside in the presence of 2-propanol in different ratios of the mixtures.

Molar Ratio (mmol*) (Methyl-β-D-glucoside To 2-Propanol)	mmol** of Methyl-β-D-glucoside Degraded	mmol*** of D-glucose Isolated	mmol*** of D-Arabinose Isolated	pH Initial	pH Final
1 :1 (1.5 : 1.6)	0.91 ± 0.019	0.04 ± 0.0001	0.01 ± 0.0004	9.6	8.9
1 : 2 (1.5 : 3.1)	0.83 ± 0.003	0.03 ± 0.0004	0.01 ± 0.0006	9.6	9.1
1 :4 (1.5 : 6.2)	0.69 ± 0.012	0.03 ± 0.0030	0.01 ± 0.0004	9.6	9.3

* Actual amounts used.
** Calculated based on the percent recoveries.
*** Calculated based on the percentages compared to the starting material.
- All of the data are the average of triplicates.

The trends are the same as in the reactions in the presence of *tert*-BuOH. When more 2-propanol is used, greater recovery of methyl-β-D-glucoside is obtained. The recovery of methyl-β-D-glucoside in each of the three reactions (1:1, 1:2, and 1:4 ratio) is slightly higher than that in each of the three reactions in the presence of *tert*-BuOH. The hydrogen atom at C-2 (2°) in 2- propanol is more easily abstracted by hydroxyl radical than the hydrogen atoms at methyl groups (1°) in *tert*-BuOH. A secondary radical formed after the hydrogen atom abstraction from 2-propanol by hydroxyl radical is more stable than a primary radical from *tert*-BuOH because of the electron donating effect of the two vicinal methyl groups and an electron rich adjacent oxygen atom in 2-propanol. Therefore, 2-propanol is a better radical trap

than *tert*-BuOH. Figure 3.9 shows the reaction rate constants of 2-propanol and *tert*-BuOH in the hydrogen atom abstraction by hydroxyl radical (Anbar *et al.*, 1966).

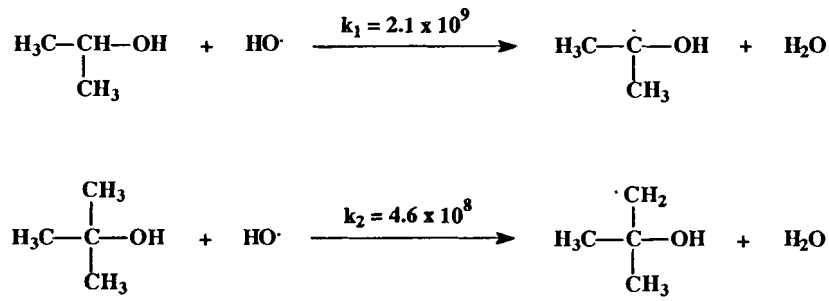

Figure 3.9. The rate constants (k) of 2-propanol and *tert*-BuOH in the hydrogen atom abstraction by hydroxyl radicals at pH 9 (modified from Anbar *et al.*, 1966).

The amounts of D-glucose and D-arabinose isolated also showed the same trend as in the reactions with *tert*-BuOH. The final pH values of the solution mixtures were slightly higher than those in the reaction with *tert*-BuOH in each case. This is expected if 2-propanol more effectively inhibits oxidation by hydroxyl radical.

In the reaction between 2-propanol and hydroxyl radical, the reaction product is acetone (Figure 3.10). Acetone was detected by the SPME-GC/MS method. The SPME- GC/MS data are shown in Appendix D.

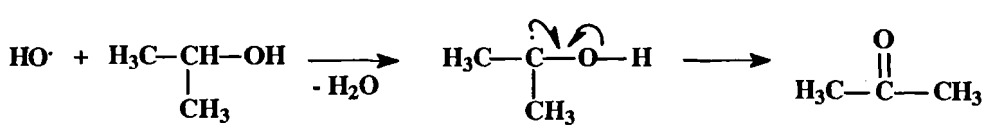

Figure 3.10. The reaction mechanism of 2-propanol with hydroxyl radical (Based on Hislop and Bolton,1999).

With regard to the analysis of methyl-β-D-glucoside-derived products by HPLC and GC/MS, it is clear that the overall chemistry was not different from the results of reaction Control IV. The HPLC chromatograms are in Appendix B and GC/MS spectra are in Appendix C.

Using the hydroxyl radical inhibition effect of the scavengers shown in this study, we designed experiments to investigate the roles of hydroxyl radicals in the UV/H_2O_2 reactions with methyl-β-D-glucoside in detail. This study is described in the following section. The supporting idea of these experiments is that the first step to form aldonic acids from aldoses is hydrogen atom abstraction at C-1 position by hydroxyl radicals as proposed by Guay (1999). Under this assumption, therefore, we determined qualitatively the inhibition effect in the formation of the major aldonic acids mentioned earlier. The results in this work showed greater hydroxyl radical inhibition effects in the formation of some aldonic acids than in the formation of others. Details are shown in the following section.

3.2.1.3. Results of qualitative GC/MS analysis of the organic acids derived from methyl-β-D-glucoside

To investigate the role of hydroxyl radicals during the formation of aldonic acids from carbohydrates, the six organic acid products, glycolic, D-glyceric, D-erythronic, tartaric, D-arabinoic, and D-gluconic acid, from the UV/H_2O_2 reaction of methyl-β-D-glucoside, in the absence and presence of *tert*-BuOH and 2-propanol, were analyzed.

We were not able to synthesize pure D-glyceric, D-erythronic, and D-arabinoic acid and therefore could not make standard calibration tables for them. As a result, the analyses of the six organic acids were performed qualitatively.

For the qualitative study, the products from the reactions with methyl-β-D-glucoside in different ratios of methyl-β-D-glucoside to the scavengers were freeze-dried, silylated, and analyzed with GC/MS. Benzoic acid was used in the GC/MS analysis as an internal standard. The relative percentage of each organic acid was calculated as the percent peak area relative to the area of benzoic acid peak which was set as 100 %. Two runs were conducted in each reaction set.

Table 3.8 shows the amounts of the six organic acids in Control IV and reactions of methyl-β-D-glucoside in the presence of *tert*-BuOH, relative to the standard.

Table 3.8. Relative percent areas of the six organic acids calculated based on the area of benzoic acid in reaction Control IV and the reactions of methyl-β-D-glucoside in the presence of *tert*-BuOH.

	Control IV		(1.5 : 1.6)*		(1.5 : 3.1)*		(1.5 : 6.3)*	
Acid	**Trial 1**	**Trial 2**	**Trial 1**	**Trial 2**	**Trial 1**	**Trial 2**	**Trial 1**	**Trial 2**
Glycolic	**55.1**	**50.1**	**27.8**	**26.5**	**26.2**	**13.4**	**0.0**	**0.0**
Glyceric	**29.0**	**23.7**	**7.9**	**4.9**	**2.1**	**0.5**	**2.4**	**1.0**
Erythronic	**35.7**	**31.9**	**13.1**	**10.5**	**6.3**	**0.0**	**10.5**	**4.9**
Tartaric	**26.4**	**21.9**	**0.1**	**0.1**	**0.3**	**2.8**	**0.0**	**0.0**
Arabinoic	**73.6**	**67.5**	**16.0**	**9.9**	**1.5**	**0.0**	**0.0**	**0.0**
Gluconic	**82.6**	**80.9**	**32.5**	**11.5**	**11.9**	**0.2**	**0.0**	**0.0**

* Molar ratio of methyl-β-D-glucoside to *tert*-BuOH.

One distinct trend in Table 3.8 is that greater amounts of *tert*-BuOH used result in less formation of the organic acids. This result is related to the total amount of methyl-β-D-glucoside degraded. As mentioned earlier, greater amounts of *tert*-BuOH used result in less degradation of methyl-β-D-glucoside.

The relative percent areas between the two trials in each reaction were not reproducible (Table 3.8). The inconsistency got worse when smaller amounts of organic acids were present in the solutions. This is probably caused by the poor reproducibility in silylation of the freeze-dried products. Before silylation, the freeze-dried samples contain organic acids mixed with the sodium hydroxide and sodium bicarbonate used as the buffer. These salts are hygroscopic, so that water in the atmosphere can be absorbed in the freeze-dried samples. This water can interfere with the silylation of the organic acids by the silylating reagent, Sylon BTZ (Supelco). To overcome the interference, usually an excess amount of silylating reagent is used. However, the use of an excess amount of silylating reagent causes an unstable baseline in the GC/MS chromatogram because of the decomposition of the silylating agent. With the unstable baseline, the precise determination of peak areas of the organic acids was not possible.

The GC/MS chromatograms in Figure C7 in Appendix C were obtained in the experiments for Section 3.2.1.2 in this thesis in which excess amounts of silylating reagent used. Chromatograms in Figure C10 are for this section. Because of the inconsistent silylation, especially with a 1.5:6.3 ratio, some products are found in one experiment, but not another (C7 versus C10 in Appendix C), although they had the

same ratios of methyl-β-D-glucoside to *tert*-BuOH. This demonstrates more clearly the inconsistency of silylation, especially when amounts of the products are small.

Nevertheless, there are some clear trends in the results in Table 3.8. As greater amounts of *tert*-BuOH were used, for example, the quantity of gluconic and arabinoic acid decreased more significantly than other acids, except tartaric acid. This suggests that *tert*-BuOH inhibited the formation of gluconic and arabinoic acid more than others.

These results support the role of hydroxyl radicals in the formation of aldonic acids from D-glucose. Guay *et al.* (2000) in our laboratory proposed that hydroxyl radicals abstract hydrogen atom at C-1 position of an aldose, such as D-glucose, and aldonic acid is formed through the reaction of the aldose radical with any of the three potential oxygen species (H_2O_2, $HO^{\cdot}$, and $HOO^{\cdot}$/Baeyer-Villiger oxidation). Hydrogen peroxide is likely the most important of the three oxygen species, since radical coupling reactions are minor. As a result, the scavenging of hydroxyl radicals by *tert*-BuOH suppressed the hydrogen atom abstraction from of aldoses.

The mechanism of formation of tartaric acid in these experiments is still a question because of little evidence. However, the results in Table 3.8 definitely indicate that hydroxyl radicals are heavily involved in the formation of tartaric acid since its formation was more drastically decreased than any other organic acid when higher amounts of *tert*-BuOH were used.

Table 3.9 shows the amounts of the six organic acids in Control IV and reactions of methyl-β-D-glucoside in the presence of 2-propanol, relative to the standard.

The results in Table 3.9 do not give much information because of the small amounts of the products determined. However, the trends are probably similar to those in the reactions of methyl-β-D-glucoside in the presence of *tert*-BuOH, and in the reactions with other carbohydrates described in previous sections.

Table 3.9. Relative percent areas of the six organic acids calculated based on the area of benzoic acid in reaction Control IV and the reactions of methyl-β-D-glucoside in the presence of 2-propanol.

	Control IV		(1.5 : 1.6)*		(1.5 : 3.1)*		(1.5 : 6.2)*	
Acid	**Trial 1**	**Trial 2**	**Trial 1**	**Trial 2**	**Trial 1**	**Trial 2**	**Trial 1**	**Trial 2**
Glycolic	**55.1**	**50.1**	**5.7**	**0.0**	**0.0**	**0.0**	**0.0**	**0.0**
Glyceric	**29.0**	**23.7**	**0.0**	**0.0**	**0.0**	**0.0**	**0.0**	**0.0**
Erythronic	**35.7**	**31.9**	**1.7**	**0.6**	**0.0**	**0.0**	**0.0**	**0.0**
Tartaric	**26.4**	**21.9**	**0.0**	**0.0**	**0.0**	**0.0**	**0.0**	**0.0**
Arabinoic	**73.6**	**67.5**	**3.8**	**0.4**	**0.0**	**0.0**	**0.0**	**0.0**
Gluconic	**82.6**	**80.9**	**77.0**	**34.1**	**0.0**	**0.0**	**0.0**	**0.0**

* Molar ratio of methyl-β-D-glucoside to 2-Propanol.

For all reactions described so far, we used methyl-β-D-glucoside as our model cellulose. Methyl-β-D-glucoside is the simplest cellulose model, so that we have the smallest numbers of variables in the reactions. However, the structure of methyl-β-D-glucoside is more similar to cellulose, which has (1→ 4)-β ether linkages between glucose units. Therefore, we ran the UV/H_2O_2 reactions with methyl-β-D-cellobioside, which is a more realistic cellulose model, to reinforce our knowledge in the oxidative degradation of cellulose. The results follow in the next section.

3.2.2. Methyl-β-D-cellobioside

3.2.2.1. Control reactions

Table 3.10 shows the results of Control V and Control VI which contained 0.3 mmol of methyl-β-D-cellobioside only and 0.3 mmol methyl-β-D-cellobioside with 2.3 mmol of hydrogen peroxide in the buffer solution, respectively. The two controls were irradiated with UV light at 254 nm.

Table 3.10. The results of control reactions with methyl-β-D-cellobioside: UV treated.

	mmol* of Methyl-β-D-cellobioside Degraded	mmol** of Methyl-β-D-glucoside Isolated	mmol** of D-glucose Isolated	mmol** of D-Arabinose Isolated	pH Initial	pH Final
Control V	0	0	0	0	9.5	9.6
Control VI	0.24 ± 0.0012	0.02 ± 0.0019	0.03 ± 0.0023	0.01 ± 0.0001	9.6	7.3

* Calculated based on the percent recoveries.
** Calculated based on the percentages compared to the starting material.
- All of the data are the average of triplicates.

In Control V, no methyl-β-D-cellobioside was degraded since there was no radical source in the mixture. Also, the final pH value of the reaction mixture was unchanged within experimental error. The HPLC chromatograms and GC/MS spectra are in Appendices B and C, respectively. On the other hand, methyl-β-D-cellobioside was severely degraded in Control VI. The major reaction products were the same as for Control IV for methyl-β-D-glucoside, except cellobiose and cellobionic acid as shown in Table 3.11 and Figure 3.11.

Table 3.11. The major reaction products from UV/H_2O_2 reaction of methyl-β-D-cellobioside.

Product	Retention time (min)
Glycolic Acid	**8.57**
D-Glyceric Acid	**16.86**
D-Erythronic Acid	**22.51**
D-Arabinose	**24.17**
Tartaric Acid	**24.76**
D-Arabinoic Acid	**27.94**
Methyl-β-D-glucoside	**30.72**
D-Glucose	**33.09**
D-Gluconic Acid	**33.45**
D-Cellobiose	**55.79**
D-Cellobionic Acid	**56.42**

- All of the GC/MS data match with those of the authentic compounds.

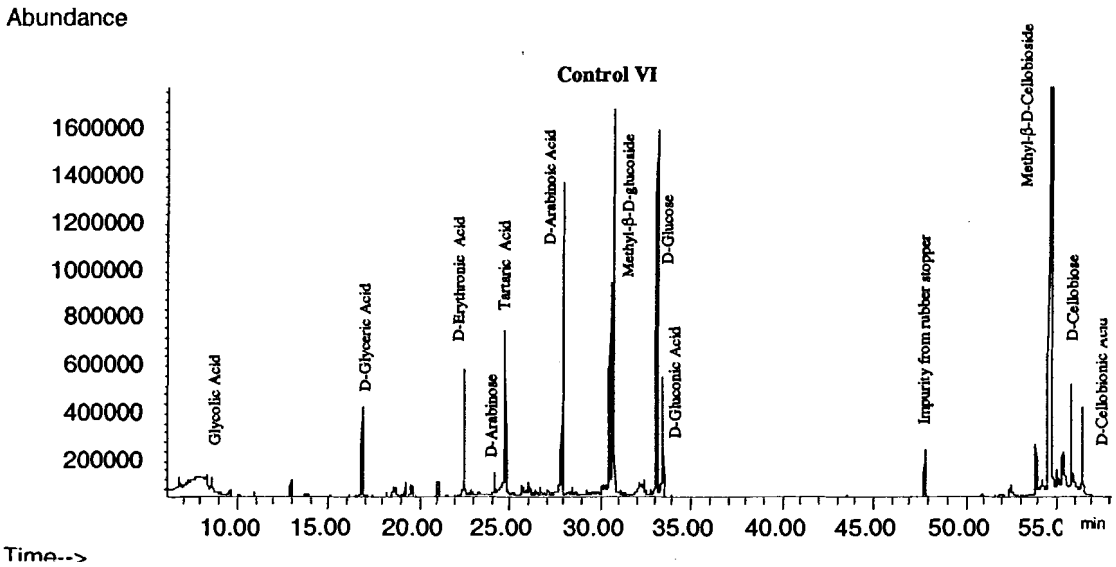

Figure 3.11. GC/MS result of UV/H_2O_2 reaction of methyl-β-D-cellobioside (Control VI).

The GC/MS chromatograms and spectra of authentic compounds are included in Appendix A.

There are two anomeric carbons in methyl-β-D-cellobioside, which are the primary targets in the reaction with hydroxyl radicals (Guay *et al.*; 2001). One is C-1 attached to the methoxyl group in the first ring. The other is C-7 connected to the methyl-β-D-glucoside ring. When hydroxyl radicals react at the C-1 position, the methoxy group is cleaved, and methyl-β-D-cellobiose is formed. If C-7 reacts with hydroxyl radicals, the ether linkage is cleaved, and methyl-β-D-glucoside and D-glucose are produced. The methyl-β-D-glucoside formed from methyl-β-D-cellobioside reacts with other hydroxyl radicals, and degrades to smaller aldoses and organic acids by the same reaction pathways as described previously. Likewise, the methyl-β-D-cellobiose and D-glucose formed from methyl-β-D-cellobioside are degraded into the smaller aldoses and organic acids. The formation of organic acids results in the low final pH in the reaction Control VI.

In Control VI, the amounts of D-glucose and D-arabinose are much higher than in the degradation of methyl-β-D-glucoside in reaction Control IV. This likely results from the cleavage of one molecule of methyl-β-D-cellobioside being a source of two D-glucose molecules, which are converted to D-arabinose.

3.2.2.2. Reactions of methyl-β-D-cellobioside in the presence of hydroxyl radical scavengers

In the presence of hydroxyl radical scavengers, the reaction products are the same as in the reaction Control VI. The HPLC and GC/MS chromatograms and spectra are included in Appendix B, and SPME-GC/MS spectra are contained in Appendix C.

The results of the reactions in the presence of *tert*-BuOH are shown in Table 3.12.

Table 3.12. The results of UV/H_2O_2 reactions with methyl-β-D-cellobioside in the presence of *tert*-BuOH in different ratios of the mixtures.

Molar Ratio (mmol*) (Methyl-β-D-cellobioside To *tert*-BuOH)	mmol** of Methyl-β-D-cellobioside Degraded	mmol*** of Methyl-β-D-glucoside Isolated	mmol*** of D-glucose Isolated	mmol*** of D-Arabinose Isolated	pH Initial	pH Final
1 : 1 (0.3 : 0.3)	0.24 ± 0.0037	0.02 ± 0.0002	0.03 ± 0.0005	Trace	9.6	7.2
1 : 2 (0.3 : 0.6)	0.24 ± 0.0015	0.02 ± 0.0003	0.03 ± 0.0005	0.01 ± 0.0002	9.7	7.3
1 : 4 (0.3 : 1.1)	0.22 ± 0.0068	0.02 ± 0.0002	0.03 ± 0.0012	Trace	9.7	7.4
1 : 8 (0.3 : 2.3)	0.17 ± 0.0035	0.02 ± 0.0003	0.02 ± 0.0005	Trace	9.7	8.5

* Actual amounts used.
** Calculated based on the percent recoveries.
*** Calculated based on the percentages compared to the starting material.
- All of the data are the average of triplicates.

From the results in Table 3.10, the amounts of methyl-β-D-cellobioside degraded in the reactions in the first three rows (1:1, 1:2, and 1:4 ratio) are almost the same as that in Control VI. Only with 1:8 ratio of methyl-β-D-cellobioside to *tert*-BuOH, are significantly lower amounts of methyl-β-D-cellobioside degraded. These results indicate that greater amounts of *tert*-BuOH are required to achieve effective

scavenging of hydroxyl radicals in the reactions with methyl-β-D-cellobioside than with methyl-β-D-glucoside.

To explain the different scavenging effect between the reactions with methyl-β-D-glucoside and with methyl-β-D-cellobioside, the structural differences between them must be taken into account. At least two moles of hydroxyl radicals are used when a methyl-β-D-glucoside molecule is degraded to a gluconic acid molecule: one when methyl-β-D-glucoside is cleaved D-glucose, and the other to form D-gluconic acid from D-glucose (Guay *et al.,* 2000). However, a methyl-β-D-cellobioside molecule will consume four hydroxyl radical molecules and produce two gluconic acid molecules in each of the three different reaction pathways due to the dimeric structure of methyl-β-D-cellobioside (Figure 3.12). As a result, methyl-β-D- cellobioside competes more effectively with *tert*-BuOH for hydroxyl radicals than does methyl-β-D-glucoside. At a 1 : 8 ratio, the concentration of *tert*-BuOH is high enough to dominate the competition, and results in significantly less degradation of methyl-β-D-cellobioside. The implication of this observation is that methyl-β-D-cellobioside is more reactive toward hydroxyl radicals than methyl-β-D-glucoside. Since the methoxyl environment is the same in both, the cleavage at the ring junctions must be more facile than methoxyl cleavage. Guay's (1999) computed values of heat of formation (ΔH), which is shown in Figure 2.32 in the review section, support this observation.

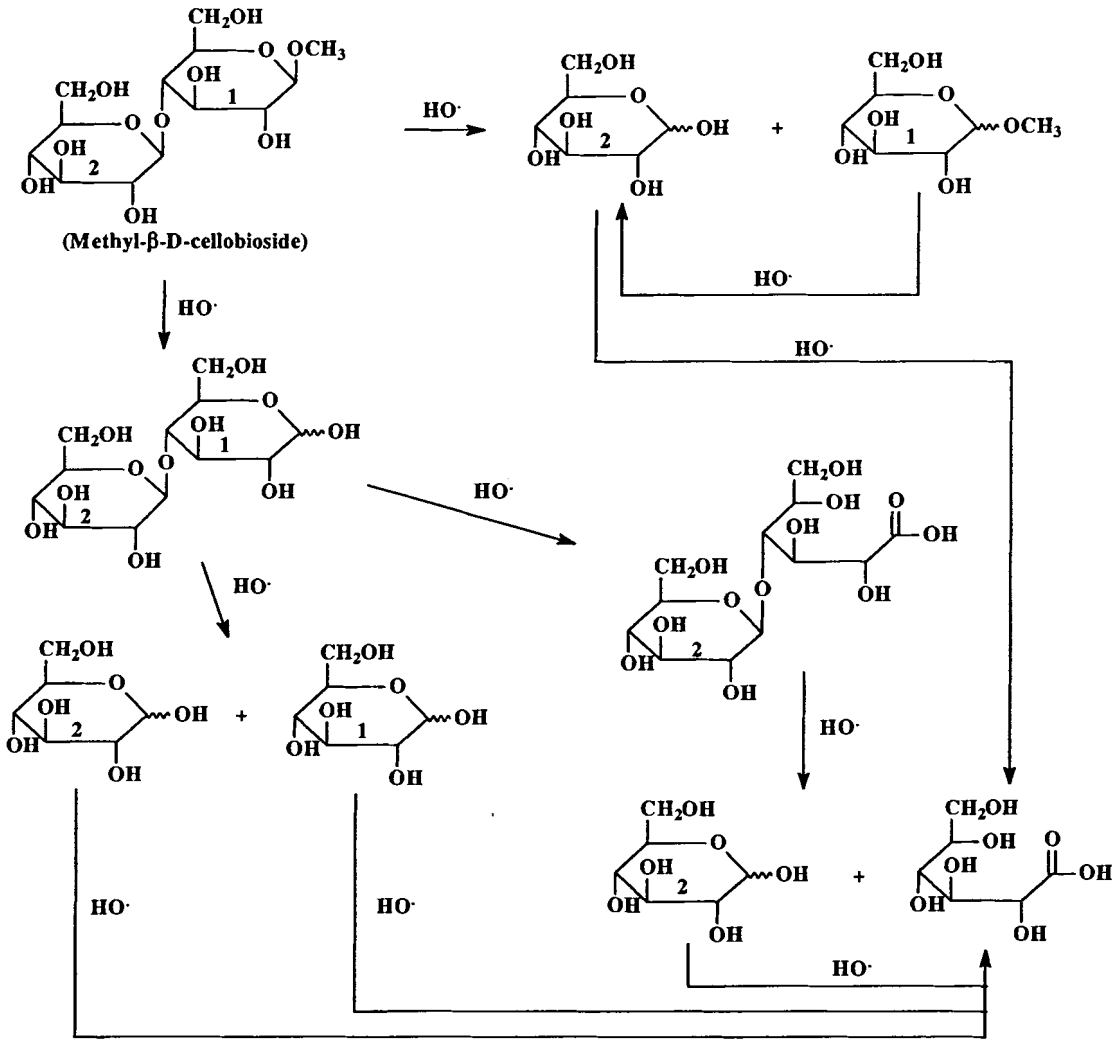

Figure 3.12. Proposed reaction pathways between methyl-β-D-cellobioside and hydroxyl radicals.

As shown in Table 3.13, the more effective hydroxyl radical scavenger, 2-propanol, leads to slightly less degradation of methyl-β-D-cellobioside in all concentration ranges. However, the trends are the same as produced by *tert*-BuOH, confirming our conclusions about relative reactivity.

Table 3.13. The results of UV/H_2O_2 reactions with methyl-β-D-cellobioside in the presence of 2-propanol in different ratios of the mixtures.

Molar Ratio (mmol*) (Methyl-β-D-cellobioside To 2-Propanol)	mmol** of Methyl-β-D-cellobioside Degraded	mmol*** of Methyl-β-D-glucoside Isolated	mmol*** of D-glucose Isolated	mmol*** of D-Arabinose Isolated	pH Initial	pH Final
1 : 1 (0.3 : 0.3)	0.24 ± 0.0065	0.02 ± 0.0002	0.02 ± 0.0013	Trace	9.5	7.2
1 : 2 (0.3 : 0.6)	0.23 ± 0.0039	0.02 ± 0.0003	0.02 ± 0.0010	Trace	9.6	7.4
1 : 4 (0.3 : 1.1)	0.20 ± 0.0071	0.02 ± 0.0013	0.02 ± 0.0010	Trace	9.6	7.7
1 : 8 (0.3 : 2.3)	0.16 ± 0.0041	0.02 ± 0.0008	0.02 ± 0.0005	Trace	9.7	8.6

* Actual amounts used.
** Calculated based on the percent recoveries.
*** Calculated based on the percentages compared to the starting material.
- All of the data are the average of triplicates.

3.2.3. Cellulose fiber

Having demonstrated inhibition of hydroxyl cleavage with two model systems, we decided to look at cellulose itself. For this purpose, disintegrated filter paper (Whatman 1) was used.

Because most product fragments were expected to be too large for chromatographic analysis, intrinsic viscosity was used to distinguish the differences in the degradation of cellulose in the different reactions. Also, the degree of

polymerization (DP) and Chain Scission numbers were calculated from the intrinsic viscosity.

Results of controls and the reactions with cellulose fiber in the presence of hydroxyl radical scavengers

To determine if cellulose fibers in filter paper are affected by UV light alone and by hydroxyl radicals, three control reactions were conducted. The filter paper used for Control VII was untreated. For Control VIII, the filter paper was irradiated with UV light only. The filter paper in Control IX was conducted in the presence of both UV light and hydrogen peroxide. The UV light irradiation time was 120 minutes at 254 nm. After the reaction, the cellulose fibers were dried in a conditioning room overnight, were mixed with deionized water and cupriethylenediamine (CED) under nitrogen, and used for the viscosity analysis. A Cannon-Fensk routine viscometer (No. 50) was used for the viscosity measurement. Based on the traveling times of the mixture and CED and the consistency of the analyte, we calculated intrinsic viscosity [η] of the cellulose fibers. From the intrinsic viscosity, Degree of Polymerization (DP) was calculated as followed: $DP^{0.9}=1.65\ [\eta]$ (Evans and Willis, 1989). Also Chain Scission Number (CS) were obtained using DPs of cellulose fibers before and after treatment as following equation:

$$CS = DP_{Before}[(1/DP_{After}) - (1/DP_{Before})]$$ (Bouchard *et al.*, 1997)

Table 3.14 contains the results of the intrinsic viscosity, degree of polymerization, and chain scission number in controls and the UV/H_2O_2 reactions in the presence of hydroxyl radical scavengers.

Table 3.14. The results of controls and the UV/H_2O_2 reactions in the presence of *tert*-BuOH and 2-propanol for cellulose fiber.

	Intrinsic Viscosity [η]	Degree of Polymerization (DP)	Chain scission number
Control VII	**684.7 ± 6.1**	**2465.2 ± 24.7**	**N/A**
Control VIII	**581.1 ± 4.7**	**2058.5 ± 20.6**	**N/A**
Control IX	**214.9 ± 6.4**	**680.7 ± 22.3**	**2.0 ± 0.10**
***tert*-BuOH**	**305.1 ± 9.8**	**1005.1 ± 35.9**	**1.0 ± 0.07**
2-Propanol	**340.7 ± 11.6**	**1134.1 ± 40.0**	**0.8 ± 0.06**

- All of the data are the average of triplicates.
- Control VII: Untreated filter paper.
- Control VIII: UV irradiated filter paper.
- Control IX: UV irradiated paper in the presence of H_2O_2.

It was found that the intrinsic viscosity of filter paper in Control VIII was lower than that in Control VII. This indicates that the filter paper was degraded by UV light. However, the carbohydrate models, methyl-β-D-glucoside and methyl-β-D-cellobioside, were not degraded by UV light alone, as shown in the previous sections in this study. The UV degradation of the filter paper must be caused by the reaction between the chromophores existing in the filter paper, such as binders, and UV light. Therefore, it is unlikely that hydroxyl radicals produced this change. Therefore, the viscosity changes in filter paper by hydroxyl radicals are compared with the viscosity of filter paper in reaction Control VIII.

In Control IX, the intrinsic viscosity of the filter paper was decreased substantially compared to reaction VIII. This result indicates that cellulose chains in the filter paper in Control IX were significantly shortened by the photochemically produced hydroxyl radicals. According to the results, each cellulose chain was cleaved twice by hydroxyl radicals during the reaction, so that an average cellulose chain consists of about 677 glucose units.

Two hydroxyl radical scavengers, *tert*-BuOH and 2-propanol, were used in the UV/H_2O_2 system to determine the inhibition in the degradation of cellulose fibers.

Compared to Control IX, the intrinsic viscosity of filter paper increased in the presence of both *tert*-BuOH and 2-propanol as shown in Table 3.14.

These results suggest that *tert*-BuOH and 2-propanol scavenged the hydroxyl radicals, so that the degradation of cellulose chains in filter paper was limited. Also, as in the UV/H_2O_2 reactions with methyl-β-D-glucoside and methyl-β-D-cellobioside, 2-propanol showed stronger protection of the filter paper from the degradation by hydroxyl radicals than *tert*-BuOH.

The CS number in the treatment of *tert*-BuOH indicates that each cellulose chain was cleaved once by hydroxyl radicals. This means that *tert*-BuOH inhibited hydroxyl radical attack on the cellulose chain, so that each cellulose chain contains about 1,012 glucose units. In the presence of 2-propanol, the inhibition was greater, and thus it resulted in a smaller CS number (0.8) and longer cellulose chains, containing about 1,141 glucose units, than the ones treated with *tert*-BuOH.

The evidence of the radical scavenging effects of *tert*-BuOH and 2-propanol is the formation of acetone in the reaction solutions as described previously. Acetone was

found in the two reaction solutions in these experiments and the SPME-GC/MS chromatograms and spectra are included in Appendix D.

CHAPTER 4

CONCLUSIONS AND SUGGESTED WORK

4.1. Conclusions

In the experiments to investigate the oxidative degradation of lignin and carbohydrates occurring during oxygen delignification, the pressurized oxygen reactions with guaiacol (a model lignin), methyl-β-D-glucoside (a carbohydrate model), and the combination of the two support the previous notion that lignin affects the degradation of carbohydrates during oxygen delignification. In the presence of guaiacol, methyl-β-D-glucoside was degraded significantly in the pressurized oxygen reactions under alkaline conditions, whereas no methyl-β-D-glucoside was decomposed in the absence of guaiacol. According to the previous suggestions, guaiacol reacts with molecular oxygen to produce phenoxy radical by hydrogen atom abstraction and demethylation. The phenoxy radicals react with superoxide radicals, and the aromatic ring is cleaved subsequent to production of organic acids. Also, molecular oxygen is converted to hydroperoxy radical by hydrogen atom abstraction from the hydroxyl group in guaiacol. This hydroperoxy radical can be converted into various other oxygen species *via* proton and electron transfer in solution. Thus, methyl-β-D-glucoside could be degraded by hydroxyl radicals originating from the molecular oxygen and guaiacol. As strong evidence for radical reactions occurring in these experiments, the reaction products from the degradation of guaiacol were the same as the products in the UV/H_2O_2 reactions which were used to specifically generate hydroxyl radicals. However, the exact pathway of methyl-β-D-glucoside oxidation under these conditions is unknown because we were unable to identify the

products derived from methyl-β-D-glucoside. This may result from the difficulty of silylation of the products. Therefore, we cannot definitely state that hydroxyl radical is the culprit.

The results of UV/H_2O_2 reactions with methyl-β-D-glucoside, methyl-β-D-cellobioside, and cellulose fibers reinforce the previously proposed oxidative reaction mechanisms of carbohydrates during oxygen delignification in our group. The reaction products were the same as in the previous research in our laboratory, in that hydroxyl radicals cleave the carbohydrates at the anomeric position to degrade them into smaller aldoses and aldonic acids.

The results of UV/H_2O_2 reactions in the presence of hydroxyl radical scavengers, *tert*-BuOH and 2-propanol, strongly support the idea that hydroxyl radicals are the major oxygen species to degrade methyl-β-D-glucoside and methyl-β-D-cellobioside. The hydroxyl radical scavengers retard the hydroxyl radical attack on methyl-β-D-glucoside and methyl-β-D-cellobioside, so that less methyl-β-D-glucoside and methyl-β-D-cellobioside are degraded in the UV/H_2O_2 reactions. Furthermore, *tert*-BuOH and 2-propanol protect the filter paper from cellulose chain cleavage by hydroxyl radicals.

The qualitative analyses of the organic acids derived from methyl-β-D-glucoside provide evidence about our previously proposed reaction pathways. They support the formation of D-gluconic and D-arabinoic acid from D-glucose and D-arabinose *via* acyl hydrogen atom abstraction by hydroxyl radicals. Although the reproducibility of the analysis was not good because of difficulties in sample preparation, there were still trends to interpret the differences in the formation of the organic acids. When the

radical scavengers are used in the reactions, the quantities of D-gluconic, D-arabinoic, and tartaric acid significantly decreased. This is consistent with the scavenging of hydroxyl radicals by *tert*-BuOH and 2-propanol, so that fewer radicals are available to react with the acyl hydrogen atoms of D-glucose and D-arabinose. The mechanism for the formation of tartaric acid is not yet worked out, but the decreased quantity is strong evidence that hydroxyl radicals have an important role in the formation of tartaric acid.

Of the two hydroxyl radical scavengers treated in this study, 2-propanol has a stronger scavenging effect than *tert*-BuOH. 2-propanol gave better protection of methyl-β-D-glucoside, methyl-β-D-cellobioside, and cellulose fibers.

4.2. Suggested work

In the study of the pressurized oxygen reaction with the mixture of guaiacol and methyl-β-D-glucoside in alkaline conditions, it is still question if methyl-β-D-glucoside was degraded by hydroxyl radicals. To answer that question, a direct determination of the reaction solution without any work-up or silylation will be desirable. To perform this, LC/MS analysis can be suggested. In LC/MS analysis, the sample solution can be used directly. One other suggestion to investigate if hydroxyl radicals are generated during the reactions, is using *tert*-BuOH and 2-propanol (hydroxyl scavengers) in the reaction solutions. If hydroxyl radicals are present, we can determine acetone produced from the reaction shown in the previous section by the SPME method.

Also, there was difficulty in the quantitative analysis of the organic acids derived from methyl-β-D-glucoside in the UV/H_2O_2 reactions. That was probably caused by experimental error in silylation of the samples. LC/MS analysis will be an answer for this.

Although this study provided strong support for our previous mechanisms in the oxidative degradation of carbohydrates by photochemically generated hydroxyl radicals, another method that would provide stronger evidence in the hydroxyl radical attack on the anomeric position in carbohydrates is possible. The suggestion is to use labeled hydrogen peroxide ($H_2{}^{18}O_2$) in the UV/H_2O_2 reactions. $H_2{}^{18}O_2$ will give labeled hydroxyl radicals ($H^{18}O^{\cdot}$) by the irradiation of UV light at 254 nm. Thus, the labeled D-glucose and/or D-cellobiose could be detected by GC/MS or LC/MS as products in the UV/H_2O_2 reactions with methyl-β-D-glucoside and methyl-β-D-cellobioside.

CHAPTER 5

EXPERIMENTAL PROCEDURES

5.1. Materials

The following chemicals were used for pressurized oxygen reactions, UV/H_2O_2 reactions, synthesis of the model carbohydrate, and as authentic standards for HPLC, GC/MS, and viscosity analysis: Acetone (EM Science), Acetic anhydride (Fisher Scientific), D-Arabinose (ICN), N,O-bis(trimethylsiyl)trifluoroacetamide (BSTFA) (Supelco), bromine (Aldrich), *tert*-buthyl alcohol (Aldrich), n-buthylamine (Aldrich), calcium chloride (Aldrich), calcium sulfate (Aldrich), D-cellobiose (Sigma), α-D-cellobiose octaacetate (Fluka), chloroform (EM Science), cupriethylenediamine (LabChem), D-erythrose (Aldrich), ethanol (Quantum), ether (Fisher Scientific), filter paper (Whatman 1), L-fucose (Fluka), fumaric acid (Aldrich), D-gluconic acid (Aldrich), D-gluconic acid lactone (Sigma), (Aldrich), D-glucose (Sigma), D-glyceraldehyde (Aldrich), glycolic acid (Aldrich), guaiacol (Aldrich, 98%), hydrobromic acid (33%) in acetic acid (Acros), hydrogen peroxide (30%) (Aldrich), iodine (Aldrich), magnesium sulfate (Fischer Science), maleic acid (Aldrich), malic acid (Aldrich), malonic acid (Aldrich), methanol (EM Science), methyl-α-D-glucopyranoside (Aldrich), methyl-β-D- glucopyranoside (Sigma), methylene chloride (EM Science), oxalic acid (Aldrich), 2-propanol (Fisher Scientific), 4-propyl guaiacol (Aldrich), pyridine (Fluka), silver carbonate (Aldrich), sodium bicarbonate (Aldrich), sodium hydroxide (Aldrich), 50% sodium hydroxide (Alfa Aesar), sodium

sulfate (Aldrich), sodium thiosulfate (Fisher Scientific), succinic acid (Aldrich), Sylon BTZ (Supelco), DL-tartaric acid (Aldrich).

5.2. Preparation of buffer solutions

For UV/hydrogen peroxide reactions, three different buffers were used. Preparation of buffer solutions was based on the literature by Robinson (1981). Each of 5.0, 6.2, 12.2, and 13.8 mL sodium hydroxide solutions (2 M) was added to four 50 mL aliquots of 1 M sodium bicarbonate solutions, and the mixtures were diluted to 100mL with nanopure water for pH 9.6, 9.7, 10.1, and 10.2, respectively.

5.3. Synthesis procedures

To perform this study, methyl-β-D-cellobioside, D-cellobionic acid, D-arabinoic acid, D-erythronic acid, and D-glyceric acid were synthesized. The synthesis procedure of methyl-β-D-cellobioside was adopted from the method of Wolform and Haq (1964).

The synthesis procedures for the aldonic acids were those described by Guay (1999).

5.3.1. Methyl-β-D-cellobioside

The synthesis of methyl-β-D-cellobioside consists of three steps: Step one : α-D-cellobiose octaacetate to 1-bromo-1-deoxycellobiose heptaacetate, Step two : 1-

bromo-1-deoxycellobiose heptaacetate to methyl-β-D-cellobioside heptaacetate, and Step three : methyl-β-D-cellobioside heptaacetate to methyl-β-D-cellobioside.

α-D-Cellobiose octaacetate (2 g; 3.0 mmol) was dissolved in 15 mL of hydrobromic acid (33%) in acetic acid and stirred for 90 minutes at ambient temperature in a 250 mL round bottom flask. At the end of the reaction, the solution was dissolved in 100 mL chloroform. The mixture was washed twice successively with 25 mL nanopure water, with 10% sodium bicarbonate, and with nanopure water again. The chloroform layer was then dried over sodium sulfate, and concentrated to approximately 5 mL. The concentrated solution was transferred to a 50 mL Erlenmyer flask, with addition of four drops of ethyl ether to initiate crystallization, and kept in a cold water bath for twelve hours. The crystals were filtered, washed with several drops of cold ethyl ether, and collected. The crystals were dissolved in methylene chloride for the determination of purity of the crystals by GC/MS. The chromatogram and spectrum are in Appendix A.

1-Bromo-1-deoxycellobiose heptaacetate (1.5 g; 2.1 mmol) was dissolved in a mixture of chloroform (30mL) and methanol (30 mL) in a 250 mL round bottom flask. Calcium sulfate (10 g) was added to the mixture as drying reagent. Silver carbonate (2.0 g; 7.3 mmol) and a small crystal of iodine were added. The flask was wrapped with aluminum foil to block light, and guarded by a calcium chloride drying tube. After stirring for 24 hours, the mixture was filtered and washed with chloroform, followed by solvent removal by rotary evaporation. The residue was dissolved in 50 mL chloroform and washed twice with 25 mL aliquots of 10% sodium thiosulfate and then twice with 25 mL nanopure water. Methyl-β-D-cellobioside

heptaacetate was crystallized in methanol after solvent removal. Its purity was determined by GC/MS. The chromatogram and spectrum are in Appendix A.

Methyl-β-D-cellobioside heptaacetate (400 mg; 0.6 mmol) was dissolved in 20 mL methanol with 0.5 mL n-butylamine (5.1 mmol) in a 200 mL round bottom flask, guarded with a calcium chloride drying tube. The solution was refluxed for six hours. Crystals of methyl-β-D-cellobioside were collected by filtration after cooling the solution. To determine the purity of methyl-β-D-cellobioside with GC/MS, it was silylated with Sylon BTZ. The chromatogram and spectrum are in Appendix A.

5.3.2. D-Cellobionic acid

Preparation of D-cellobionic acid was performed by bromine oxidation of D-cellobiose. 100 mg D-cellobiose (0.3 mmol), 0.0155 mL bromine (0.3 mmol), and 10 mL 0.1 M pH 9.6 buffer were placed in a 20 mL vial with a magnetic stir bar. The solution mixture was stirred for 40 hours at ambient temperature. The solution was neutralized to pH ~7.2 with 1 M sodium hydroxide after the reaction. The neutralized solution was freeze-dried and silylated with Sylon BTZ for GC/MS analysis, which is shown in Appendix A.

5.3.3. D-Arabinoic acid

Preparation of D-arabinoic acid was performed by bromine oxidation of D-arabinose. 50 mg D-arabinose (0.3 mmol), 0.0175 mL bromine (0.3 mmol), 5 mL nanopure water, and 5 mL 0.1 M pH 9.6 buffer were placed in a 20 mL vial with a

magnetic stir bar. The solution mixture was stirred for 40 hours at ambient temperature. The solution was neutralized to pH ~7.2 with 1 M sodium hydroxide after 40 hours of the reaction. The neutralized solution was freeze-dried and silylated with Sylon BTZ for GC/MS analysis, shown in Appendix A.

5.3.4. D-Erythronic acid

Preparation of D-erythronic acid was performed by bromine oxidation of D-erythrose. 50 mg D-erythrose (0.4 mmol), 0.0225 mL bromine (0.4 mmol), 5 mL nanopure water, and 5 mL 0.1 M pH 9.6 buffer were placed in a 20 mL vial with a magnetic stir bar. The solution mixture was stirred for 40 hours at ambient temperature. The solution was neutralized to pH ~7.2 with 1 M sodium hydroxide after 40 hours of the reaction. The neutralized solution was freeze-dried and silylated with Sylon BTZ for GC/MS analysis, the results of which are shown in Appendix A.

5.3.5. D-Glyceric acid

Preparation of D-glyceric acid was performed by bromine oxidation of D-glyceraldehyde. 50 mg D-glyceraldehyde (0.6 mmol), 0.0300 mL bromine (0.6 mmol), 5 mL nanopure water, and 5 mL 0.1 M pH 9.6 buffer were placed in a 20 mL vial with a magnetic stir bar. The solution mixture was stirred for 40 hours at ambient temperature. The solution was neutralized to pH ~7.2 with 1 M sodium hydroxide after 40 hours of the reaction. The neutralized solution was freeze-dried and silylated with Sylon BTZ for GC/MS analysis, which is shown in Appendix A.

5.4. Procedures of the pressurized alkali-oxygen reaction

There were two controls in the pressurized alkali-oxygen reaction. One (Control I) was guaiacol (0.1625 mL; 1.5 mmol) dissolved in 9.8375 mL NaOH solution (160 mM). The other (Control II) was methyl-β-D-glucoside (0.3 grams; 1.5 mmol) dissolved in 10 mL NaOH solution (13mM). Sample solutions were designed in different molar ratios between methyl-β-D-glucoside and guaiacol. There were two batches of sample reactions. One batch had the ratios of 1 : 1, 2 : 2, and 1 : 4 of guaiacol to methyl-β-D-glucoside. These solutions contained 0.1625 mL guaiacol plus 0.3 (1.5), 0.6 (3.1), and 1.2 (6.2) grams (mmol) of methyl-β-D-glucoside in 9.8375 mL NaOH solutions (170 mM), respectively. The other batch had the ratios of 2 : 1 and 2 : 2 of guaiacol to methyl-β-D-glucoside and contained 0.3250 mL guaiacol (3.0 mmol) plus 0.3, and 0.6 grams of methyl-β-D-glucoside in 9.6750 mL NaOH solutions (320 mM), respectively. The total volume of each solution was 10 mL. The initial pHs of the solutions were 12.

Each solution was placed in a 60 mL borosilicate Griffin-Worden pressure vessel (KONTES) with a magnetic stir bar. The reaction vessel was wrapped with aluminum foil to block out the light, and was placed in an oil bath that was pre-heated to 95 °C. The reactions were conducted under 65 psi of oxygen pressure for 4 hours. The reaction solutions were stirred during the reaction. After the reaction, the solution in the vessel was cooled down in the air for 30 minutes before analyzed. The cool reaction solution was divided into two equal portions; one half was used for the analysis of guaiacol and its derivatives, and the other half was used for the analysis of

methyl-β-D-glucoside and its derivatives. The portion for guaiacol analysis was acidified to pH 1 with HCl (6 M). All the reactions were conducted in triplicate.

5.5. UV/hydrogen peroxide reaction procedures: Hydroxyl radical generation system and radical scavengers

A Rayonet photochemical reactor was used to produce hydroxyl radicals by ultraviolet (UV) light irradiation of hydrogen peroxide. In the Rayonet reactor, twelve lamps were used to emit UV light at 254 nm. There were three different reactions for methyl-β-D-glucoside, methyl-β-D-cellobioside, and cellulose fiber. The target pH of all the solutions was 9.5. Each solution was prepared in a 20 mL quartz tube before it was placed in the reactor. The temperature inside of the reactor was about 35 °C during the reactions.

The batch of reactions of methyl-β-D-glucoside contained two control reactions and sample reactions. One (Control III) of the controls was the blank reaction of methyl-β-D-glucoside in pH 9.6 buffer solution. The other control (Control IV) was the reaction of methyl-β-D-glucoside in the presence of hydrogen peroxide in pH 10.1 buffer solution. The sample reaction solutions included the mixtures of methyl-β-D-glucoside, hydrogen peroxide, and *tert*-butanol or 2-propanol in buffer solutions with different molar ratios.

The details are shown in table 5-1.

Table 5.1. Reaction mixtures of methyl-β-D-glucoside (MβG) in UV treated reactions.

	MβG (g) (mmol)	H_2O_2 (mL) (mmol)	*t*-BuOH (mL) (mmol)	Buffer (mL) (pH)
Control III	0.30 (1.5)	0	0	10.00 (9.6)
Control IV	0.30 (1.5)	1.15 (11.3)	0	8.85 (10.1)
1 : 1*	0.30 (1.5)	1.15 (11.3)	0.15 (1.6)	8.70 (10.1)
1 : 2*	0.30 (1.5)	1.15 (11.3)	0.30 (3.1)	8.55 (10.1)
1 : 4*	0.30 (1.5)	1.15 (11.3)	0.60 (6.3)	8.25 (10.1)
	MβG (g) (mmol)	**H_2O_2 (mL) (mmol)**	**2-Propanol (mL) (mmol)**	**Buffer (mL) (pH)**
1 : 1*	0.30 (1.5)	1.15 (11.3)	0.12 (1.6)	8.73 (10.1)
1 : 2*	0.30 (1.5)	1.15 (11.3)	0.24 (3.1)	8.62 (10.1)
1 : 4*	0.30 (1.5)	1.15 (11.3)	0.48 (6.2)	8.38 (10.1)

* The ratios were the molar ratios of methyl-β-D-glucoside to *tert*-BuOH or 2-Propanol

The total volume was 10 mL in each solution. The molar ratio of methyl-β-D-glucoside to hydrogen peroxide was 1 : 8 in every solution mixtures, except Control III. The run time of each reaction was 45 minutes. All the reactions were run in triplicate.

The reaction solution mixtures of methyl-β-D-cellobioside were designed in a similar way to those of methyl-β-D-glucoside as shown in Table 5-2, except one more reaction ratio (1 : 8) of methyl-β-D-cellobioside to *tert*-butanol or 2-propanol. The total

Table 5.2. Reaction mixtures of methyl-β-D-cellobioside (MβC) in UV treated reactions.

	MβC (g) (mmol)	H_2O_2 (mL) (mmol)	*t*-BuOH (mL) (mmol)	Buffer (mL) (pH)
Control V	0.10 (0.3)	0	0	3.3300 (9.6)
Control VI	0.10 (0.3)	0.2300 (2.3)	0	3.1000 (9.7)
1 : 1*	0.10 (0.3)	0.2300 (2.3)	0.0270 (0.3)	3.0730 (9.7)
1 : 2*	0.10 (0.3)	0.2300 (2.3)	0.0540 (0.6)	3.0460 (9.7)
1 : 4*	0.10 (0.3)	0.2300 (2.3)	0.1100 (1.1)	2.9900 (9.7)
1 : 8*	0.10 (0.3)	0.2300 (2.3)	0.2200 (2.3)	2.8800 (9.7)
	MβC (g) (mmol)	**H_2O_2 (mL) (mmol)**	**2-Propanol (mL) (mmol)**	**Buffer (mL) (pH)**
1 : 1*	0.10 (0.3)	0.2300 (2.3)	0.0215 (0.3)	3.0785 (9.7)
1: 2*	0.10 (0.3)	0.2300 (2.3)	0.0430 (0.6)	3.0140 (9.7)
1 : 4*	0.10 (0.3)	0.2300 (2.3)	0.0860 (1.1)	2.9710 (9.7)
1 : 8*	0.10 (0.3)	0.2300 (2.3)	0.1720 (2.2)	2.9280 (9.7)

* The ratios were the molar ratios of methyl-β-D-cellobioside to *tert*-BuOH or 2-Propanol

volume of the solutions was 3.3 mL. The molar ratio of methyl-β-D-cellobioside to hydrogen peroxide was 1 : 8 in the mixtures. The run time of each reaction was 45 minutes. All the reactions were conducted in triplicate.

To conduct the experiments with cellulose fiber, about 5 grams of filter paper was blended in 100 mL nanopure water until the fibers of filter paper were totally separated. The fibers were filtered and washed with acetone to make a fluffy pad. The pad was placed in a conditioning room at 25 °C overnight. The amount of filter

paper used in each reaction was15 mg, which was measured in the conditioning room. There were three control and two sample reactions in the experiments with filter paper. Each reaction mixture was prepared in a 20 mL quartz tube before UV treatment in a Rayonet reactor.

Control V contained 15 mg filter paper in 5 mL pH 9.6 buffer solution. Control VI included 15 mg filter paper and 1 mL (10 mmol) hydrogen peroxide (30 %) in 4 mL pH 10.2 buffer solution. One sample reaction contained 15 mg filter paper, 3.12 mL *tert*-(33 mmol) BuOH, 1.00 mL (10 mmol) hydrogen peroxide (30 %) , and 0.88 mL pH 10.2 buffer. The other sample reaction contained 15 mg filter paper, 2.51 mL (33 mmol)

2-propanol, 1.00 mL (10 mmol) hydrogen peroxide, and 1.49 mL pH 10.2 buffer. For all the mixtures, buffer solution was added first to separate all the fibers by stirring the solution. Subsequently, other reagents were added into the stirred mixtures. The total volume in each reaction mixture was 5.00 mL. For each case, twelve reactions were run. The reaction time was 120 minutes. A stir plate was placed into the bottom of the reactor to stir the mixtures during the reaction time. After the reaction finished, the solution was filtered and washed with nanopure water and acetone. The collected substrates from the twelve reactions were combined together and placed in the conditioning room overnight. Then, the filter paper sample was divided into three portions of 50 mg for the triplicate viscosity analysis.

5.6. High performance liquid chromatography (HPLC) analysis

Two sets of HPLCs were used to carry out analyses in this study. For carbohydrate analysis, the HPLC was composed of Hewlett Packard 1100 series pumps, degasser, and a Hewlett Packard 1049A electrochemical detector. A Dionex Carbopac PA1 column (4 x 250 mm) with a guard column (Dionex Carbopac PA1 Guard) was used to separate carbohydrate samples as Guay (1999) had modified the method of Wright *et al.* (1996). The mobile phase was 100 % nanopure water with the flow rate of 1.0 mL/min.. After the separation, the column was washed with 350 mM sodium hydroxide for 1.9 minutes with the flow rate of 1.0 mL/min.. L-Fucose was used as an internal standard for quantitation of carbohydrates. For the determination of the percent recovery of methyl-β-D-glucoside in the pressurized oxygen reaction and UV/H_2O_2 reactions, each HPLC sample contained 0.0335 mL reaction solution, 0.4000 mL (9.75×10^{-3} mmol) L-fucose (4 mg/mL), and 1.5665 mL nanopure water. The run time of analysis was 12 minutes. In the determination of the percentages of glucose and arabinose isolated, the reaction solution (0.8000 mL) was mixed with 0.2000 mL (4.87×10^{-3} mmol) L-fucose (4 mg/mL). The percentages of glucose and arabinose isolated were calculated based on the concentration of the starting material (methyl-β-D-glucoside). The run time of analysis was 35 minutes. The percent recovery of methyl-β-D-cellobioside and the percentages of methyl-β-D-glucoside isolated in UV/H_2O_2 reactions were determined at the same time in the mixture of 0.0335 mL reaction mixture, 0.4000 mL (9.75×10^{-3} mmol) L-fucose (4mg/mL), and 1.5665 mL nanopure water. The run time of analysis was 12 minutes.

Percentages of glucose and arabinose isolated were calculated in the mixture of 0.3000 mL reaction mixture, 0.2000 mL (4.87×10^{-3} mmol), and 0.5000 mL nanopure water. The percent formation of methyl-β-D-glucoside, glucose, and arabinose were calculated based on the concentration of the starting material (methyl-β-D-cellobioside). From all the percentages calculated, the actual amounts of each compound degraded and isolated were calculated in millimoles. The injection volume was 20 μL in each run. The run time of analysis was 35 minutes.

Guaiacol analyses were conducted on a Hewlett Packard 1090 series HPLC that was equipped with an automatic sampler (HP 1090 series II) and UV-detector. A C8 column (Phenomenex Prodigy 5μm 150 x 4.60 mm) was used for separation of guaiacol from the reaction solutions. The mobile phase was 60:40 of 0.1 % acetic cid:acetonitrile.

The flow rate was 1.0 mL/min. The injection volume was 10μL and the draw speed was 16.7 μL/min.. The column temperature was 40 °C. The detection wavelengths were 254 and 280 nm. The run time of analysis was 12 minutes. Quantitation of guaiacol was performed using 4-propylguaiacol (4-PG) as an internal standard. The HPLC chromatograms of the standard and reaction solutions were attached in Appendix B. For determination of guaiacol recovery in the pressurized oxygen reaction, 0.01 mL reaction solution, 0.50 mL (0.0016 mmol) 4-PG (0.0032 M), and 0.49 mL NaOH (0.16 M) were mixed in a 2 mL vial thoroughly before the injection.

5.7. Solid phase microextraction (SPME) procedure

The SPME technique was used to determine *tert*-butanol, 2-propanol, and acetone which were not detectable in the GC/MS method. The SPME fiber used in this study was Carbowax/Divinylbenzene (CW/DVB) (SUPELCO 57336-U, 70 μm). For sampling, 0.2 mL of the each aqueous reaction solution was transferred to a 2 mL glass vial capped tightly with a septum. The solution in the vial sat for twenty minutes at 35 °C in a heated sand bath prior to sampling. For headspace sampling, the CW/DVB fiber was introduced into the vial by piercing through the septum. The CW/DVB fiber was exposed to the sample matrix headspace for five minutes to extract the target analytes. Then the fiber was inserted into the injection port of GC/MS using a SPME inlet guide (SUPELCO, 57356-U). The GC/MS conditions for SPME are described in the next section.

5.8. Gas chromatography and mass spectroscopy (GC/MS) analysis

The GC/MS used in this study was a Hewlett Packard 6890 series with an automatic sampler (HP 6890). The GC column was a HP-5% crosslinked phenyl methylsiloxane column (ID 0.25 mm, film thickness 0.25 μm, and length 30.0 m). For the SPME samples, a DB-WAX column (J & W Scientific, ID 0.25 mm, film thickness 0.5 μm) was used. The length of the column was shortened to approximately 15 meters from the original length (30 meters). The injection sleeve used was a Hewlett Packard 4 mm ID inlet liner packed with deactivated glass wool, except in the case of the SPME analysis. The injection sleeve was used with a

Therm-O-Ring seal (Supelco). For SPME samples, a Hewlett Packard 0.75 mm ID injection sleeve was used with a Therm-O-Ring seal (Supelco). The septum in the injection port was a pre-pierced 11 mm SOLSEPT (Hewlett Packard). The ion source in the MS was an electron impact (70eV). The injection port temperature of the GC/MS was 250 °C and the detector temperature was 280 °C. There were five GC/MS temperature programs used for five different analytes. The analytes are guaiacol, methyl-β-D-glucoside, methyl-β-D-cellobioside and their derivatives, intermediate products during synthesis of methyl-β-D-cellobioside, and SPME samples.

In the analysis of guaiacol and its derivatives, the initial oven temperature was 70 °C with 6 minutes of holding time. The temperature then was increased to 250 °C at a rate of 10 °C/min. The holding time at 250 °C was 10 minutes to make the total run time 34 minutes. The acidified solution, which is mentioned in the section of the pressurized oxygen reaction, was extracted with methylene chloride. The solute of the methylene chloride layer was dried over magnesium sulfate, and the solvent was removed by rotary evaporation to analyze the water insoluble substrates. The residue was dissolved with 1.5 mL methylene chloride and was transferred to a 2 mL vial before GC/MS injection. The aqueous layer was freeze-dried for 36 hours. The products were extracted with acetone from the remaining salts. After the acetone was removed by a rotary evaporator, the residue was silylated with 0.2 mL N,O-bis(trimethylsiyl)trifluoroacetamide (BSTFA) for one hour at 60 °C. The silylated products were mixed with 1 mL methylene chloride in a 2 mL vial, and injected to GC/MS.

For methyl-β-D-glucoside and its derivatives, the initial oven temperature and holding time were the same as the case of guaiacol analysis. After the initial six minutes, the oven temperature was increased to 175 °C at a rate of 5 °C/min., and then to 240 °C at a rate of 2.5 °C/min.. The total run time was 53 minutes. The reaction solutions from the pressurized oxygen reaction and UV/H_2O_2 reaction were freeze-dried for 36 hours for GC/MS analysis. The residues were extracted with 2 mL pyridine from the salts. Sylon BTZ (1 mL) was added to the pyridine phase solution for silylation. After waiting for 10 minutes, 0.2 mL of the silylated mixture was transferred to a 2 mL vial, and diluted with 1 mL pyridine before injection to GC/MS. Additionally, for analysis of methyl-β-D-glucoside derivatives from the solutions mixture in the pressurized oxygen reaction, acetylation was performed. After the reaction, dilute NaOH solution was added to the mixture to adjust the pH of the solution to 12. The mixture was extracted with CH_2Cl_2. The solution was divided into aqueous and organic phase. For the organic phase, which will contain neutral compounds, the solvent was removed by rotary evaporation. The residue was mixed with 5 mL acetic anhydride and 0.5 mL pyridine, and the reaction was conducted over night at 50 °C. The aqueous phase, which is expected to contain organic acids, was mixed with dilute HCl until the pH of solution reach to 5 and extracted with CH_2Cl_2. From the organic phase, CH_2Cl_2 was removed by rotary evaporation. The residue was mixed with 5 mL acetic anhydride and 0.5 mL pyridine, and the reaction was conducted over night at 50 °C. From the acetylated solutions, the remaining acetic anhydride, pyridine, and acetic acid were removed by vacuum evaporation at 70 °C. The final products were dissolved in CH_2Cl_2 for GC/MS analysis.

In the case of methyl-β-D-cellobioside and its derivatives, the initial oven temperature, holding time, and the temperature program up to 240 °C were the same as for the methyl-β-D-glucoside-related samples. After 240 °C, the oven temperature was increased to 300 °C at a rate of 10 °C/min. with 3 minutes of holding time at 300 °C. The total run time was 62 minutes. The reaction products were silylated and analyzed simultaneously to the methyl-β-D-glucoside samples.

In the analyses of α-D-cellobiose octaacetate, 1-bromo-1-oxycellobiose heptaacetate, and methyl-β-D-cellobioside heptaacetate, the initial oven temperature was 150 °C with no holding time. The temperature was increased to 200 °C at a rate of 8 °C/min. with 6 minutes holding time at 200 °C and to 300 °C at a rate of 25 °C/min.. The holding time at 300 °C was 6 minutes. The total run time was 16.25 minutes.

All GC/MS methods mentioned above were conducted with a 10 to 1 split mode.

For SPME samples, the oven temperature was 200 °C with 10 minutes of holding time, and then it was raised to 240 °C at a rate of 50 °C/min. The holding time at 240 °C was 1 minute. The total run time was 11.8 minutes. SPME samples were analyzed using a splitless mode.

5.9. Viscosity analysis

Filter paper was prepared as previously described in UV/H_2O_2 reaction procedure section. A Cannon-Fenske routine viscometer (Cannon Instrument Co., Viscometer No. 50) was used. The viscometer was placed into a water bath (25 °C) with the two

bubbles of the viscometer submerged before the viscosity samples were prepared. Each portion (50 mg) of the filter paper was torn into very small pieces manually, and placed into a 20 mL vial. Nanopure water (5 mL) was added to the vial, and the mixture was stirred for 15 minutes to disperse it, until it had no fiber bundles. Subsequently, cupriethylenediamine (CED) (5 mL) was added into the dispersed fiber mixture under nitrogen purging. The vial was capped tightly, and the solution mixture was stirred for another 15 minutes. After the stirring, the solution (7 mL) was transferred into the viscometer allowed to sit for 5 minutes to bring the solution to the bath temperature. The solution was drawn slightly above the top line on the viscometer using a suction rubber bulb. The travel time of the solution between the two lines in the viscometer was measured. To calculated intrinsic viscosity [η], the measured travel time (t) in seconds of the analyte, consistency (c) of the analyte, and the relative viscosity ($[\eta]_{rel} = t/T$) were determined. The "T" in the equation of relative viscosity is the travel time of CED only in the viscometer. The consistency of each analyte was 0.005 since 0.05 grams of filter paper was dispersed in 10 mL solution (5 mL nanopure water plus 5 mL CED). Once the relative viscosity was determined, the value of [η]c was found in the table of "the intrinsic viscosity at different values of relative viscosity" in the American Society for Testing and Materials (ASTM) D-1795. The value ([η]c) found was divided by the consistency (c) to calculate the intrinsic viscosity [η]. Additionally, Degree of Polymerization (DP) was calculated with the following equation: $DP^{0.9} = 1.65\ [\eta]$ (Evans and Willis, 1989). The Chain Scission number (CS) of the filter paper was calculated based on

the degree of polymerization (DP_o) of filter paper before the UV/H_2O_2 treatment and the DP after the treatment: $CS = DP_o\ [(1/DP)-(1/DP_o)]$ (Bouchard *et al.*, 1997).

REFERENCES

Afanas'ev, I.B., In Superoxide ion: Chemistry and Biochemical Implications, Volume I, CRC Press, Florida, 1989.

Afanas'ev, I.B., Grabovetskii, V.V., and Kuprianova, N.S., "Kinetics and mechanism of the reactions of superoxide ion in solution. V. Kinetics and mechanism of interaction of superoxide ion with vitamin E and ascorbic acid", J. Chem. Soc, Perkin Trans. 2, 281 (1987).

Afanas'ev, I.B., Grabovetskii, V.V., Kuprianova, N.S., and Gunar, V.I., "Kinetics and mechanism of the reaction of $O_2^{\cdot-}$ with ascorbic acid and α-tocopherol" in Superoxide and superoxide dismutase in chemistry, biology, and medicine, Rotilio, G. (ed.), p. 50, Elsevier, New York, 1986.

Afanas'ev, I.B. and Polozova, N.I., "The formation of semiquinones in the reaction of $O_2^{\cdot-}$ with hydroquinones", Zh. Org. Khim., 12, 1833 (1976).

Afanas'ev, I.B., Prigoda, S.V., Malzeva, T.Ya., and Samokhvalov, G.I., "One-electron transfer reactions between superoxide ion and quinones", Dokl. Akad. Nauk SSSR, 209, 376 (1973).

Atkinson, R., "Kinetics and mechanisms of the gas-phase reactions of the hydroxyl radical with organic compounds under atmospheric conditions", Chem. Rev., 69 (1985).

Atkinson, R., Perry, R.A., and Pitts, Jr., J.N., "Rate constants for the reaction of the OH radical with CH_3SH and CH_3NH_2 over the temperature range 299-426 °K", J. Chem. Phys., 66, 1578 (1977).

Atkinson, R., Perry, R.A., and Pitts, Jr., J.N., "Rate constants for the reaction of the OH radical with $(CH_3)_2NH$, $(CH_3)_3N$, and $C_2H_5NH_2$ over the temperature range 298-426 °K", J. Chem. Phys., 68, 1850 (1978).

Barnes, A.R. and Sugden, J.K., "The hydroxyl radical in aqueous media", Pharm. Acta Helv., 61, 218 (1986).

Biermann, C.J., Handbook of Pulping and Papermaking, 2nd Edition, p. 32-33, Academic Press, Inc., San Diego, 1996.

Bouchard, J., Morelli, E., and Berry, R., "Gas-phase addition of methanol or acetic acid with ozone in high consistency ozone bleaching of softwood kraft pulp", Paprican report PPR 1305 (1997).

Brunow, G., University of Helsinki, Website: www.helsinki.fi/~orgkm_ww/lignin_structure.html, 1998.

Buxton, G.V., Greenstock, C.L., Helman, W.P., and Ross, A.B., "Critical review of rate constants for reactions of hydrated electrons, hydrogen atoms and hydroxyl radicals ($^{\cdot}OH/^{\cdot}O^-$) in aqueous solution", J. Phys. Chem. Ref. Data, 17, 513 (1988).

Chitose, N., Katsumura, Y., Domae, M., Zuo, Z., Murakami, T., and La Verne, J.A., "Radiolysis of aqueous solutions with pulsed helium ion beams. 3. Yields of OH radicals and the sum of e_{aq}^- and H atom yields determined in methyl viologen solutions containing formate", J. Phys. Chem. A, 103, 4769 (1999).

Cohen, G., "The Fenton reactions" in Handbook of Methods for Oxygen Radical Research, Greenwald, R.A. (ed.), p. 55, CRC Press, Florida, 1985.

Collaman, J. P., "Synthetic models for the oxygen-binding hemoproteins", Acc. Chem. Res. 10, 265 (1977).

Dietz, R., Forno, A.E.J., Larcombe, B.E., and Peover, M.E., "Nucleophilic reactions of electro-generated superoxide ion", J. Chem. Soc. B, 816 (1970).

Dixon, W.T., Norman, R.O.C., and Buley, A.L., "Electron resonance studies of oxidation. Part II. Aliphatic acids and substituted acids", J. Chem. Soc., 3625 (1970).

Evans, R. and Willis, A.F.A., "Cellulose molecular weight determined by viscometry", J. Appl. Polym. Sci., 37, 2331 (1989).

Forrester, A.R. and Purushotham, V., "Mechanism of hydrolysis of ester by superoxide", J. Chem. Soc., Chem. Commun., 1505 (1984).

Frimer, A., "The organic chemistry of superoxide anion radical" in Superoxide Dismutase, Vol. II, Chapter 5, p. 83, Larry, W. (ed.), CRC Press, Florida, 1982.

Frimer, A. and Rosenthal, I., "Nucleophilic radical aromatic substitution with superoxide ion", Tetrahedron Lett., 2809 (1976).

Gibian, M.J., Sawyer, D.T., Ungermann, T., Tangpoonpholvivat, R., and Morrison, M.M., "Reactivity of superoxide ion with carbonyl compounds in aprotic solvents", J. Am. Chem. Soc., 101, 640 (1979).

Gierer, J., "Mechanisms of bleaching with oxygen-containing species" in Proceedings of The International Symposium on Wood and Pulping Chemistry, Vol. 1, p. 279, Paris, 1987.

Gierer, J., "The reactions of lignins with oxygen-containing species" in Proceedings of The InternationalSymposium on Wood and Pulping Chemistry, Vol. 1, p. 301, CTAPI, Beijing, 1993a.

Gierer, J., "The role of superoxide anion radicals ($O_2^{\cdot-}$) in delignification" in Proceedings of The International Symposium on Wood and Pulping Chemistry, Vol. 1, p. 240, CTAPI, Beijing, 1993b.

Gierer, J., "Formation and involvement of superoxide ($O_2^{\cdot-}/HO_2^{\cdot}$) and hydroxyl ($OH^{\cdot}$) radicals in TCF bleaching processes: A review[1]", Holzforschung, 51, 34-46 (1997).

Gierer, J., Reitberger, T., Yang, E., and Yoon, B.-H., "Formation and involvement of radicals in oxygen delignification studies by the autoxidation of lignin and carbohydrate model compounds", J. Wood Chem. Technol., 21, 313 (2001).

Gierer, J., Yang, E., and Reitberger, T., "On the significance of the superoxide radical ($O_2^{\cdot-}/HO_2^{\cdot}$) in oxidative delignification, studied with 4-*t*-butylsyringol and 4-*t*-butylguaiacol", Holzforschung, 48, 405 (1994).

Guay, D.F., "Mechanisms of oxidative degradation of carbohydrates during oxygen delignification", Ph.D. Thesis, University of Maine, 1999.

Guay, D.F., Cole, B.J.W., Fort Jr., R.C., Genco, J.M., and Hausman, M.C., "Mechanism of oxidative degradation of carbohydrates during oxygen delignification. I. Reaction of photochemically generated hydroxyl radicals with Me-β-D-glucoside", J. Wood. Chem. Technol., 20, 375 (2000).

Guay, D.F., Cole, B.J.W., Fort Jr.,R.C., Hausman, M.C., Genco, J.M., Elder, T.J., and Overly, K.R., "Mechanism of oxidative degradation of carbohydrates during oxygen delignification. II. Reaction of photochemically generated hydroxyl radicals with Me-β-D-cellobioside", J. Wood. Chem. Technol., 21, 67 (2001).

Hatakeyama, S. and Akimoto, H., "Reactions of OH radicals with methanethiol, dimethyl sulfide, and dimethyl disulfide in air", J. Phys. Chem., 87, 2387 (1983).

Hausman, M., "A mechanistic study of the degradation of lignin model compounds with oxygen species", Ph.D. Thesis, University of Maine, 1999.

Hislop, K.A. and Bolton, J.R., "The photochemical generation of hydroxyl radicals in the UV-vis/Ferrioxalate/H_2O_2 system", Environ. Sci. Technol., 33, 3119 (1999).

Hoare, D.E. and Peacock, G.B., "Studies of the reactions of hydroxyl radicals. II.", Proc. R. Soc. London, Ser. A., 291, 85 (1966).

Hoyermann, K. and Sievert, R., "Die reaktion von OH-radikalen mit propen: I. Bestimmung der primärprodukte bei niedrigen drücken", Ber. Bunsen-Ges. Phys. Chem., 83, 933 (1979).

Hoyermann, K. and Sievert, R., "Elementarreaktionen in der oxidation von alkene", Ber. Bunsen-Ges. Phys. Chem., 87, 1027 (1983).

Jefcoate, C.R.E. and Norman, R.O.C., "Electron spin resonance studies. Part XIV. Hydroxylation. Part III. Reactions of anisole, acetanilide, fluorobenzene, and some phenols with the titanium(III)-hydrogen peroxide system", J. Chem. Soc. B, 48 (1968).

Johnson, R.A., "Superoxide chemistry. A new, convenient synthesis of diacyl peroxides", Tetrahedron Lett., 331 (1976).

Jones, C.W. Application of Hydrogen Peroxide and Derivatives, Chapter 2, Clark, J.H. (Ser. ed.), Royal Society of Chemistry, Cambridge, UK, 1999.

Kadla, J.F., Chang, H.-M., Jameel, H., and Gratzl, J.S., "High temperature reactions of lignin and lignin model compounds with stabilized hydrogen peroxide" in Proceedings of The International Symposium on Wood and Pulping Chemistry, Montreal, p. D3-1, 1997.

Karhunen, P., Rummakko, P., Sipilä, J., Brunow, G., and Kilpeläinen, I., "Dibenzodioxocins: A novel type of linkage in softwood lignins", Tetrahedron Lett., 36, 169 (1995).

Kerr, J.A. and Sheppard, D.W., "Kinetics of the reactions of hydroxyl radicals with aldehydes studied under atmospheric conditions", Environ. Sci. Technol., 15, 960 (1981).

Kim, S., DiCosimo, R., and San Filippo, J., Jr., "Spectrometric and chemical characterization of superoxide", Anal. Chem., 51, 769 (1979).

Kobayashi, S., Tezuka, T., and Ando, W., "Nucleophilic and elelctron transfer oxidations of troponoid compounds by superoxide ion", J. Chem. Soc., Chem. Commun., 508 (1979).

Kornblum, N. and Singaram, S., "Conversion of nitriles to amides and esters to acids by the action of sodium superoxide", J. Org. Chem., 44, 4727 (1979).

Lachenal, D., "Hydrogen peroxide as a delignifying agent" in Pulp Bleaching – Principles and Practice, Section IV, Chapter 6, p 349, Dence ,C.W. and Reeve, D.W. (eds.), Tappi Press, Atlanta, 1996.

Lachenal, D. and Papadopoulos, J., "Improvement of hydrogen peroxide delignification" in Proceedings of The International Symposium on Wood and Pulping Chemistry, p. 295, Paris, 1987.

Lee, J. and Grabowski, J., "Reactions of atomic oxygen radical anion and the synthesis of organic reactive intermediates", Chem. Rev., 92, 1611 (1992).

Lee-Ruff, E., Lever, A.S.P., and Ringandy, J., "The reaction of catechol and derivatives with potassium superoxide", Can. J. Chem., 54, 1837 (1976).

Legrini, O., Oliveros, E., and Braun, A.M., "Photochemical process for water treatment", Chem. Rev., 93, 671 (1993).

Lenhardt, T.M., McDade, C.E., and Bayes, K.D., "Rates of reaction of butyl radicals with molecular oxygen", J. Chem. Phys., 72, 304 (1980).

Long, C.A. and Bielski, B.H.J., "Rate of reaction of superoxide radical with chloride-containing species", J. Phys. Chem., 84, 555 (1980).

Luo, N., Kombo, D.C., and Osman, R., "Theoretical studies of hydrogen abstraction from 2-propanol by OH radical", J. Phys. Chem. A, 101, 926 (1997).

March, J., Advanced Organic chemistry; Reactions, Mechanisms, and Structure, Second Edition, McGraw-Hill Book Company, New York, 1977.

Mayo, F.R., "Comparison of liquid-phase and gas-phase reactions of free radicals", J. Am. Chem. Soc., 89, 2654 (1967).

McDonald, R.N. and Chowdhury, A.K., "Gas-phase ion-molecule reactions of dioxygen anion radical ($O_2^{\cdot-}$)", J. Am. Chem. Soc., 107, 4123 (1985).

McDonough, T.J., "Oxygen Delignification" in Pulp Bleaching – Principles and Practice, Section IV, Chapter 1, p. 215, Dence, C.W. and Reeve, D.W. (eds.), Tappi Press, Atlanta, 1996.

McMillen, D.F. and Golden, D.M., "Hydrocarbon bond dissociation energies", Ann. Rev. Phys. Chem., 33, 493 (1982).

McMurry, J., Organic Chemistry, 4th Edition, Books/Cole Publishing Company, Pacific Grove, CA, 1996.

Merier, U., Grotheer, H.H., Riekert, G., and Just, T., "Temperature dependence and branching ratio of the CH_3OH + OH reaction", Chem. Phys. Lett., 106, 97 (1984).

Merier, U., Grotheer, H.H., Riekert, G., and Just, T., "Study of hydroxyl radical reactions with methanol and ethanol by laser-induced fluorescence", Ber. Bunsen-Ges. Phys. Chem., 89, 325 (1985).

Merritt, M.V. and Johnson, R.A., 'Spin-trapping, alkylperoxy radicals, and superoxide-alkyl halide reaction", J. Am. Chem. Soc., 86, 2321 (1977).

Merritt, M.V. and Sawyer, D.T., "Electrochemical studies of the reactivity of superoxide ion with alkyl halide in dimethyl sulfoxide", J. Org. Chem., 35, 2157 (1970).

Miller, R.W., "Reactions of superoxide anion, catechols, and cytochrome C", Can. J. Biochem., 48, 935 (1970).

Moro-oka, Y. and Foote, C.S., "Chemistry of superoxide ion. I. Oxidation of 2,5-di-tert-butyl catechol with KO_2", J. Am. Chem. Soc., 98, 1510 (1976).

Nanni, E.J., Jr. and Sawyer, D.T., "Free radical and electron-transfer mechanisms for tertiary aminoxide", J. Am. Chem. Soc., 102, 7591 (1980).

Nanni, E.J., Jr., Stallings, M.D., and Sawyer, D.T., "Does superoxide ion oxidize catechol, α-tocopherol, and ascorbic acid by direct electron transfer?", J. Am. Chem. Soc., 102, 4481 (1980).

Necker, D.C. and Hauck, G., "Reactions of diphenylcyclopropenone and tetracyclones with potassium superoxide", J. Org. Chem., 48, 4691 (1983).

Nishikimi, M., "Oxidation of ascorbic acid with superoxide anion generated by the xanthine-xanthine oxidase system", Biochem. Biophys. Res. Comm., 63, 463 (1975).

Pan, X., Lachenal, D., Lapierre, C., and Monties, B., "Structure and reactivity of spruce mechanical pulp lignins. Part III. Bleaching and photoyellowing of isolated lignin reactions", J. Wood Chem. Technol., 13(2), 145 (1993).

Peller, J., Wiest, O., and Kamat, P.V., "Sonolysis of 2,4-dichlorophenoxyacetic acid in aqueous solutions. Evidence for ·OH-radical-mediated degradation", J. Phys. Chem. A, 105, 3176 (2001).

Perry, R.A., Atkinson, R., and Pitts, J.N., Jr., "Rate constants for the reaction of the OH radicals with CH_2=CHF, CH_2=CHCl, and CH_2=CHBr over the temperature range 299-426 °K", J. Chem. Phys., 67, 458 (1977).

Pigman, W. and Horton, D., The carbohydrates, Chemistry and Biochemistry, Second Edition, Academic Press, New York, 128 (1972).

Poupko, R. and Rosenthal, I., "Electron transfer interactions between superoxide ion and organic compounds", J. Phys. Chem., 77, 1722 (1973).

Rao, P.S. and Hayon, E., "Ionization constants and spectral characteristics of some semiquinone radicals in aqueous solution", J. Phys. Chem., 77, 2274 (1973).

Reitberger, T., Gierer, J., Yang, E., and Yoon, B.-H., "Involvement of oxygen-derived free radicals in chemical and biological degradation of lignin" in Oxidative Delignification Chemistry – Fundamentals and Catalysis, ACS Symposium Series 785, Chapter 15, p. 255, Argyropoulos, D.S. (ed.), American Chemical Society, Washington, DC, 2001.

Roberts, J.L., Jr. and Sawyer, D.T., "Activation of superoxide ion by reactions with protons, electrophiles, secondary amines, radicals, and reduced metal ions", Isr. J. Chem., 23, 430 (1983).

Robinson, R.A., "Buffer solutions operational definitions of pH" in CRC Handbook of Chemistry and Physics, 62nd Edition, p. D-126, Robert, C.W. and Melvin, J.A. (eds.), CRC Press, Florida, 1981.

Rosenthal, I. and Frimer, A., "The reaction between tetracyclone and superoxide anion radical", Tetrahedron Lett., 3731 (1975).

Samuel, D. and Steckel, F., "The physico-chemical properties of molecular oxygen" in Molecular Oxygen in Biology, p. 6, Hayaishi, O. (ed.), North-Holland Publishing Company, Amsterdam, 1974.

San Filippo, J., Jr., Chern, C.-I., and Valentine, J.S., "Oxidative cleavage of α-ketones, esters, and carboxylic acids by superoxide", J. Org. Chem., 41, 1077 (1976).

Sawyer, D.T., Oxygen Chemistry, Oxford University Press, New York, 1991.

Sawyer, D.T., "The chemistry and activation of dioxgen species (O_2, $O_2^{\cdot-}$, and HOOH) in biology" in Oxygen Complexes and Oxygen Activation by Transition Metals, p. 131-148, Martell, A.E. and Sawyer, D.T. (eds.), Plenum, New York, 1988.

Sawyer, D.T. and Gibian, M.J., "The chemistry of superoxide ion", Tetrahedron, 35, 1471 (1979).

Sawyer, D.T. and Nanni, E.J., Jr., "Redox chemistry of dioxygen species and their chemical reactivity" in Oxygen and Oxy-radicals in Chemistry and Biology, p. 15, Rogers, M.A.J. and E.L. Powers (eds.), Academic Press, London, 1981.

Sawyer, D.T., Stamp, J.J., and Menton, K.A., "Reactivity of superoxide ion with ethyl pyruvate, α-diketones, and benzyl in dimethylformamide", J. Org. Chem., 48, 3733 (1983).

Sawyer, D.T. and Valentine, J.S., "How super is superoxide ion ?", Acc. Chem. Res., 14, 393 (1981).

Schuchmann, M.N., Bothe, E., von Sonntag, J., and von Sonntag, C., "Reaction of OH radicals with benzoquinone in aqueous solutions. A pulse radiolysis study", J. Chem. Soc., Perkin Trans. 2, 791 (1998).

Schumb, W.C., Satterfield, C.N., and Wentworth, R.L., Hydrogen peroxide, p. 406-412, Reinhold Publishing Corporation, New York, 1955.

Schwarz, H.A. and Bielski, B.H.J., "Reactions of hydroperoxo and superoxide with iodine and bromine and the iodide (I_2^-) and iodine atom reduction potentials", J. Phys. Chem., 96, 1445 (1986).

Shibata, K., Saito, Y., Urano, K., and Matsui, M., "Reaction of Schiff bases with superoxide ion in acetonitrile", Bull. Chem. Soc. Jpn., 59, 3323 (1986).

Singleton, D.L., Irwin, R.S., and Cvetanivic, R.J., "Arrhenius parameters for the reactions of $O(^3P)$ atoms with several aldehydes and the trend in aldehydic C-H bond dissociation energies", Can. J. Chem., 55, 3321 (1977).

Sjöström, E., Wood Chemistry; Fundamentals and Application, 2nd Edition, Academic Press, Inc., San Diego, 1993.

Sutton, H.C. and Downes, M.T., "Reactions of the HO_2 radical in aqueous solution with bromine and related compounds", J. Chem. Soc., Faraday Trans., 1, 1498 (1972).

Tatsumi, K. and Terashima, N., "Oxidative degradation of lignin. VI. Demethylation mechanism of lignin with hydroxyl radical", Mokuzai Gakkaishi, 29, 530 (1984).

Tatsumi, K. and Terashima, N., "Oxidative degradation of lignin. VII. Cleavage of the β-O-4 linkage of guaiacylglycerol-β-guaiacyl ether by hydroxyl radicals", Mokuzai Gakkaishi, 31, 316 (1985a).

Tatsumi, K. and Terashima, N., "Oxidative degradation of lignin. VIII. Degradation of dehydrodivanillic acid with hydroxyl radicals", Mokuzai Gakkaishi, 31, 761 (1985b).

Tauber, A., Mark, G., Schuchmann, H.-P., and von Sonntag, C., "Sonolysis of *tert*-butyl alcohol in aqueous solution", J. Chem. Soc., Perkin Trans., 2, 1129 (1999).

Temps, F. and Wagner, H. Gg., "Rate constants for the reactions of OH-radicals with CH_2O and HCO", Ber. Bunsen-Ges. Phys. Chem., 88, 415 (1984).

Tripathi, G.N.R., "Electron-transfer component in hydroxyl radical reactions observed by Time Resolved Resonance Raman Spectroscopy", J. Am. Chem. Soc., 120, 4161 (1998).

Tsang, P.K.S. and Sawyer, D.T., "Electron-transfer thermodynamics and bonding for the superoxide ($O_2^{\cdot-}$), dioxygen ($^{\cdot}O_2^{\cdot}$), and hydroxyl ($^{\cdot}OH$) adducts of (Tetrakis (2,6-dichlorophenyl)prophinato)iron, -manganese, and -cobalt in dimethylformamide", Inorg. Chem., 29, 2848 (1990).

van Lierop, B., Skothos, A., and Liebergott, N., "Ozone Delignification" in Pulp Bleaching – Principles and Practice, Section IV, Chapter 5, p. 323, Dence ,C.W. and Reeve, D.W. (eds.), Tappi Press, Atlanta, 1996.

Walling, C. and Kato, S., "The oxidation of alcohols by Fenton's reagent. The effect of copper ion", J. Am. Soc., 93, 4275 (1971).

Whytock, D.A., Micheal, J.V., Payne, W.A., and Stief, V.J., "Absolute rate of the reaction of atomic hydrogen with acetaldehyde", J. Chem. Phys., 65, 4771 (1976).

Willson, R.L., "Pulse radiolysis studies of electron transfer in aqueous quinone solutions", Trans. Faraday Soc., 67, 3020 (1971).

Wolform, M.L. and Haq, S., "A polymer-homologous series of methyl-β-D-glycoside from cellulose", TAPPI, 47, 183 (1964).

Wright, P.J. and Wallis, F.A.A., "Rapid determination of carbohydrates in hardwoods by high performance anion exchange chromatography", Holzforschung, 50, 518 (1996).

APPENDICES

APPENDIX A

GC/MS Scans of Authentic Compounds

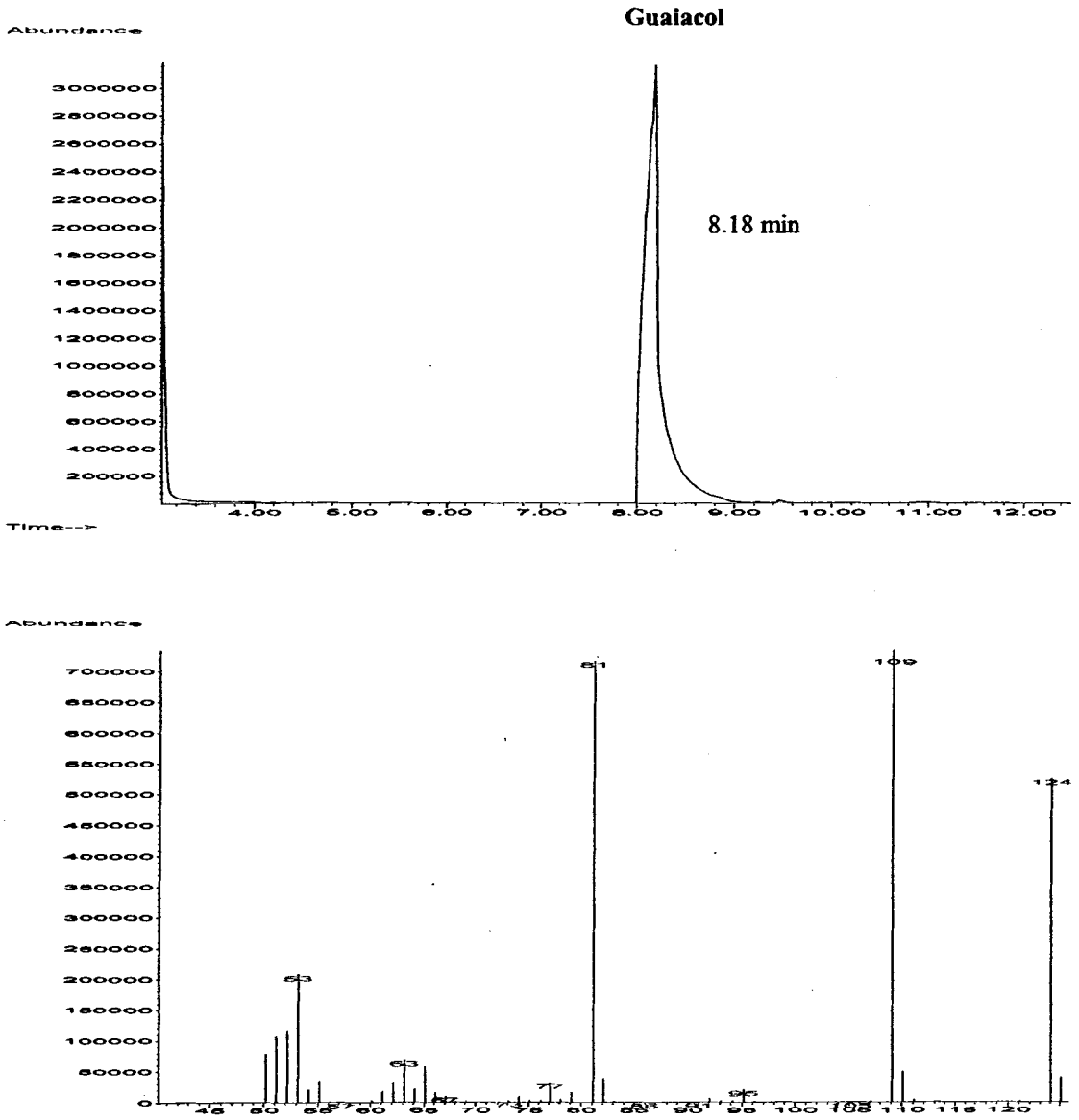

Figure A.1. GC/MS scan of guaiacol.

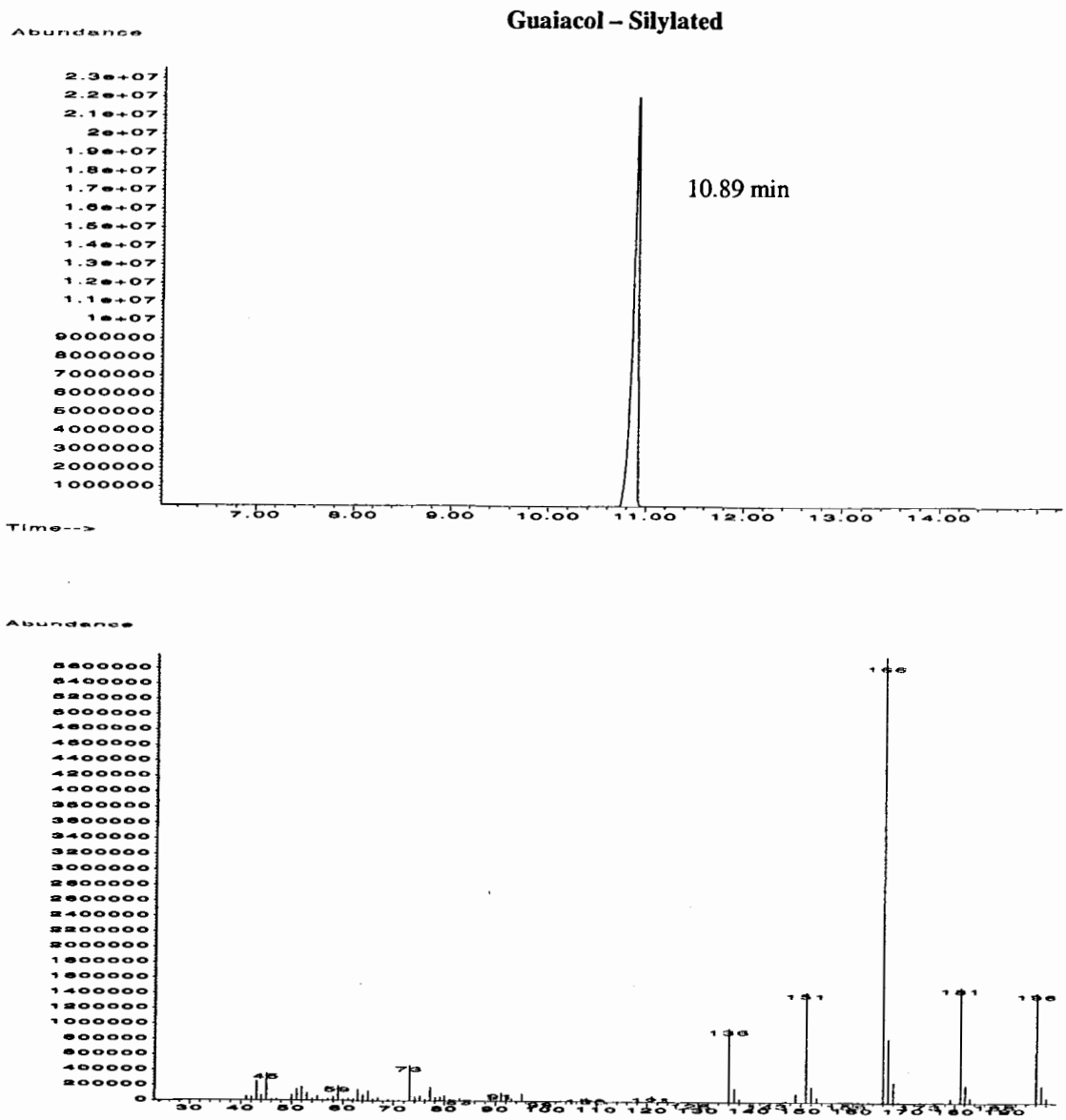

Figure A.2. GC/MS scan of silylated guaiacol.

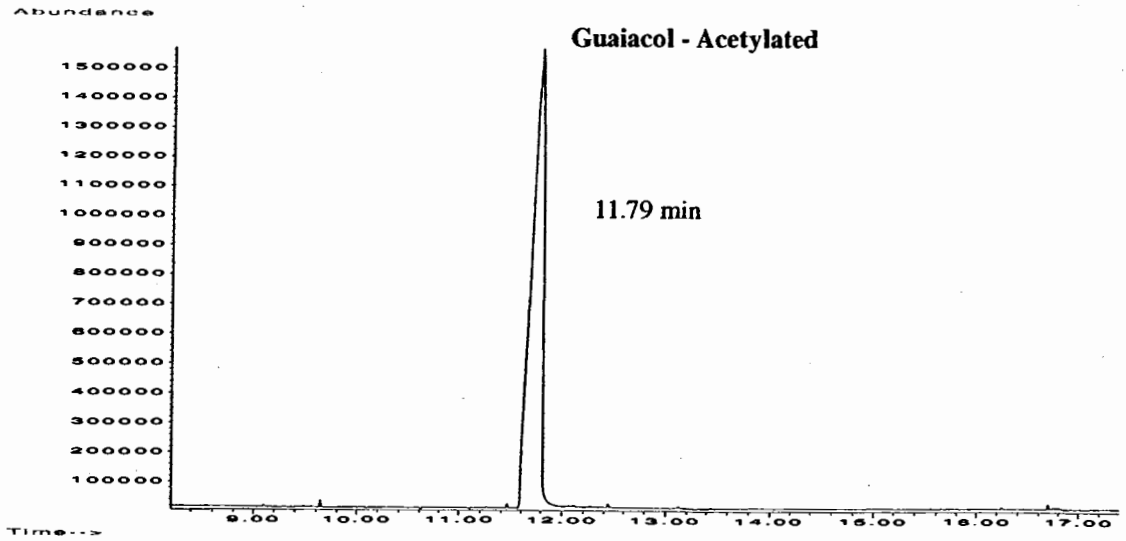

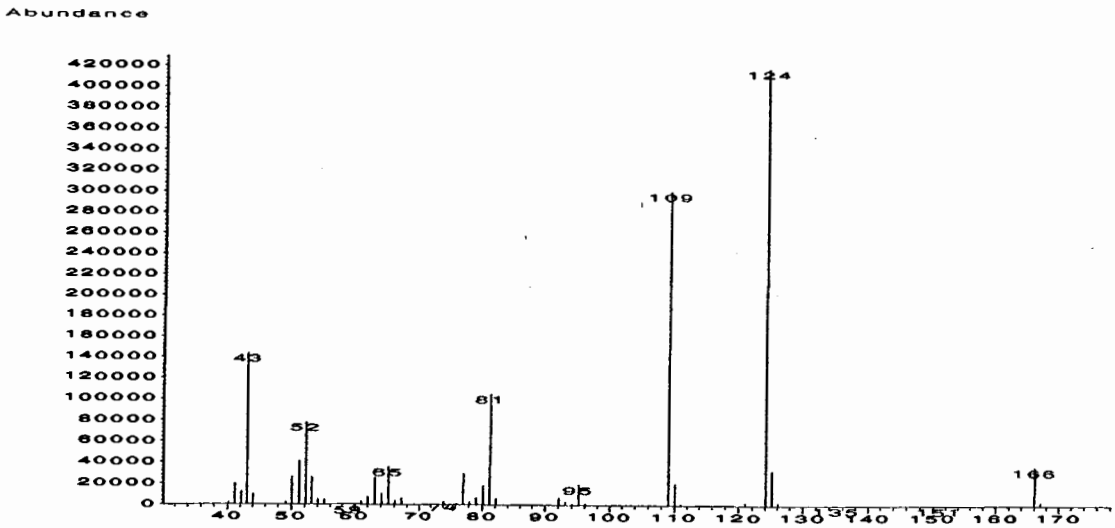

Figure A.3. GC/MS scan of acetylated guaiacol.

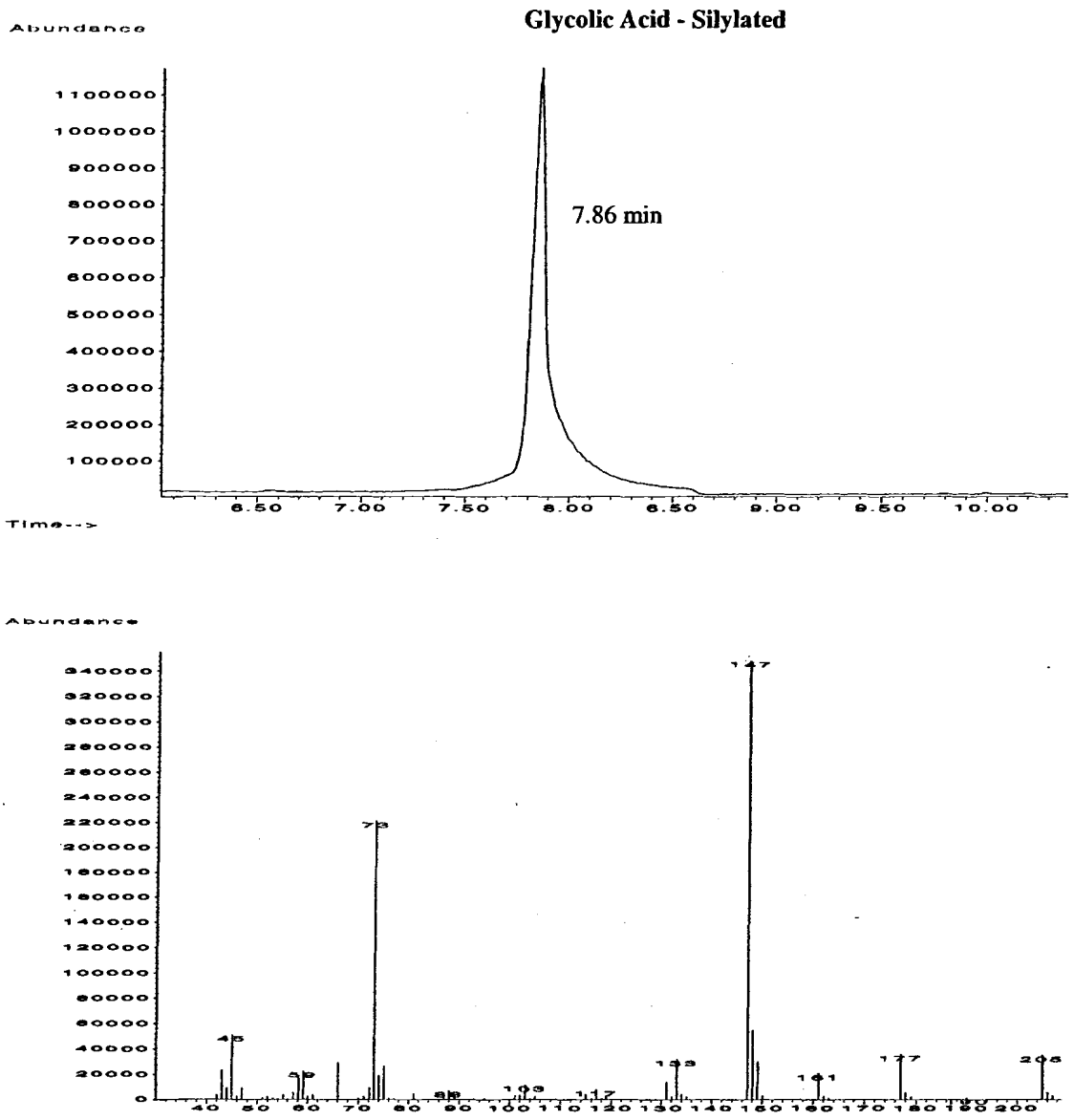

Figure A.4. GC/MS scan of silylated glycolic acid.

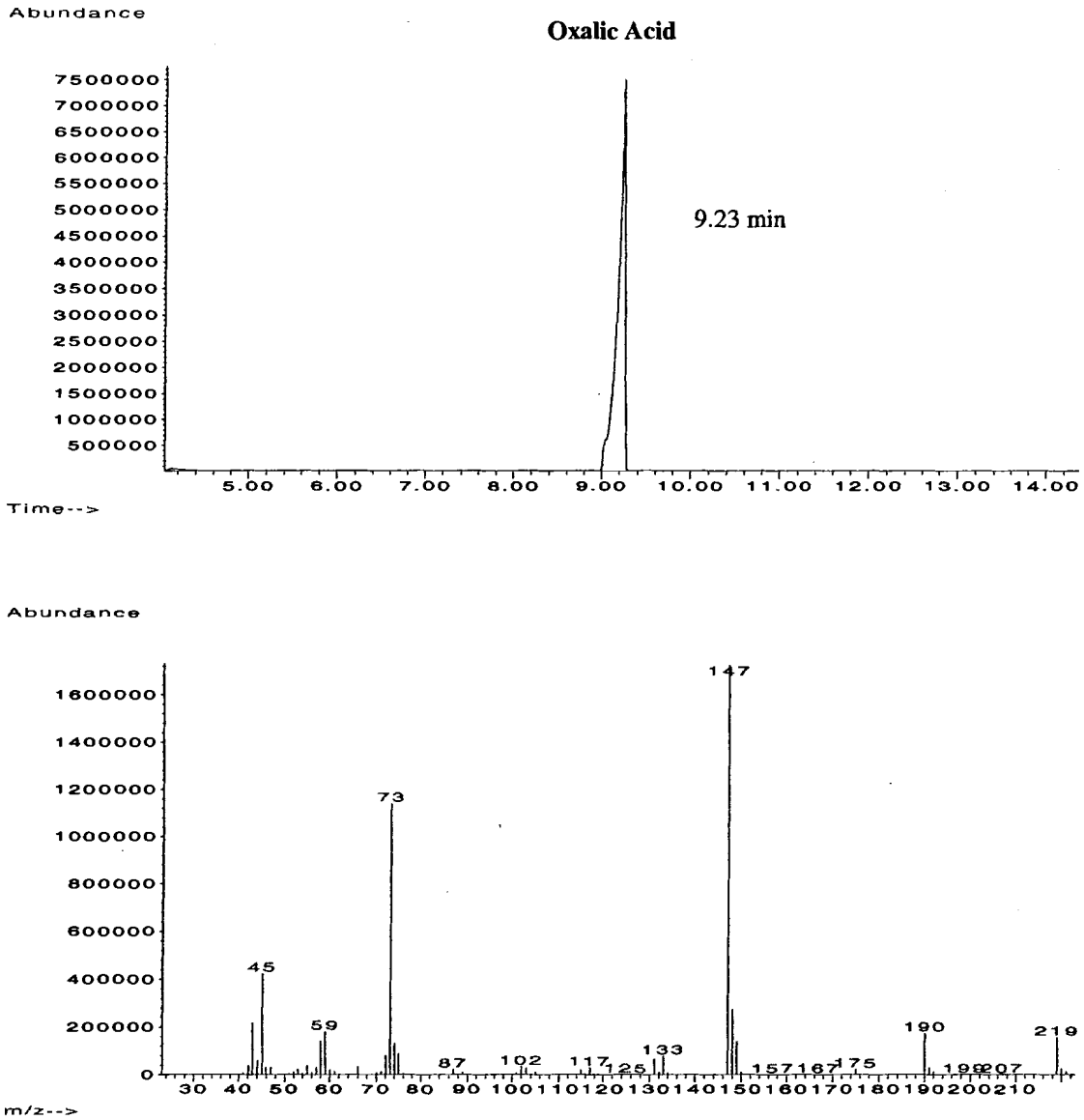

Figure A.5. GC/MS scan of silylated oxalic acid.

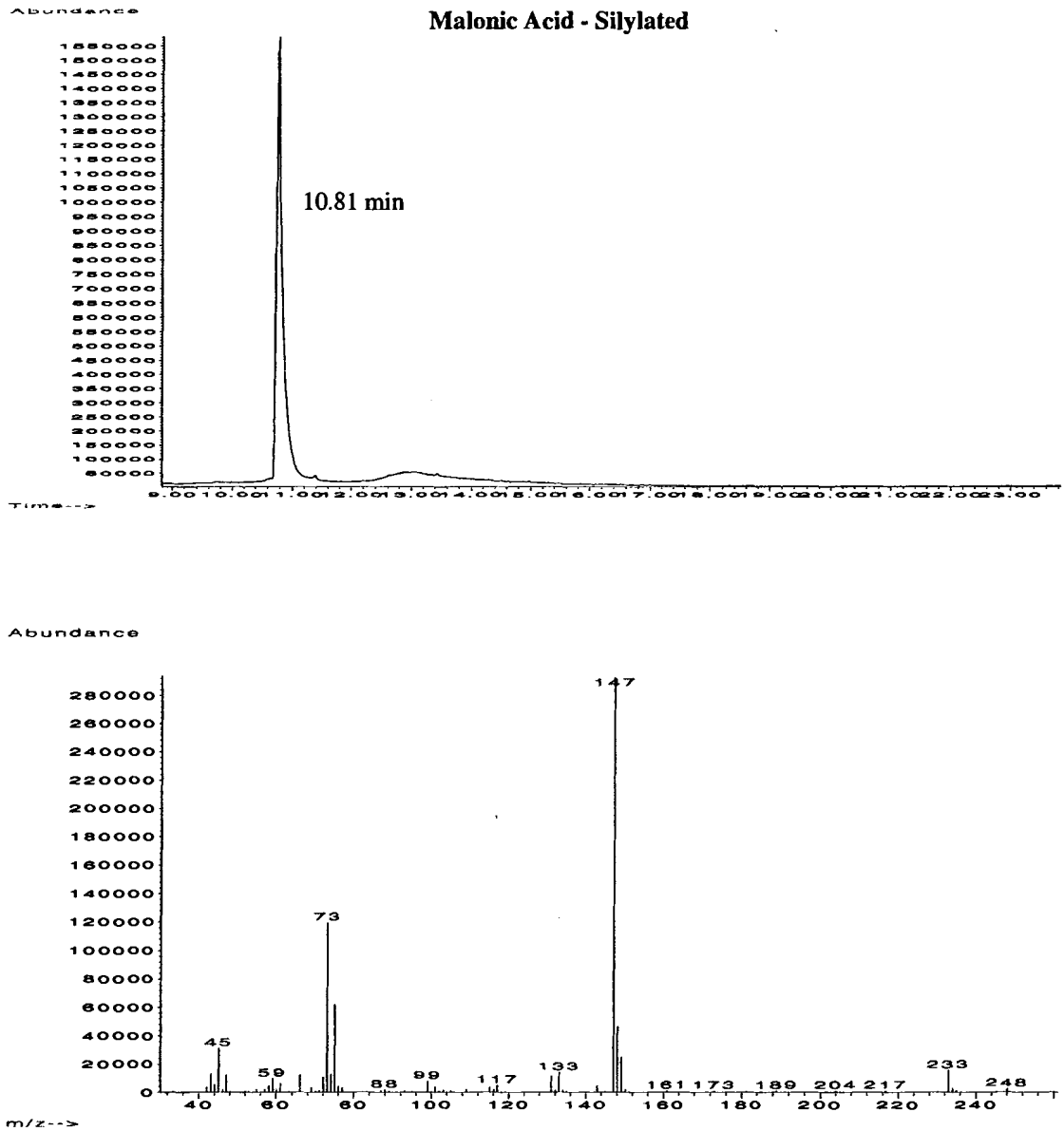

Figure A.6. GC/MS scan of silylated malonic acid.

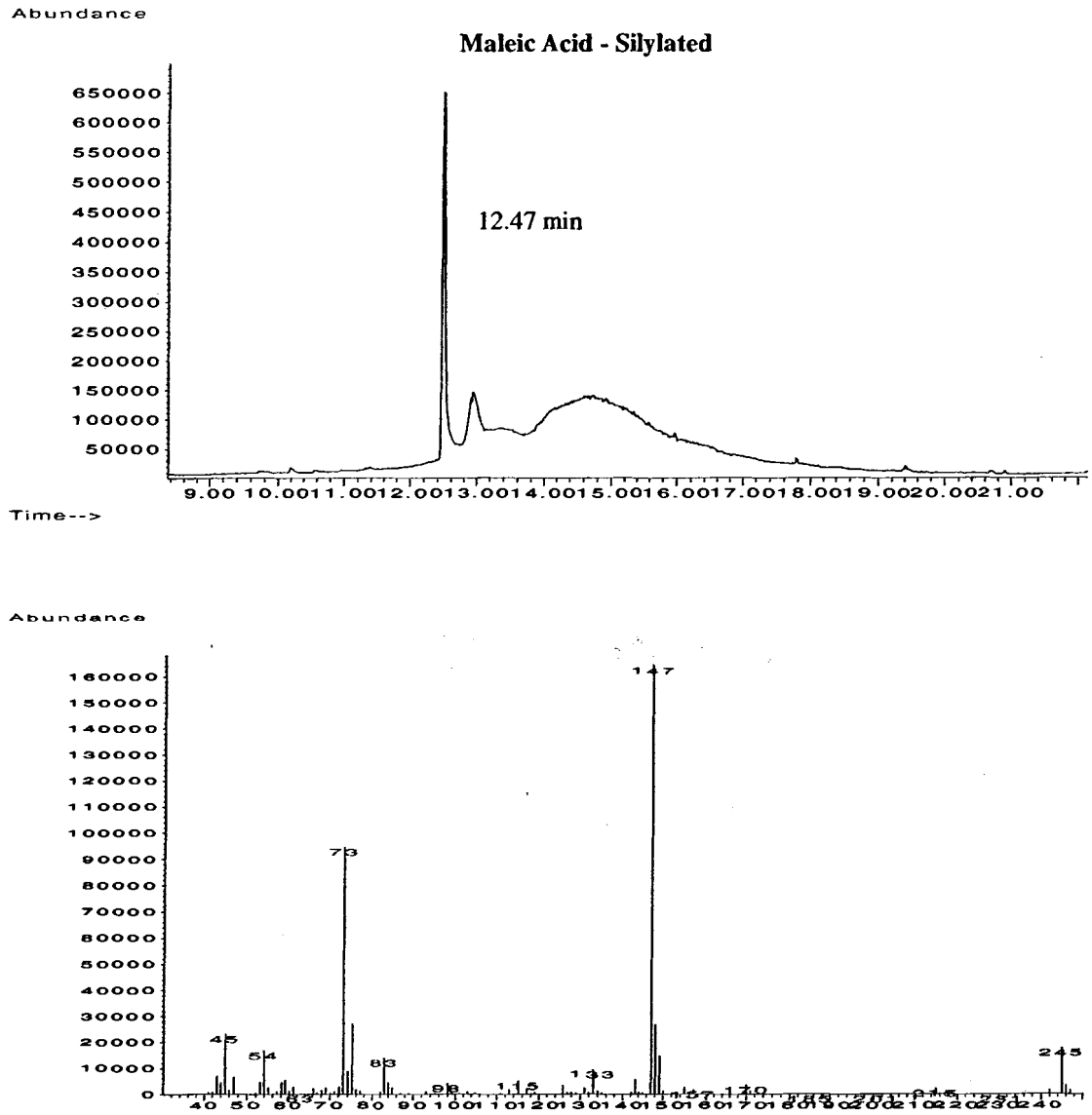

Figure A.7. GC/MS scan of silylated maleic acid.

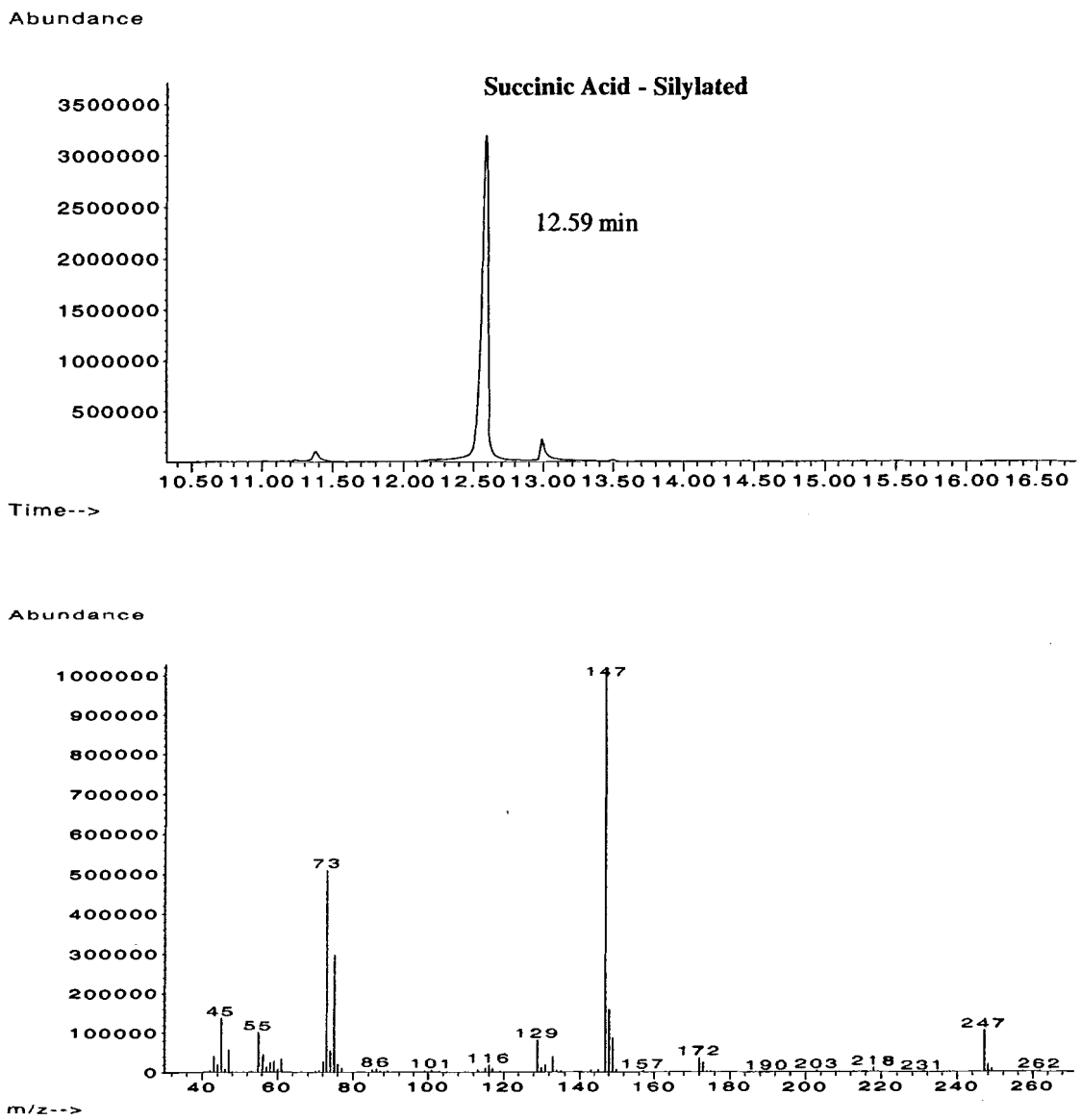

Figure A.8. GC/MS scan of silylated succinic acid.

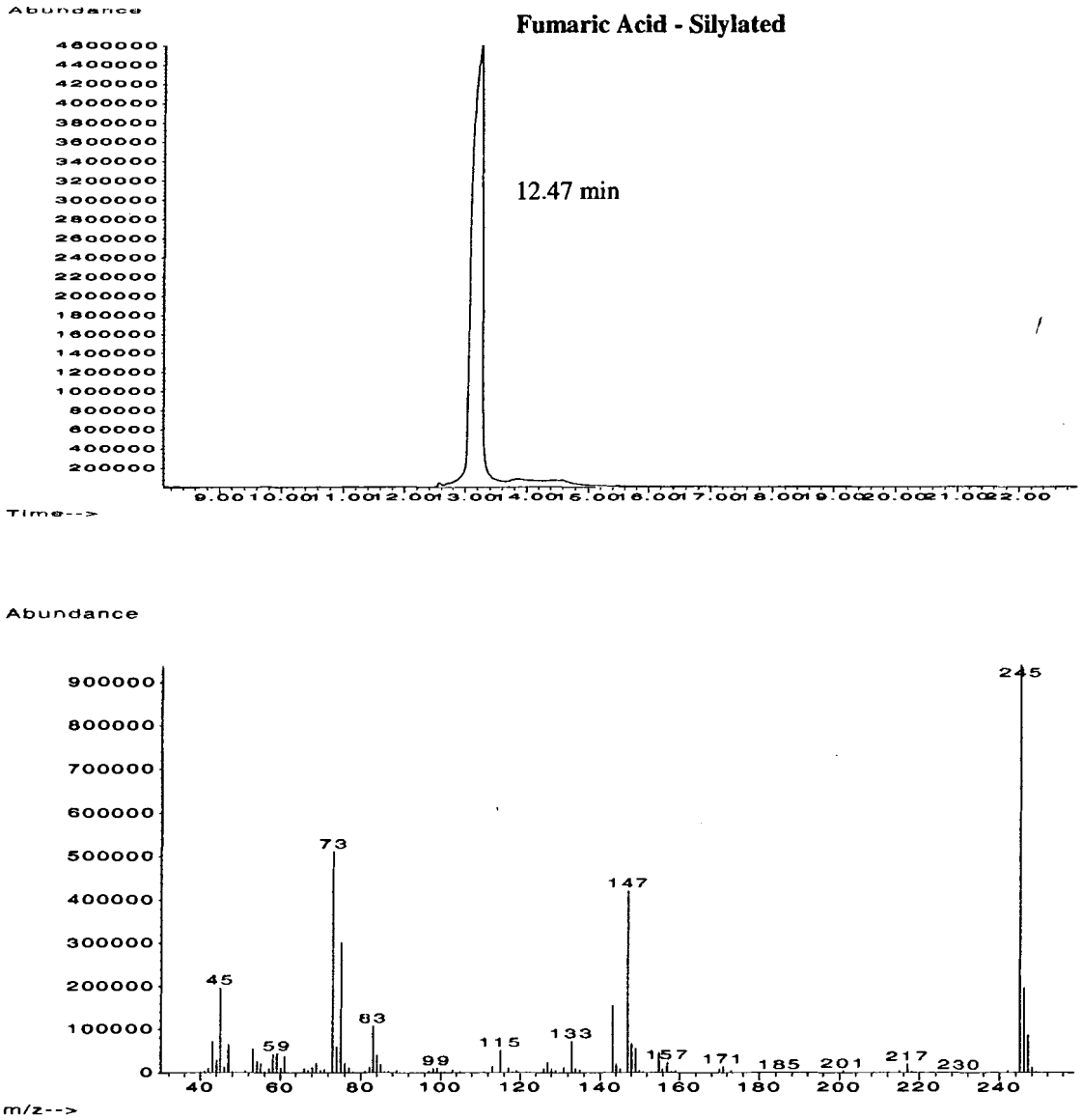

Figure A.9. GC/MS scan of silylated fumaric acid.

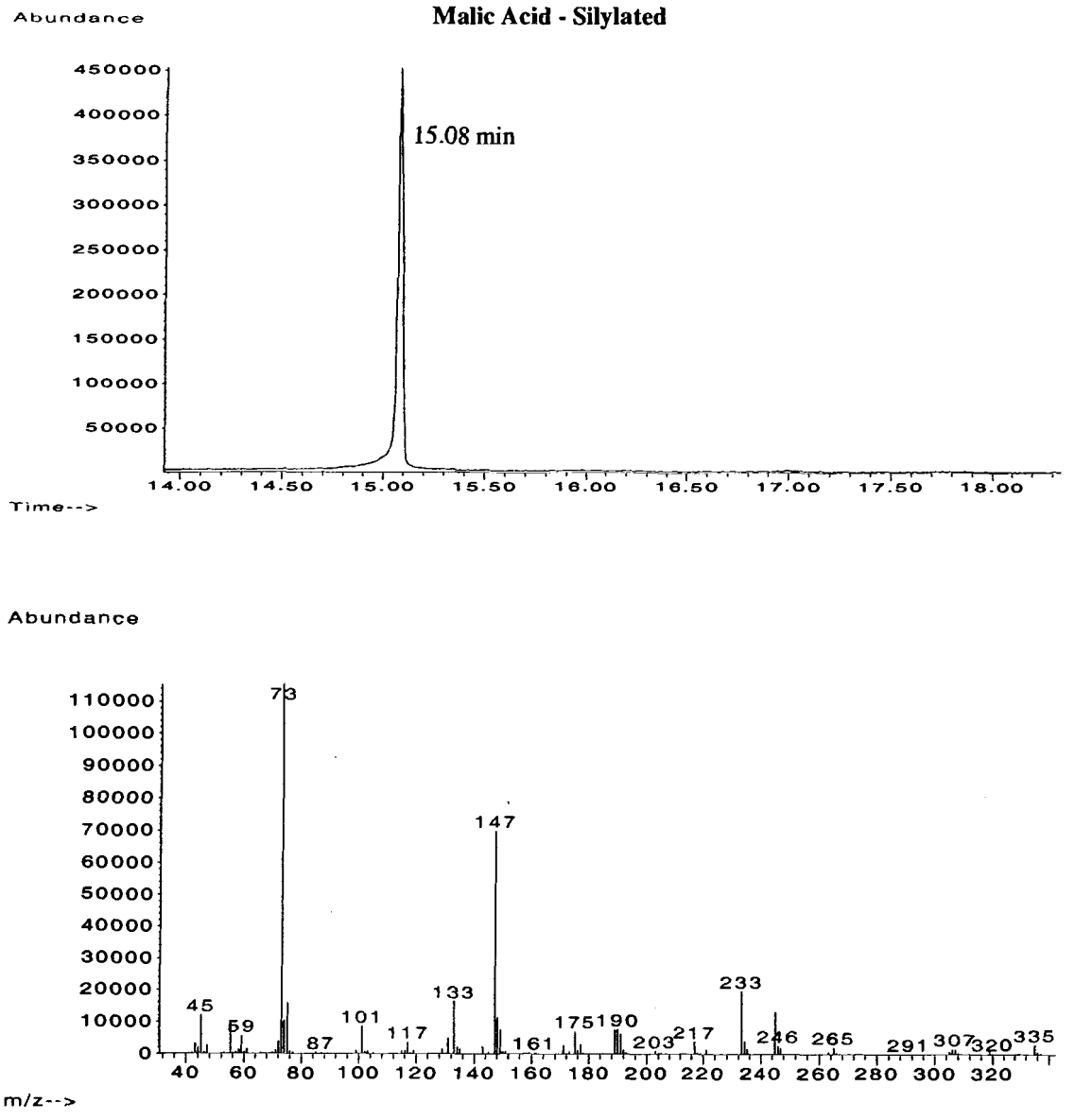

Figure A.10. GC/MS scan of silylated malic acid.

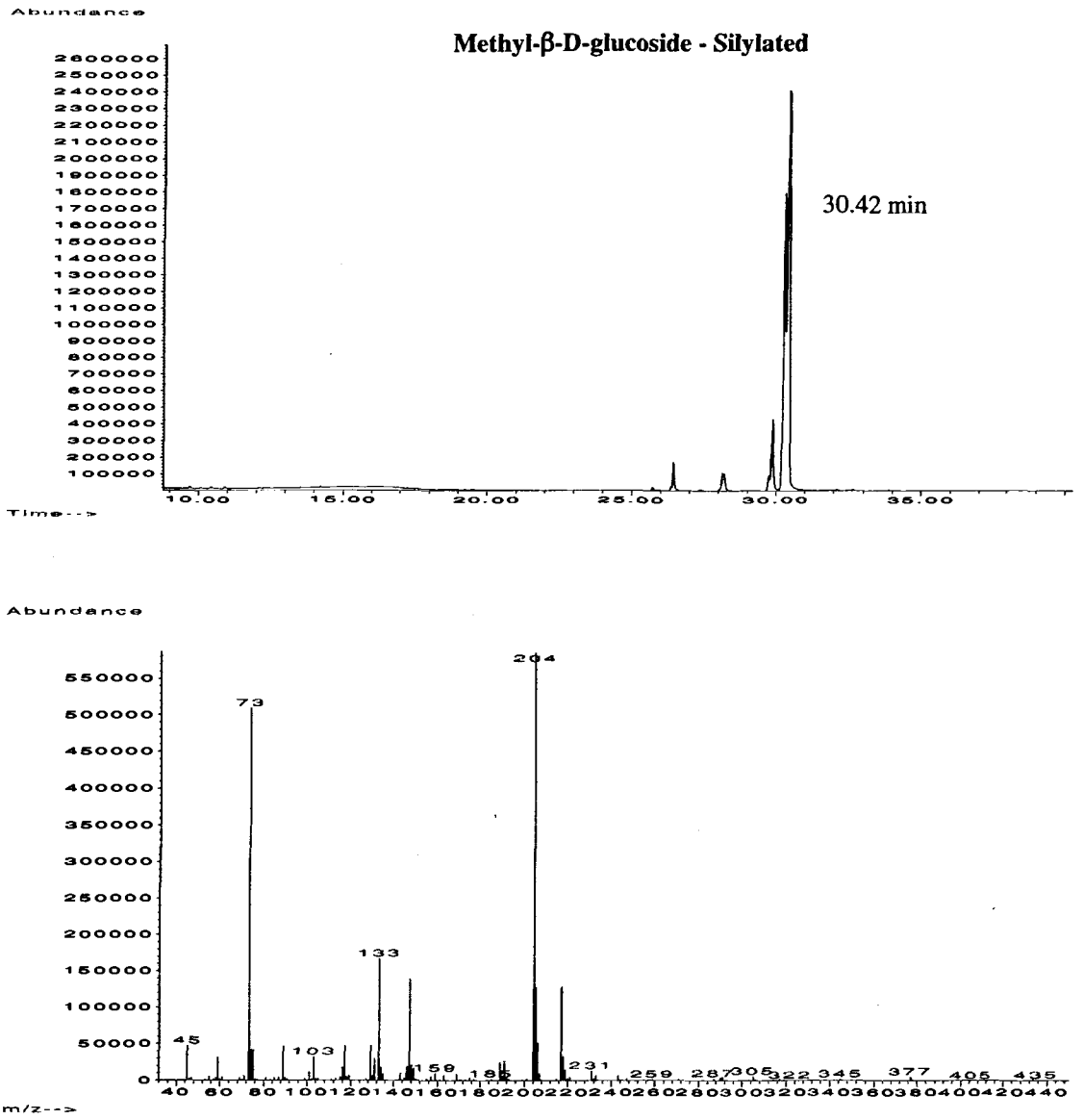

Figure A.11. GC/MS scan of silylated methyl-β-D-glucoside.

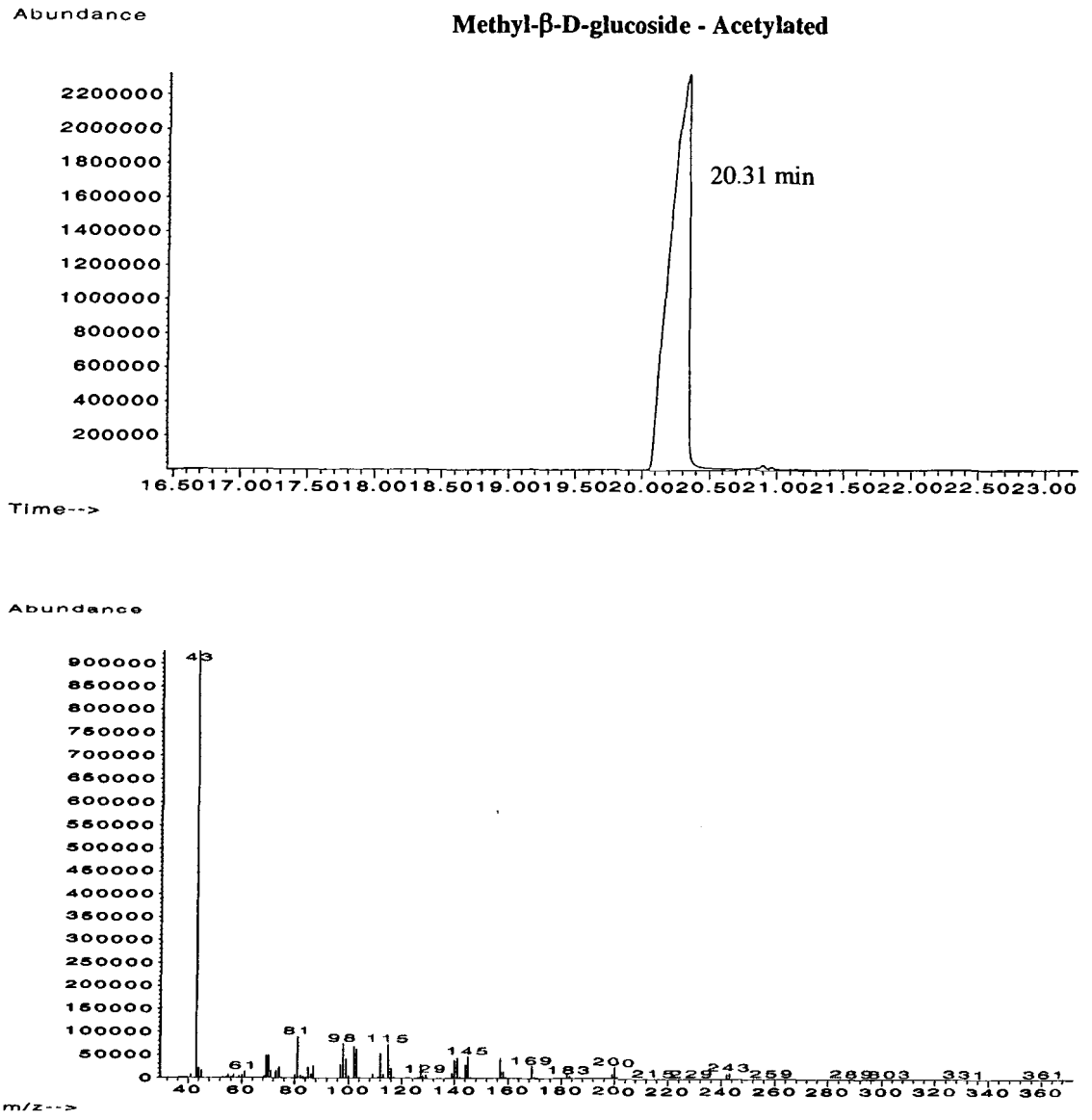

Figure A.12. GC/MS scan of acetylated methyl-β-D-glucoside.

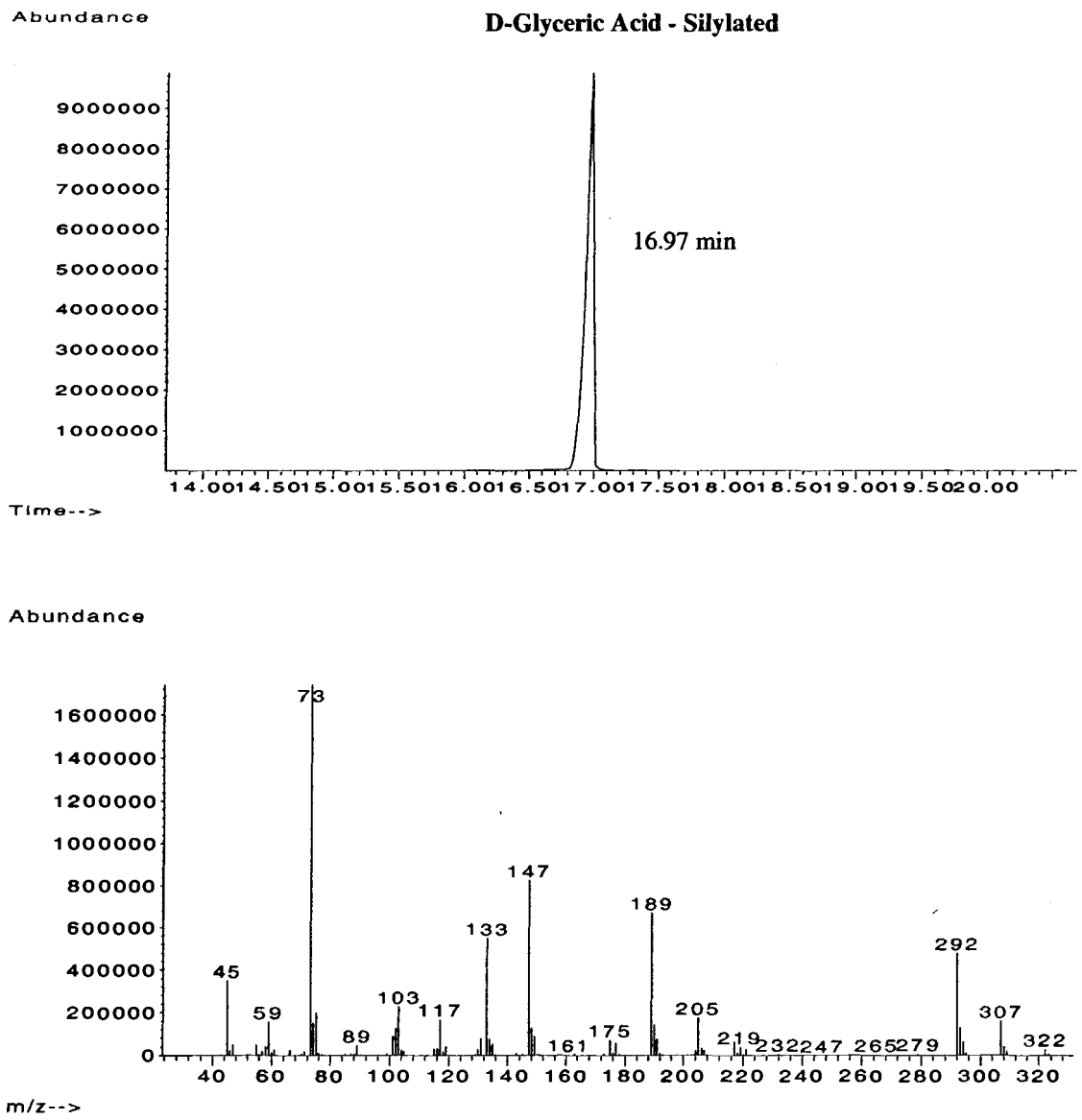

Figure A.13. GC/MS scan of silylated D-glyceric acid.

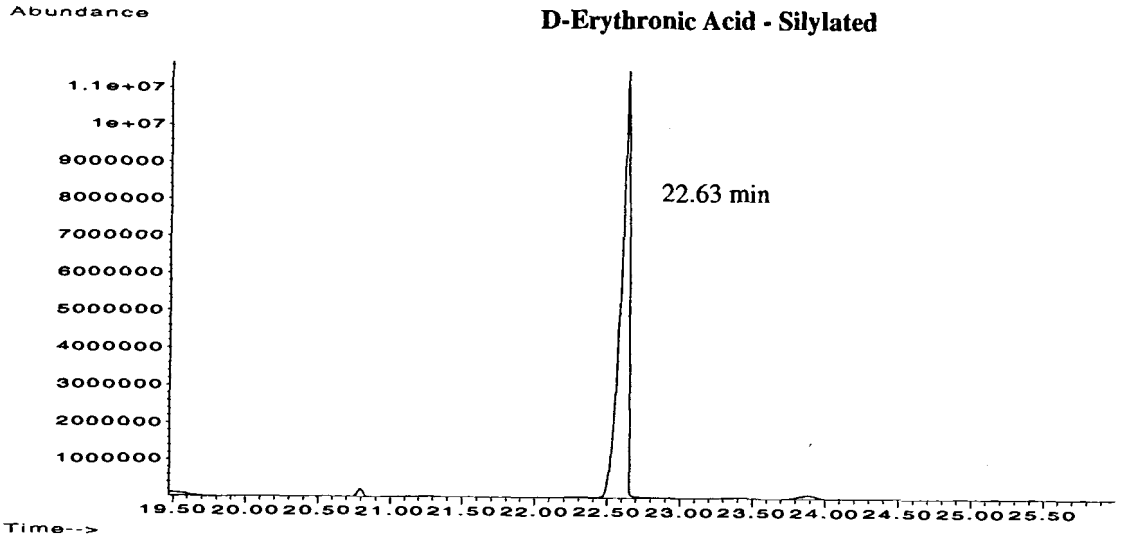

Figure A.14. GC/MS scan of silylated D-erythronic acid.

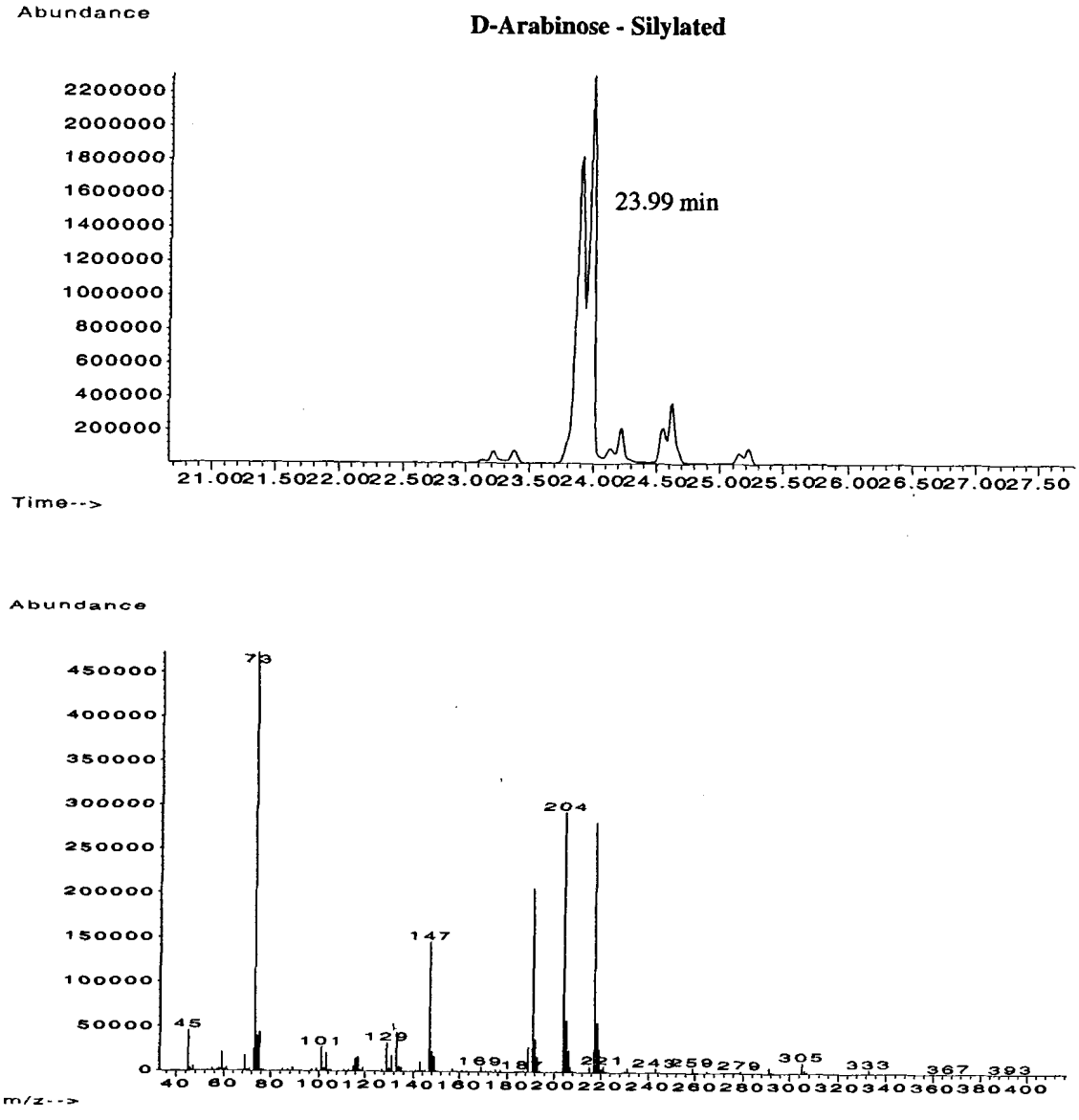

Figure A.15. GC/MS scan of silylated D-arabinose.

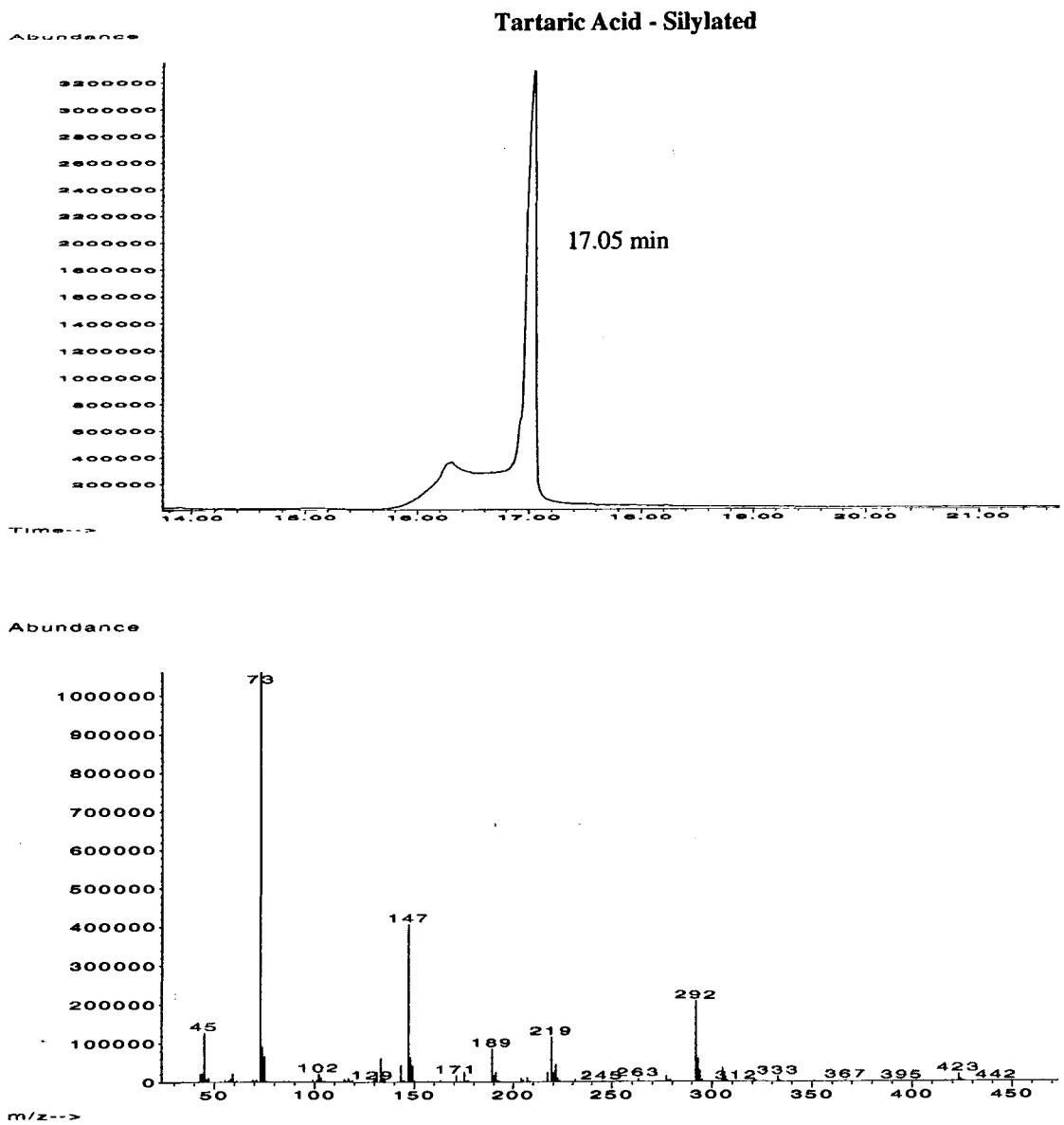

Figure A.16. GC/MS scan of silylated tartaric acid.

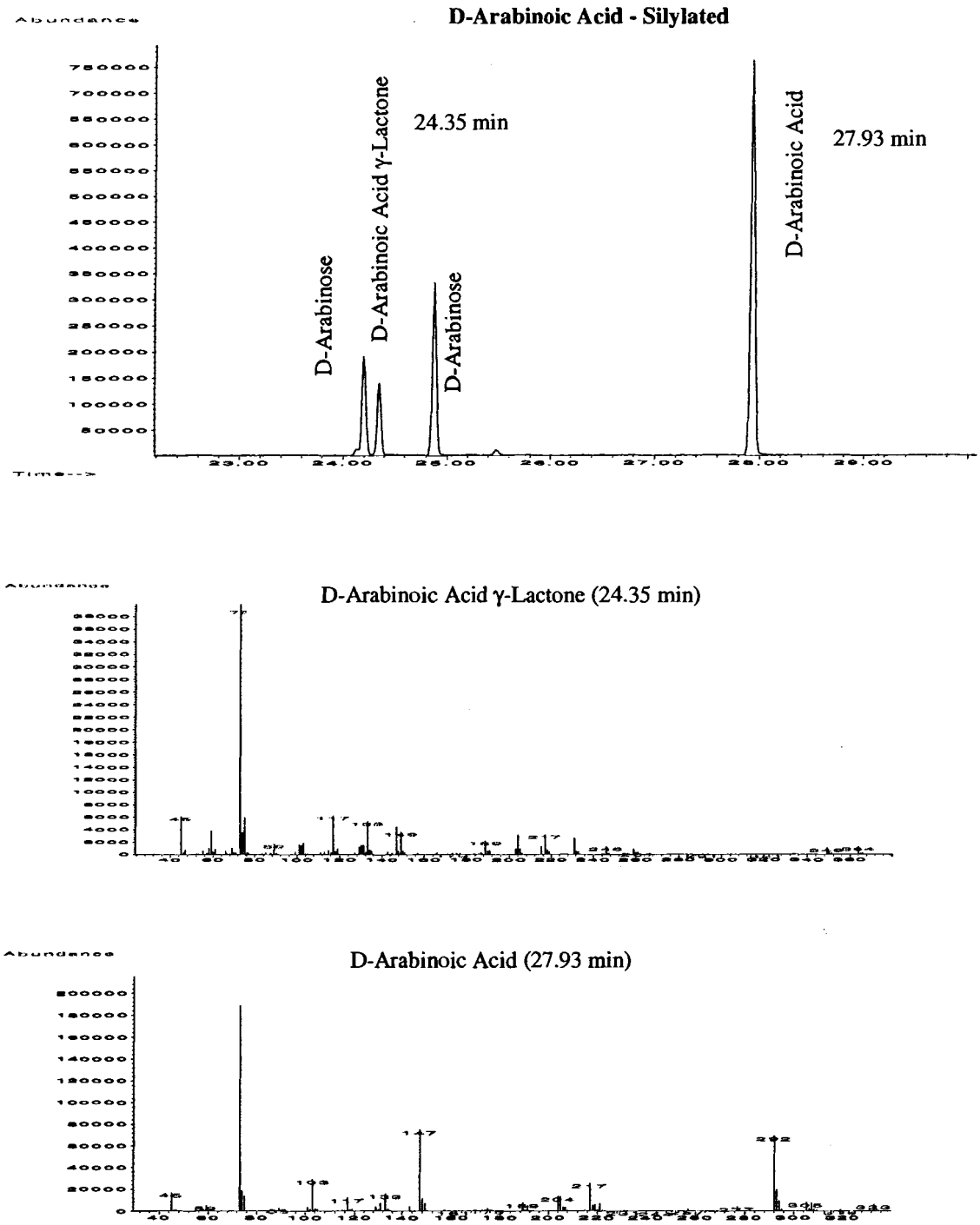

Figure A.17. GC/MS scan of silylated D-arabinoic acid.

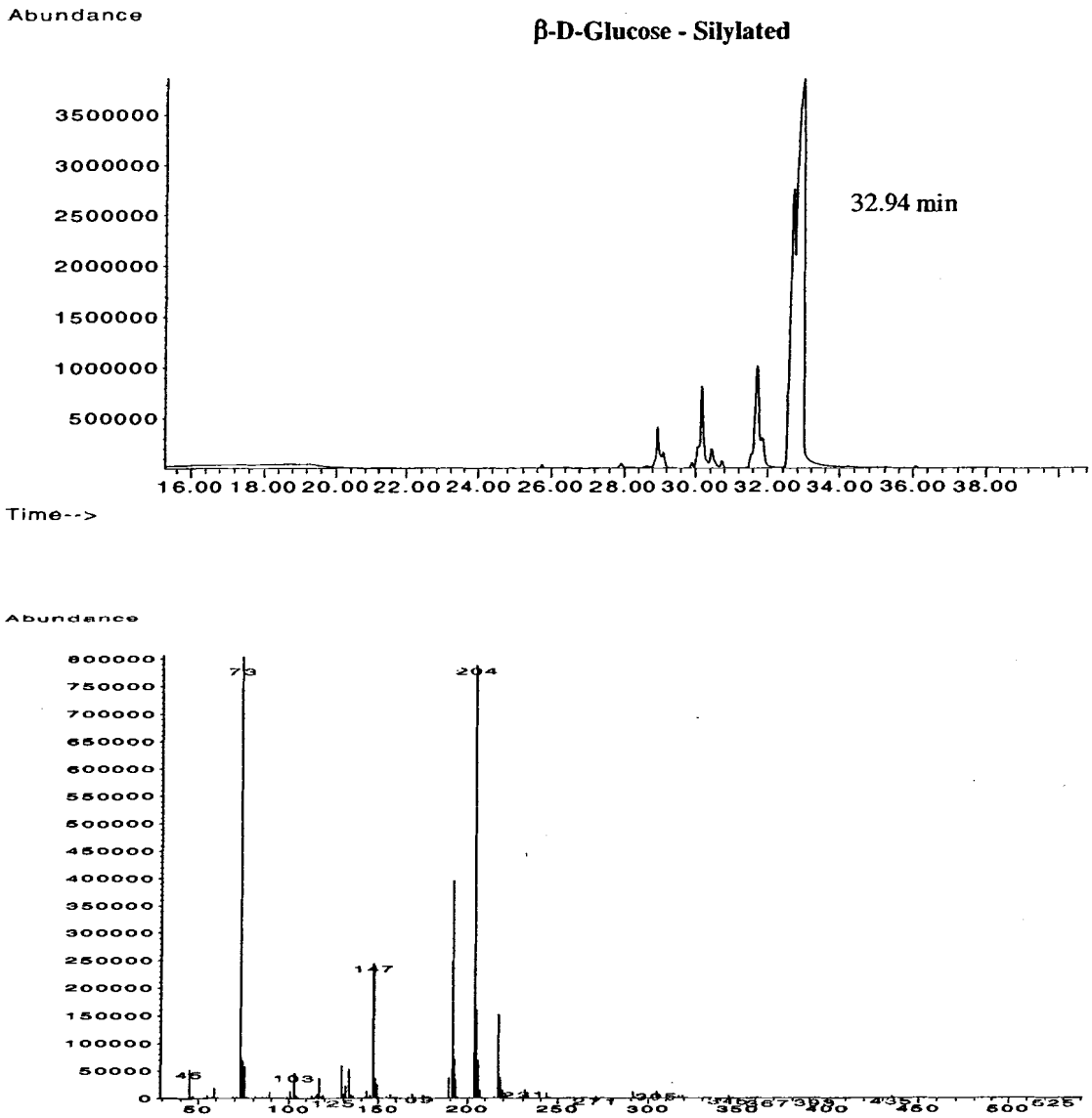

Figure A.18. GC/MS scan of silylated β-D-glucose.

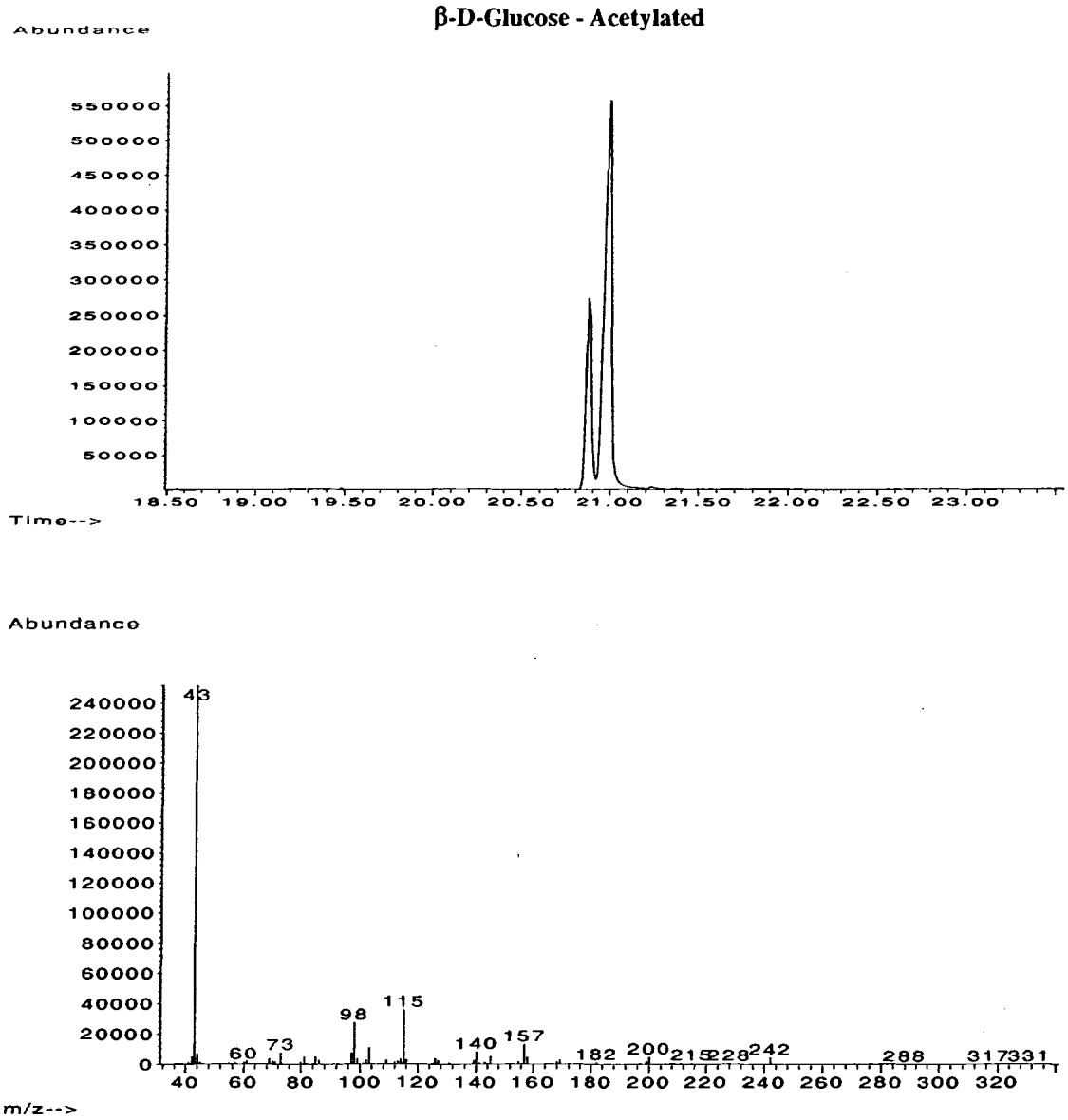

Figure A.19. GC/MS scan of acetylated β-D-glucose.

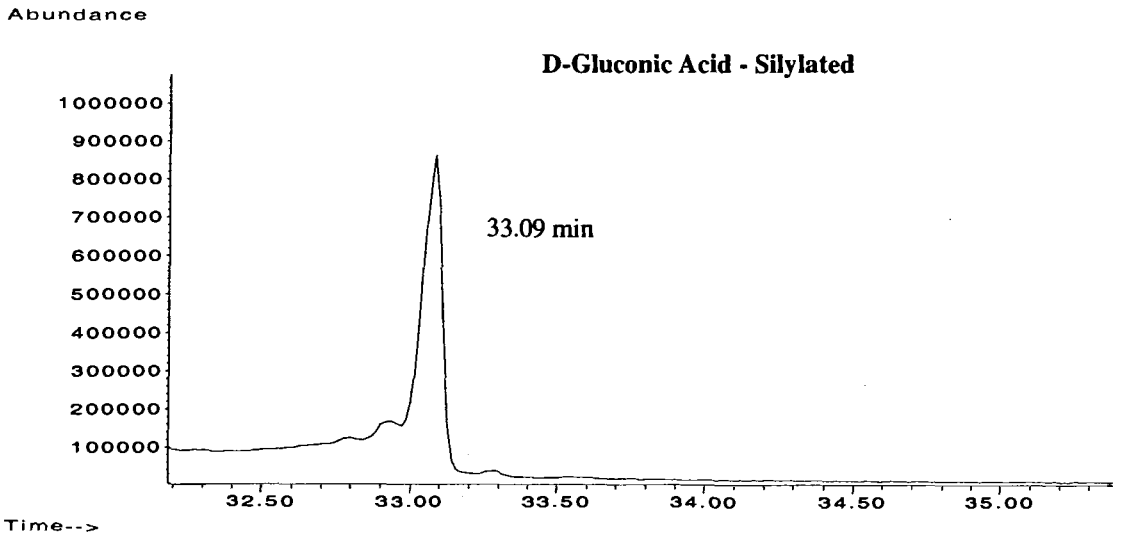

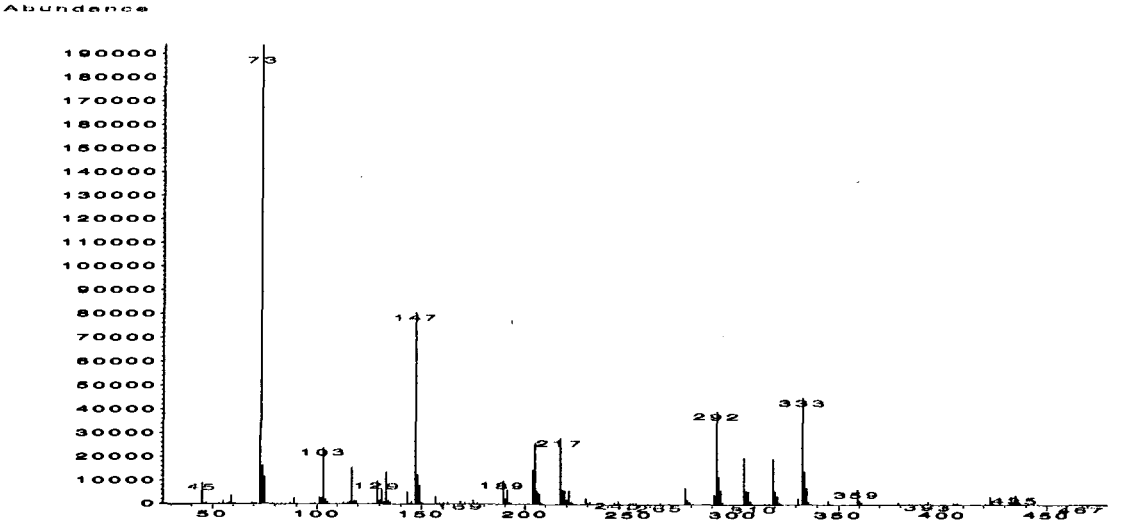

Figure A.20. GC/MS scan of silylated D-gluconic acid.

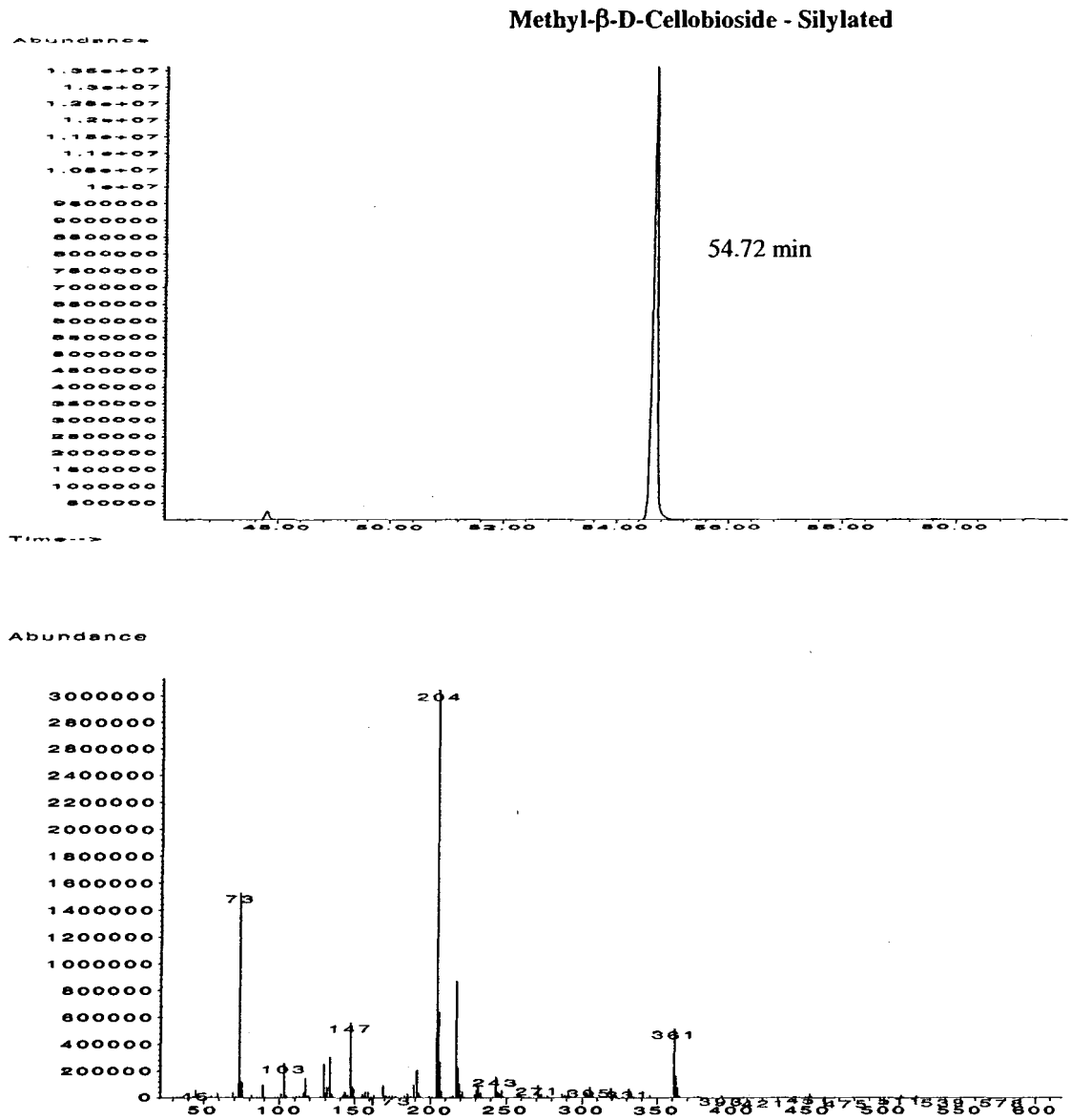

Figure A.21. GC/MS scan of silylated methyl-β-D-cellobioside.

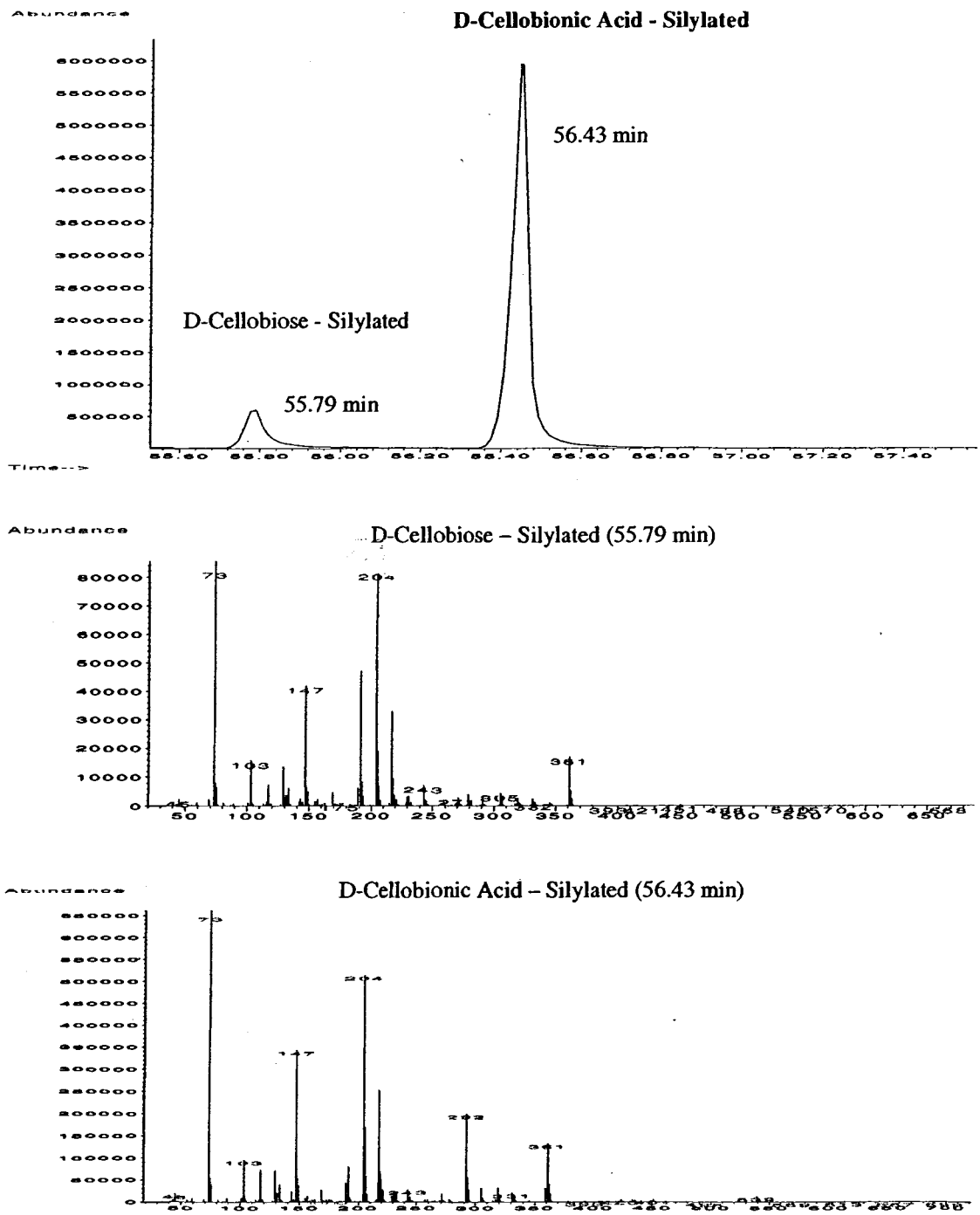

Figure A.22. GC/MS scan of silylated D-cellobiose and D-cellobionic acid.

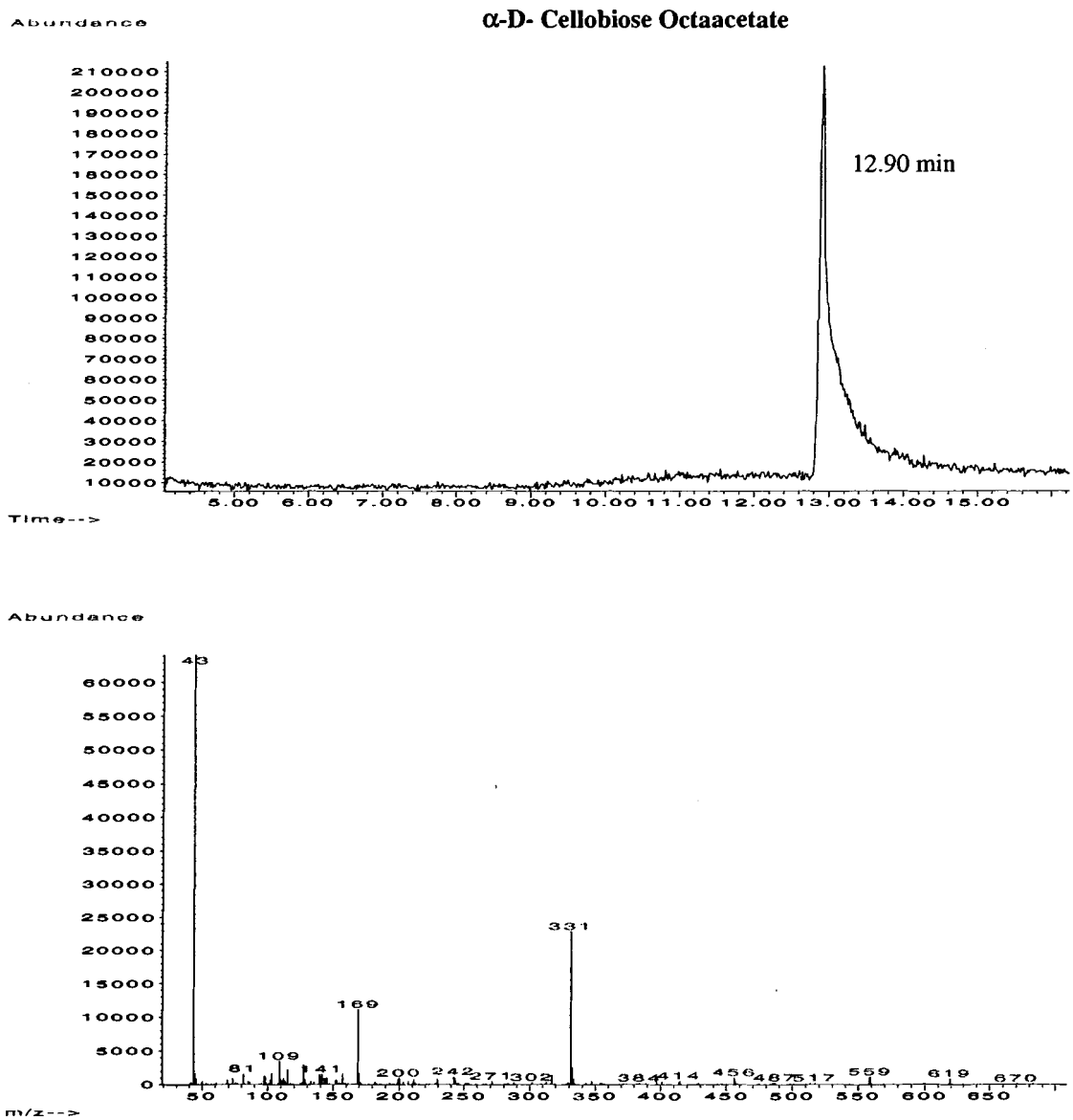

Figure A.23. GC/MS scan of α-D-cellobiose octaacetate.

1-Bromo-1-deoxycellobiose Heptaacetate

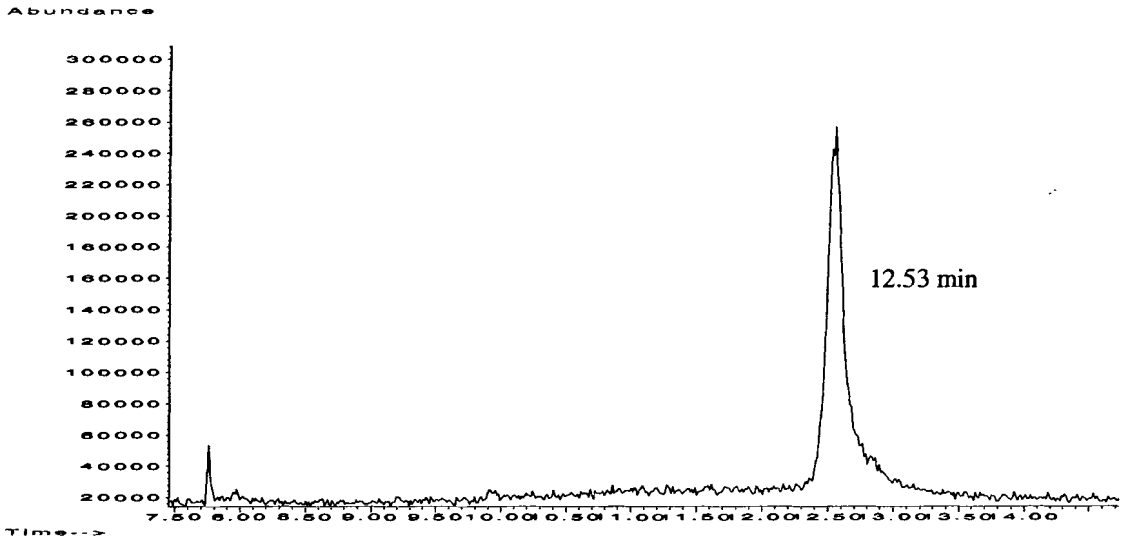

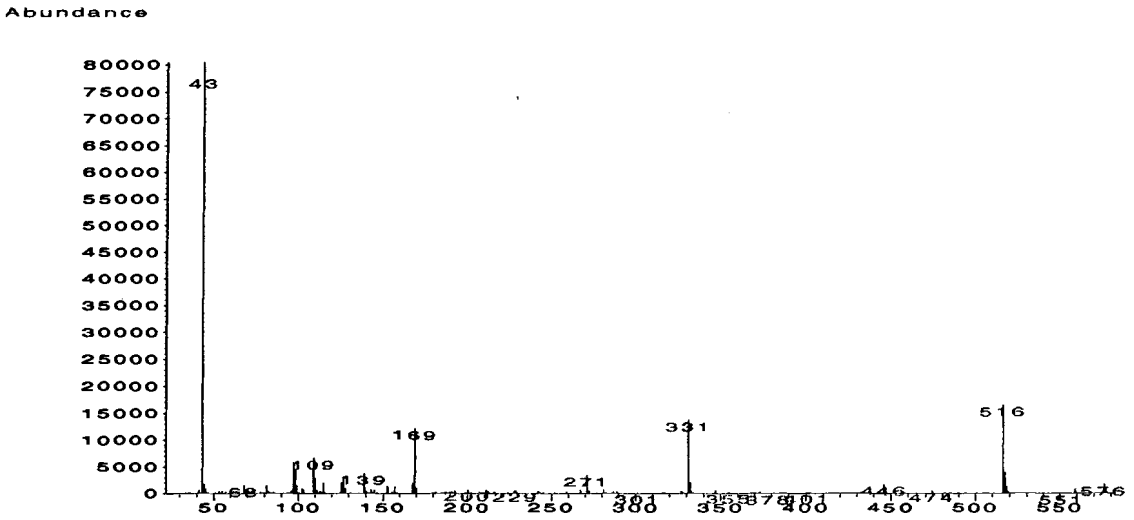

Figure A.24. GC/MS scan of 1-bromo-l-deoxycellobiose heptaacetate.

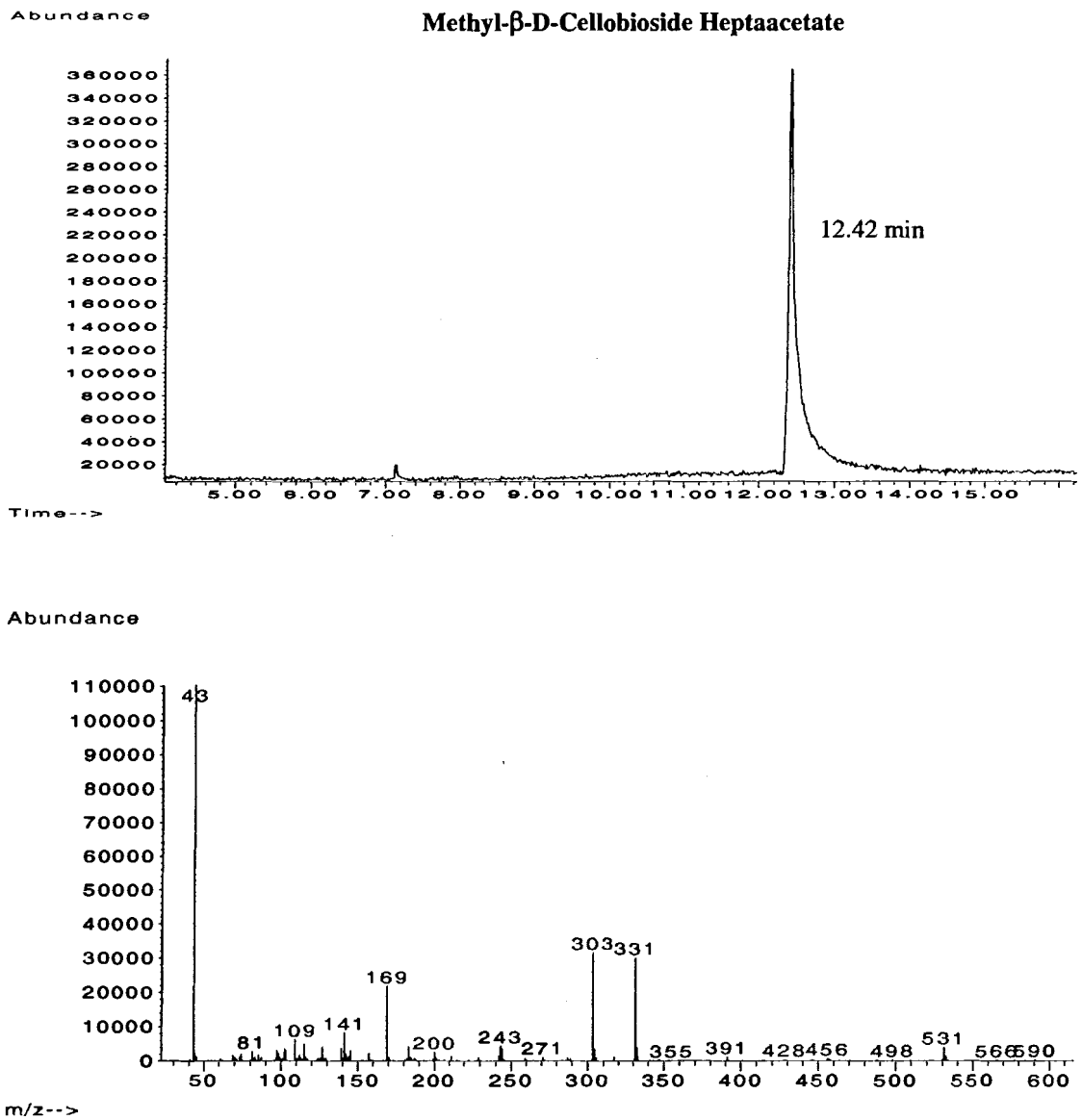

Figure A.25. GC/MS scan of methyl-β-D-cellobioside heptaacetate.

APPENDIX B

HPLC Data

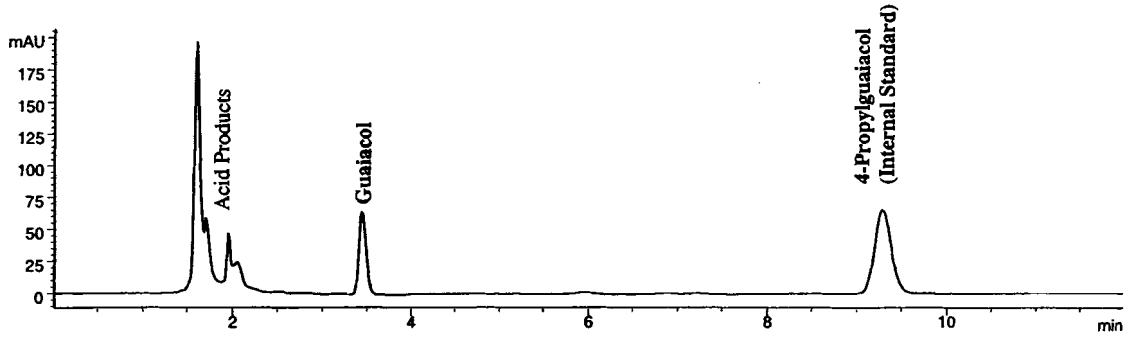

Figure B.1. HPLC scan of guaiacol (Control I) treated in the pressurized oxygen reaction.

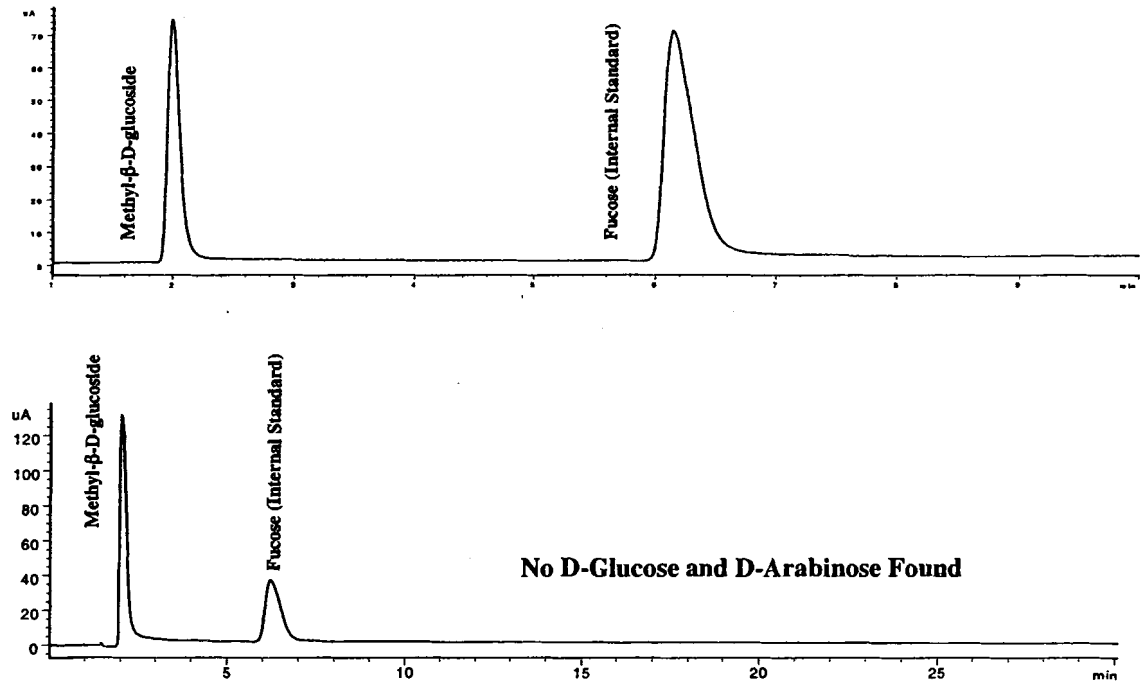

Figure B.2. HPLC scan of methyl-β-D-glucoside (Control II) treated in the pressurized oxygen reaction. Top scan is for the determination of the recovery of methyl-β-D-glucoside. The bottom scan is for the determination of D-glucose and D-arabinose.

Guaiacol : Methyl-β-D-glucoside = 1: 1

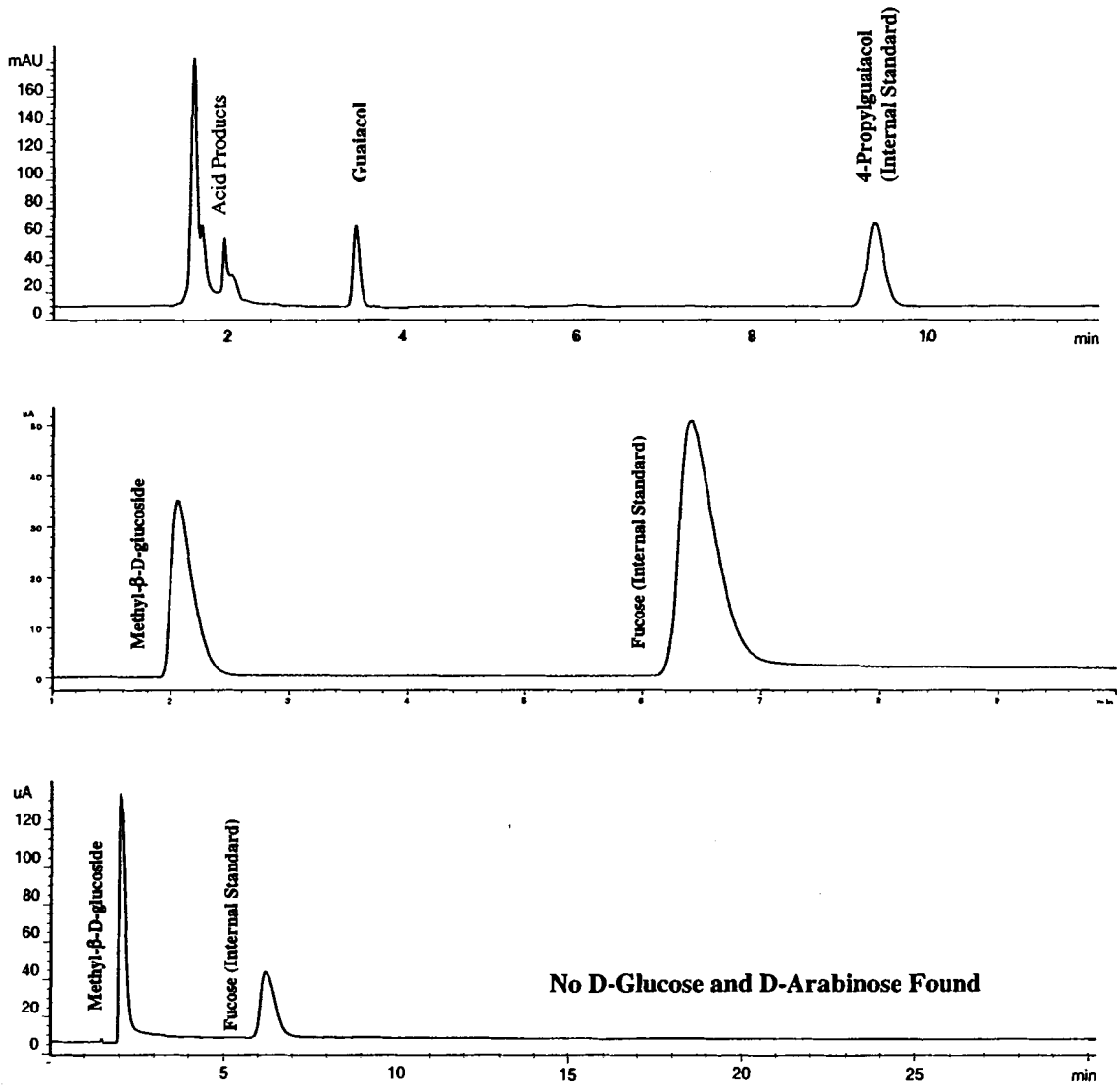

Figure B.3. HPLC scans of the pressurized oxygen reactions of the mixture of guaiacol and methyl-β-D-glucoside. The top scan is for the determination of guaiacol, the middle scan is for the determination of methyl-β-D-glucoside, and the bottom scan is for the determination of D-glucose and D-arabinose.

Guaiacol : Methyl-β-D-glucoside = 1: 2

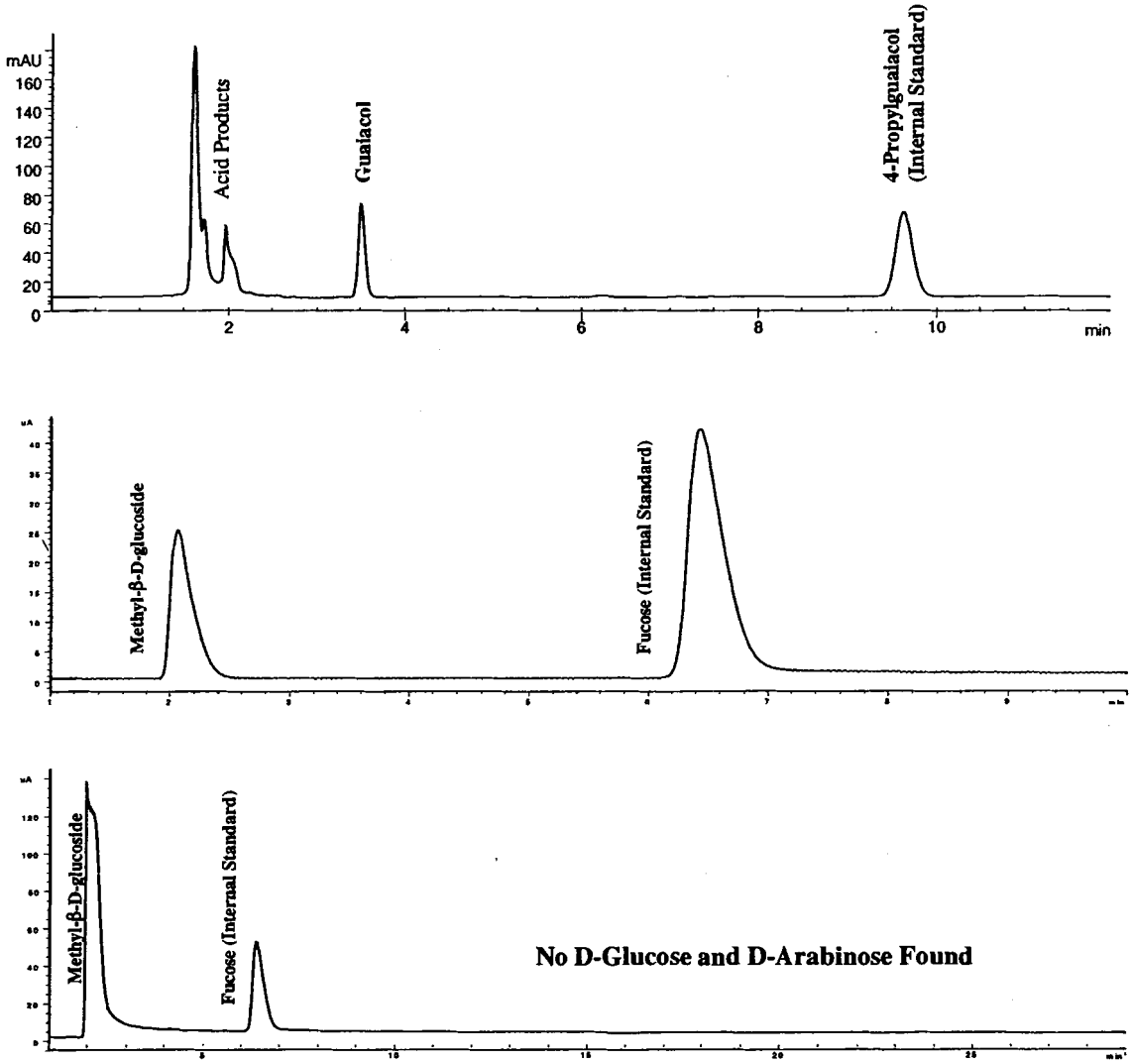

Figure B.3. Continued.

Guaiacol : Methyl-β-D-glucoside = 1: 4

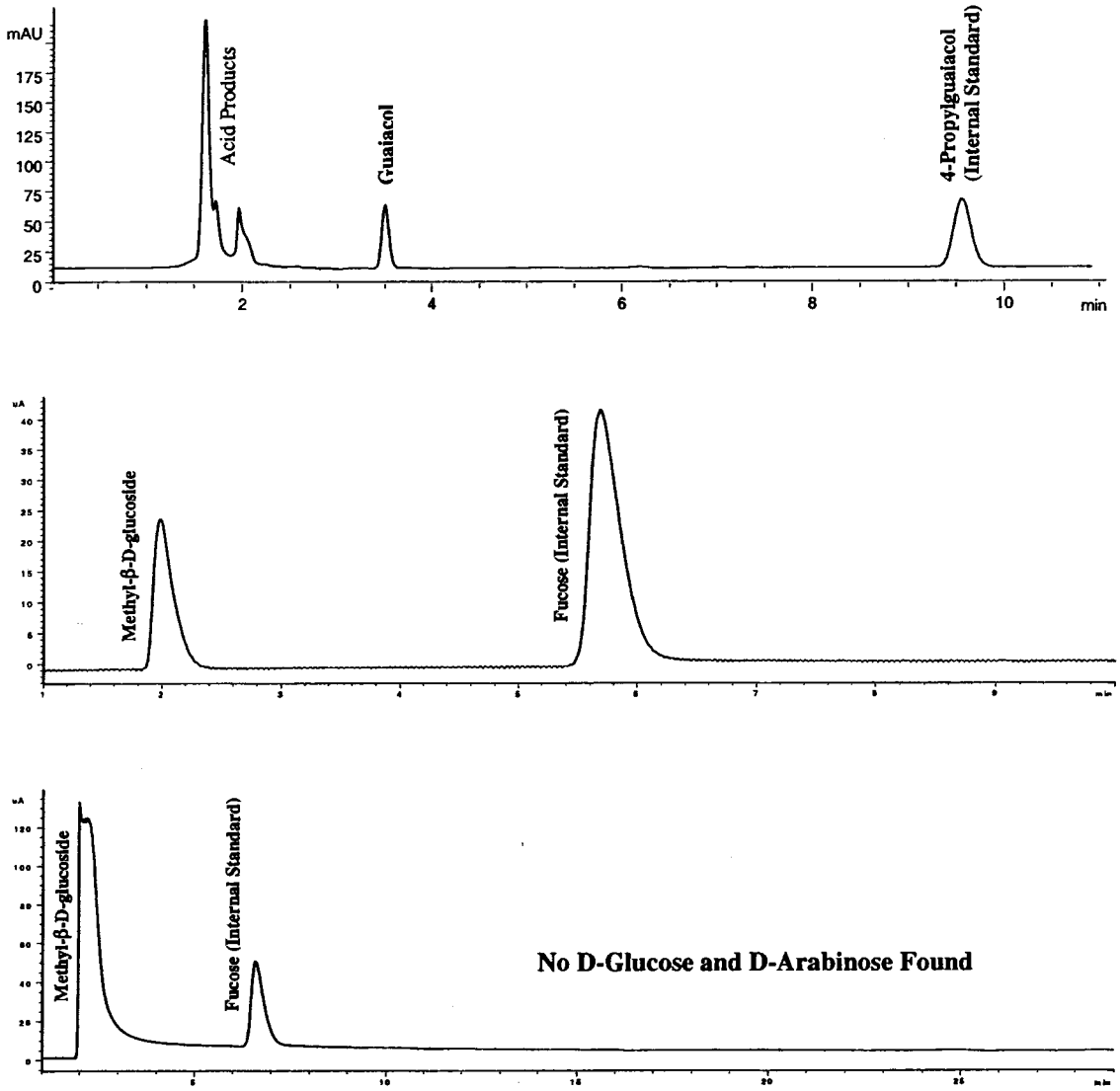

Figure B.3. Continued.

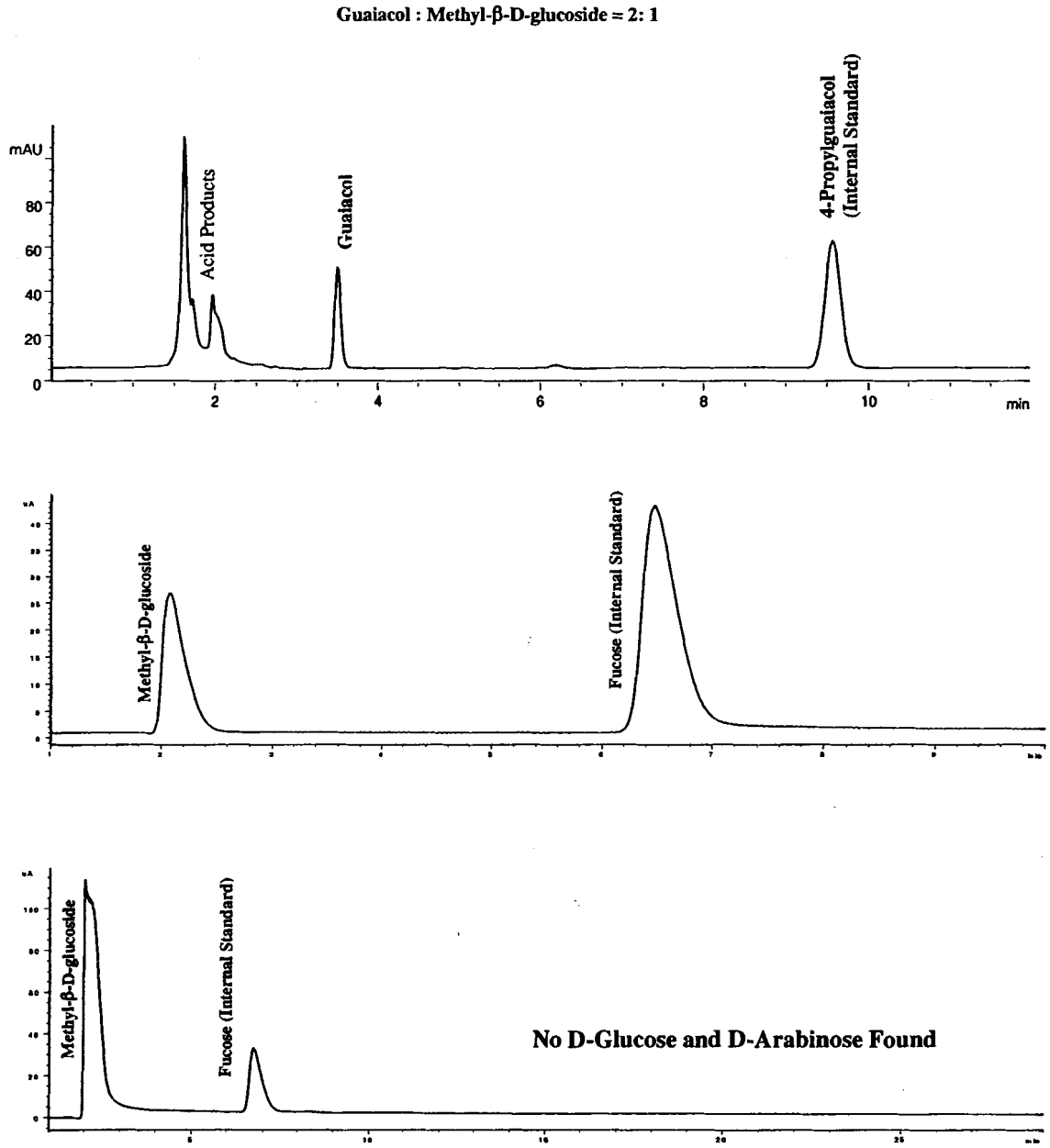

Figure B.3. Continued.

Guaiacol : Methyl-β-D-glucoside = 2: 2

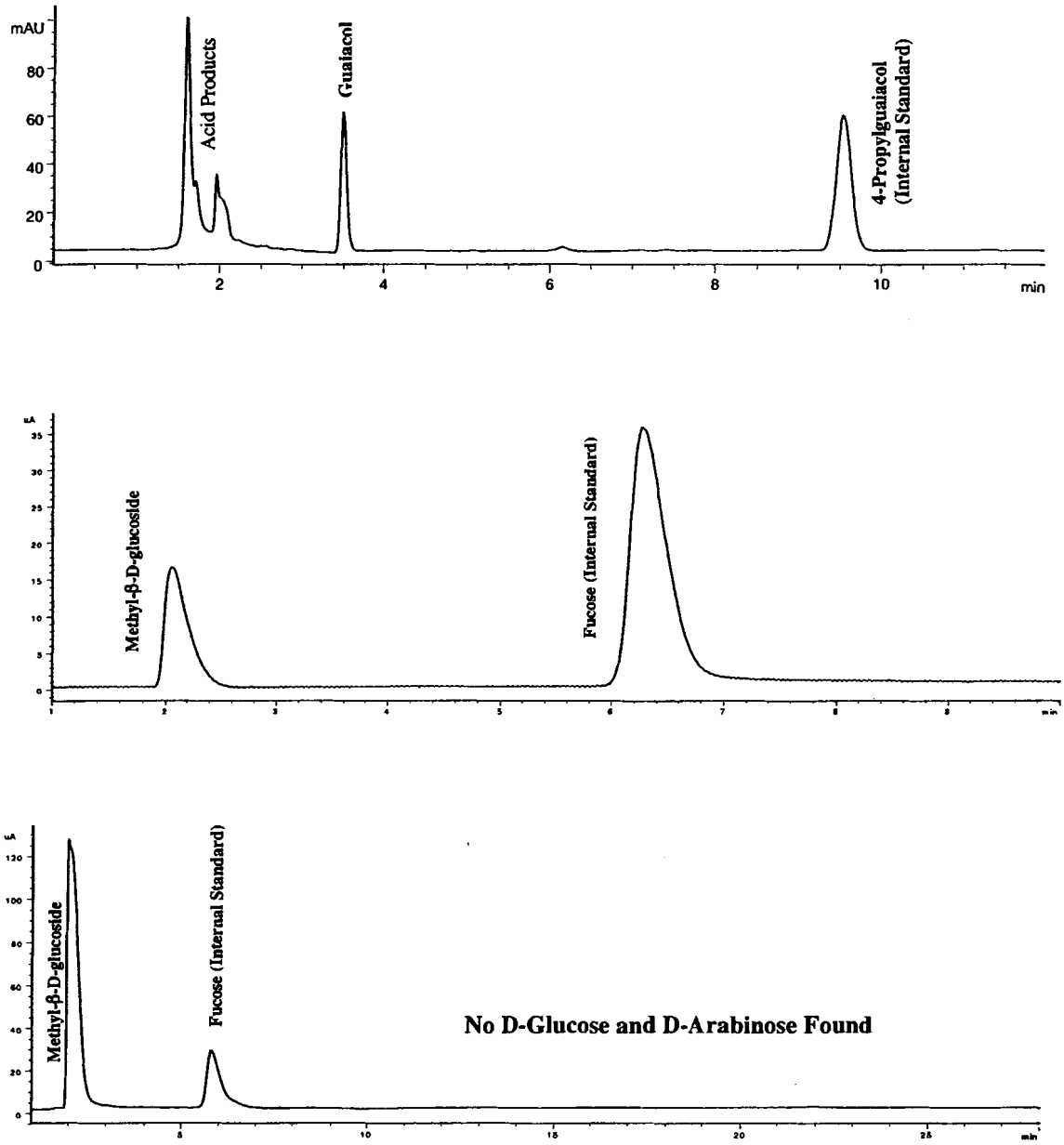

Figure B.3. Continued.

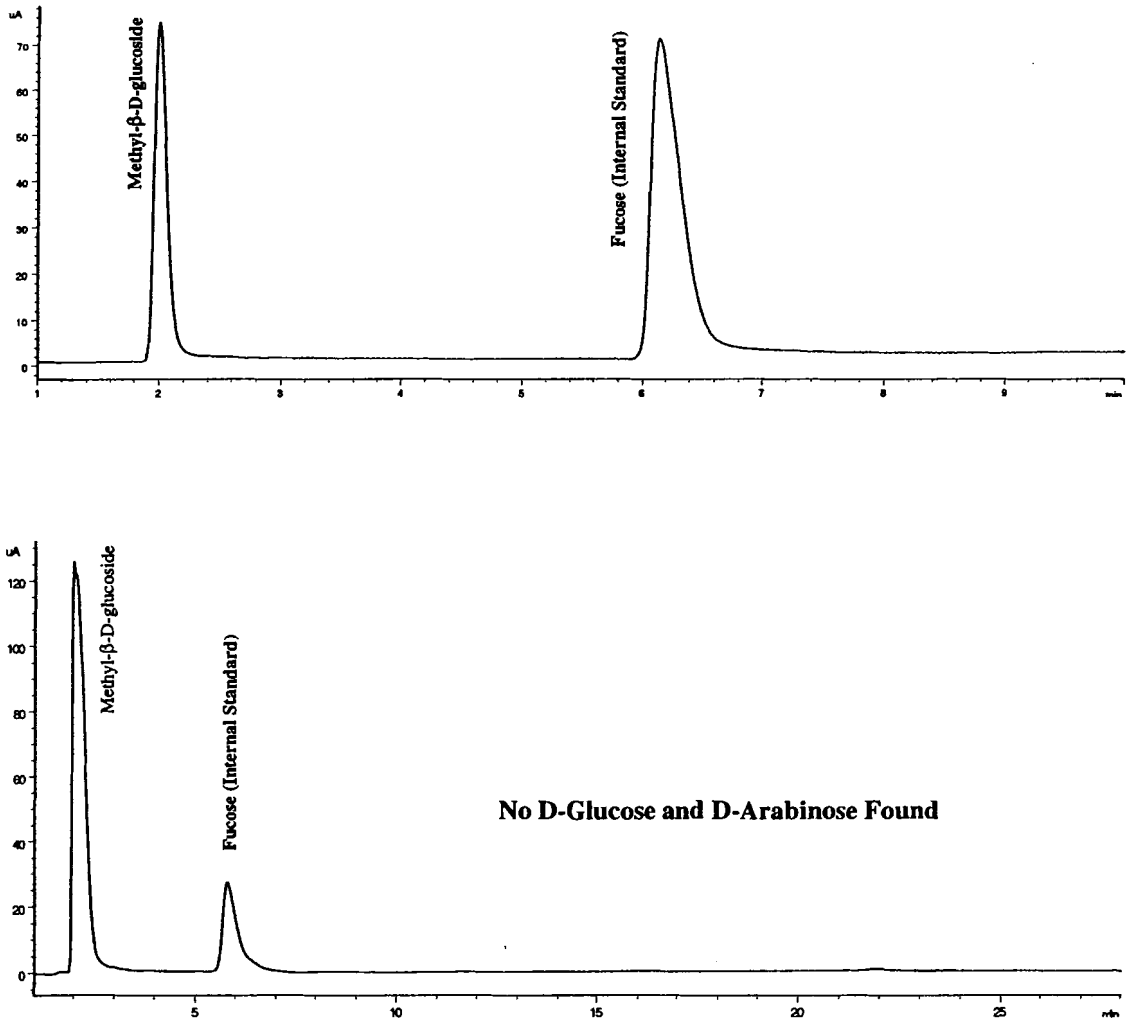

Figure B.4. HPLC scans of methyl-β-D-glucoside (Control III) treated with UV light in pH 9.6 buffer for 45 minutes. The top scan is for the dermination of the recovery of methyl-β-D-glucoside. The bottom scan is for determination of D-glucose and D-arabinose formed during the reaction.

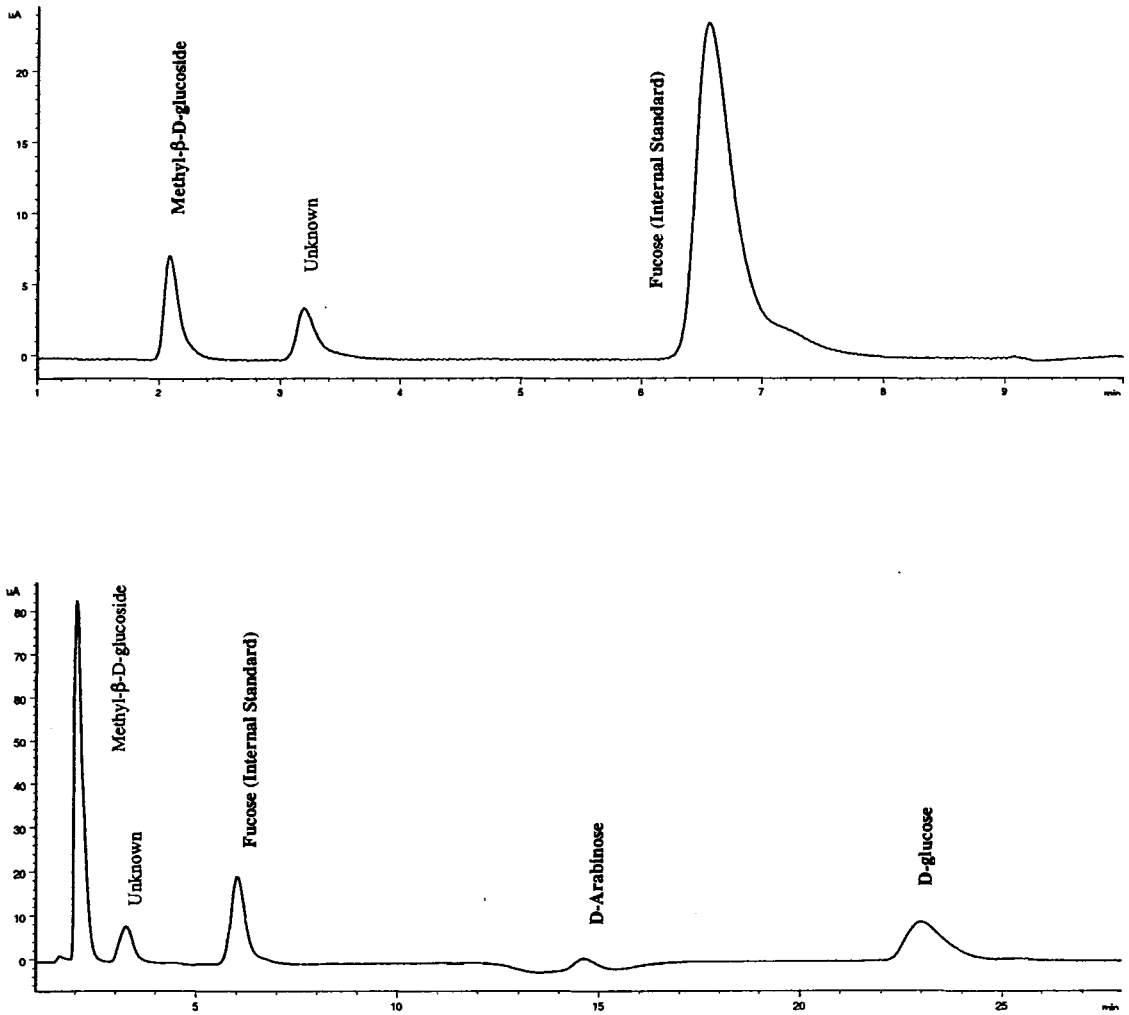

Figure B.5. HPLC scans of UV/H_2O_2 reactions with methyl-β-D-glucoside (Control IV). The top scan is for the determination of the recovery of methyl-β-D-glucoside. The bottom scan is for determination of D-glucose and D-arabinose formed during the reaction.

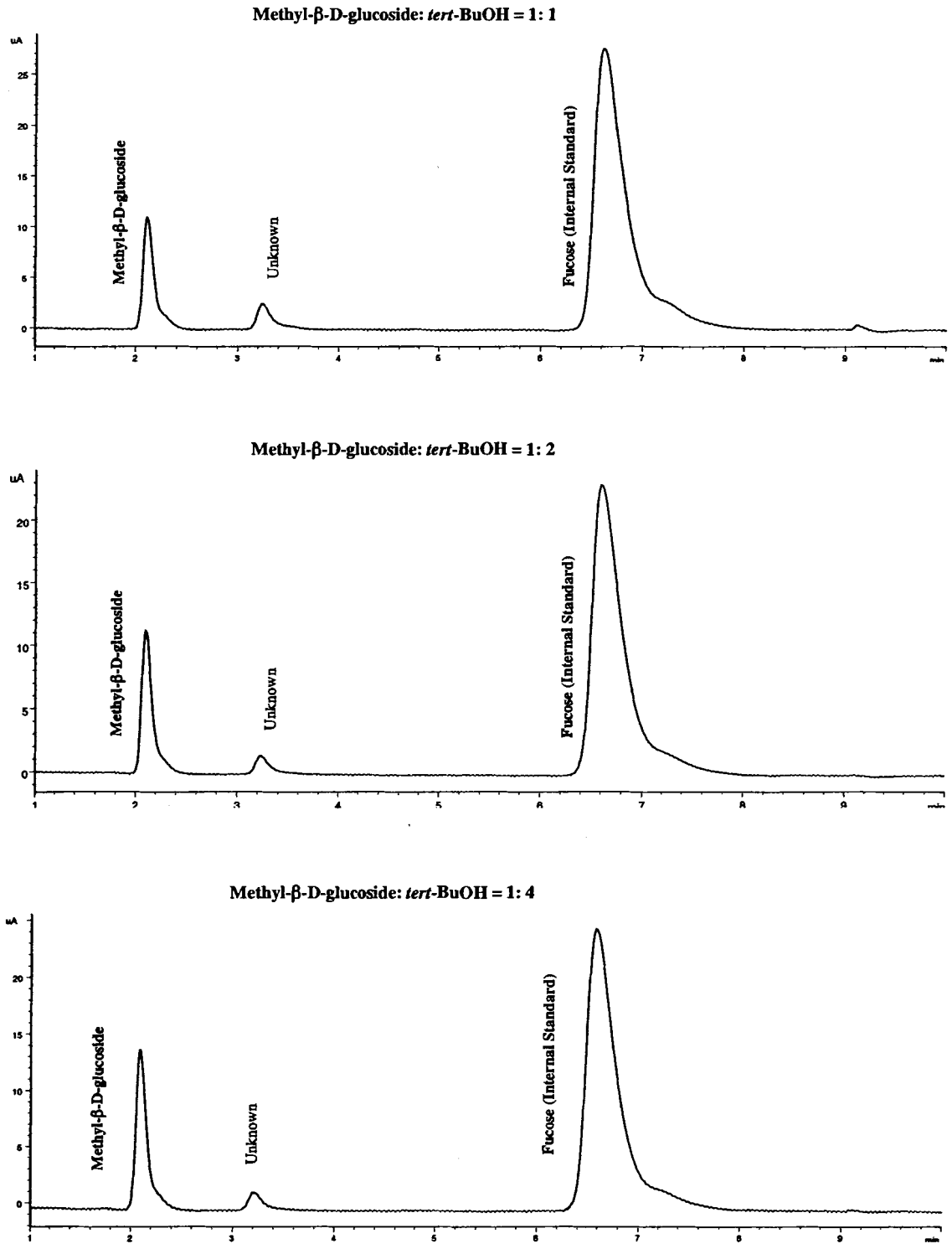

Figure B.6. HPLC scans of UV/H_2O_2 reactions with methyl-β-D-glucoside in the presence of *tert*-BuOH for the determination of the recovery of methyl-β-D-glucoside.

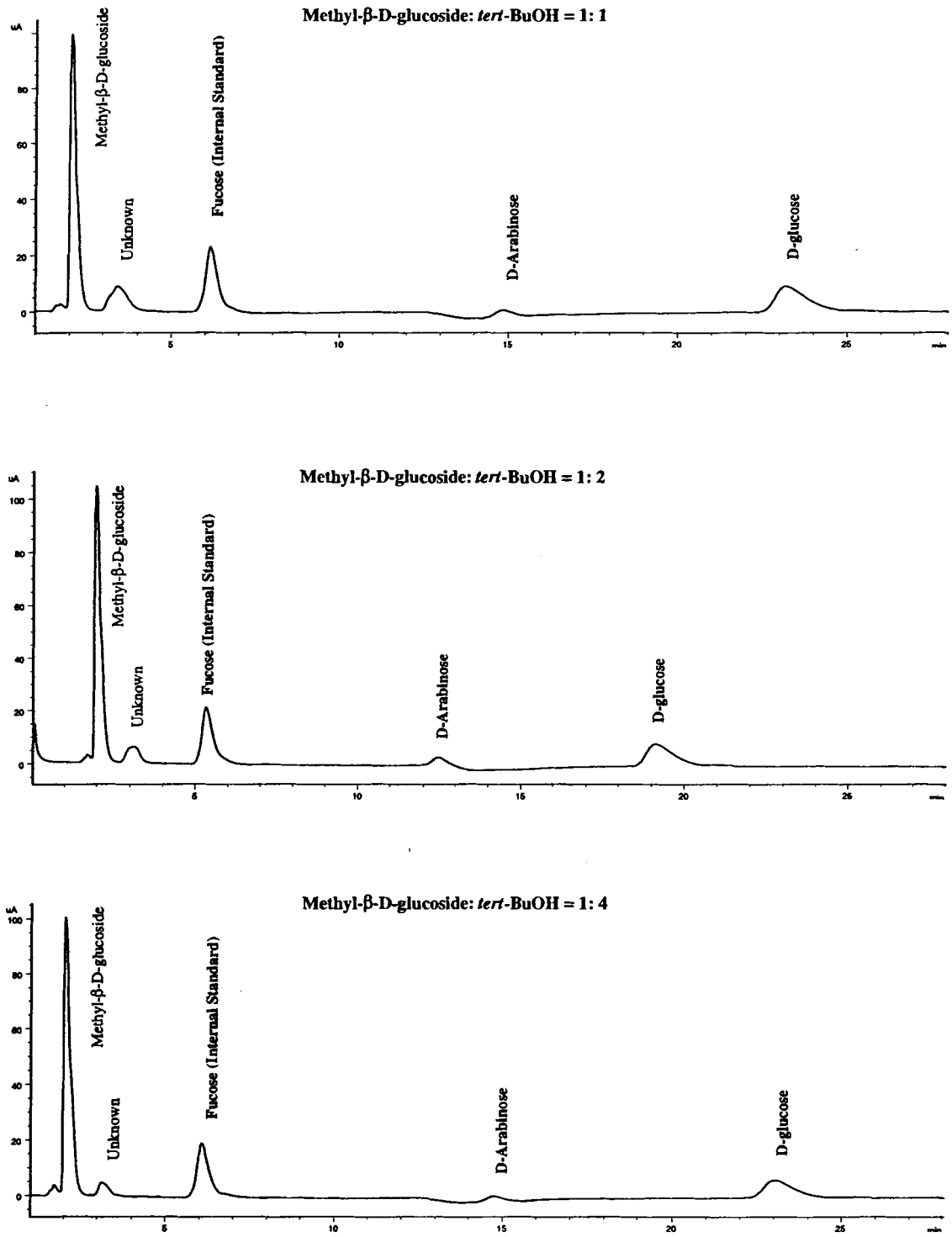

Figure B.7. HPLC scans of UV/H_2O_2 reactions with methyl-β-D-glucoside in the presence of *tert*-BuOH for the determination of the formation of D-glucose and D-arabinose.

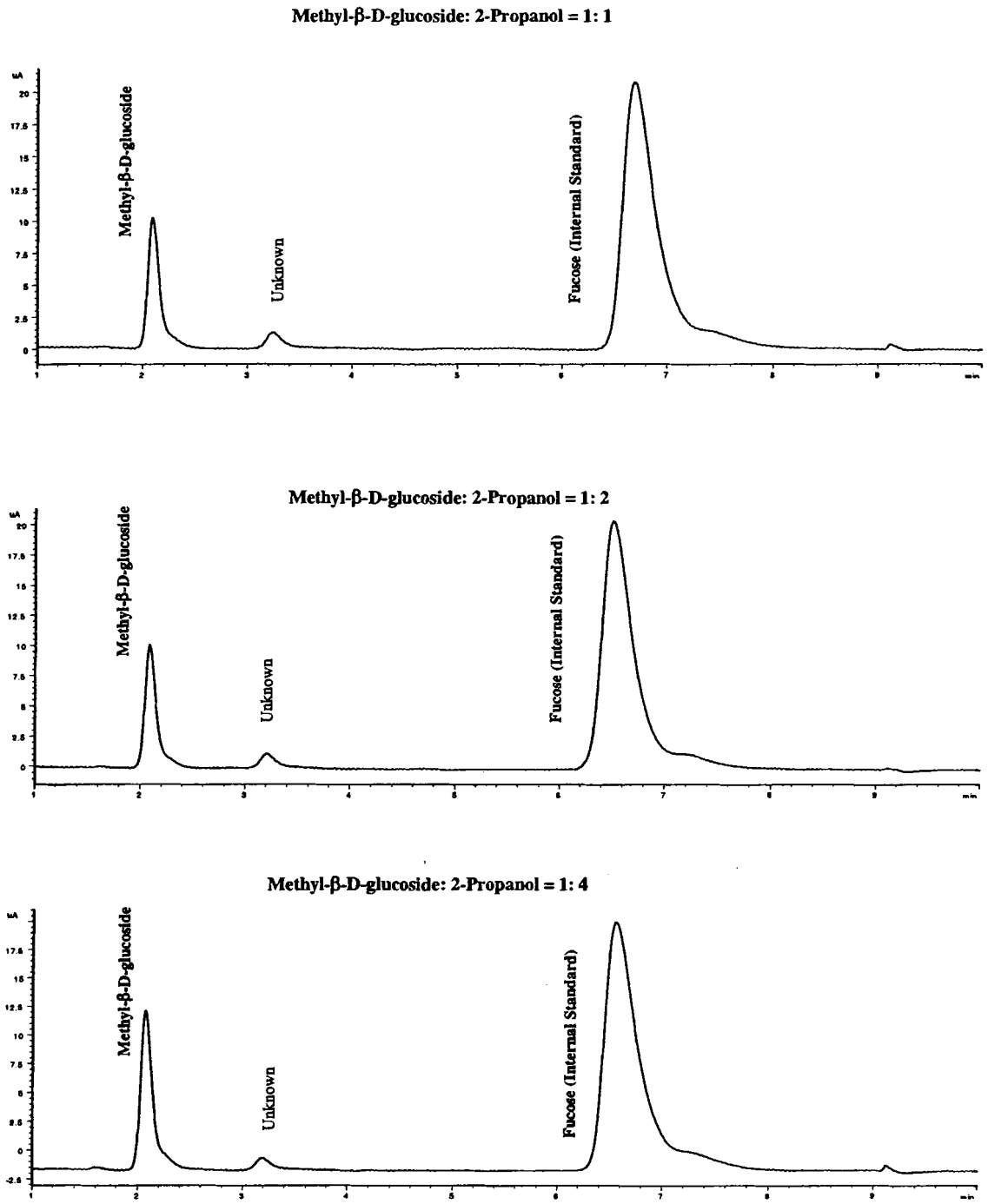

Figure B.8. HPLC scans of UV/H_2O_2 reactions with methyl-β-D-glucoside in the presence of 2-propanol for the determination of the recovery of methyl-β-D-glucoside.

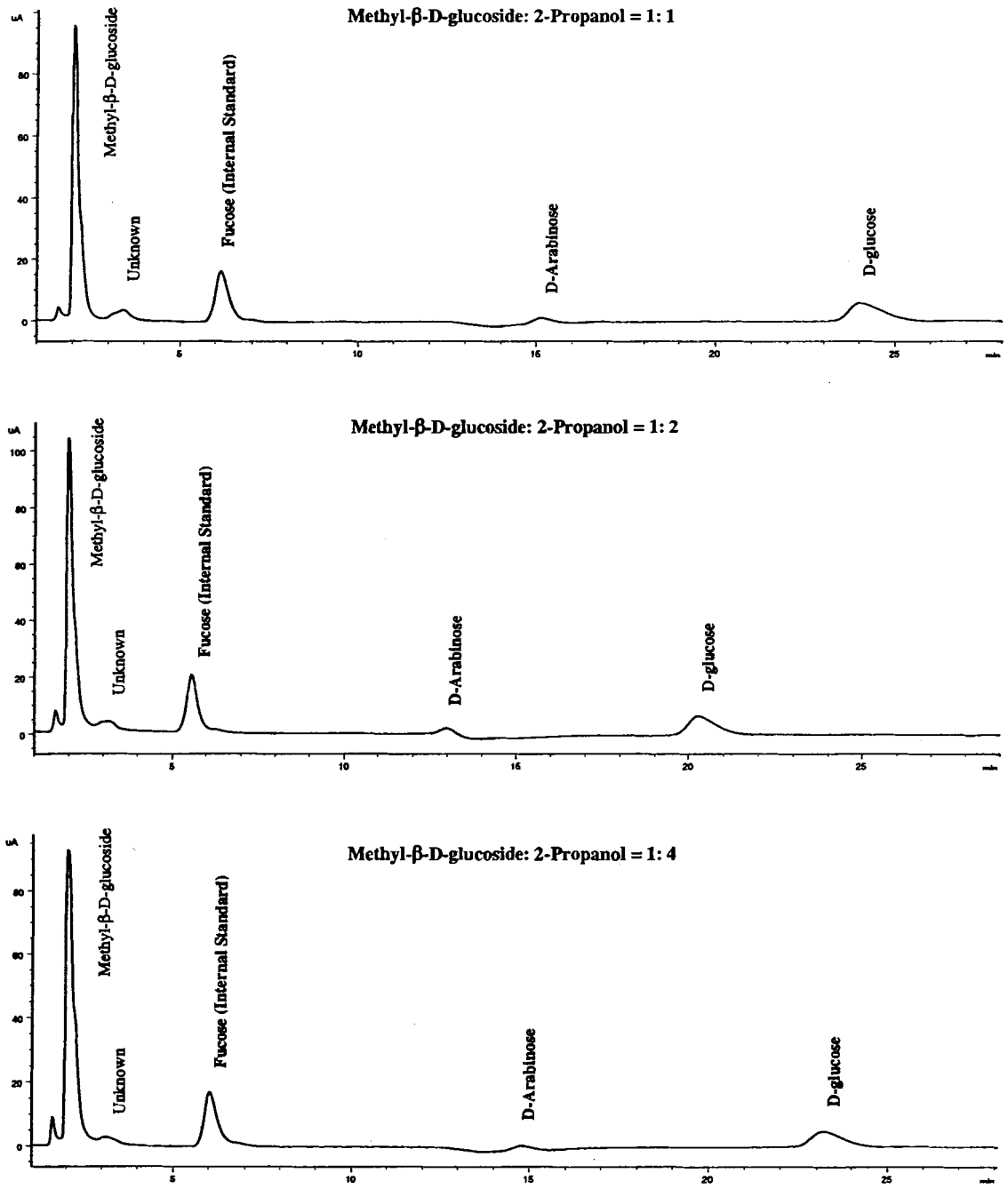

Figure B.9. HPLC scans of UV/H_2O_2 reactions with methyl-β-D-glucoside in the presence of 2-propanol for the determination of the formation of D-glucose and D-arabinose.

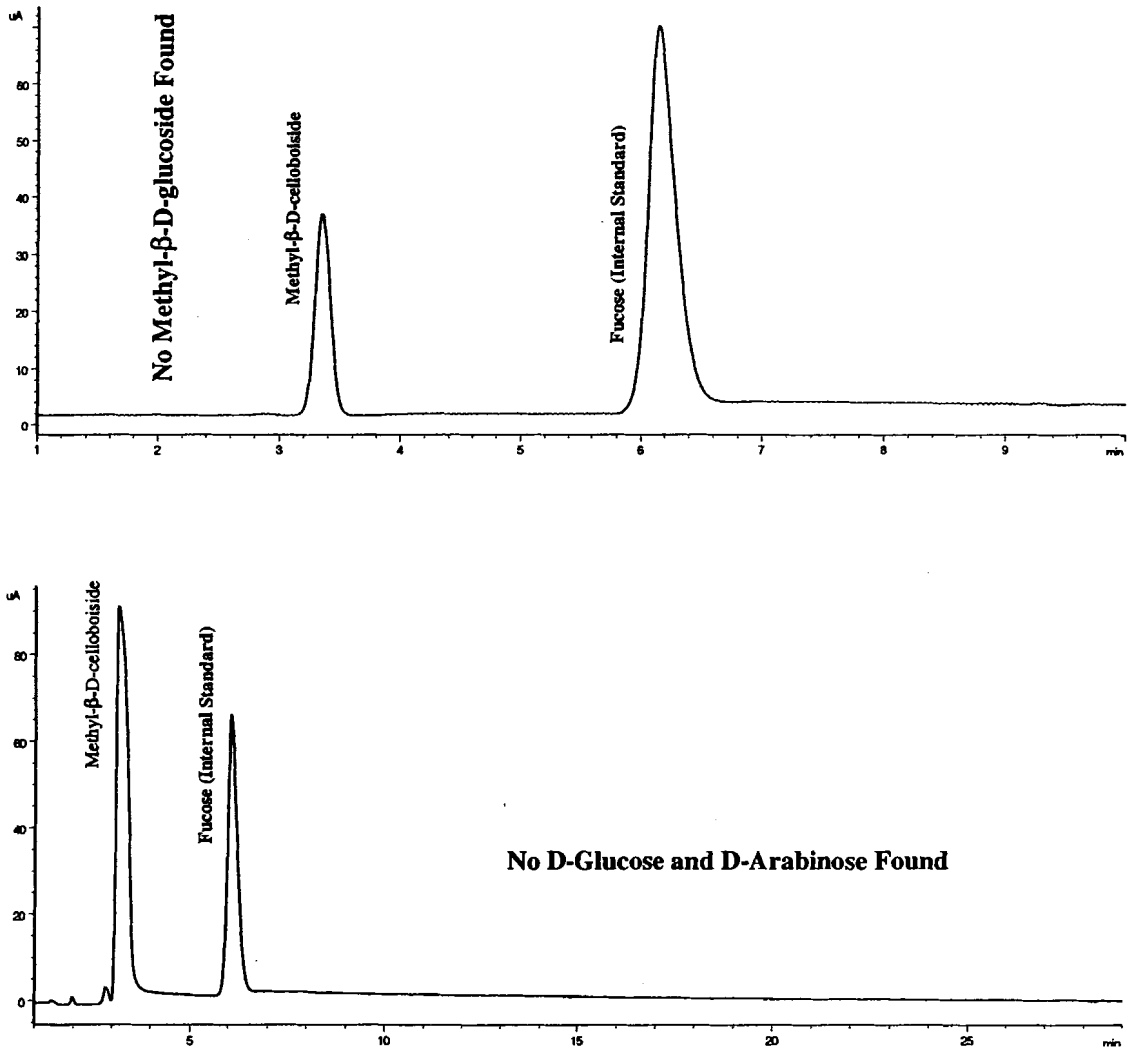

Figure B.10. HPLC scans of methyl-β-D-cellobioside treated with UV light in pH 9.6 buffer for 45 minutes. The top scan is for the determination of the recovery of methyl-β-D-cellobioside. The bottom scan is for determination of methyl-β-D-glucoside, D-glucose, and D-arabinose formed during the reaction.

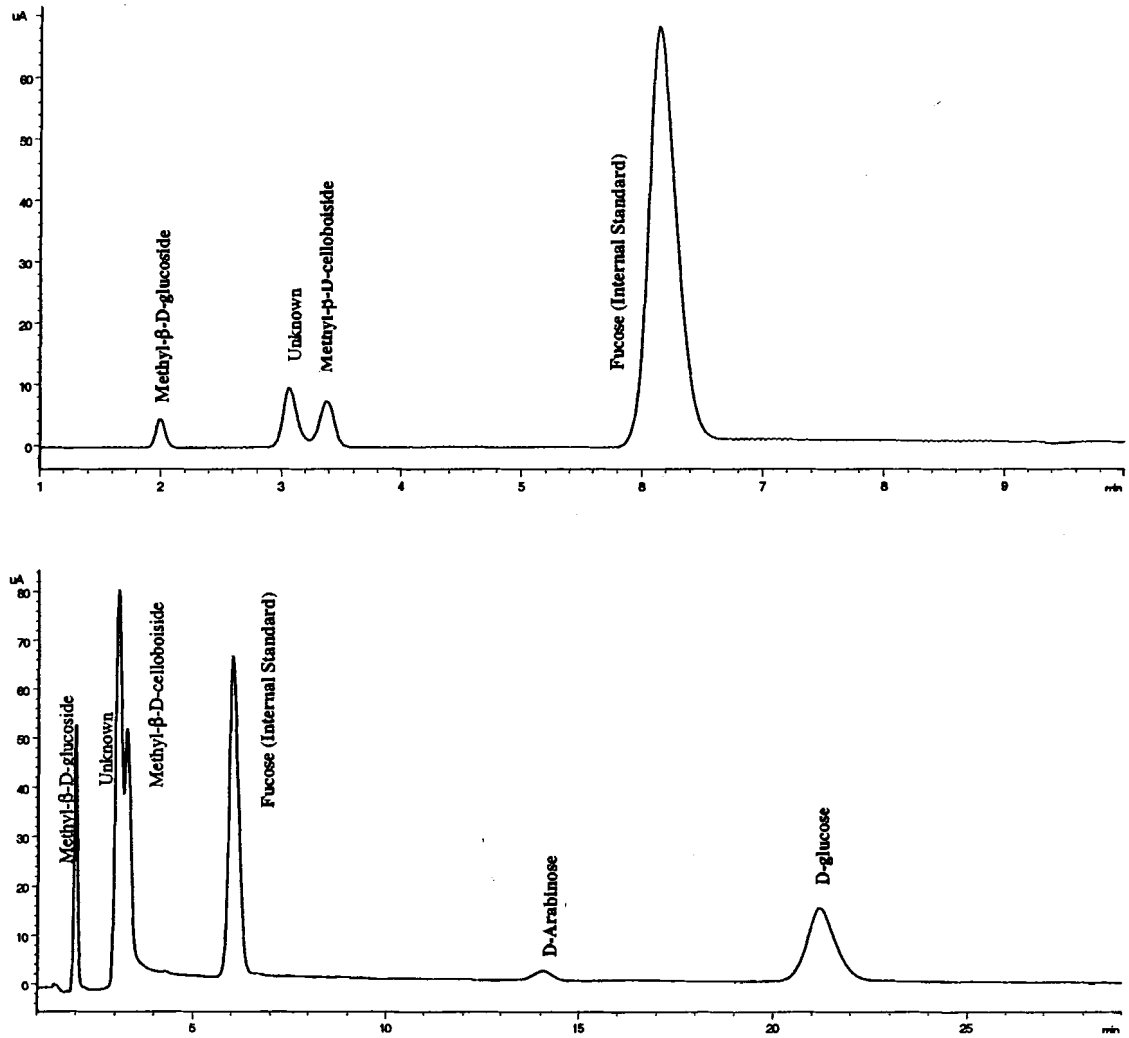

Figure B.11. HPLC scans of UV/H_2O_2 reactions with methyl-β-D-cellobioside. The top scan is for the determination of methyl-β-D-cellobioside and methyl-b-D-glucoside. The bottom scan is for determination of D-glucose and D-arabinose formed during the reaction.

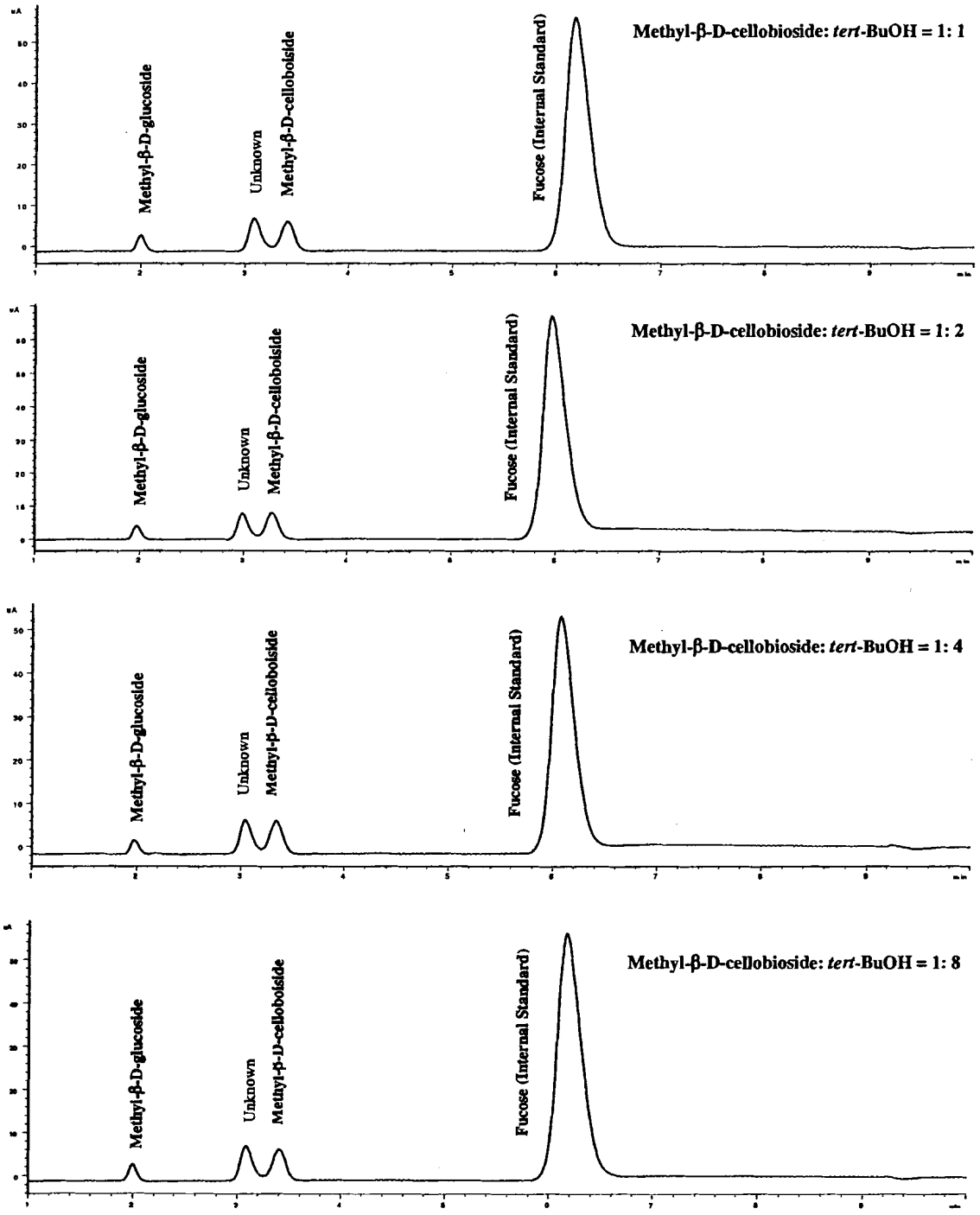

Figure B.12. HPLC scans of UV/H_2O_2 reactions with methyl-β-D-cellobioside in the presence of *tert*-BuOH for the determination of methyl-β-D-cellobioside and methyl-β-D-glucoside. Retention time varied with the column conditions.

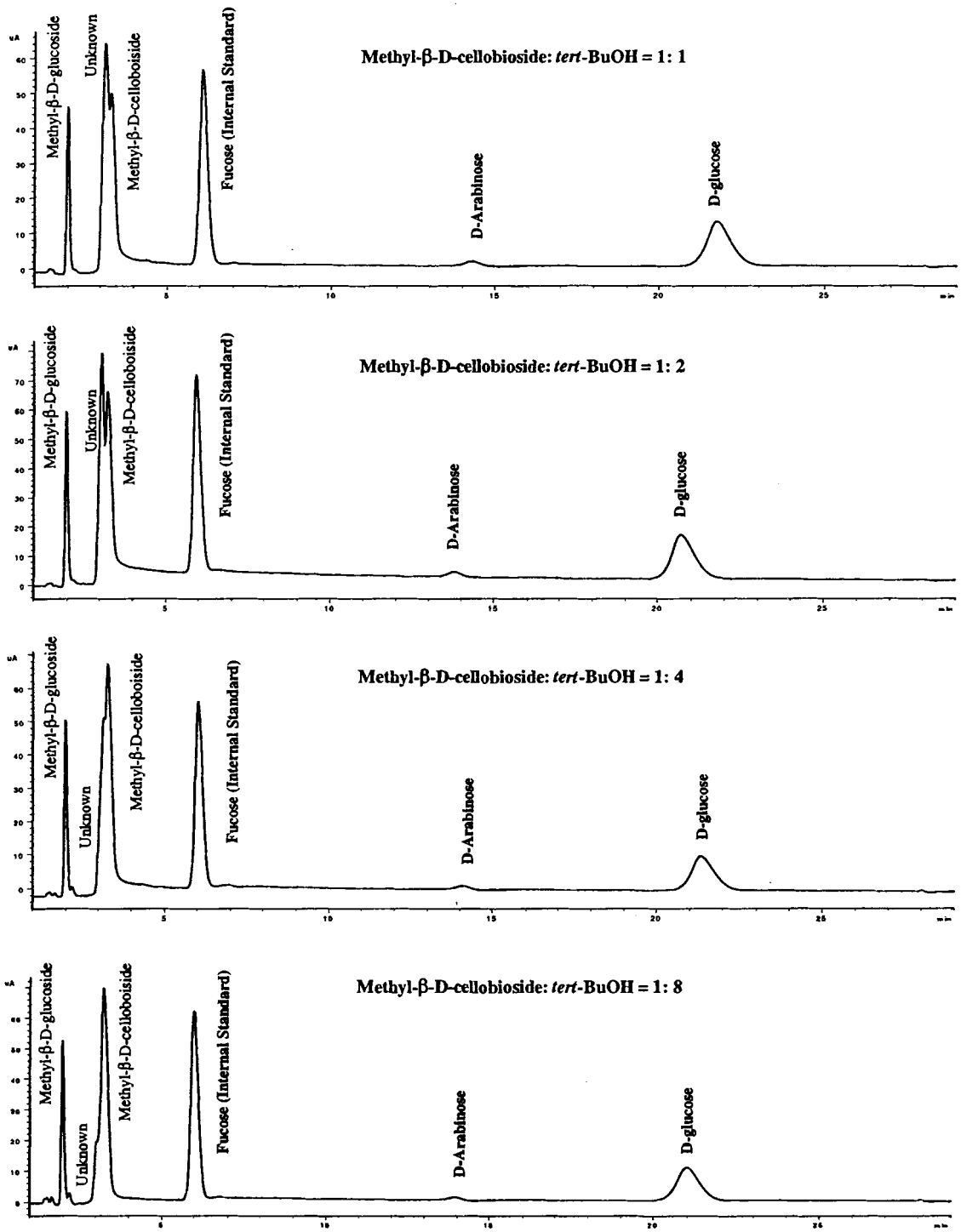

Figure B.13. HPLC scans of UV/H_2O_2 reactions with methyl-β-D-cellobioside in the presence of *tert*-BuOH for the determination of the formation of D-glucose and D-arabinose.

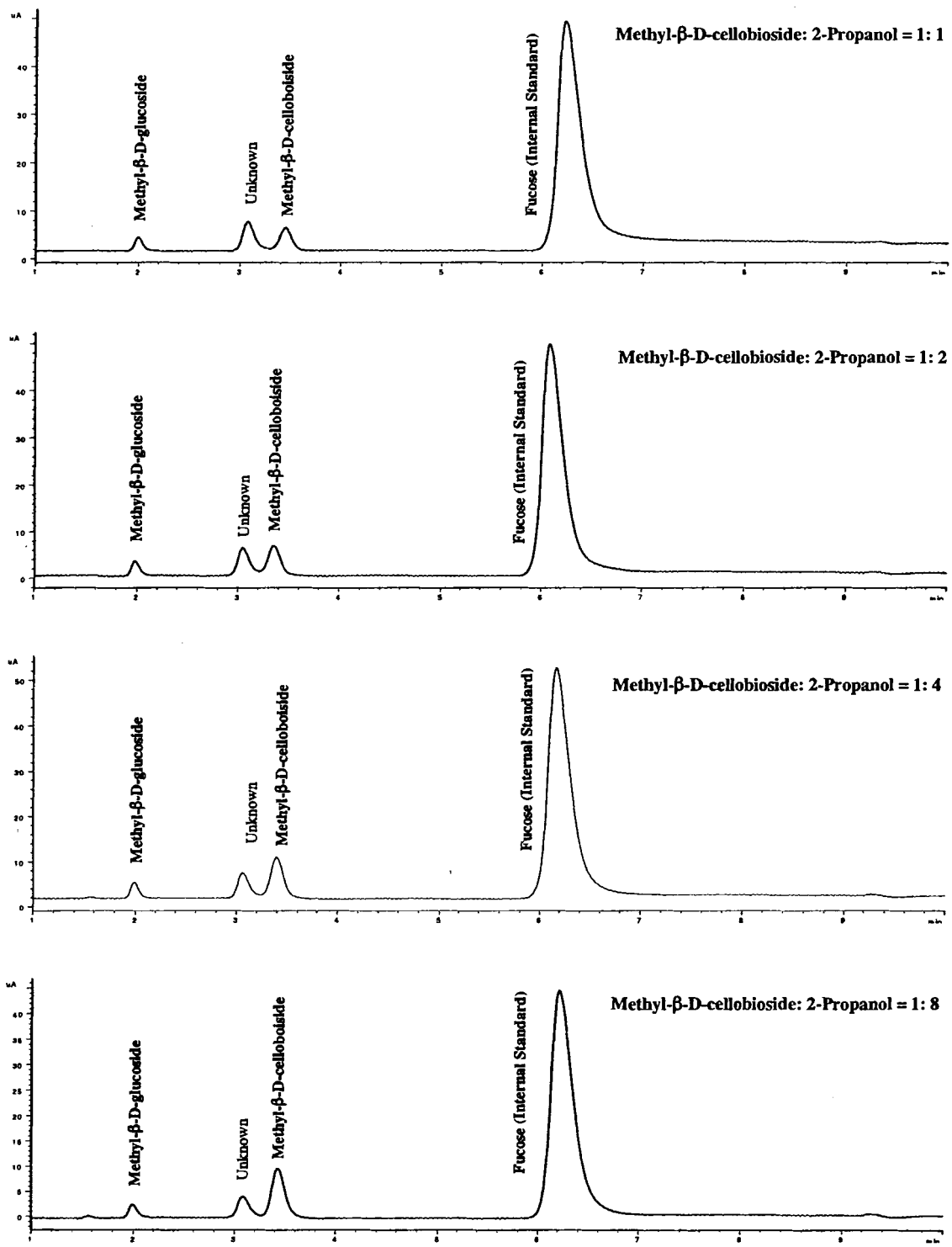

Figure B.14. HPLC scans of UV/H_2O_2 reactions with methyl-β-D-cellobioside in the presence of 2-propanol for the determination of methyl-β-D-cellobioside and methyl-β-D- glucoside. Retention time varied with the column conditions.

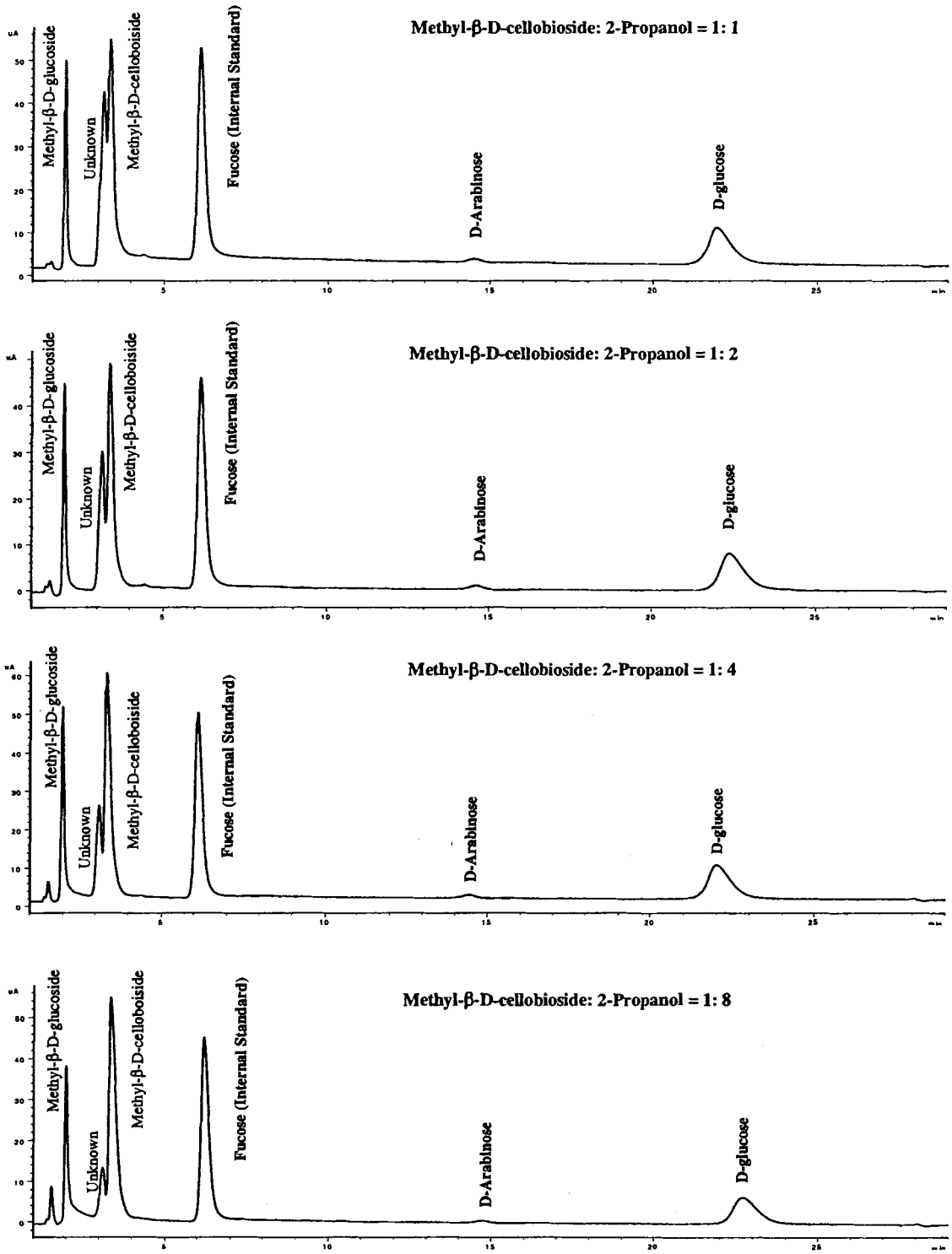

Figure B.15. HPLC scans of UV/H_2O_2 reactions with methyl-β-D-cellobioside in the presence of 2-propanol for the determination of the formation of D-glucose and D-arabinose.

APPENDIX C

GC/MS Data of The Pressurized Oxygen and UV/H_2O_2 Reactions

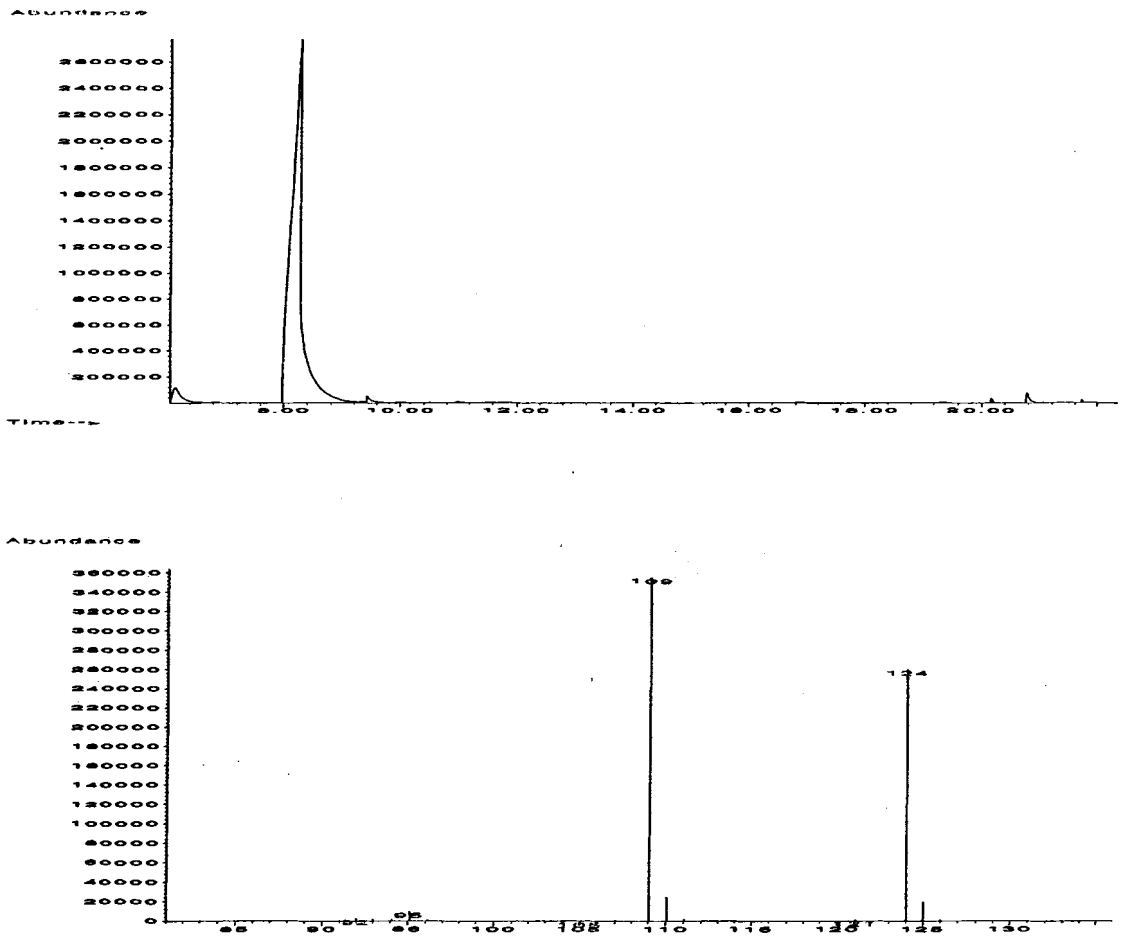

Figure C.1. GC/MS scan of guaiacol extracted from the reaction Control I.

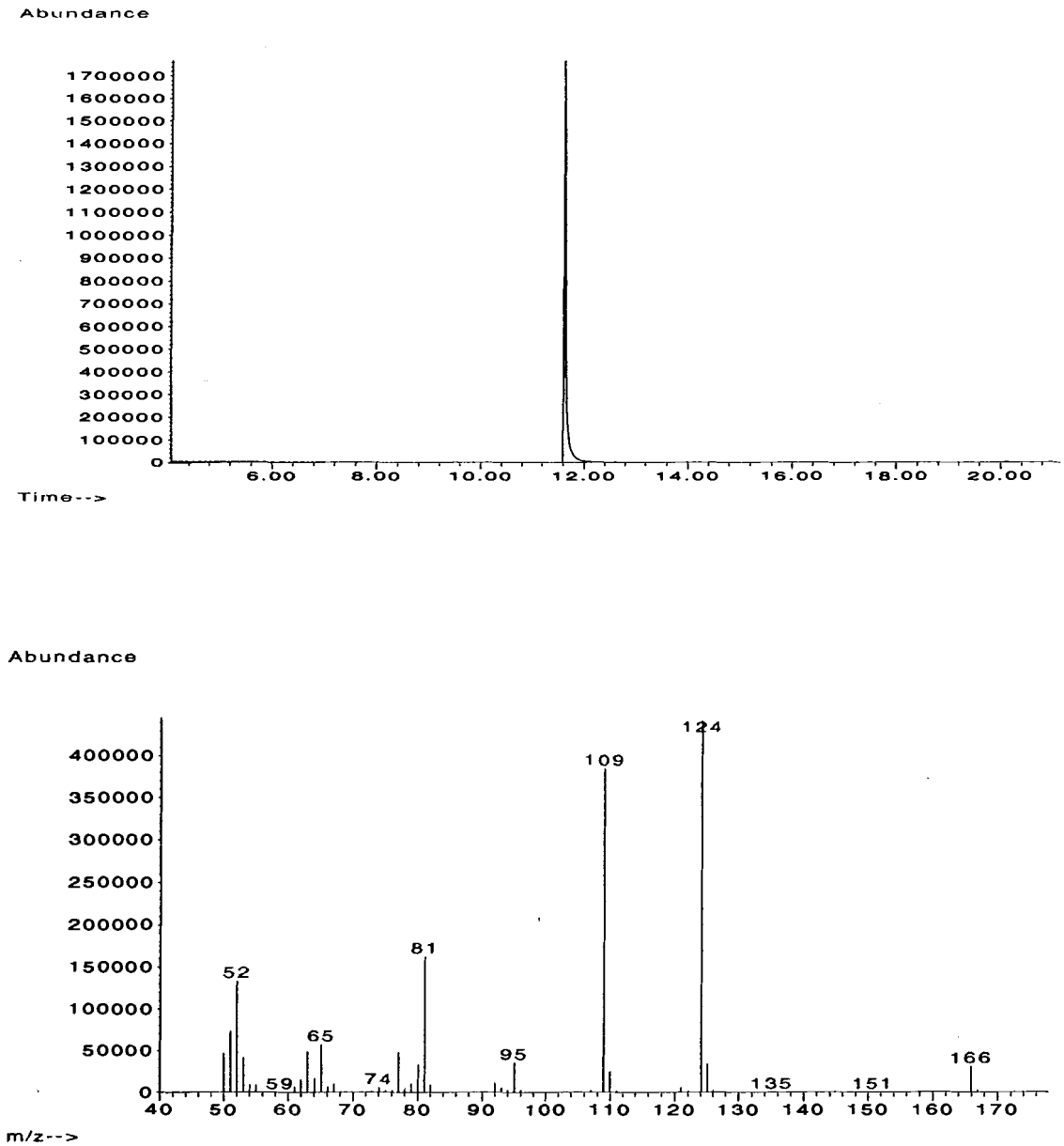

Figure C.2. GC/MS scan of acetylated guaiacol extracted from the reaction Control I reacted under pressurized oxygen.

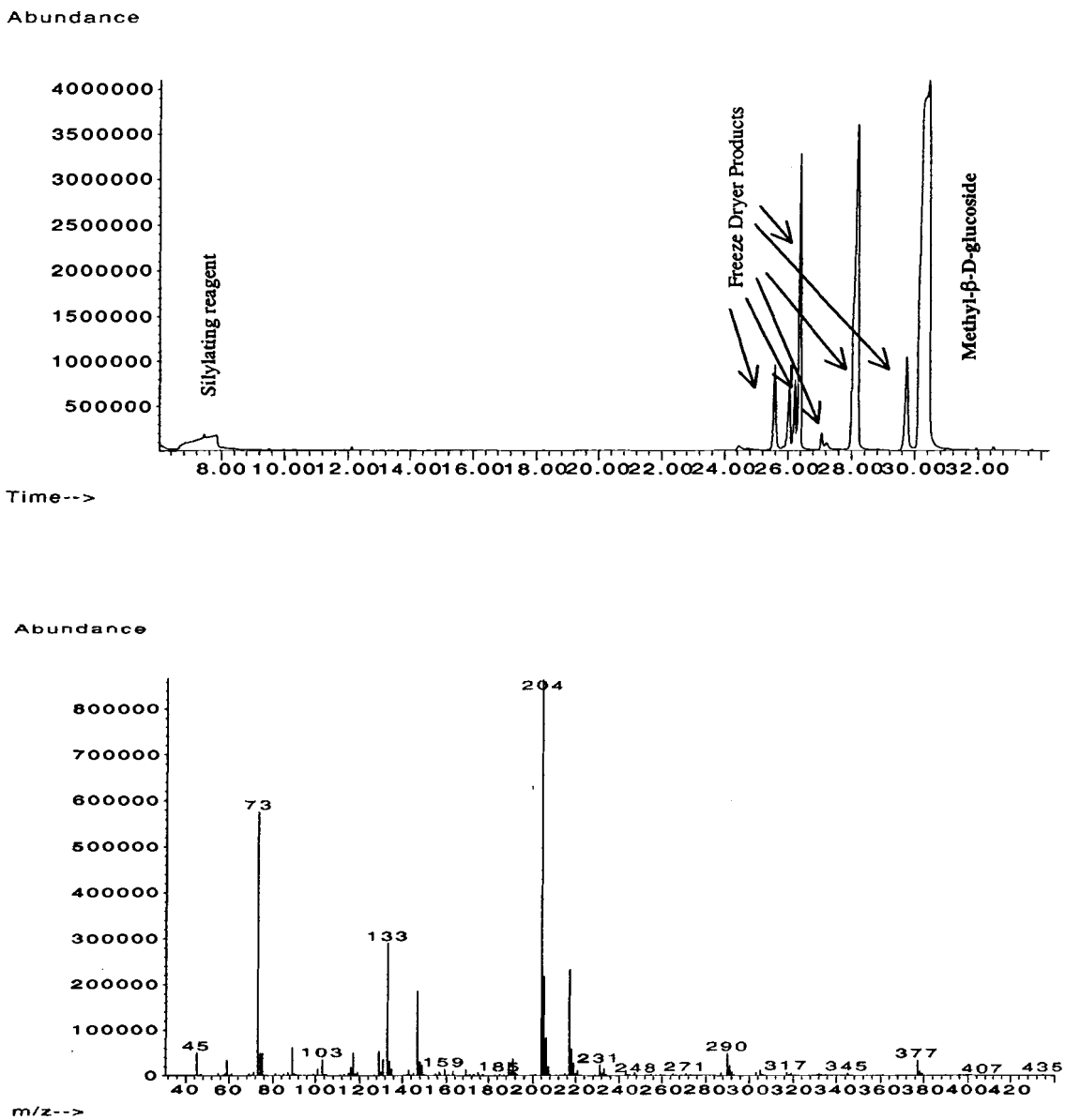

Figure C.3. GC/MS scan of silylated methyl-β-D-glucoside (Control II) reacted under pressurized oxygen.

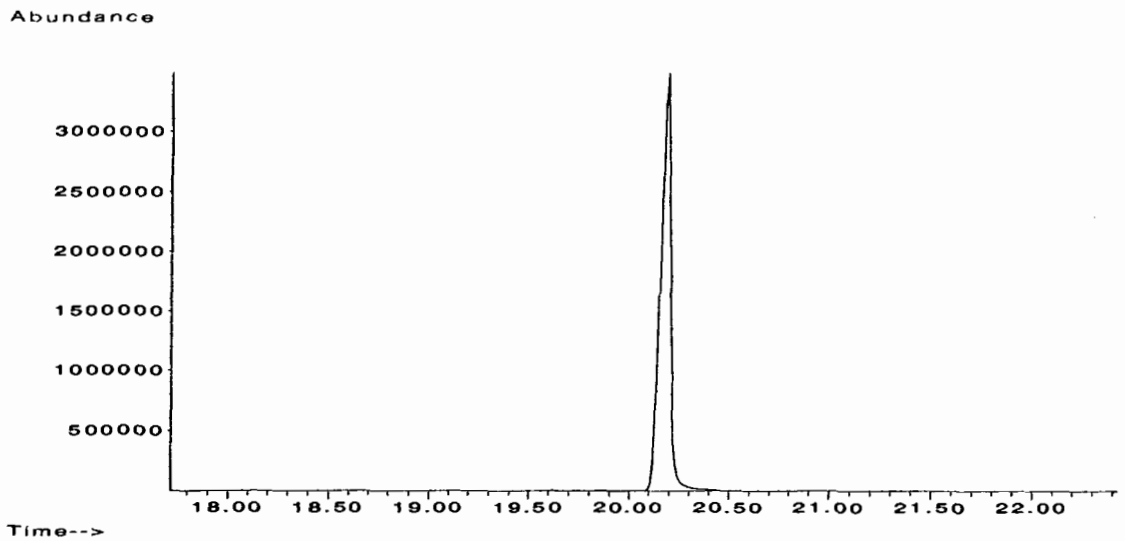

Figure C.4. GC/MS scan of acetylated methyl-β-D-glucoside (Control II) reacted under pressurized oxygen.

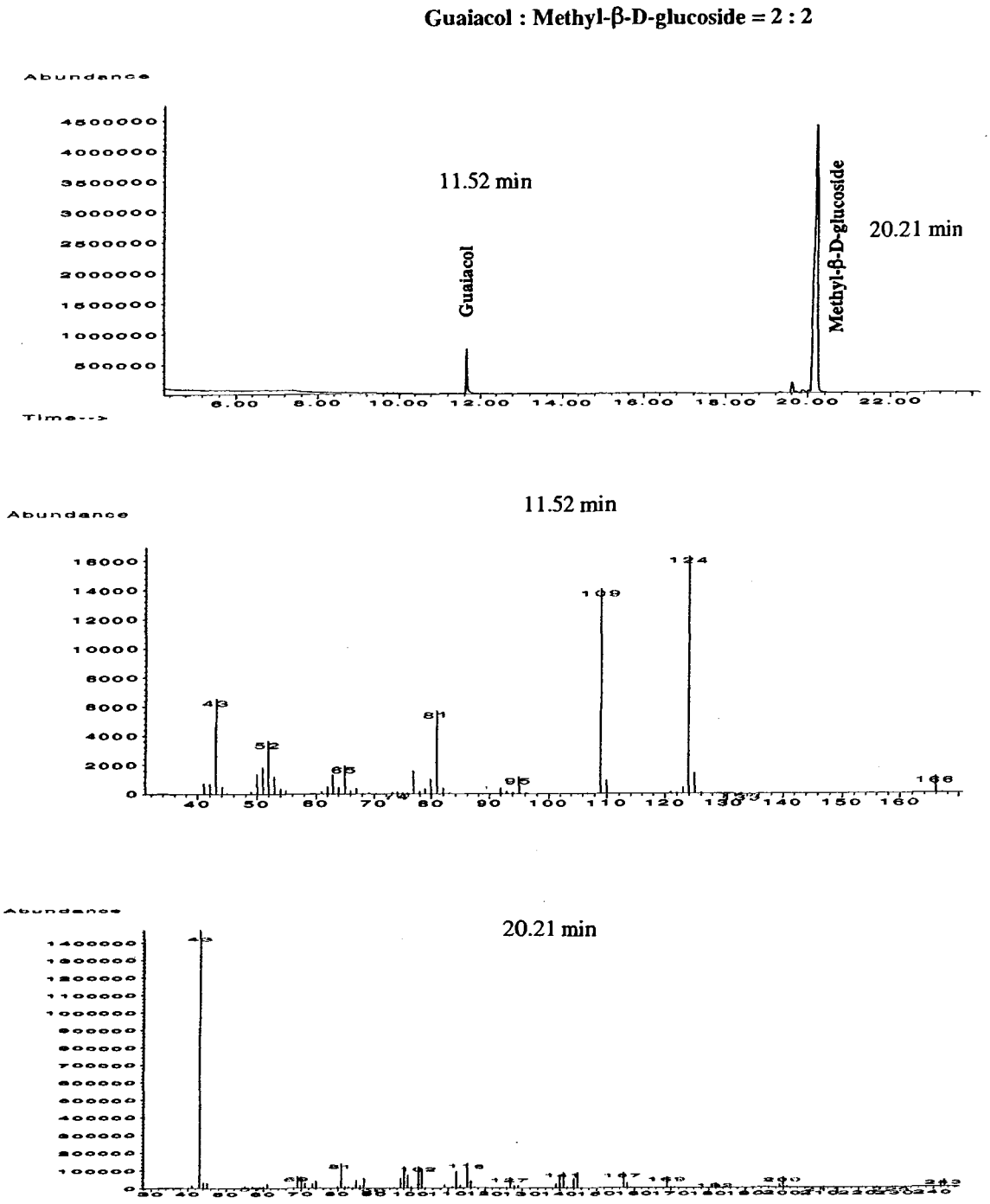

Figure C.5. GC/MS scan of acetylated mixture of guaiacol and methyl-β-D-glucoside reacted under pressurized oxygen.

Guaiacol : Methyl-β-D-glucoside = 1 : 1

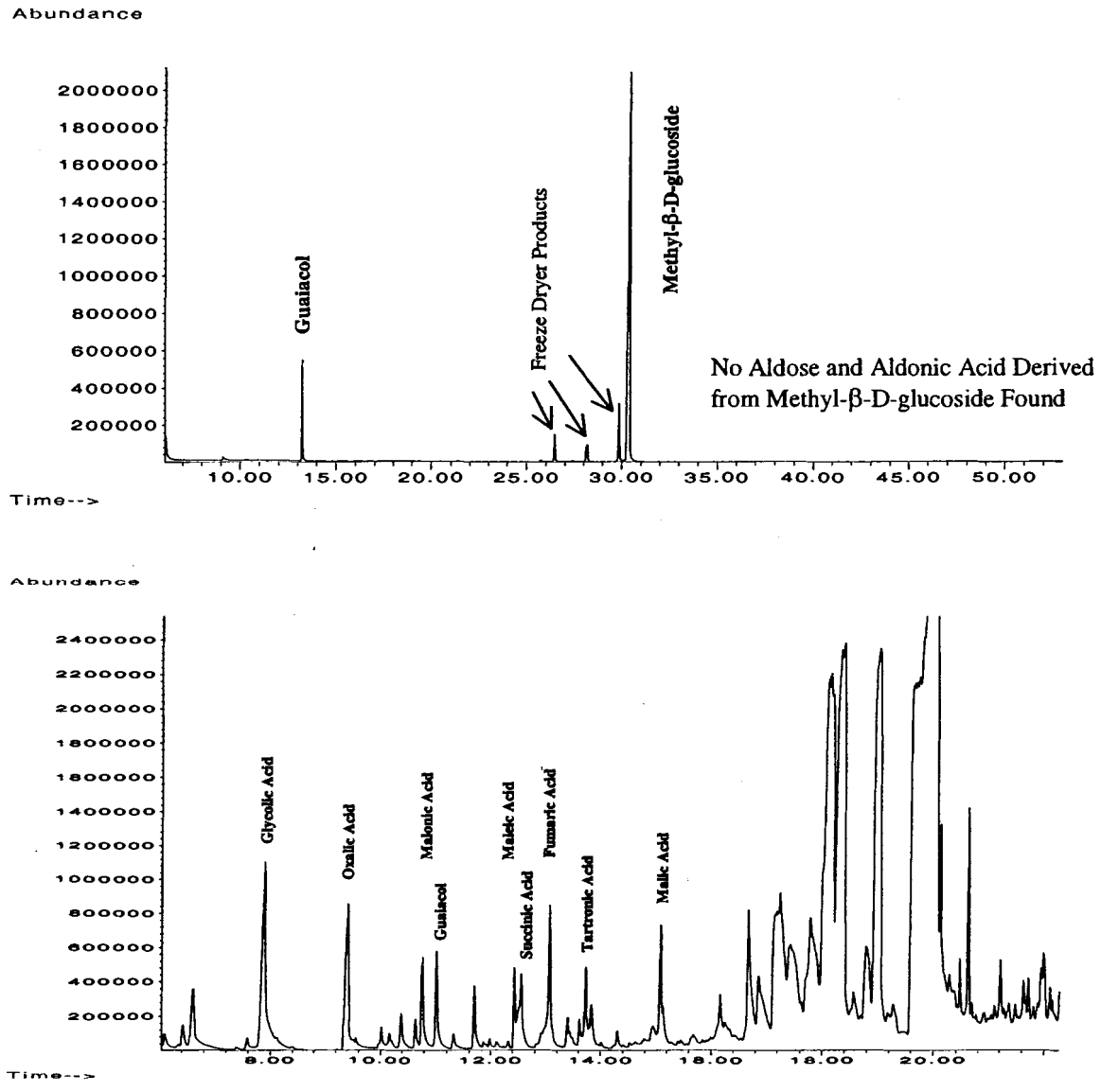

Figure C.6. GC/MS scans of the silylated mixture of guaiacol and methyl-β-D- glucoside reacted under pressurized oxygen. The top scan is for the determination of products derived from methyl-β-D-glucoside. The bottom scan is for the determination of the products derived from guaiacol.

Guaiacol : Methyl-β-D-glucoside = 1 : 2

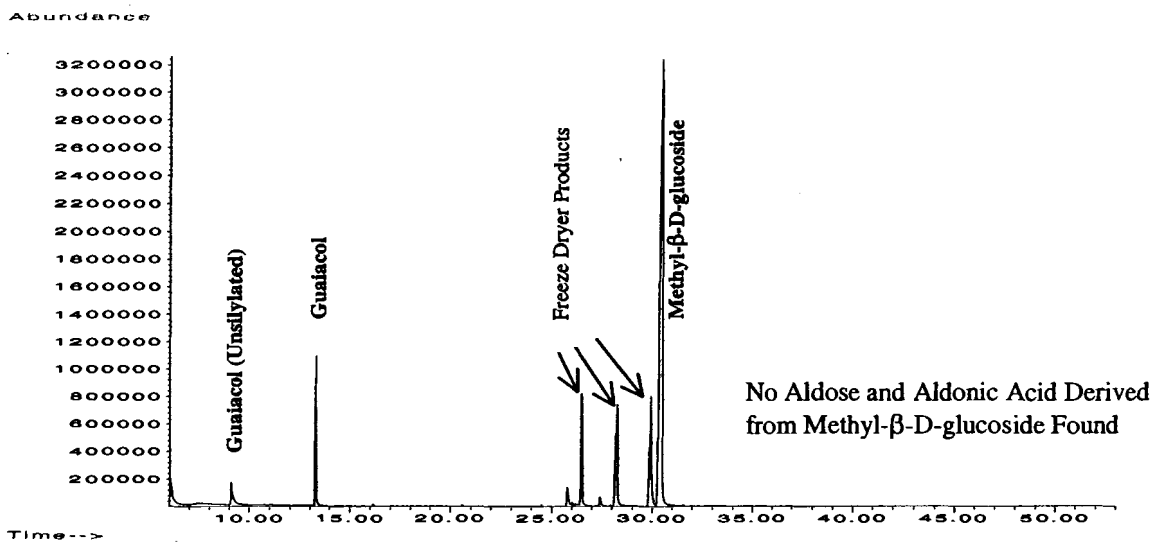

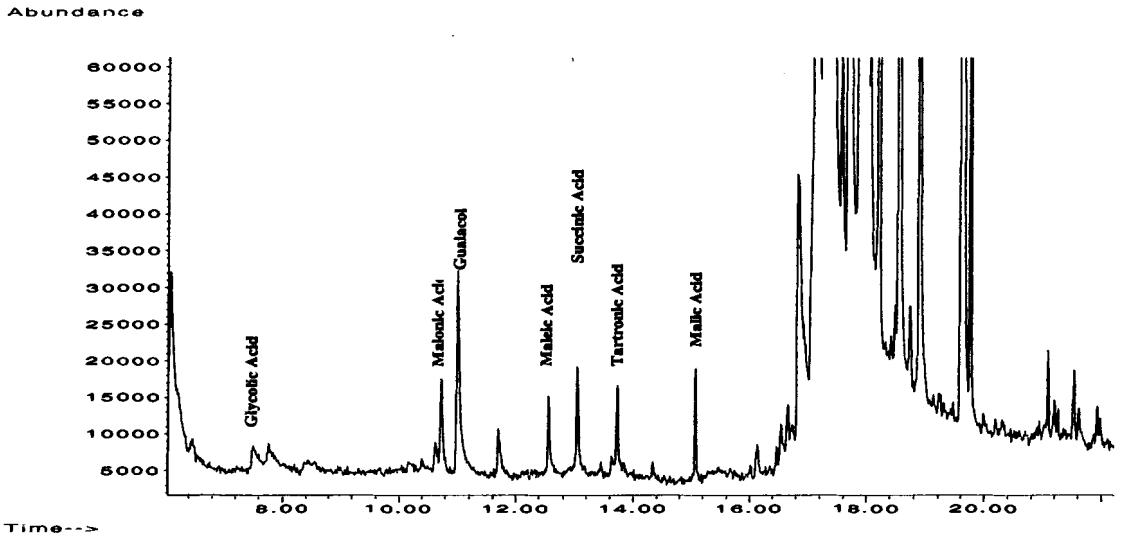

Figure C.6. Continued.

Guaiacol : Methyl-β-D-glucoside = 1 : 4

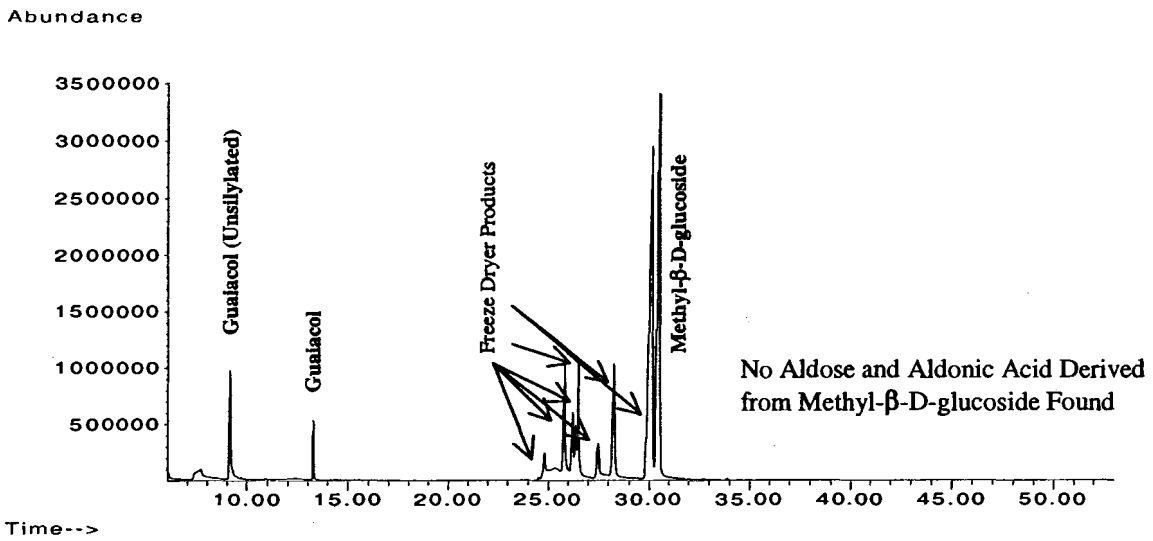

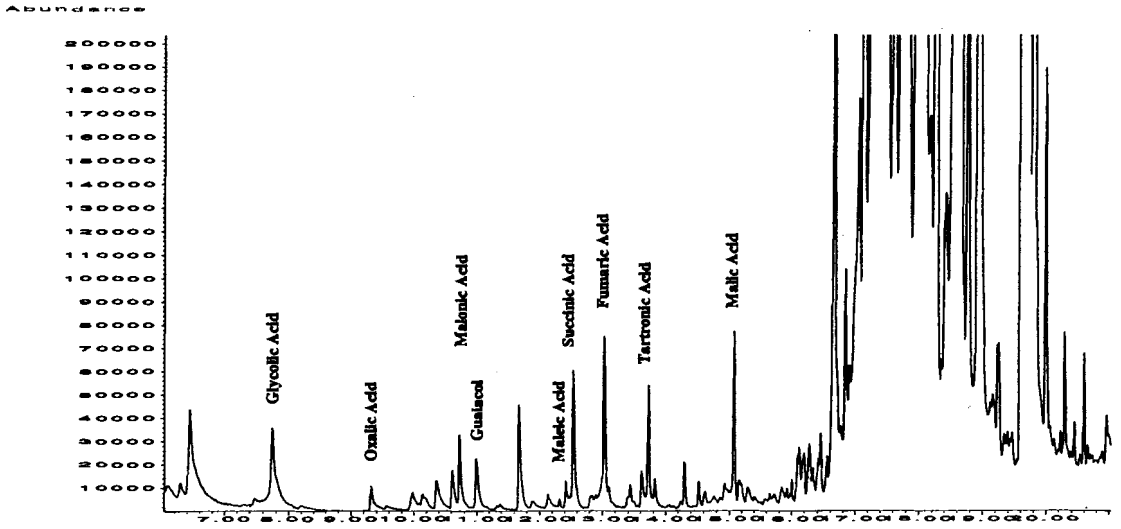

Figure C.6. Continued.

Guaiacol : Methyl-β-D-glucoside = 2 : 1

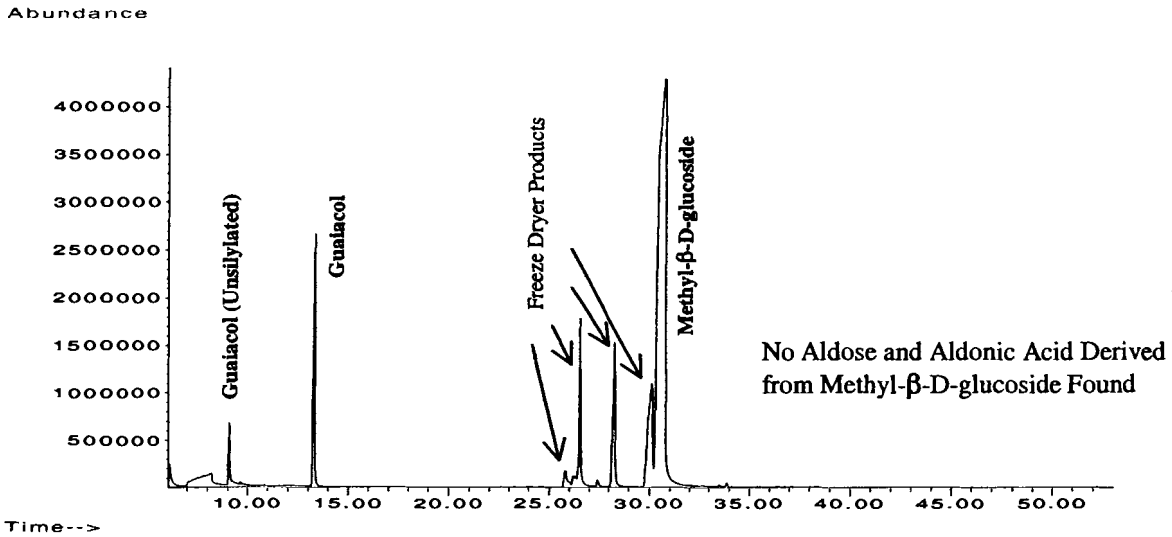

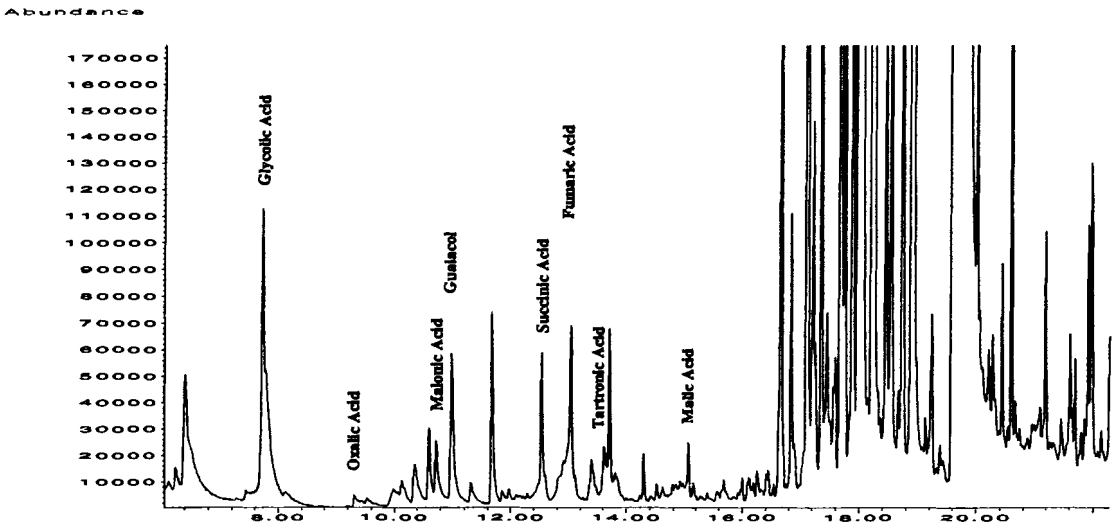

Figure C.6. Continued.

Guaiacol : Methyl-β-D-glucoside = 2 : 2

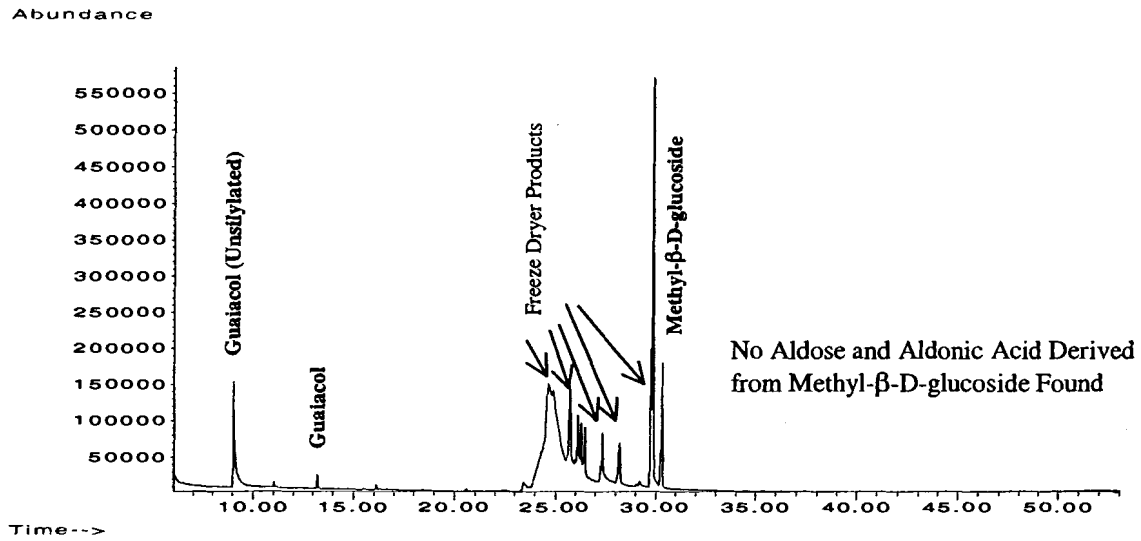

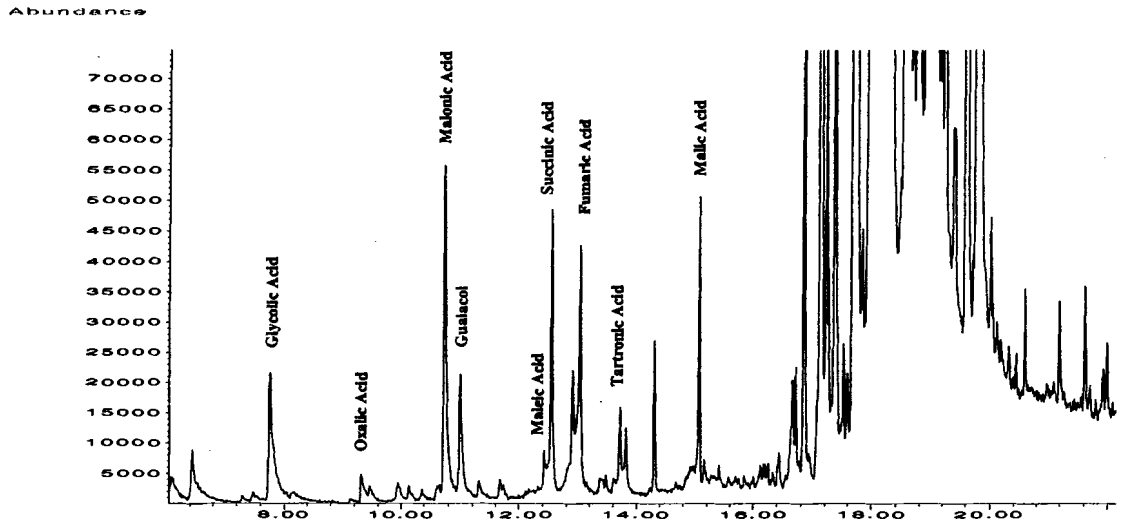

Figure C.6. Continued.

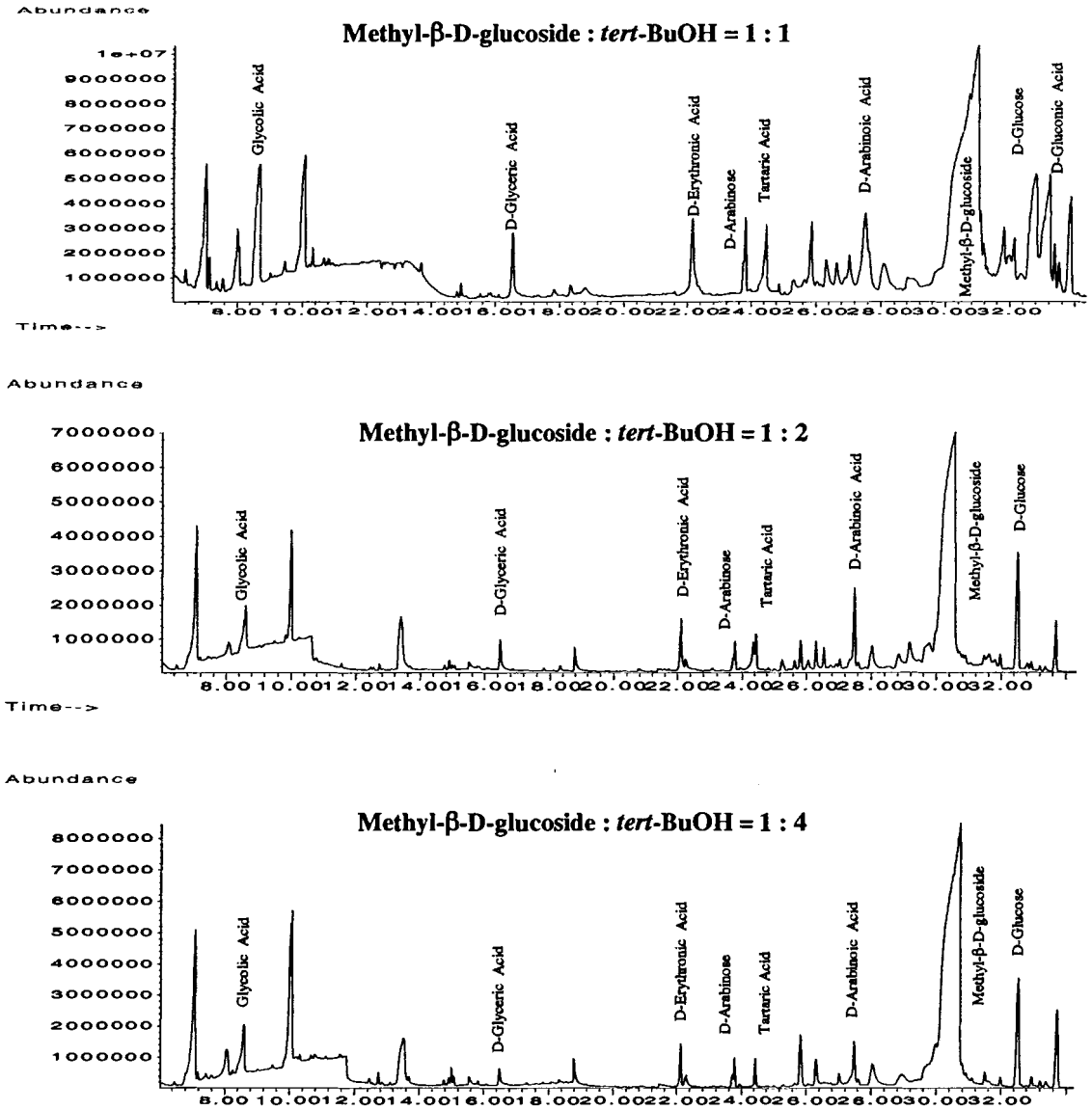

Figure C.7. GC/MS scans of UV/H_2O_2 reactions of methyl-β-D-glucoside in the presence of *tert*-BuOH.

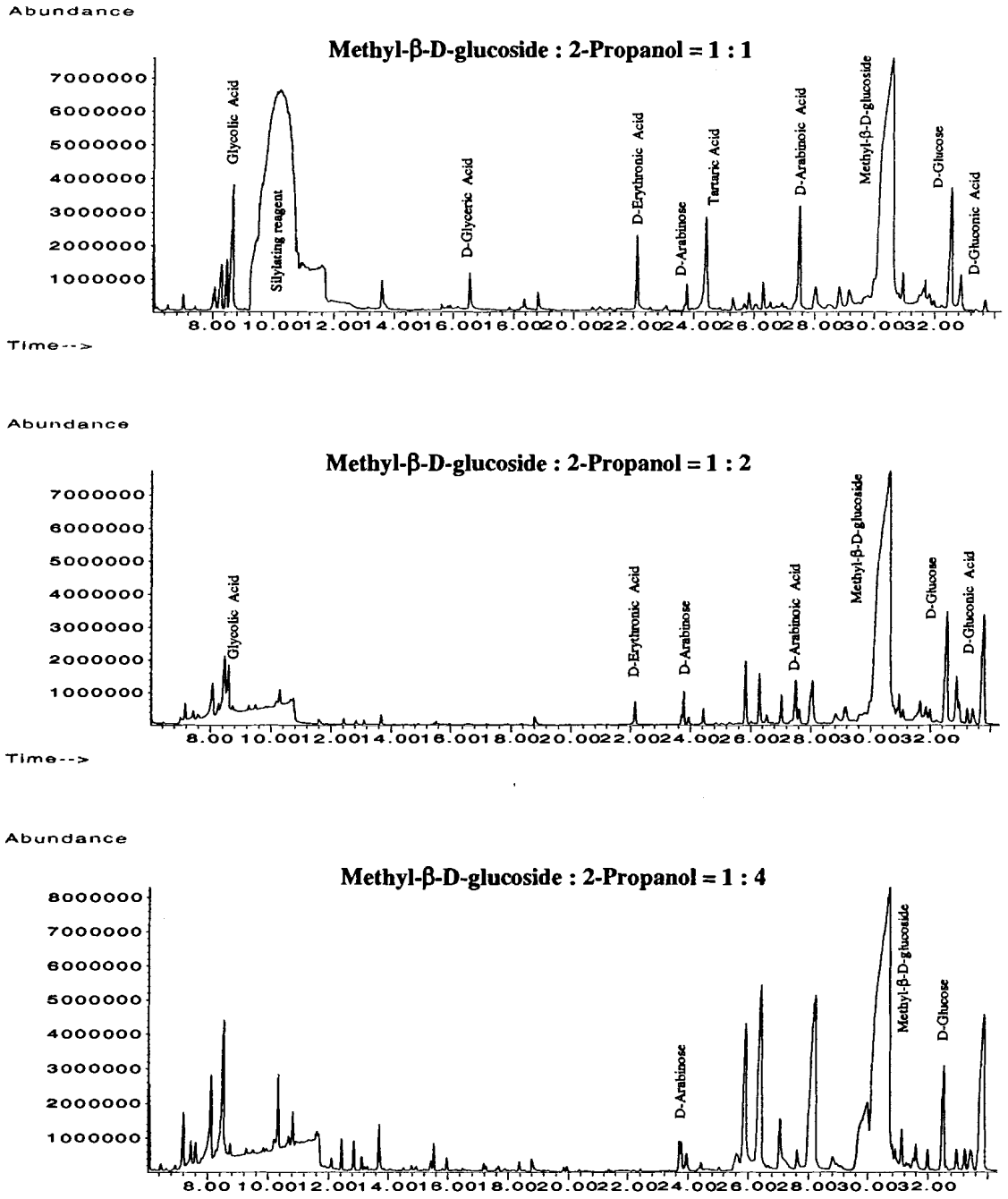

Figure C.8. GC/MS scans of UV/H_2O_2 reactions of methyl-β-D-glucoside in the presence of 2-propanol.

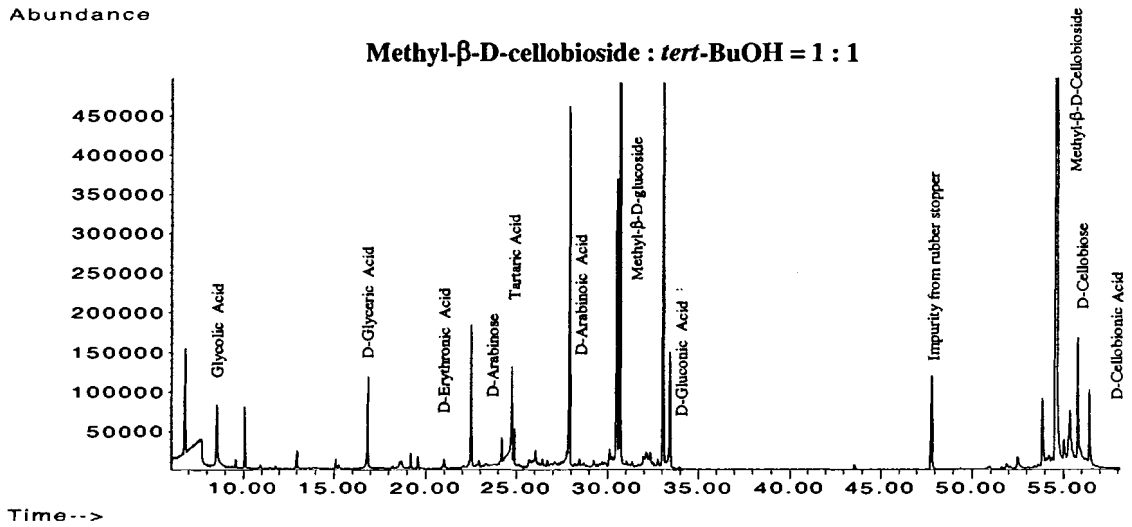

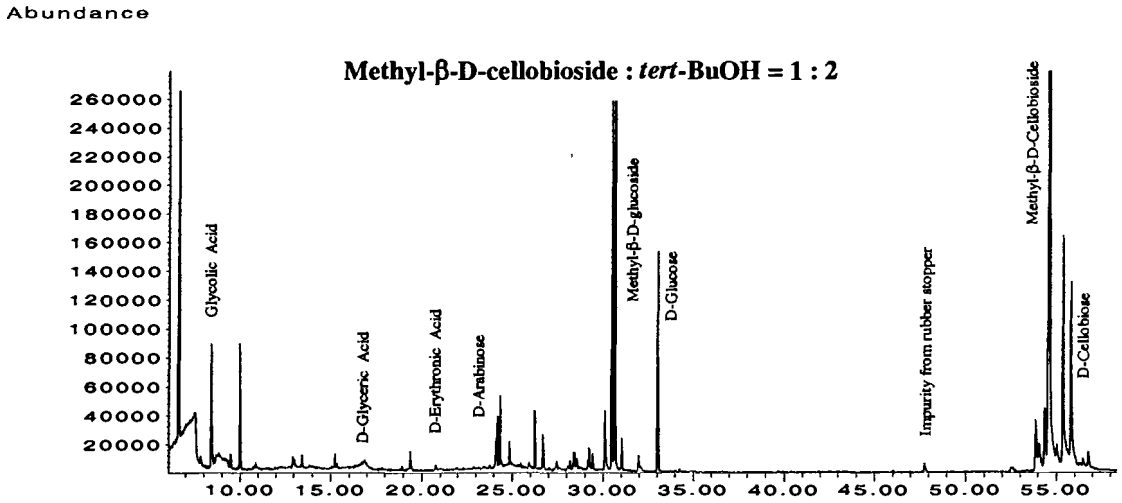

Figure C.9. GC/MS scans of UV/H_2O_2 reactions of methyl-β-D-cellobioside in the presence of *tert*-BuOH.

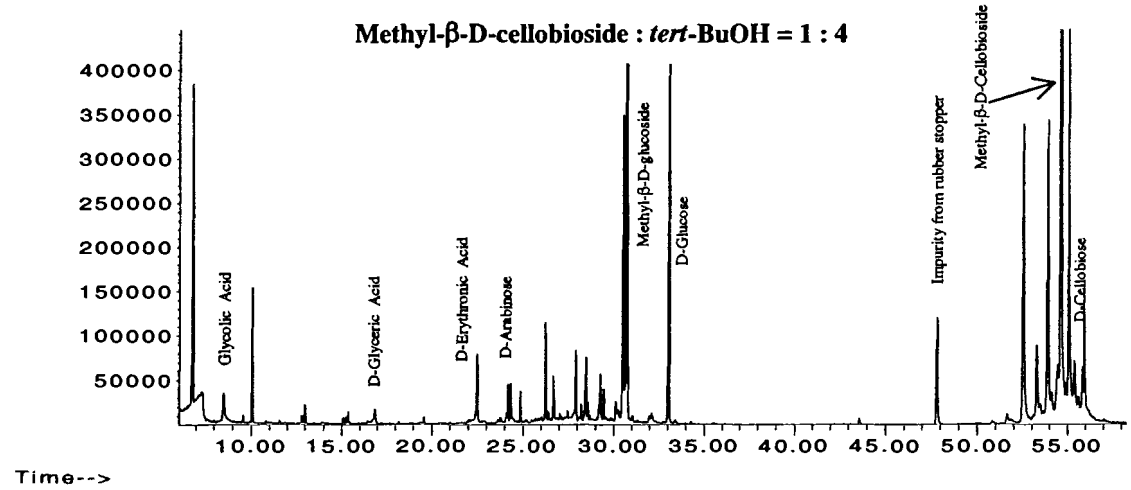

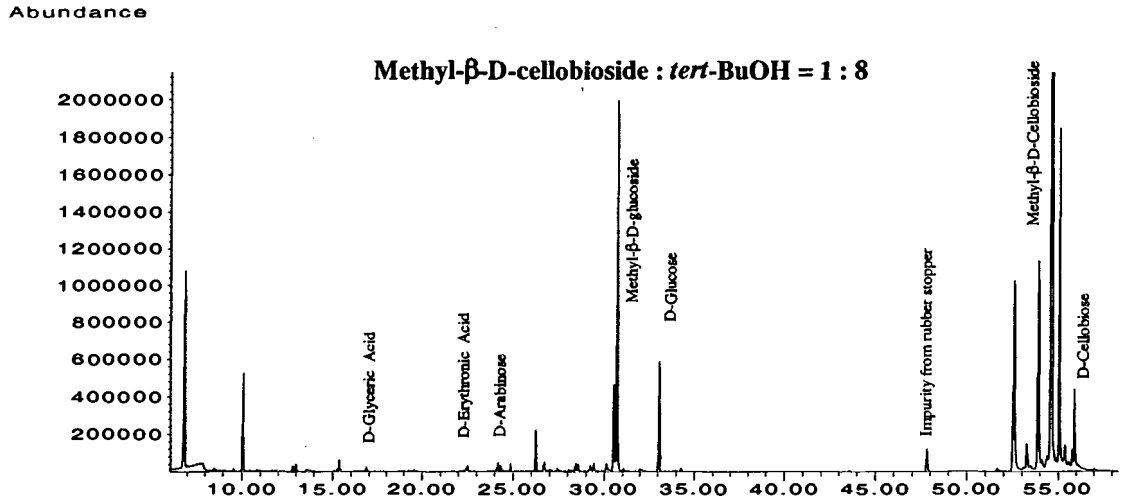

Figure C.9. Continued.

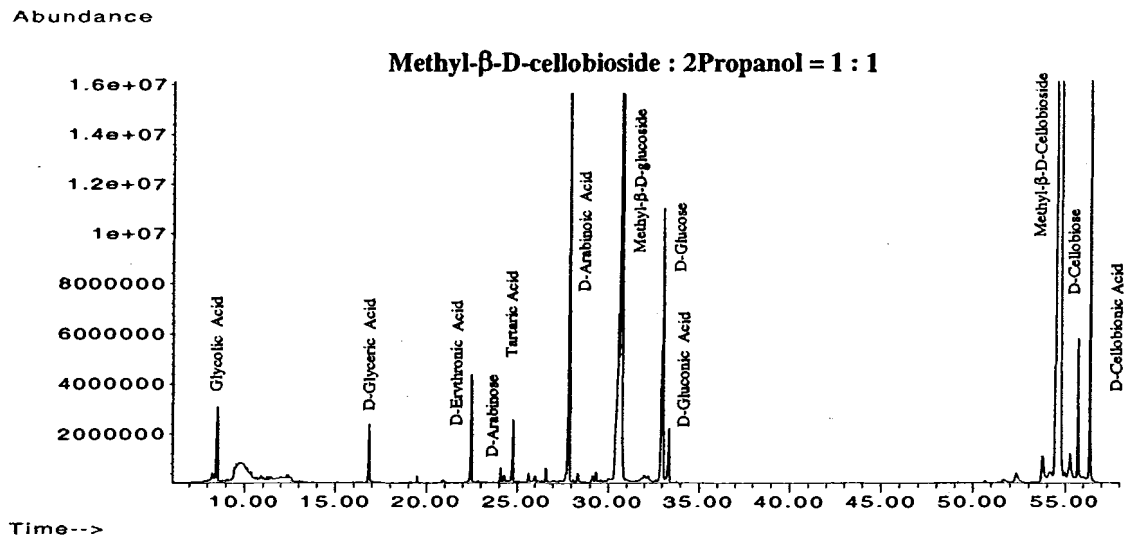

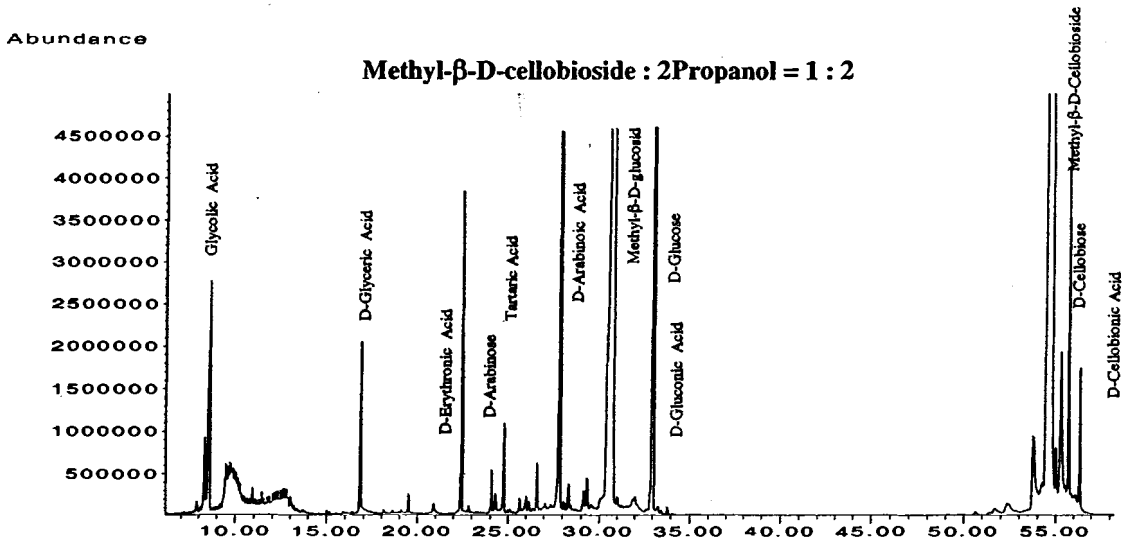

Figure C.10. GC/MS scans of UV/H_2O_2 reactions of methyl-β-D-cellobioside in the presence of 2-propanol.

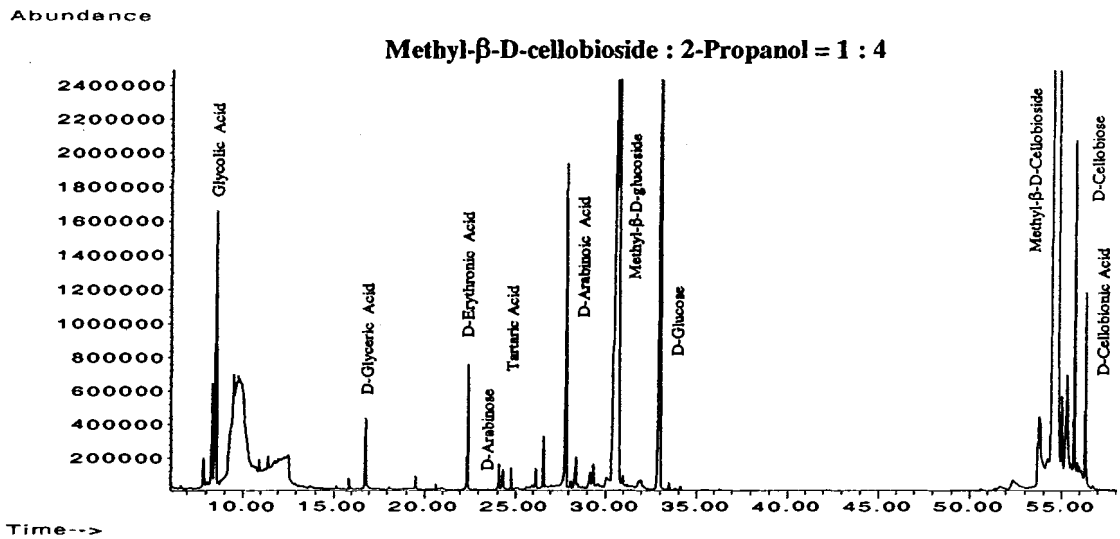

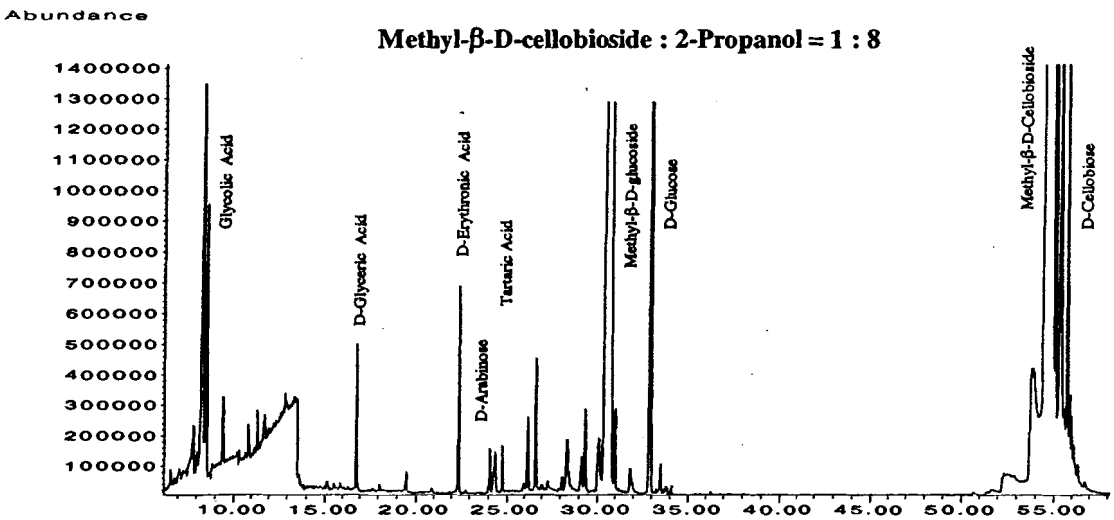

Figure C.10. Continued.

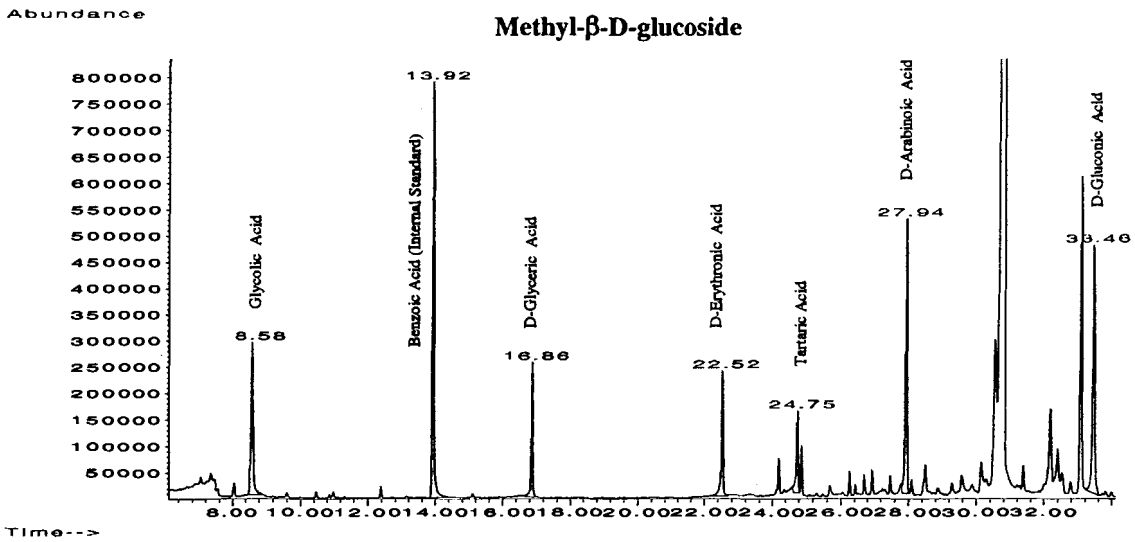

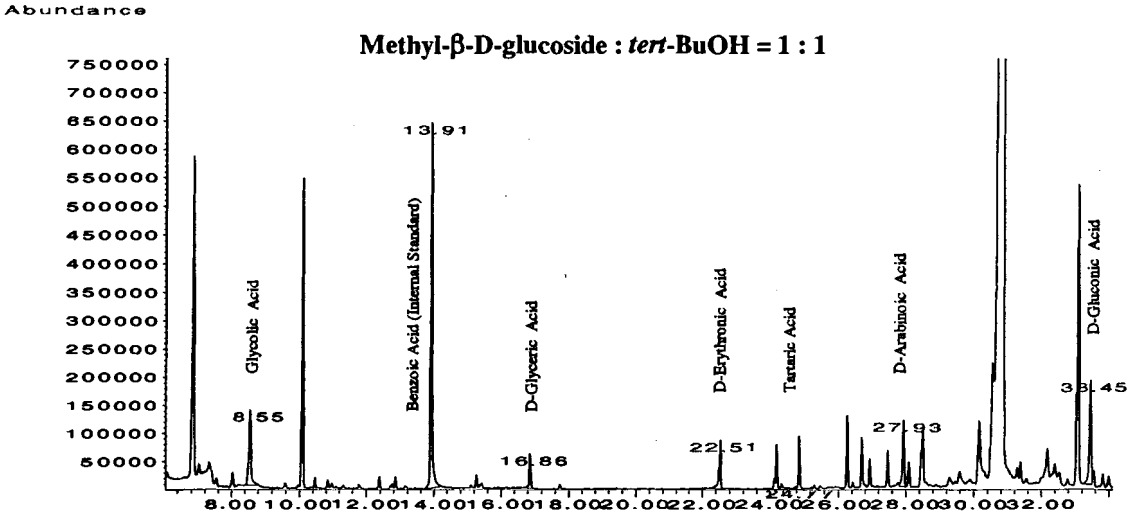

Figure C.11. GC/MS scans of UV/H_2O_2 reactions for the qualitative comparison of the amounts of organic acids in different reactions. The numbers above the peaks are the retention times.

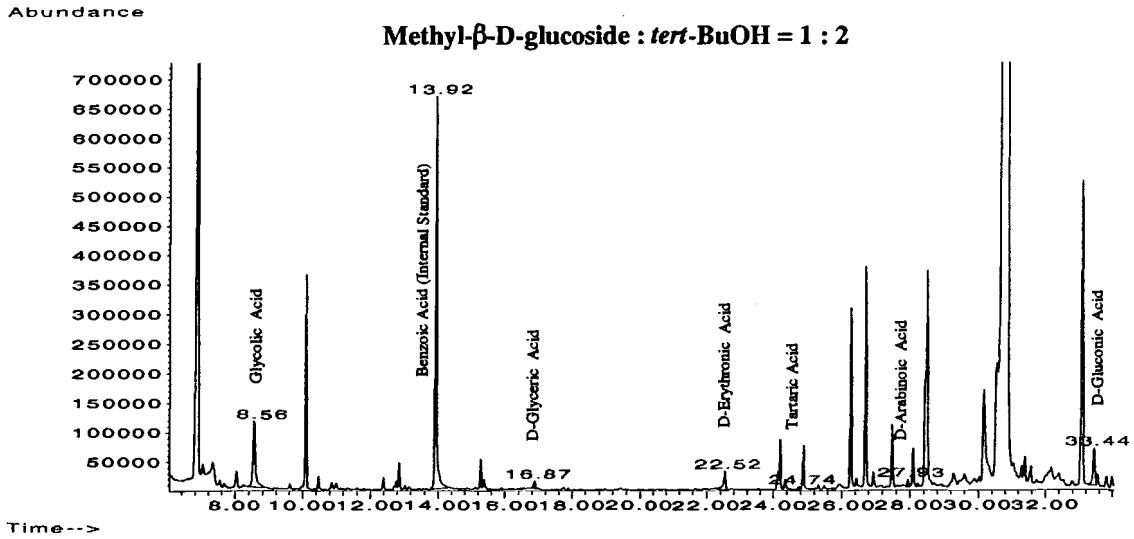

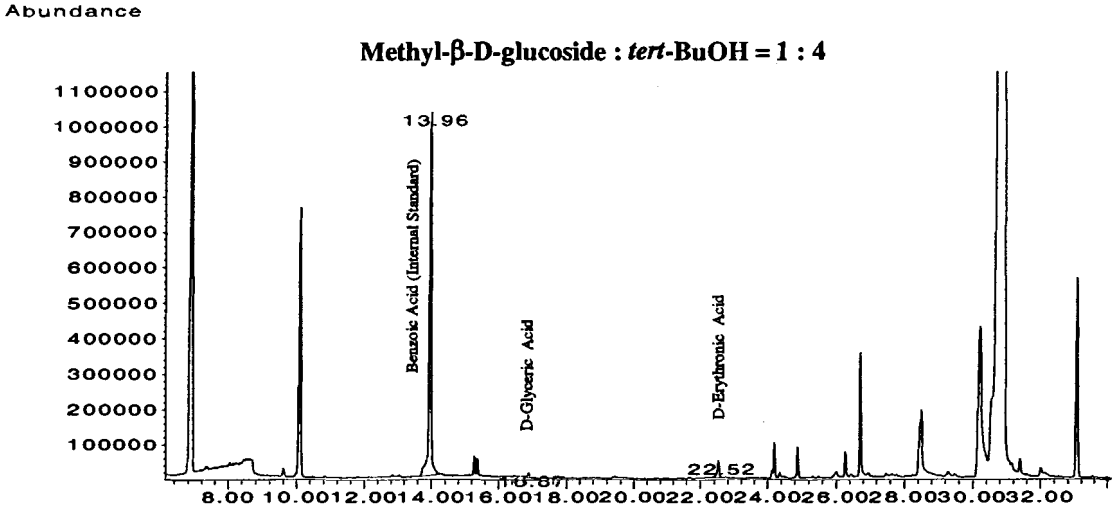

Figure C.11. Continued.

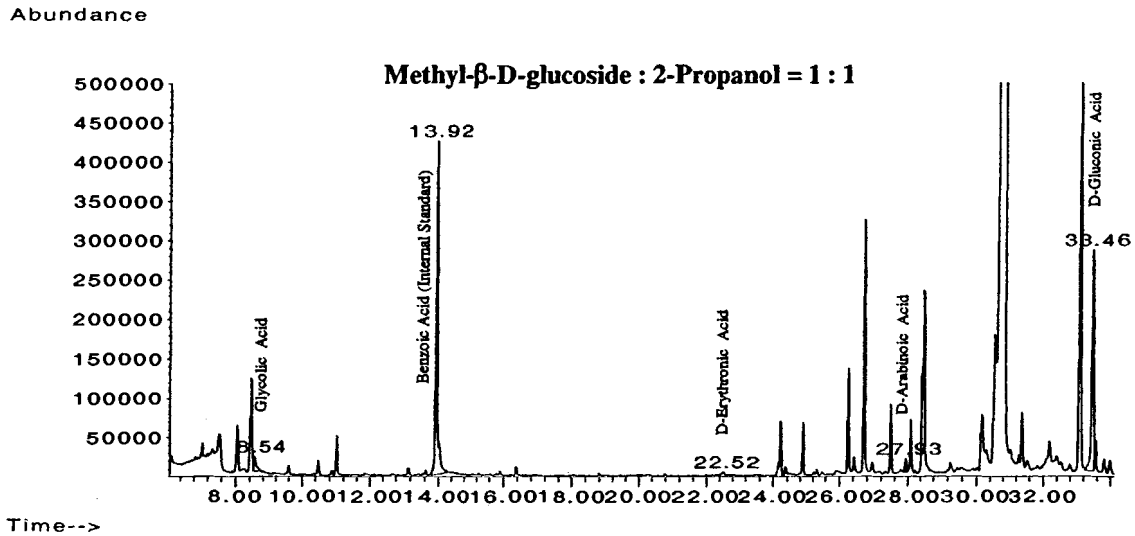

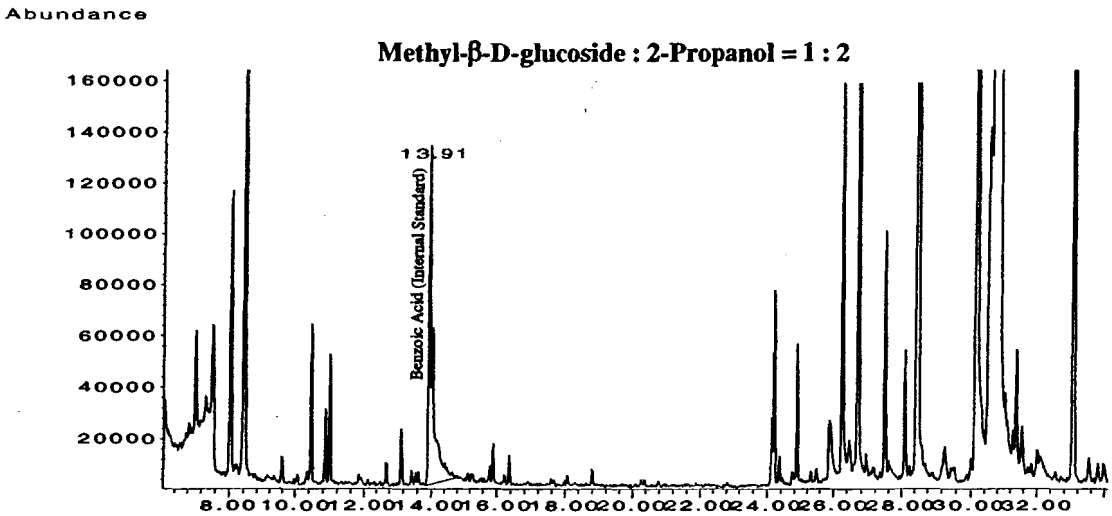

Figure C.11. Continued.

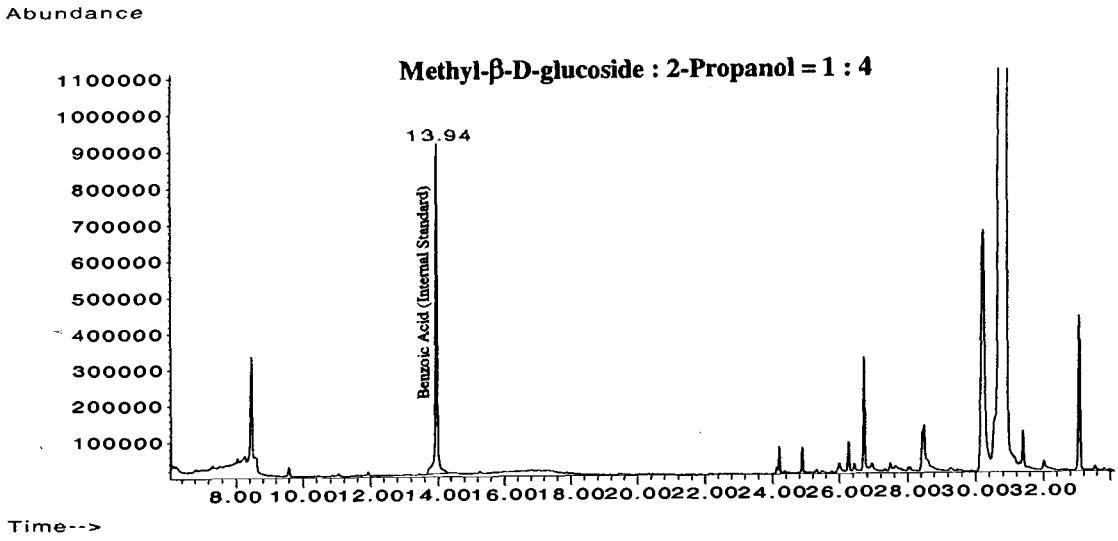

Figure C.11. Continued.

APPENDIX D

SPME-GC/MS Data

tert-BuOH

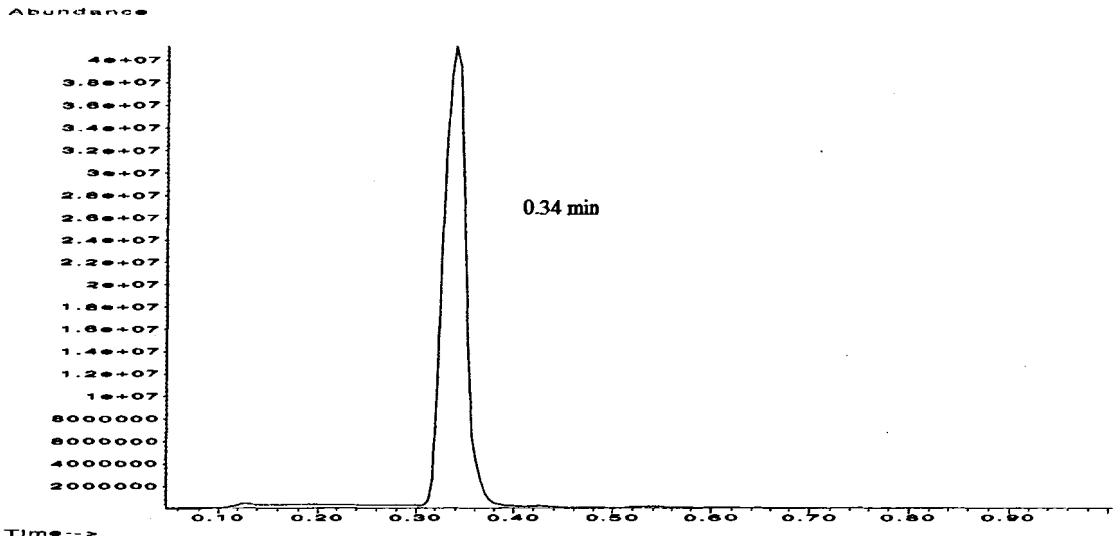

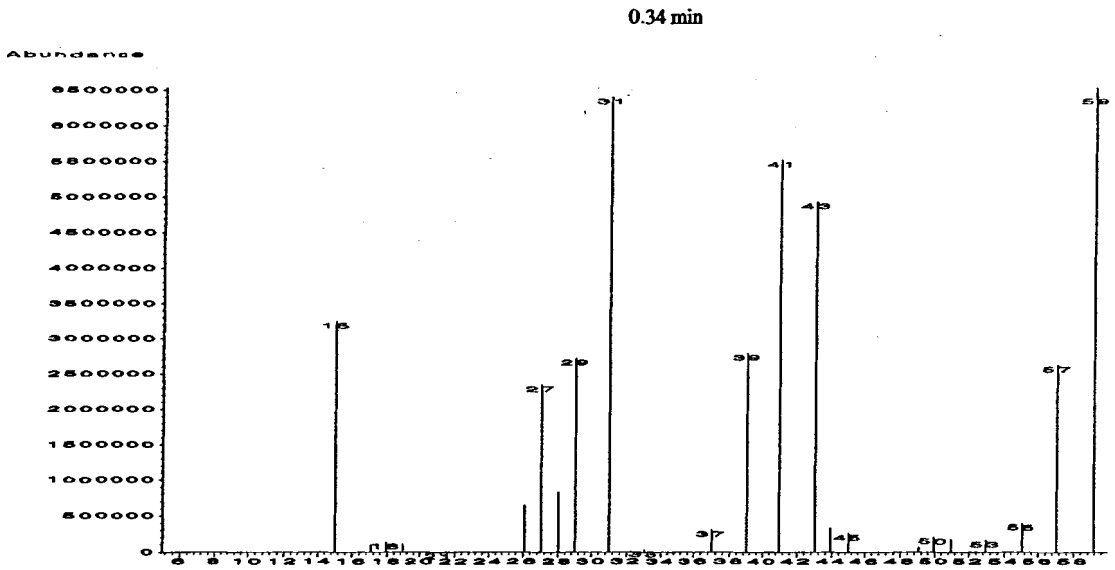

Figure D.1. SPME-GC/MS scan of *tert*-BuOH.

2-Propanol

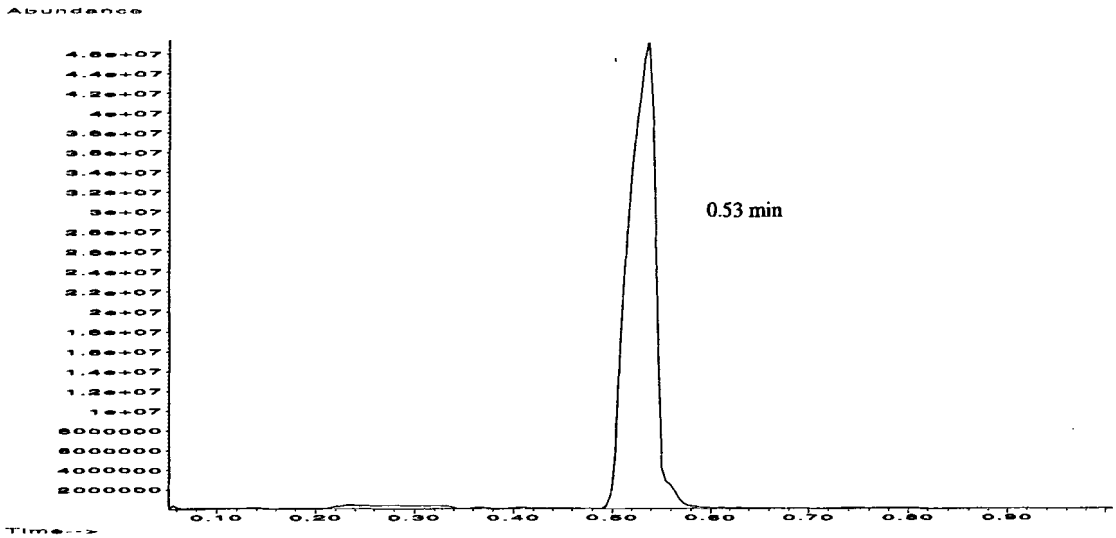

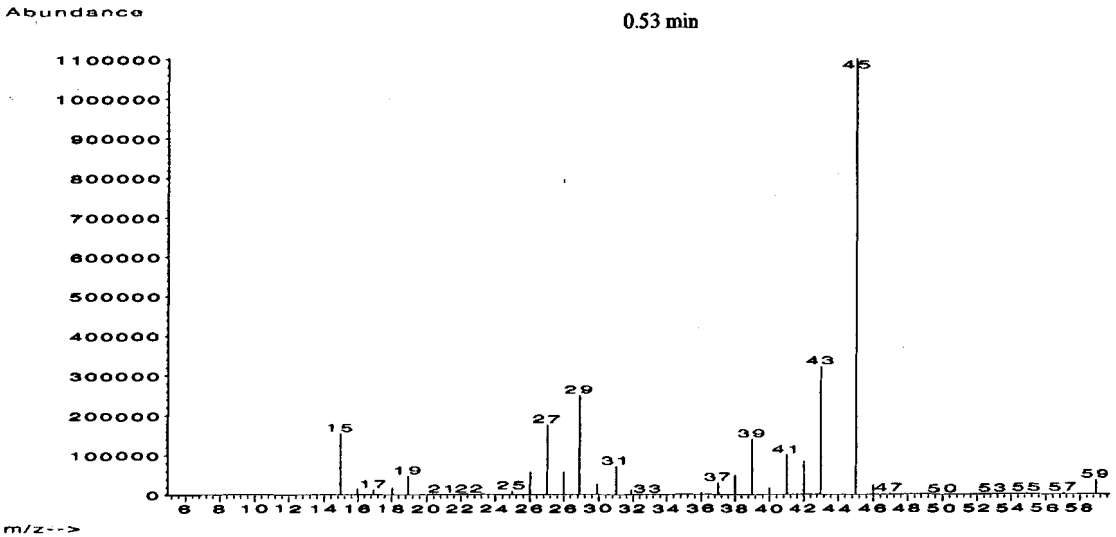

Figure D.2. SPME-GC/MS scan of 2-propanol.

Acetone

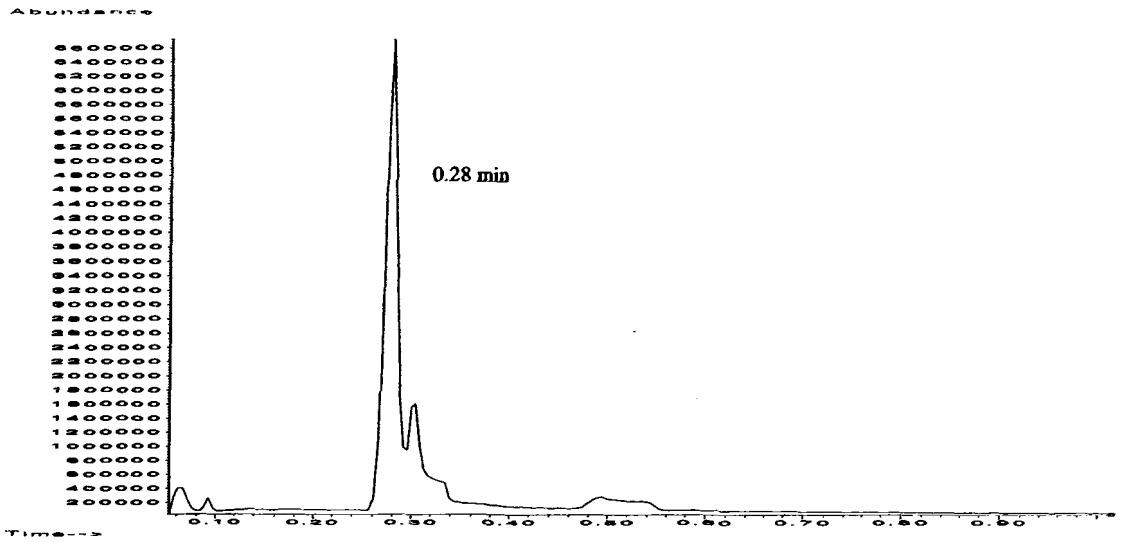

0.28 min

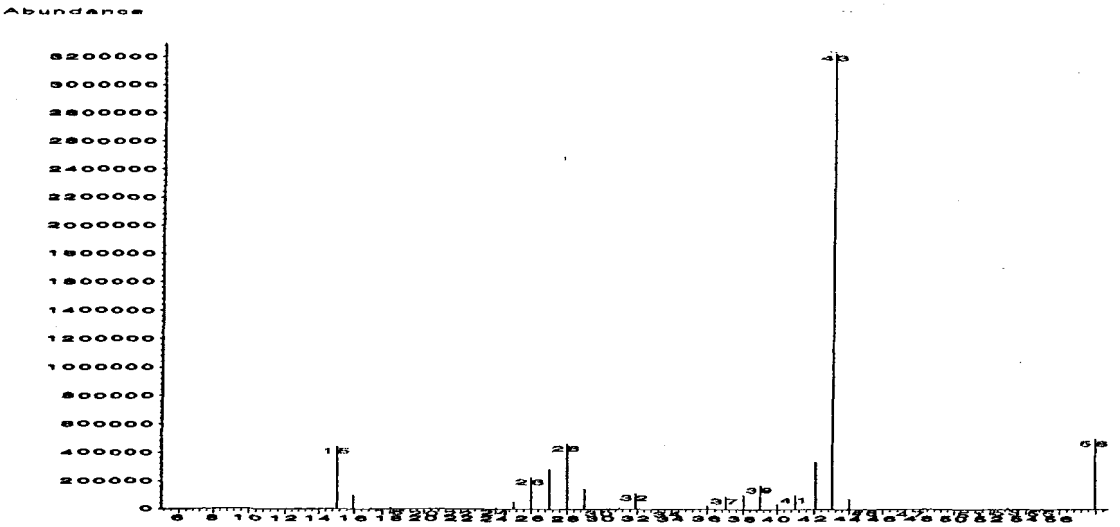

Figure D.3. SPME-GC/MS scan of acetone.

Methyl-β-D-glucoside : *tert*-BuOH = 1 : 1

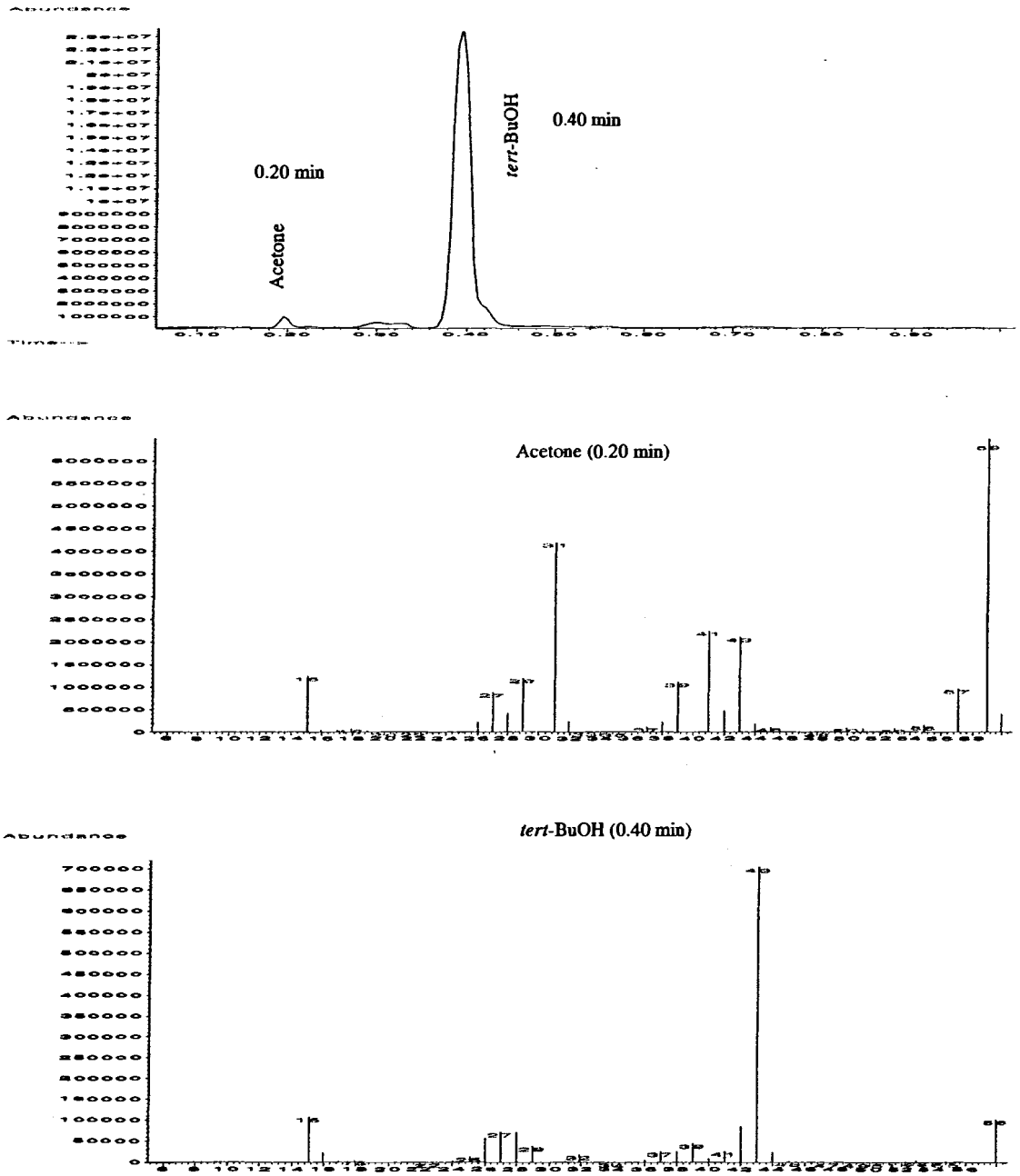

Figure D.4. SPME-GC/MS scans of UV/H_2O_2 reactions of methyl-β-D-glucoside in the presence of *tert*-BuOH. Retention times varied due to the length of column.

Methyl-β-D-glucoside : *tert*-BuOH = 1 : 2

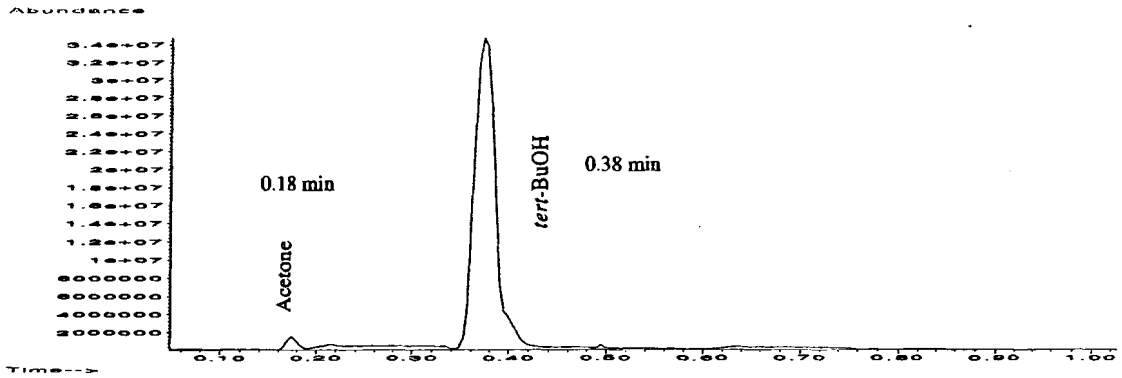

Acetone (0.18 min)

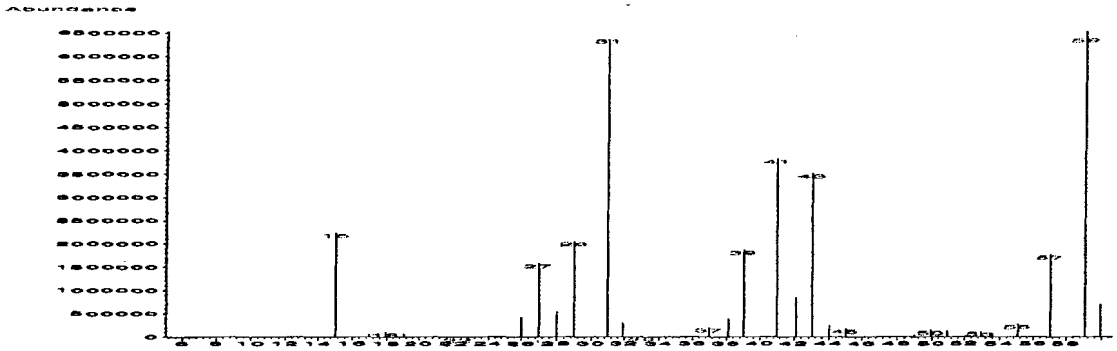

tert-BuOH (0.38 min)

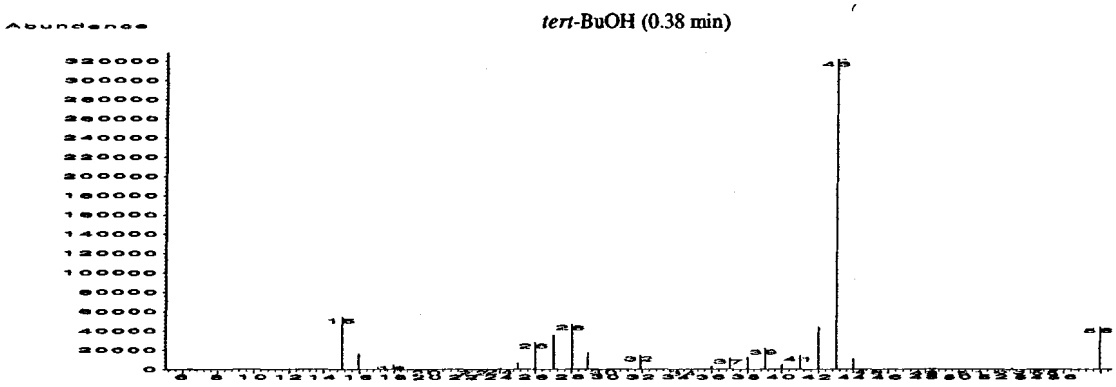

Figure D.4. Continued.

Methyl-β-D-glucoside : *tert*-BuOH = 1 : 4

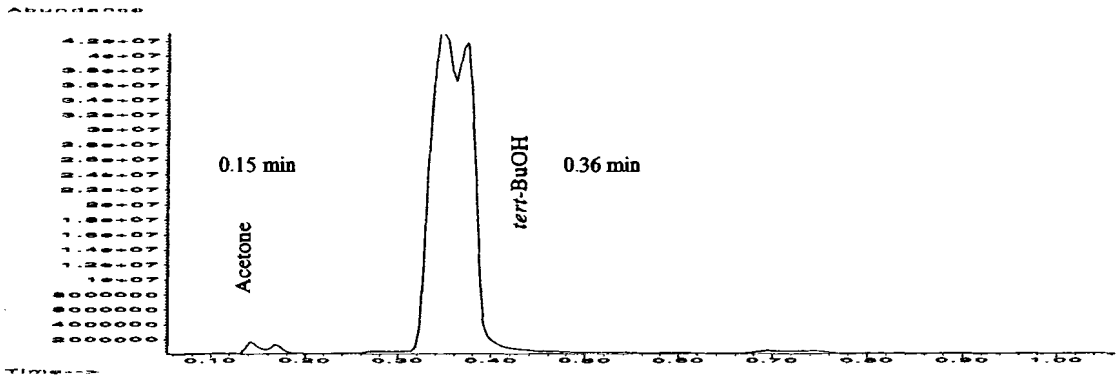

Acetone (0.15 min)

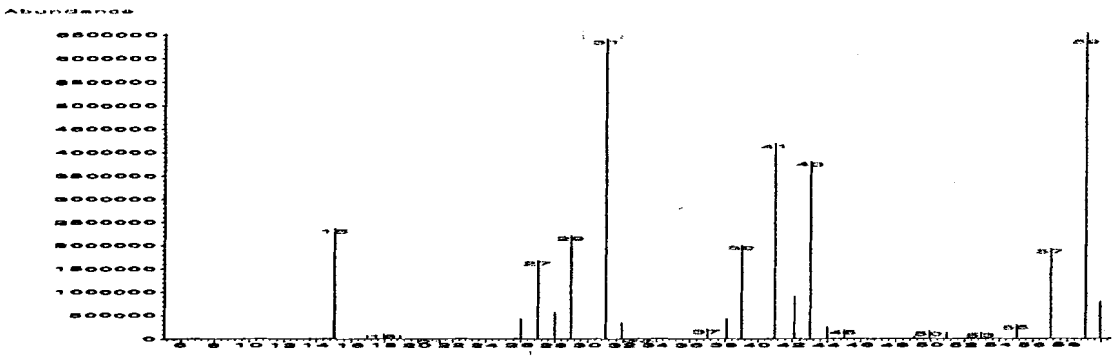

tert-BuOH (0.36 min)

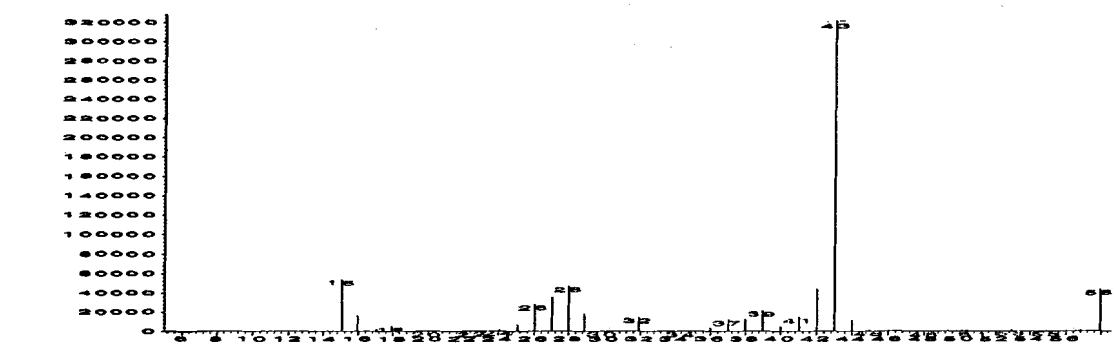

Figure D.4. Continued.

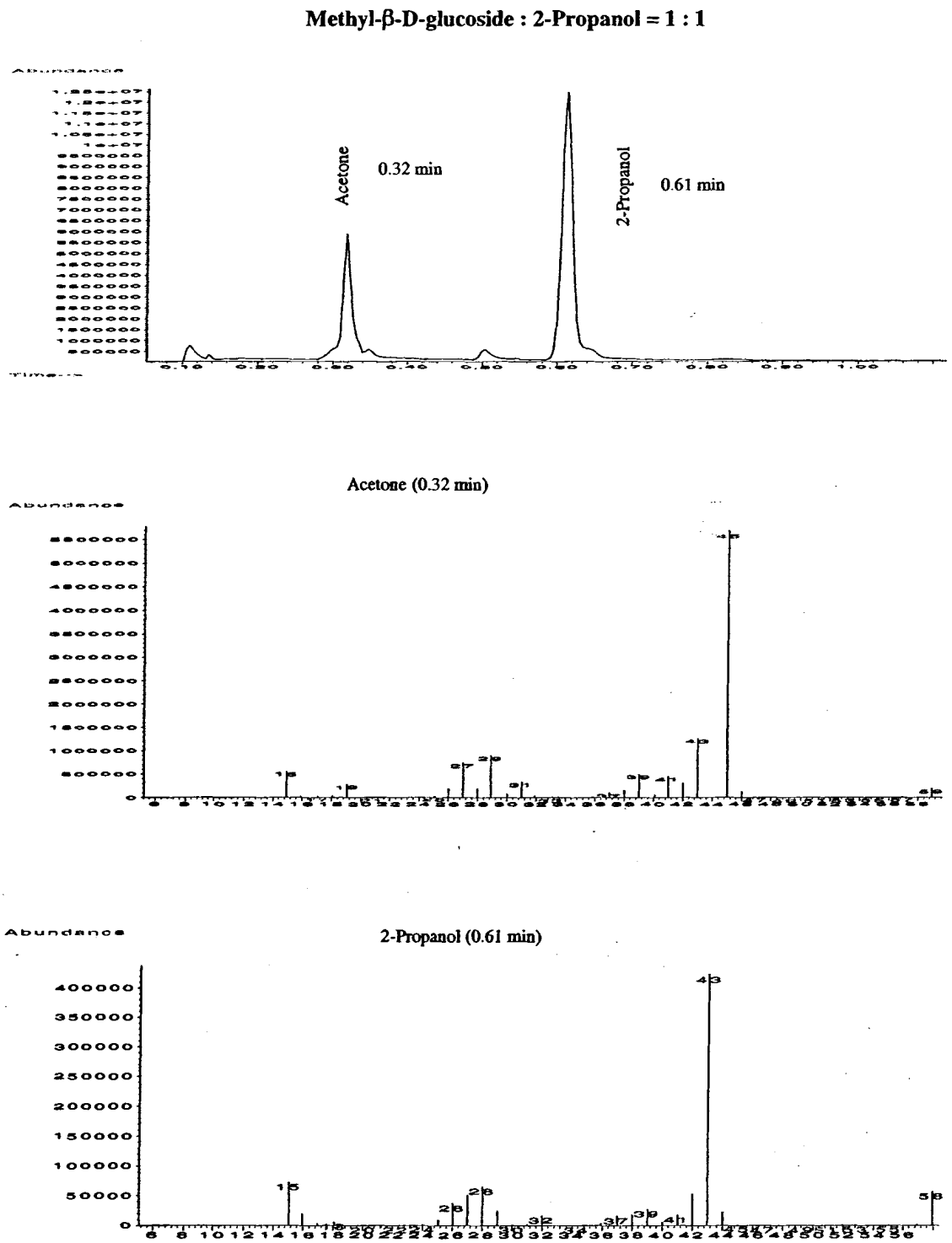

Figure D.5. SPME-GC/MS scans of UV/H_2O_2 reactions of methyl-β-D-glucoside in the presence of 2-propanol. Retention times varied due to the length of column.

Methyl-β-D-glucoside : 2-Propanol = 1 : 2

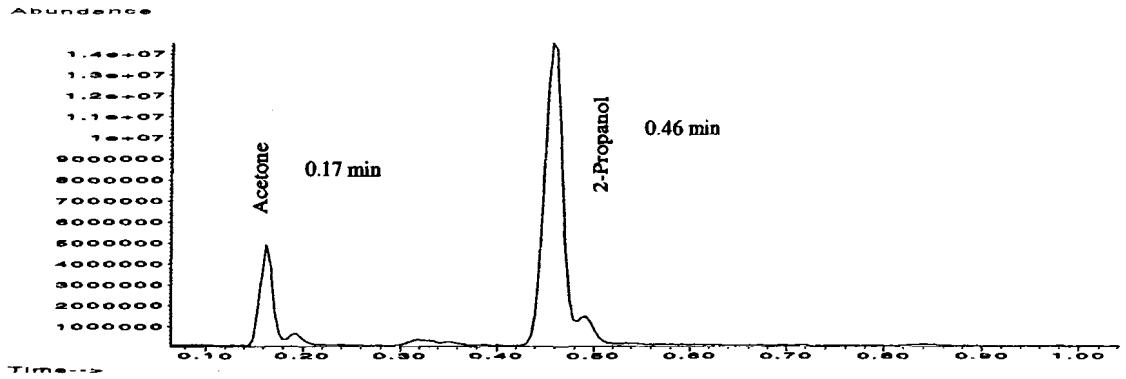

Acetone (0.17 min)

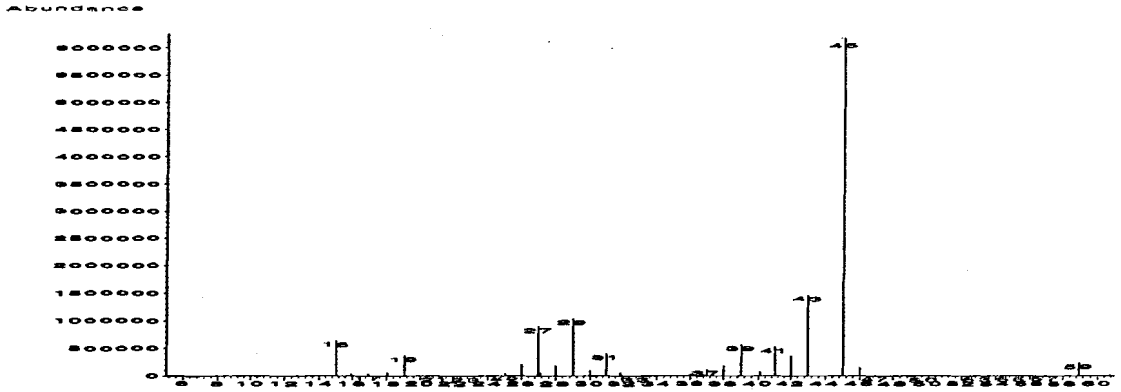

2-Propanol (0.46 min)

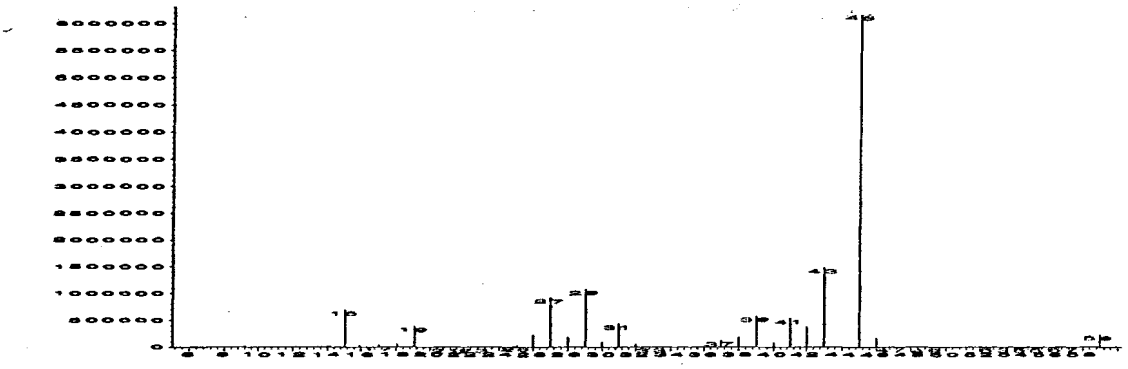

Figure D.5. Continued.

Methyl-β-D-glucoside : 2-Propanol = 1 : 4

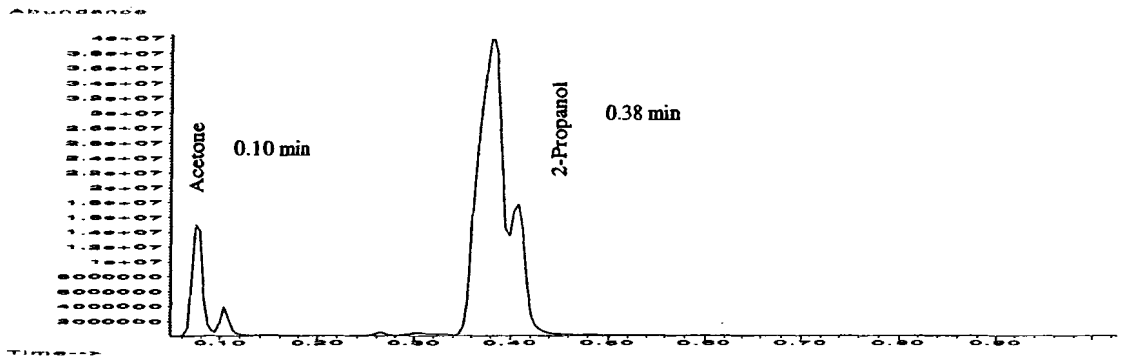

Acetone (0.10 min)

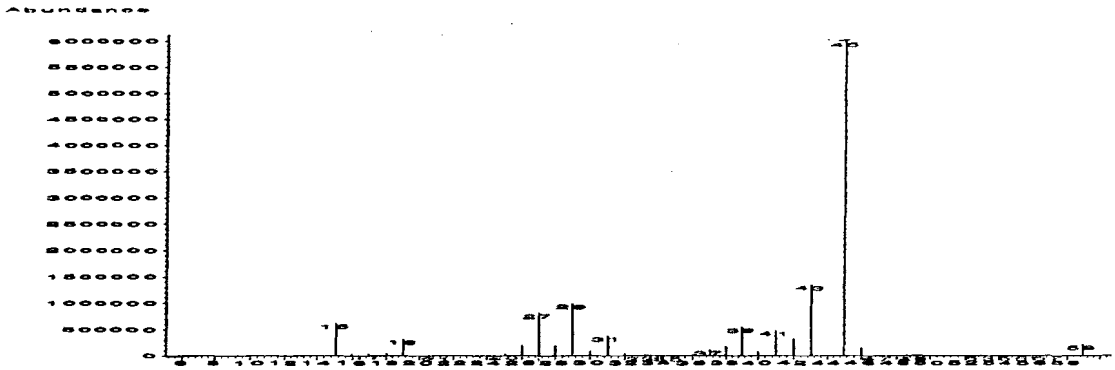

2-Propanol (0.46 min)

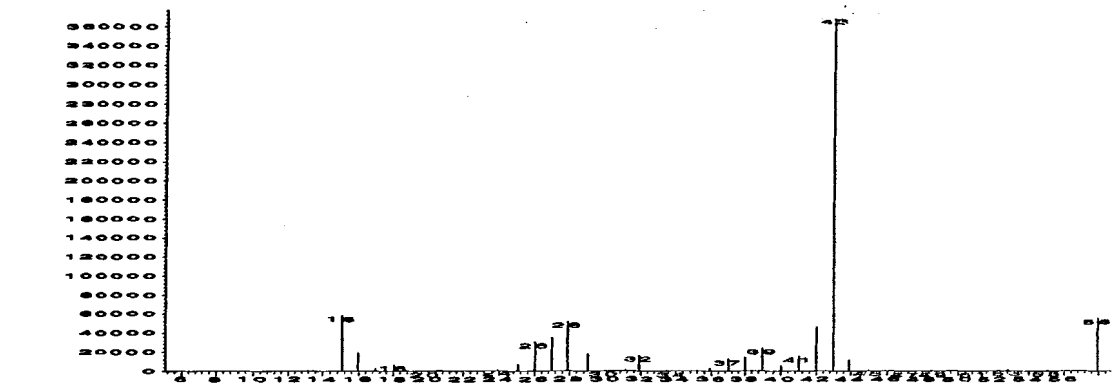

Figure D.5. Continued.

Methyl-β-D-cellobioside : *tert*-BuOH = 1 : 1

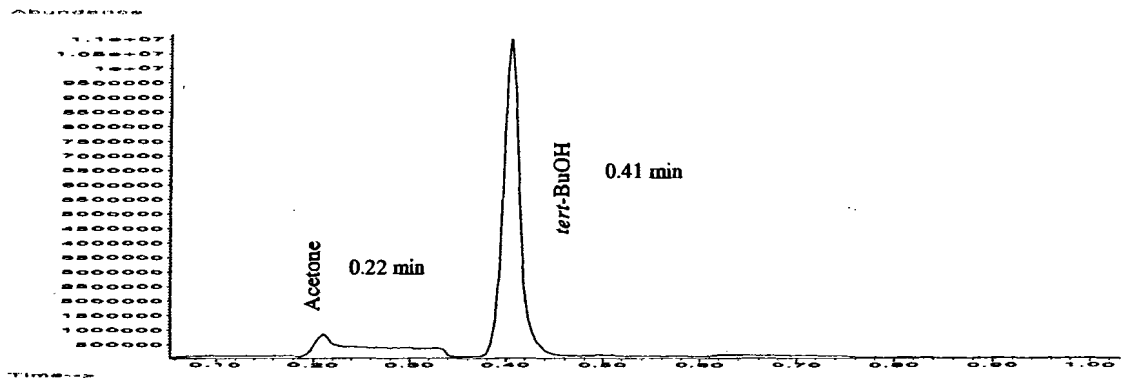

Figure D.6. SPME-GC/MS scans of UV/H_2O_2 reactions of methyl-β-D-cellobioside in the presence of *tert*-BuOH. Retention times varied due to the length of column.

Methyl-β-D-cellobioside : *tert*-BuOH = 1 : 2

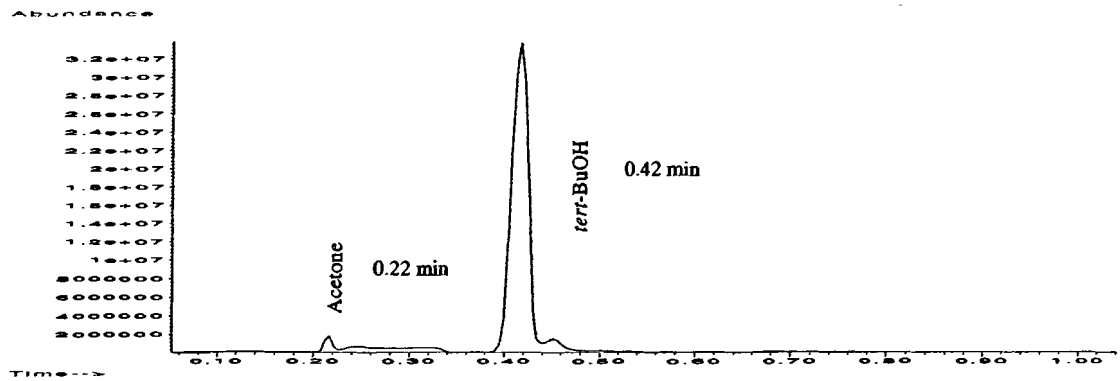

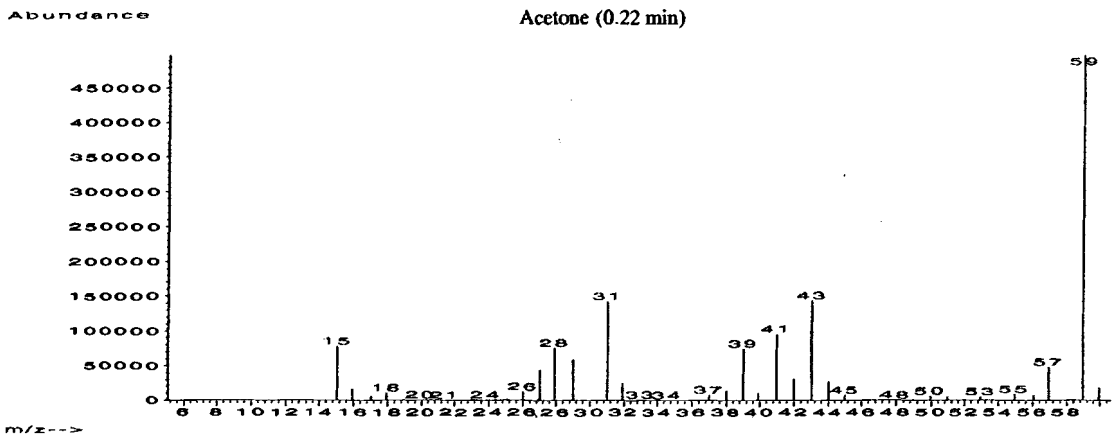

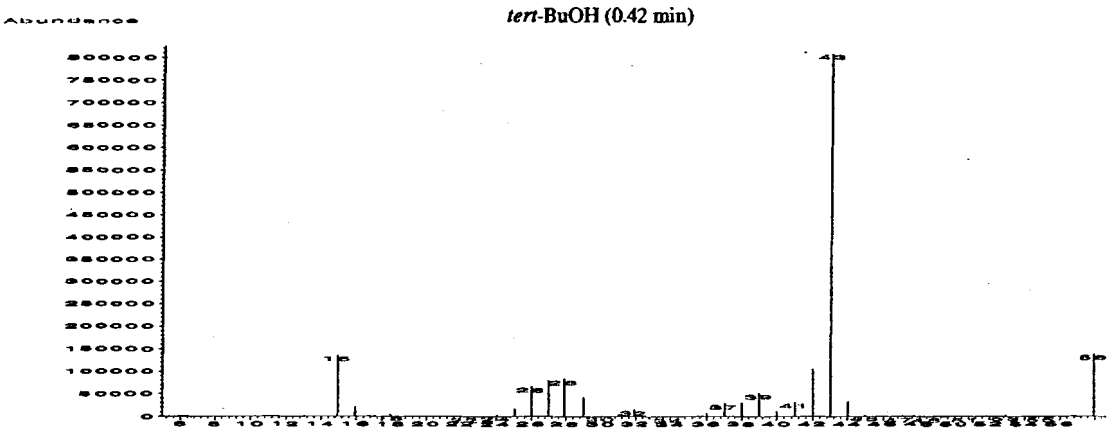

Figure D.6. Continued.

Methyl-β-D-cellobioside : *tert*-BuOH = 1 : 4

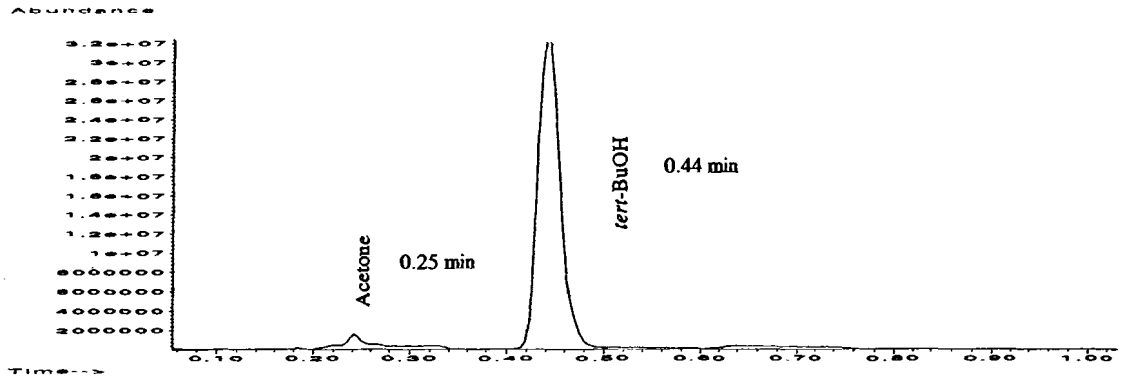

Acetone (0.25 min)

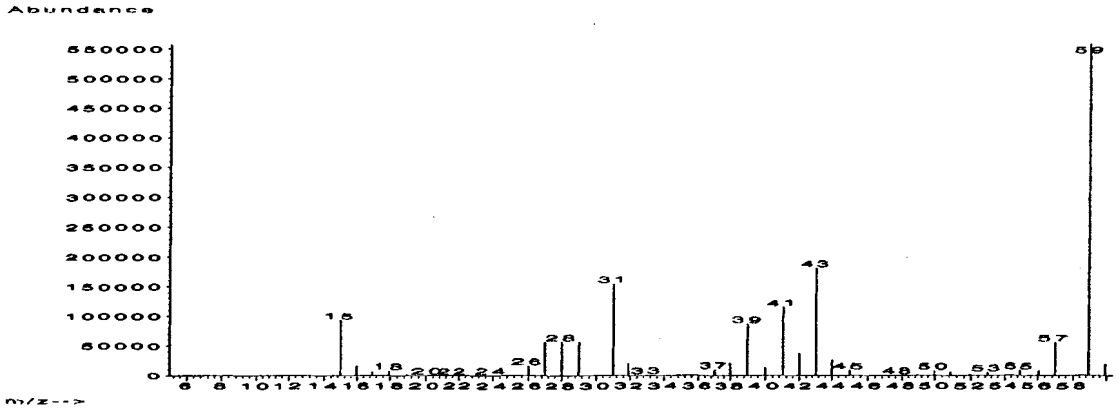

tert-BuOH (0.44 min)

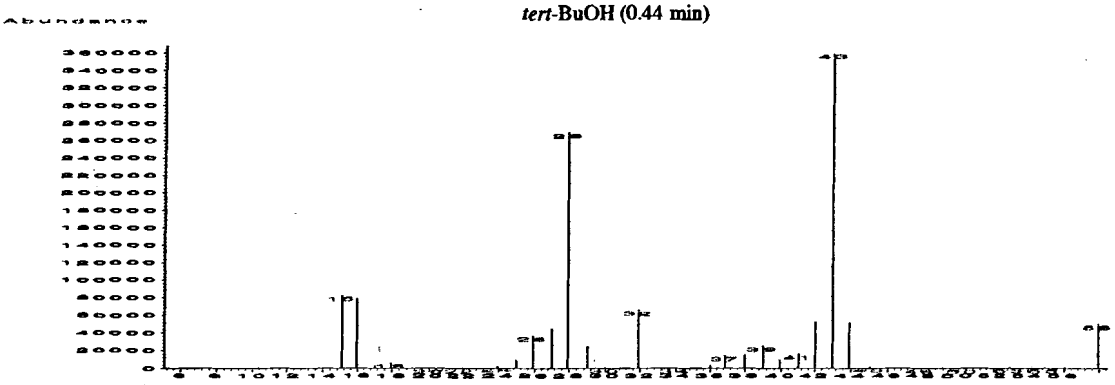

Figure D.6. Continued.

Methyl-β-D-cellobioside : *tert*-BuOH = 1 : 8

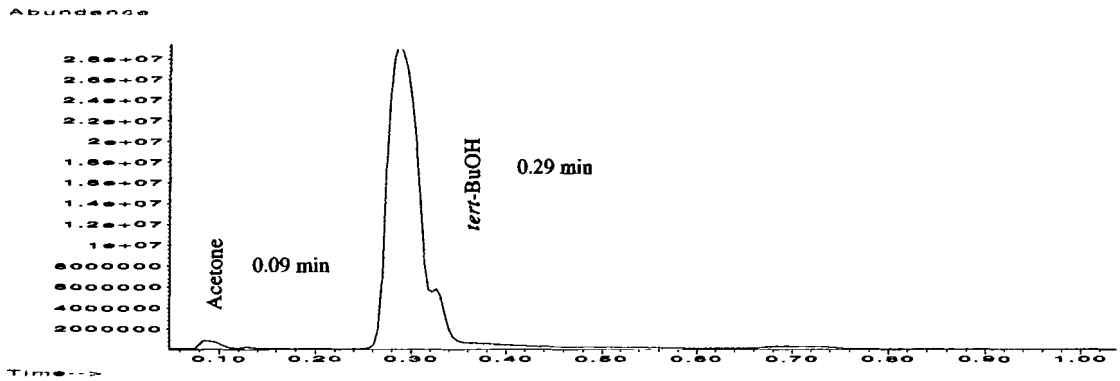

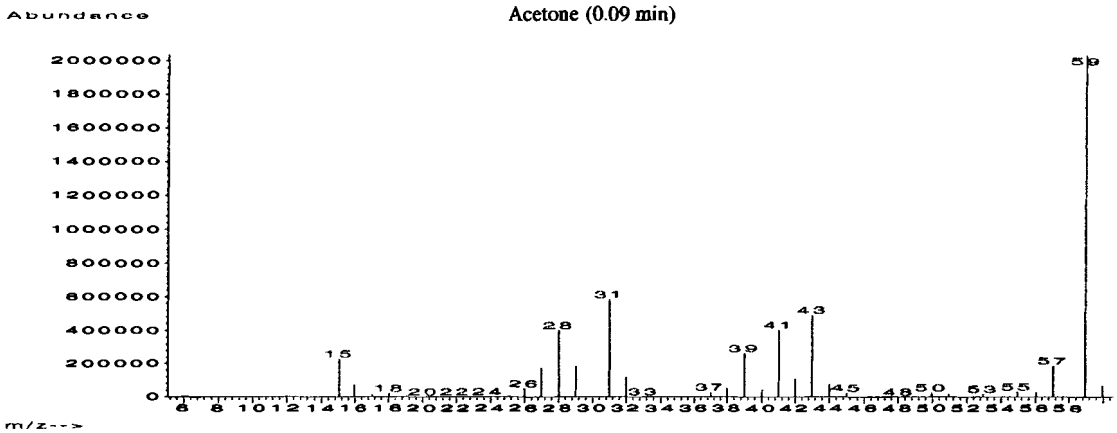

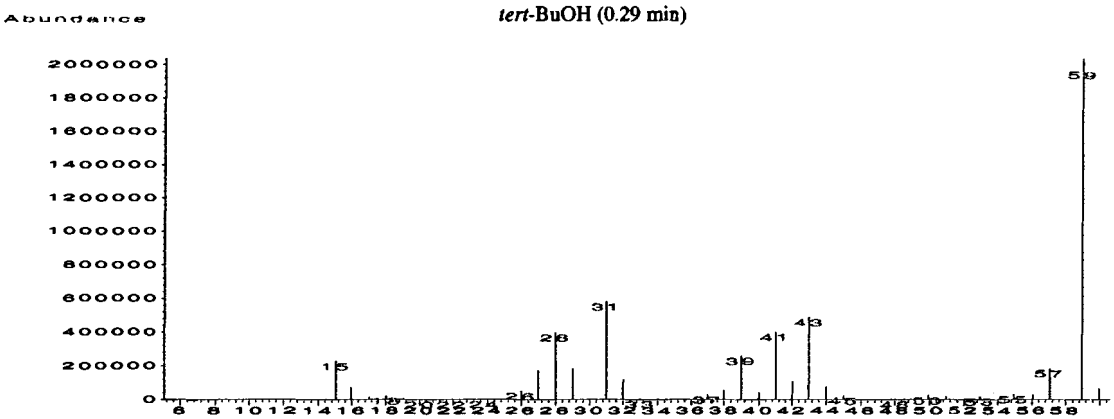

Figure D.6. Continued.

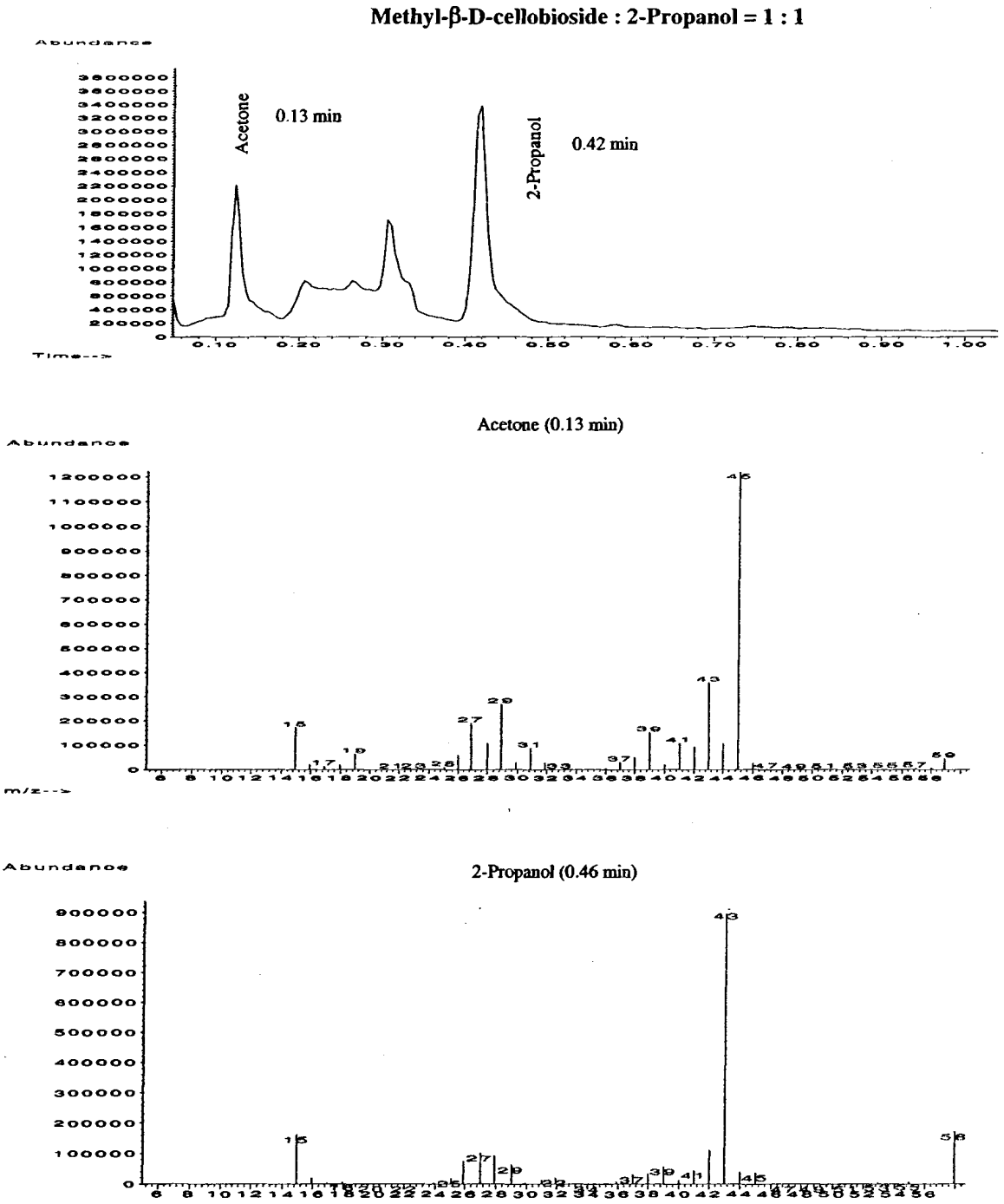

Figure D.7. SPME-GC/MS scans of UV/H_2O_2 reactions of methyl-β-D-cellobioside in the presence of 2-propanol. Retention times varied due to the length of column.

Methyl-β-D-cellobioside : 2-Propanol = 1 : 2

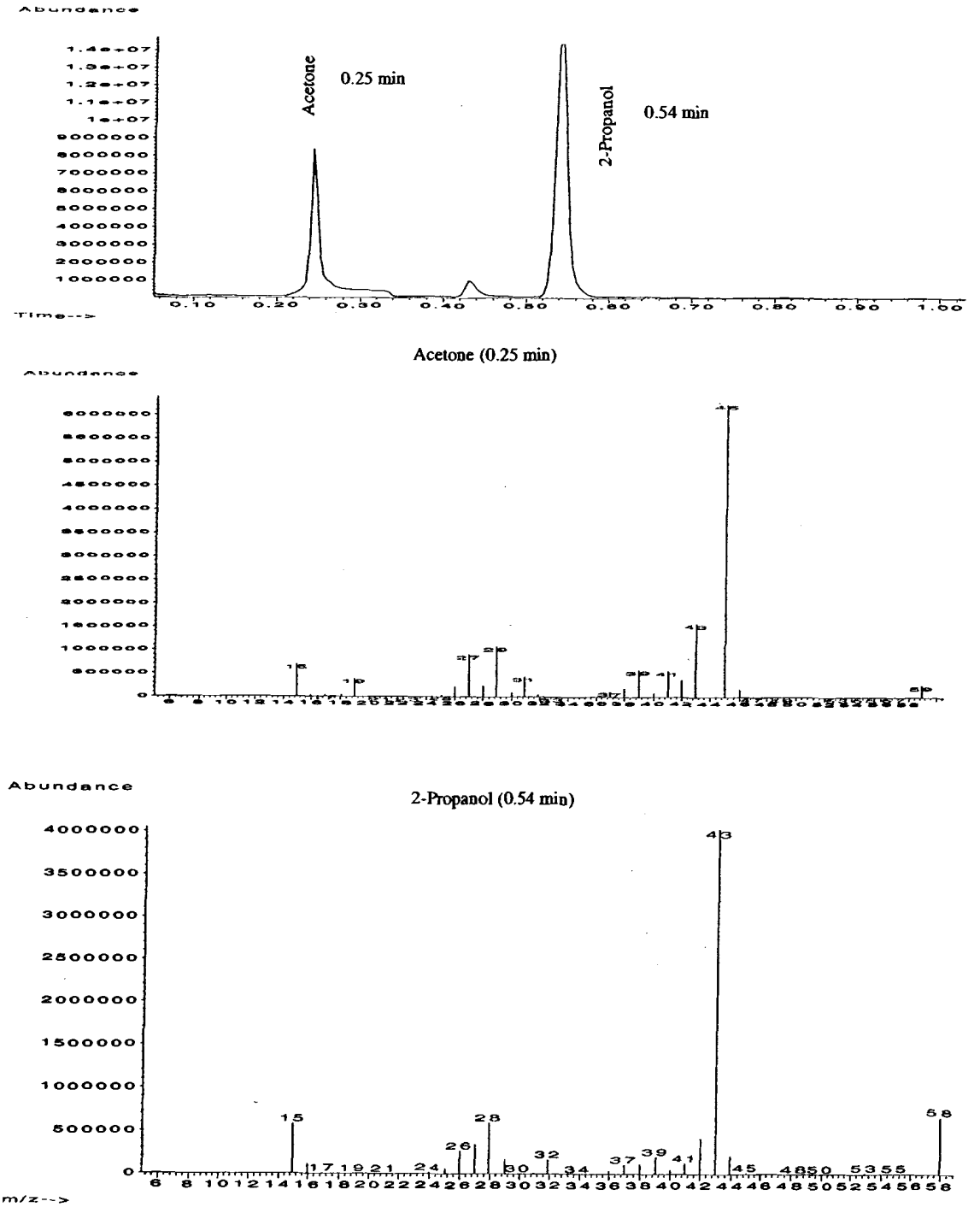

Figure D.7. Continued.

Methyl-β-D-cellobioside : 2-Propanol = 1 : 4

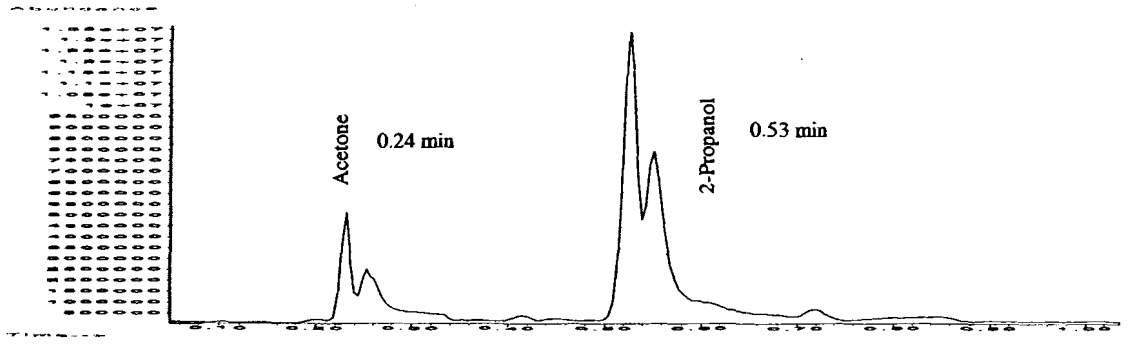

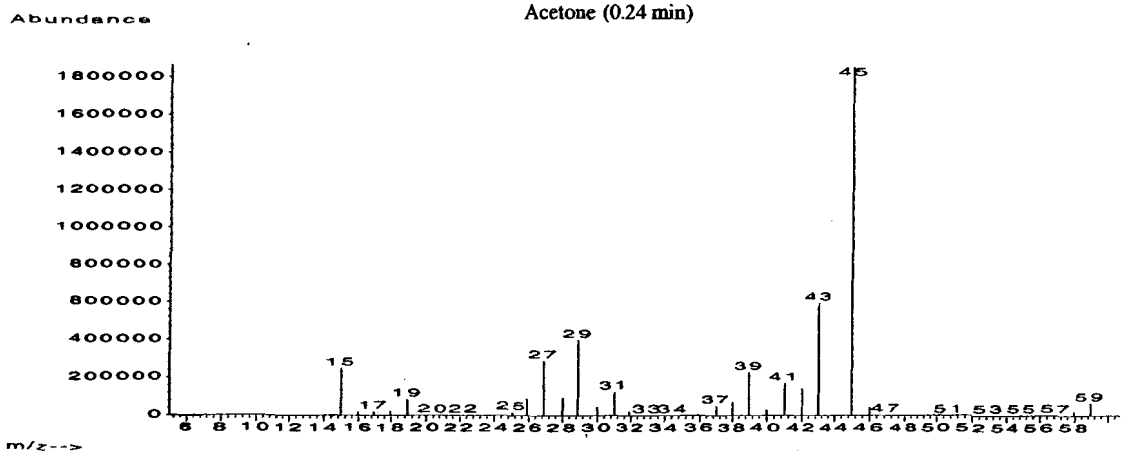

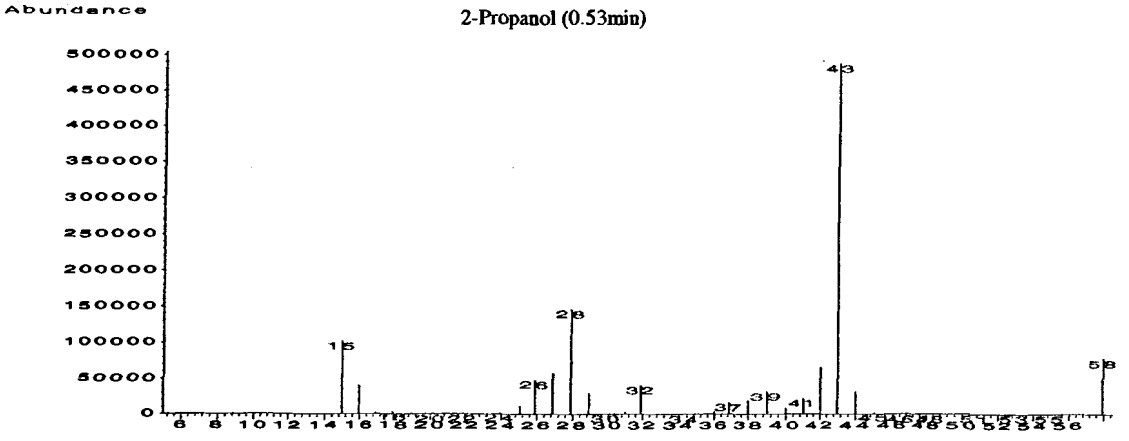

Figure D.7. Continued.

Methyl-β-D-cellobioside : 2-Propanol = 1 : 8

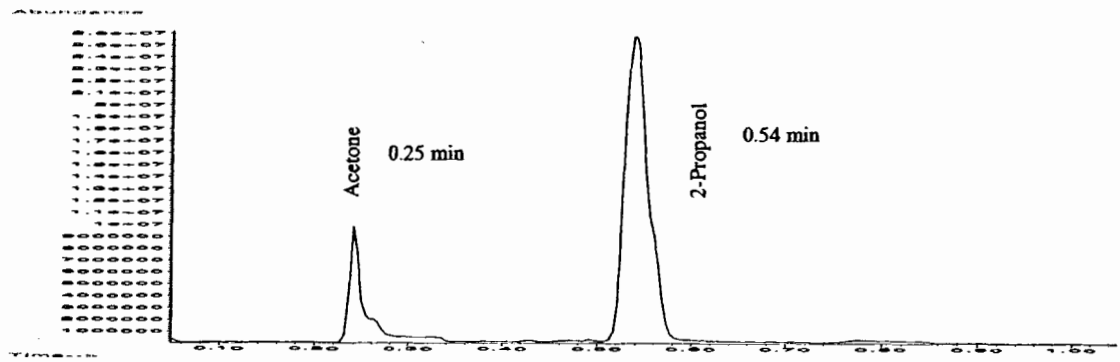

Acetone (0.25 min)

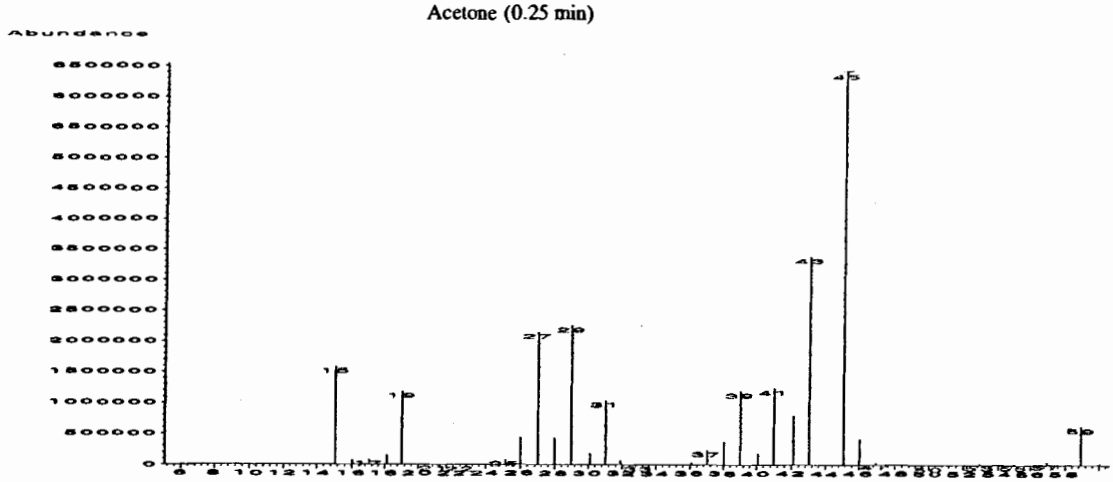

2-Propanol (0.54min)

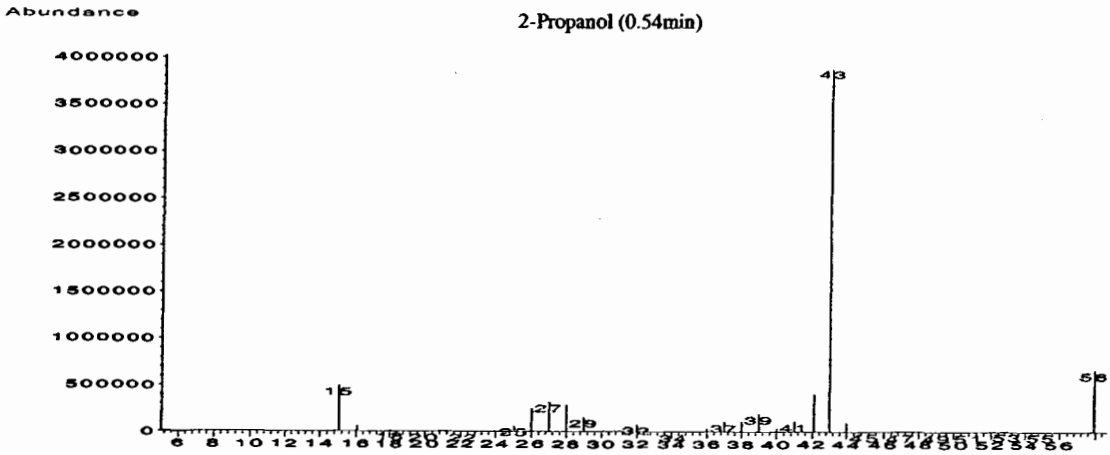

Figure D.7. Continued.

Cellulose fiber in the presence of *tert*-BuOH

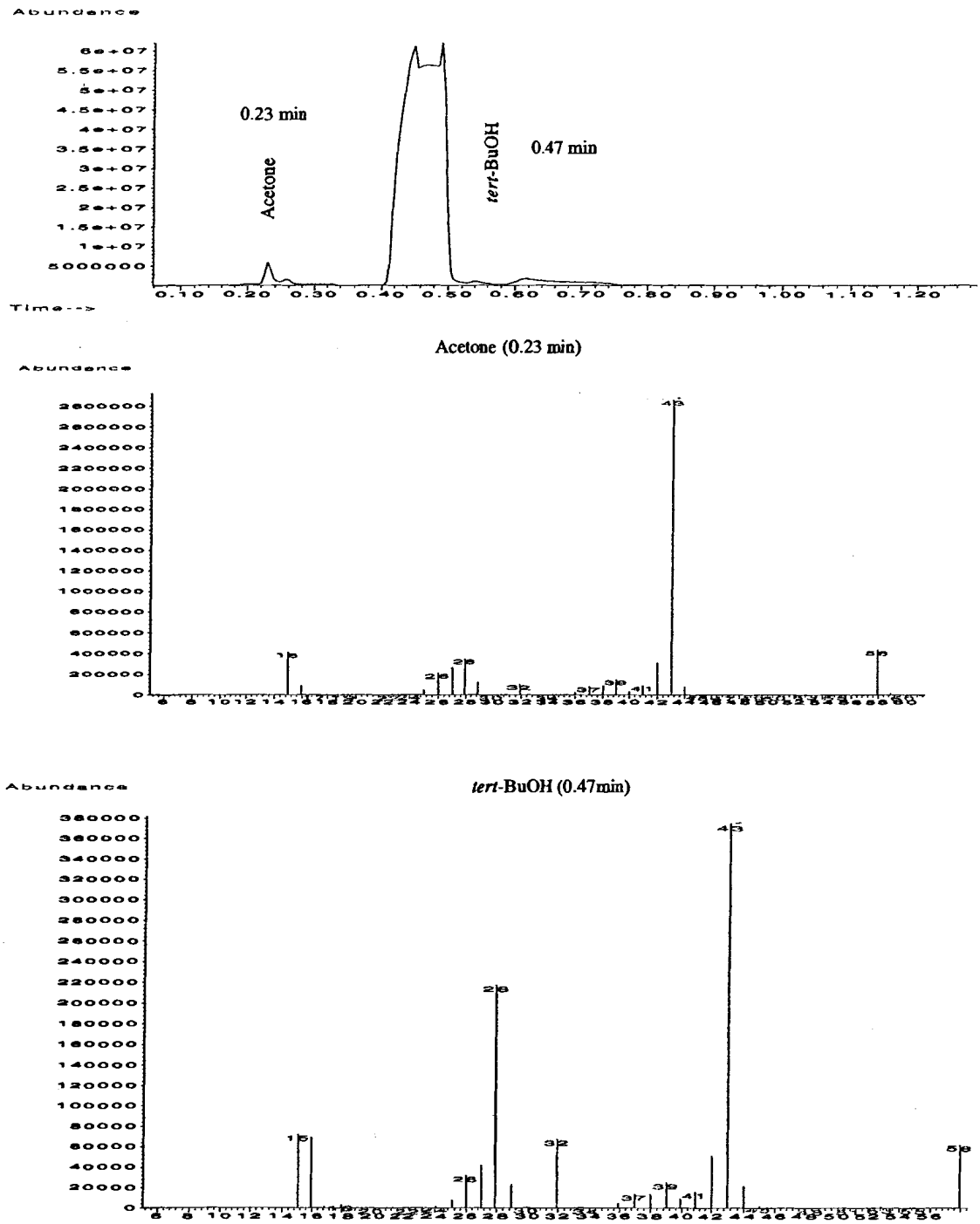

Figure D.8. SPME-GC/MS scan of UV/H_2O_2 reaction of the cellulose fiber (filter paper) in the presence of *tert*-BuOH.

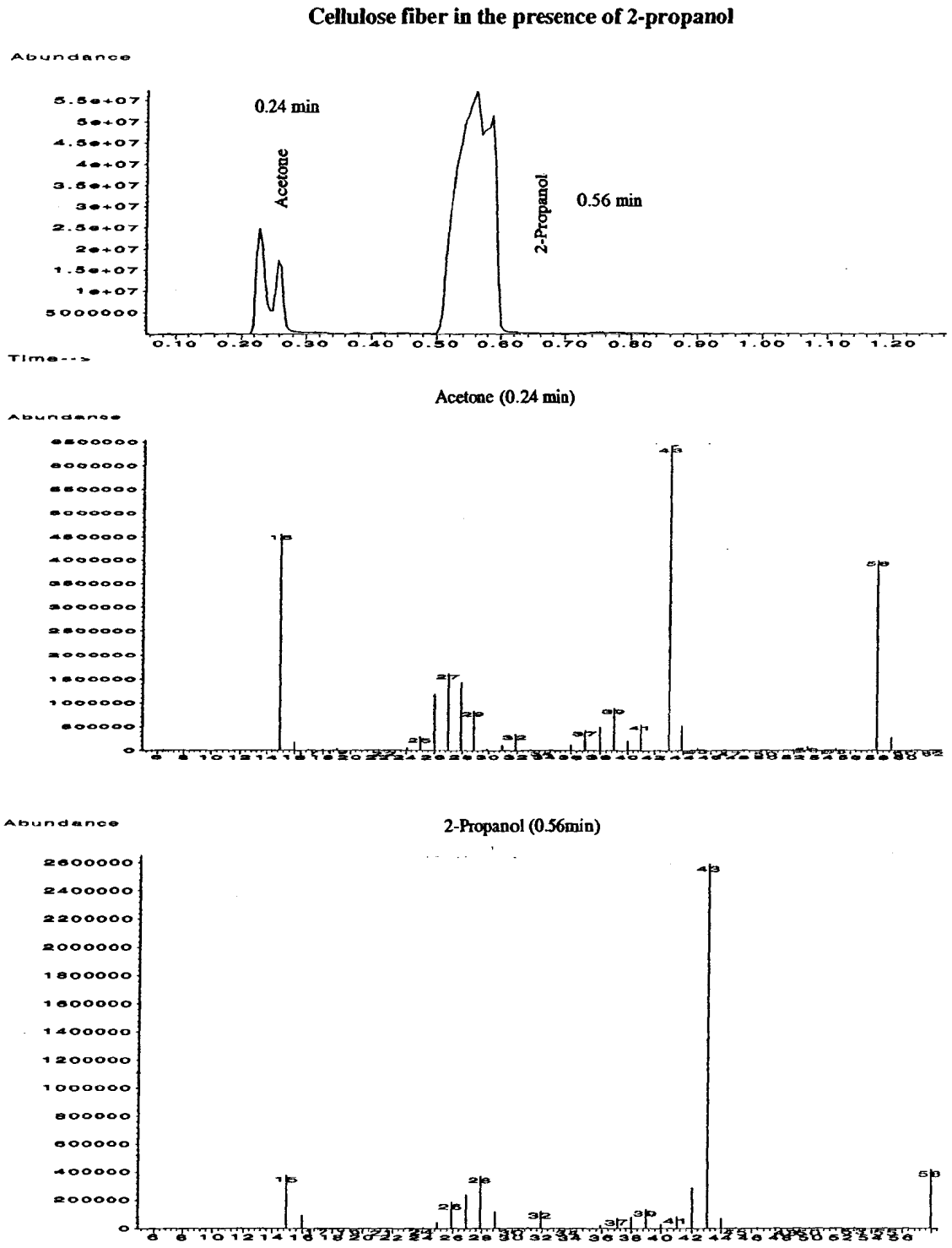

Figure D.9. SPME-GC/MS scan of UV/H_2O_2 reaction of the cellulose fiber (filter paper) in the presence of 2-propanol.

BIOGRAPHY OF THE AUTHOR

Oh-Kyu Lee was born in Kyungki-Do, Korea, June 5, 1964. He was graduated from Kyung-Shin High School in Seoul, Korea in 1983. He attended Konkuk University in Seoul, Korea and earned a Bachelor's degree in Forestry in 1988. At the same school, he entered the graduate program in the field of Forest Utilization and earned a Master of Science degree in1990. He served Korean army for two and half years (from 1990 to 1992). In 1995, he entered the Wood Science and Technology graduate program at University of Maine in Orono, Maine in the Department of Forest Management and earned a Master of Science degree in 1999. In fall of 1998, before he received the M.S. degree in the Department of Forest Management, he entered the graduate program at the same institute in the Department of Chemistry. He was a teaching assistant from 1998 to 2000 and a research assistant from 2000 to 2002.

Oh-Kyu is a candidate for the Doctor of Philosophy degree in Chemistry from The University of Maine in December, 2002.